The influence of sediment characteristics on the abundance and distribution of *E. coli* in estuarine sediments

Adam James Wyness

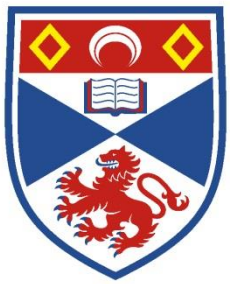

University of
St Andrews

This thesis is submitted in partial fulfilment for the degree of PhD

at the

University of St Andrews

1. Candidate's declarations:

I, Adam James Wyness hereby certify that this thesis, which is approximately 65000 words in length, has been written by me, and that it is the record of work carried out by me, and that it has not been submitted in any previous application for a higher degree.

I was admitted as a research student in September 2012 and as a candidate for the degree of Doctorate of Philosophy (PhD) in September 2013; the higher study for which this is a record was carried out in the University of St Andrews between 2012 and 2016.

Date …… signature of candidate ……

2. Supervisor's declaration:

I hereby certify that the candidate has fulfilled the conditions of the Resolution and Regulations appropriate for the degree of Doctorate of Philosophy (PhD) in the University of St Andrews and that the candidate is qualified to submit this thesis in application for that degree.

Date …… signature of supervisor ……

3. Permission for publication: (*to be signed by both candidate and supervisor*)

In submitting this thesis to the University of St Andrews I understand that I am giving permission for it to be made available for use in accordance with the regulations of the University Library for the time being in force, subject to any copyright vested in the work not being affected thereby. I also understand that the title and the abstract will be published, and that a copy of the work may be made and supplied to any bona fide library or research worker, that my thesis will be electronically accessible for personal or research use unless exempt by award of an embargo as requested below, and that the library has the right to migrate my thesis into new electronic forms as required to ensure continued access to the thesis. I have obtained any third-party copyright permissions that may be required in order to allow such access and migration, or have requested the appropriate embargo below.

The following is an agreed request by candidate and supervisor regarding the publication of this thesis:

Access to printed copy and electronic publication of thesis through the University of St Andrews

Acknowledgments

Firstly, I am eternally grateful to all of my supervisors. Thank you to Prof. Dave Paterson and Dr. Emma Defew at St Andrews University for your guidance and supervision, and for always finding time for me during my fleeting visits and the longer discussions going through chapters at a time. Your advice and suggestions on the initial project plan, to your patience reviewing chapters during the write-up was brilliant.

Thank you also to Dr. Lisa Avery and Dr. Marc Stutter at The James Hutton Institute. Lisa- thank you for your constant support and guidance, and encouragement to always 'give it a go', and the regular 'have you got 5 minutes?' resulting in me emerging from your office an hour later. I also appreciate that you could always find time for me during challenging circumstances. Marc- thank you for jumping in when things got complicated and getting your head round data for a whole chapter within a few minutes to guide me on the analysis.

Thank you to all the staff at The James Hutton Institute for having the time and patience to show me new techniques, answer 'quick' questions, and help troubleshoot the inevitable issues along the way. There are too many to mention individually, but I would especially like to thank Duncan for the smooth running of the micro-lab, Nadine for teaching me many new techniques, Claire for putting up with the muddy-ing of her lab and for her help sampling, and Betty for her endless patience discussing my stats work. Also, a big thank you to Matteo and Joe for their assistance with the fieldwork through snow and sun, wearing leaky waders and pushing the car out when it was stuck in mud, it was always a pleasure regardless of the weather!

Thank you to all the members of the Sediment Ecology Research group at St Andrews University for their invaluable expertise in field-work and sediment analysis. Special thanks to Irv and Jack for the early starts and the hard work they put in for the long days trudging from site to site pulling the sledges full of kit and samples. Without them, sampling days would have been far less efficient and enjoyable.

Thank you to the PhD student community of both The James Hutton Institute and St Andrews University, from Helen, Conor and Claire for their advice and support in the early stages, Kate and Julie for always lending a sofa, to the current PhD students for always providing some

light- hearted relief. I wish you the best of luck for your own projects. Also, thank you Sheila for the daily ‘networking’, and Nia for the chocolate.

A massive thank you to my family for supporting me throughout the whole process, from proof-reading CVs before I started, to listening to me complain about why things weren’t working when I came home. I will be coming back a lot more often now! Of course, the biggest thank you of all is to Katie- for putting up with the ups and the downs, the late nights and weekends of working and helping me sample in the wind and rain. I would not have been able to do this without your support. However, please don’t let a 3-legged dog run off with a sample again.

Finally, a thank you to the Fife Countryside Trust, and Scottish National Heritage for permitting the sampling campaigns on the beautiful Ythan and Eden estuaries.

Contents

Abstract

Microbiological water quality monitoring of bathing waters does not account for faecal bacteria in sediments. Intertidal deposits are a significant reservoir of faecal bacteria and this indicates there is a risk to human health through direct contact with the sediment, or through the resuspension of bacteria to the water column.

This project investigated factors influencing the relative abundance of faecal indicator organisms (FIOs) in intertidal estuarine sediments. The effects of physical, biogeochemical and biological sediment characteristics, environmental variables and native microbial communities were explored through field campaigns on the Ythan and Eden estuaries, Scotland. The contributory role of sediments to adverse water quality was investigated by combining FIO abundance and measurements of sediment stability. The importance of strain and sediment characteristics in the adhesion of *E. coli* to suspended sediments was also examined using laboratory experiments.

E. coli concentrations up to 5.9 $\log_{10}$ CFU 100 g dry wt^{-1} were observed, confirming that intertidal sediments are an important reservoir of faecal bacteria. The variability of *E. coli* abundance in estuarine sediments was successfully explained with multiple stepwise linear regression (Adjusted R^2 up to 87.4) using easily-obtainable measurements of sediment characteristics and environmental variables, with variability most heavily influenced by salinity and particle size gradients. Native microbial community population metrics and community constituent composition correlated with environmental gradients, but did not influence FIO abundance. The amount of *E. coli* adhering to suspended sediments ranged from 0.02 to 0.74 $\log_{10}$ CFU ml^{-1}, and was dependant on strain characteristics and sediment type rather than zeta potential, with higher cell-particle adhesion at 2 and 3.5 PSU than 0 and 5 PSU.

Monitoring of sediment characteristics will lead to more informed bathing water quality advisories to protect public health. Future research should focus on applying the findings here to the modelling of bacterial fate and transport on a catchment scale.

1. General introduction

1.1 Protecting public health

Human disease in association with pathogens from wastewater-polluted coastal waters is estimated to cause 120 million cases of gastro-intestinal disease, and 50 million cases of severe respiratory disease worldwide, resulting in an annual cost of three million disability- adjusted life years lost to poor-health and premature death, and approximately 9 billion pounds [1]. In the UK, an estimated 20 million people use the coast each year [2], with an estimated 1.75 million cases of gastrointestinal disease annually in England and Wales from beach and bathing water usage [3]. The most common illness associated with bathing in contaminated water is enteric illness [2], but bacterial skin infections, and eye, ear, nose and throat infections can also be contracted [3]. The risk of contracting gastrointestinal disease was estimated at around 51/1000 bathers, and the risk of other respiratory, ear and eye disease between 20/1000 and 54/1000 bathers in water that met the previous 'Imperative' guideline of <2000 faecal coliforms 100 ml^{-1} [4]. The likelihood of gastrointestinal illness of sea-bathers compared to non-bathing beach goers increases by an alarming 1.76 fold [5]. However, risk is not only associated with bathers, as an increase in enteric illnesses can be a direct result from increased contact with recreational beach sand [6]. The increase of disease in bathers may be because of facilitated infection pathways in water through accidental water ingestion, and also perhaps an increase in exposure to pathogens resuspended from sediments in the swash zone through wave action and human activity.

Many riverine, transitional (estuarine) and coastal waters are routinely monitored for microbial quality in order to protect recreational water users from disease. Where a body of water has been designated as 'bathing water', the required monitoring involves the culture-based enumeration of organisms that indicate recent faecal contamination, and the results used to allocate water quality classifications [7]. For coastal and estuarine waters in EU member states (including Scotland), an abundance of lower than 250 *Escherichia coli* Colony Forming Units (CFU) 100 ml^{-1} results in classification of 'Excellent' water quality, and between 250 – 500 *E. coli* CFU 100 ml^{-1} results in a 'Good' classification. Above 500 *E. coli* CFU 100 ml^{-1} results in a 'Poor' classification, where bathing is actively discouraged [7].

1.2 Human pathogens in the environment

Faecal bacteria enter the environment through point and non-point (diffuse) sources. Point sources are inputs such as improperly-treated sewage and combined sewage overflow systems. Diffuse sources include contamination from recreational beach users, and run-off from septic tanks, landfill sites and agricultural lands. Since the discontinuation of raw sewage outflows, diffuse sources are the predominant contributor to water-way contamination, however high rainfall events can result in raw sewage discharge from combined sewage overflow systems. Faecal contamination is transported down the catchment by surface run-off and groundwater into streams, rivers, and eventually reaches estuaries and the sea. Throughout the transportation process, bacterial cells can be repeatedly sedimented and resuspended to and from bottom sediments, increasing contaminant residence times within waterways compared to water-borne contaminants. The amount of rainfall (in defined periods) and subsequent river flow data is viewed as one of the most important factors causing adverse water quality. Historical correlations between these factors and faecal indicator organism (FIO) abundance are currently used by SEPA in the issuing of real-time bathing water quality advisories [8].

Faecal contamination also derives from domestic animals and wildlife. Animals act as reservoirs for several human pathogens, such as pathogenic serotypes of *E. coli* and *Salmonella* [9], and contamination from bird and dog faeces can contain up to 3.3×10^5 and 3.9×10^7 CFU g^{-1} dry weight faeces of enterococci sp. respectively [10]. The presence of FIOs such as enterococci sp. and *E. coli*, are ubiquitous in the faeces of warm blooded animals, and their presence indicates the extent of recent faecal contamination, and the likelihood of the presence of pathogenic faecal bacteria.

Faecal coliforms persist for long periods in the environment despite many associated environmental stresses [11] (discussed further in Sections 1.9 and 1.10). *Salmonella* sp. have been demonstrated to survive up to 332 days in manure-amended soils [12], and *E. coli* has demonstrated persistence for over 9 years in maritime soils [13]. Persistence in water is not as great as in the presence of soil or sediment however, with *Salmonella* sp. observed to survive for 16 days in farm pond water [14], and *Salmonella enterica* in sterile freshwater for 54 days, compared to up to 119 days in sterile freshwater sediments [15]. *E. coli* O157:H7 can survive almost 3 weeks in reservoir water, 18 days in agricultural lake water, 10 days in agricultural river water and up to 64 days in faecally contaminated puddle water [16]. Survival studies have

shown *E. coli* and *Salmonella* sp to survive in non-sterilised/ filtered estuarine water *in situ* for at least 15 days [17] and the addition of small concentrations of organic matter can support *E. coli* in seawater for almost 18 weeks [18].

1.3 Sedimentation of suspended cells

Sediments act as a reservoir for bacteria, including human pathogens, with freshwater and marine sediments containing up to 4 times the number of coliforms than the over-lying water [19-22]. Bacteria accumulate in sediments after descending in the water column, particularly when adhered to particles as they flocculate and sink. Bacteria adhere to particles as a medium for protection and survival; numbers of human pathogens are enriched several-fold when associated with suspended flocculated particulates compared to the surrounding water [23].

Two mechanisms occur that associate bacteria and sediment particles; the adhesion of bacteria to sediment particles larger than themselves, and the electrostatic attraction of smaller clay particles to the cell surface [24]. This forms an envelope of smaller colloidal clay particles that has been observed around *rhizobia* cells [25] and *E. coli* where this layer increased cell resistance to bacteriophage attack in saline sediment [24].

The speed of the deposition of suspended sediments and associated bacteria is determined by the settling velocity. The settling velocity of particles is chiefly determined by the size of the particle [26], and is calculated using Stokes' law. Generally, particles larger than 15 µm will take less than one tidal cycle to settle, but particles smaller than 15 µm, such as clay particles, will take longer than one tidal cycle and are also affected by electrostatic forces [27].

High current and tidal forces prevent the sedimentation of smaller particles, keeping them in suspension. This can result in stratification with depth in sediment beds because of temporal hydrodynamic shifts, and also results in the absence of smaller particles such as clays in areas of high current and tidal forces, such as estuary mouths, relatively narrow areas of an estuary and exposed beaches. Areas where hydrodynamic forces are low, such as bays, and in the upper sections of estuaries where the meeting of river and tidal currents create areas of slacker water usually result in underlying sediments of a finer particle size distribution [27]. 'Salt flocculation' also occurs, with particles more likely to flocculate as salinity increases [27], which increases the overall settling velocity of smaller particles.

After association with a particle in the water column, bacteria are incorporated into sediments with the sedimentation of the particle [28]. Muirhead et al. (2006) observed that, in a static system, a mean of 81 % of cells of an environmentally isolated *E. coli* strain attached to soil particles within 30 minutes of inoculation [29]. This short timescale suggests that when freely suspended cells are present in the water column through large-scale disturbance or input to the estuary, within a short time period they can adhere to particles and are susceptible to deposition.

There are various processes that can influence the persistence of bacteria in estuarine systems, many of which depend on whether the bacteria is part of the benthic sediment or in suspension, and in association or not with suspended particles (Fig. 1.1). The mechanisms of these processes are discussed in detail in this chapter.

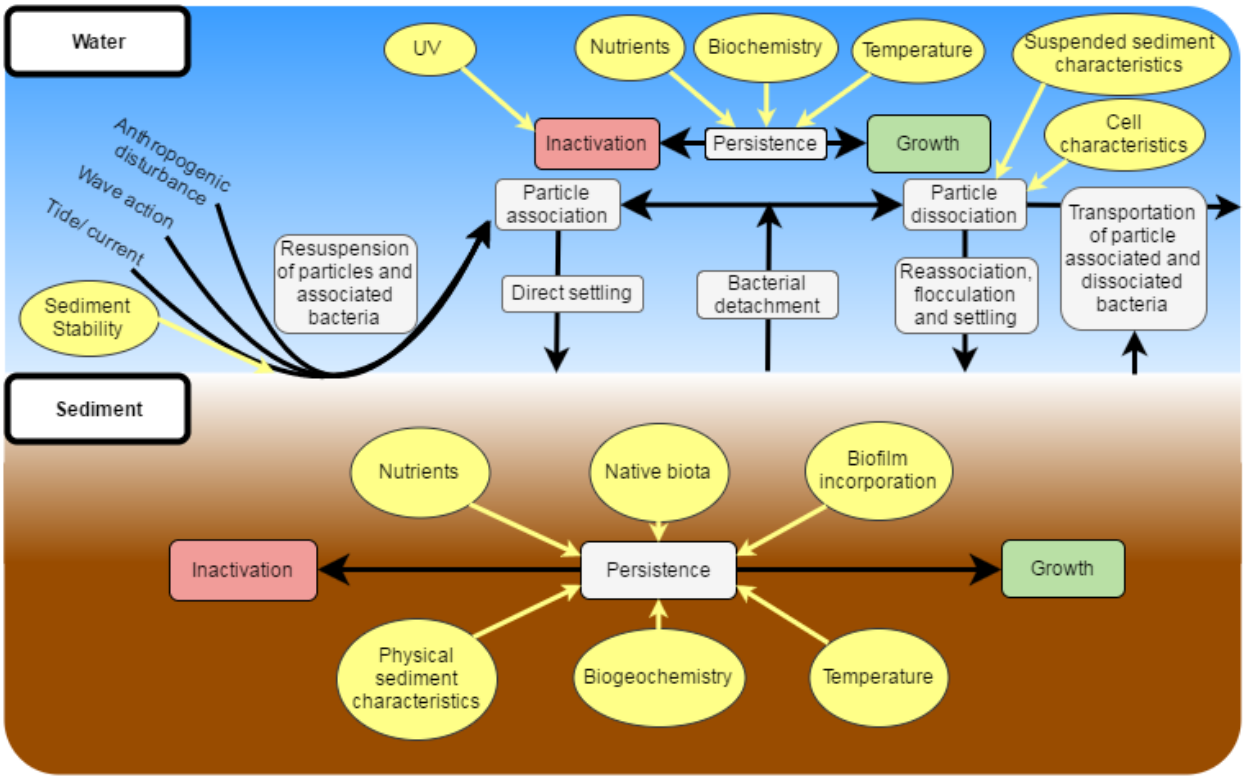

Figure 1.1 Conceptual diagram of processes that are known or suspected to influence the persistence of non-native bacteria in the estuarine system.

1.4 Cell-particle adhesion

1.4.1 Factors affecting cell adhesion

There are two widely accepted theories of active survival mechanisms used by bacteria. One is to adhere to a surface and produce a biofilm [30], the other is to adopt a dormant state [31] known as a viable but non-culturable (VBNC) state. A cell that is metabolically active, but incapable of the mitosis required to grow upon the media typically used for the detection and enumeration of that bacteria [32] is classified as VBNC.

The attachment of bacteria to surfaces is complex, and dependant on many factors including the properties of the surface, the cell, and the environment around them [33]. Cells are initially weakly (reversibly) associated with particles before they become strongly (irreversibly) associated [34]. The growth phase of the cell effects its adhesion, with log-phase bacterial cells having increased hydrophobicity [35], and adhesion rates [36] compared to stationary phase cells. Before the initial adhesion of a bacterial cell to a surface, there are changes in gene expression [37, 38], suggesting cells may sense a surface, and initiate a gene signal cascade [39]. Many changes in bacterial adhesion occur in response to environmental stresses [40] such as starvation, where extracellular polymeric substance production [41] and the formation of extracellular appendages [30] increase, and cell hydrophobicity changes to favour adhesion to surfaces [31].

1.4.2 First phase of adhesion: the physical forces of attraction

There is no definitive factor governing initial adhesion of bacteria to a surface, though many have been suggested including surface condition, mass transport, surface charge, hydrophobicity [42], surface roughness, surface micro-topography [43] and electrophoretic mobility [44]. If biological or chemical factors are ignored, there are two physical forces affecting surface to surface contact. These opposing forces are electrostatic repulsion, or the double layer of counterions, and Van der Waals attraction forces and their action known as Derjaguin-Landau-Verwey-Overbeek (DLVO) theory [45]. The principles of DLVO theory are sufficient in describing the early stages of bacterial adhesion to river sediments [46]. DLVO theory applies for colloidal particles [47], which suffices as a simple model of bacterial attachment, however the interactions between bacteria and sediment particles demonstrate bacteria are not inert, and have means of enhancing their adhesion to surfaces.

DLVO theory shows that adsorption is affected greatly by the electrostatic potentials of the surface or cell, therefore the difference between the surface charge and surrounding medium, known as the zeta potential, is an important measure. The surface charge of particles in suspension in estuaries [48] and indeed most natural surfaces, including that of bacteria [49], is negative, so cells with a less negative zeta potential or surface charge would have a smaller repulsive force to overcome when adhering to a surface. The zeta potential of *E. coli*, *Salmonella* and *Pseudomonas* sp. have been shown to vary with nutrient availability, starvation [50] and growth phase [40]. High electrolyte solutions have also been shown to supress the double layer of counterions [51], allowing the Van der Waals forces to act strongly, facilitating attachment. Conditioning films cover almost every surface in aquatic environments [52]. They are formed mostly from proteinaceous substances that are found ubiquitously in natural waters, especially that of high production environments such as estuaries. It is suggested that they could neutralise any physico-chemical features of the surface, including surface charge [52]. This would mask the negative charge of a surface, allowing greater adhesion than realised in abiotic laboratory experiments. The compression of the double layer of counterions also affects bacterial desorption; *E. coli* remains adhered to sediment particles at high salinities, but with decreasing salinity comes a critical concentration where the cells become detached from the sediment particles [24].

Laboratory experiments show substratum surface charge greatly affects *E. coli* adhesion [53], with 23 times greater cell density and enhanced biofilm structure by a factor of 37.5 on positively charged polyethene sheets compared to negatively charged polyethene sheets [53]. After high shear exposure, 40 % of biomass was retained on the positively charged sheet compared to 0 % on the negatively charged sheet. Some surfaces may also have a bactericidal effect, however dead or damaged cells can provide a structure for live cells to form a stable biofilm [53].

Attachment of indigenous groundwater bacteria is highly dependent on surface charges of the cell and mineral surface [47]. Negatively charged bacterial cells showed high adhesion to the positively charged surfaces, whereas attachment to negatively charged surfaces was significantly lower. This evidence underlines the importance of analysing the electrostatic charge of bacteria and sediment particles within the environment.

1.4.3 Second phase of adhesion: irreversible attachment

During the first phase, only inter-particle attraction forces are holding the cell to a surface; therefore cells are easily dispersed by shear forces. To create an irreversible attachment, cells will attach through extracellular appendages [54], or the exudation of extracellular polymeric substances [55], leading to biofilm formation. Biofilm synthesis initialises as bacteria sense the range of physical or chemical cues associated with surface contact such as an increase in available nutrients [37].

1.5 Extracellular appendages: facilitating bacterial adhesion to surfaces

Many types of extracellular appendages have been reported to be advantageous to bacteria during the initial adhesion or biofilm formation process. Fimbrae and pili are similar structures, the difference in nomenclature arising from their frequency; only one or two pili are found on a cell, whereas fimbriae are more numerous. Type 1 pili are composed of several proteins, one of which is FimH adhesin, and is associated with cell adhesion whereas type IV pili are usually associated with cell motility. Type 1 pili are essential for initial adhesion of *E. coli* to abiotic surfaces, while type IV pili are involved with movement along the surface [56], augmenting biofilm formation. Flagella are whip-like appendages used primarily for movement and there is contrasting evidence on whether they are essential to biofilm formation by *E. coli* [56-58], as they are for *P. aeruginosa* [59]. Curli fimbriae are extracellular proteinaceous amyloid fibres exuded by enteric pathogens to adhere to surfaces and other cells in order to facilitate biofilm formation [60]. However, the genes for curli fimbriae production are not expressed under medium to high osmotic pressure, temperatures below 30°C and during stationary growth phase [61].

Flagella are suggested to aid biofilm formation in several ways [56]. They could be used for initial anchorage to the surface before initiation of biofilm synthesis. It is suggested that the motility from flagella is required to overcome surface repulsion before initial contact with the surface, and also motility is required after surface contact to spread over the surface and develop a biofilm [56].

The motility role of extracellular appendages differs between bacterial species [56]. *E. coli* are peritrichous (have many flagella extending from random locations) and have a ‘random walk’ including swimming and tumbling [62], whereas *Pseudomonas aeruginosa* and *P. fluorescens*

are monotrichous (have one flagella at a polar end of the cell) and move in a 'straight movement, then stop, then turn' routine [63]. Single type-IV pili are used by *P. aeruginosa* to 'slingshot' itself before pulling itself in a crawling movement with many pili [64]. The slingshot movement is 20 times faster than the crawling, and is an efficient mode of motility through a viscous medium, such as a biofilm. *E. coli* mutants lacking type-IV pili show impaired biofilm formation compared to wild types [65].

Pseudomonas fluorescens mutants lacking flagella took longer to adhere to glass surfaces in high and low fluid shear than those with flagella due to lack of mobile attachment [66]. *Acinetobacter calcoaceticus* mutants not expressing genes for thin fimbriae also demonstrated how the presence of fimbriae were a crucial bacterial adhesion to polystyrene and hydrocarbon surfaces, and that fimbriae were important in the agglutination of cells [67].

Despite some contrasting views, the consensus is that the presence of several and different types of extracellular appendages and exudates are advantageous to surface adherence and consequential biofilm production (Table 1.1). Pratt [56] identified the connection between this and the evidence that large numbers of pili and presence of flagella have been associated with increased pathogenicity in enterobacteria [68, 69]. Thus, pathogens most likely to persist within the environment are also ones most likely to induce illness.

Table 1.1 Selected fecal bacteria and pathogens and their cellular appendages that are known to increase adhesion rates.

Appendage	Species	Reference
Pili	Gram - & + Bacteria	[65, 70]
F1C fimbriae	*Escherichia coli*	[71]
Curli	*Escherichia coli*	[57]
Type I pili	*Escherichia coli*	[56]
Thin aggregative fimbriae (Curli)	*Salmonella enteritidis*	[72]
Type I pili	*Klebsiella pneumoniae*	[73]
Flagella	*Pseudomonas* sp.	[58]
Type IV pili	*Pseudomonas aeruginosa*	[59]
Type IV pili	*Vibrio* sp.	[74]
Enzymatic adhesion: SSP adhesion	*Staphylococcus epidermidis*	[75]
Enzymatic adhesion: Autolysin AtlE	*Staphylococcus epidermidis*	[76]

1.6 Occurrence of fecal bacteria in intertidal sediments

Reported abundances of faecal bacteria in intertidal sediments varies considerably between sediment types, which results in difficulties comparing studies when sediment characteristics have not been comprehensively analysed, in addition to difficulties arising from sampling of different sediment depths. Nevertheless, total coliforms have been recorded in intertidal [77] and subtidal [78] estuarine sediments with up to 2.4 x 10^6 Most Probable Number (MPN) 100 ml^{-1}, and 1.3 x 10^5 CFU 100 g^{-1} found, respectively, and faecal coliforms up to 1.6 x 10^5 MPN 100 ml^{-1} [77] and 8.0 x 10^4 MPN 100 g^{-1} dry wt [79] for intertidal and subtidal estuarine sediments found, respectively. *E. coli* has been recorded in benthic estuarine sediments at a mean of 5.9 x 10^3 CFU 100 g^{-1} in the Conwy estuary (UK) [78] and up to ~8.0 x 10^4 CFU 100 g^{-1} in the Neuse River estuary (NC, USA) [80].

1.7 Survival of fecal bacteria in intertidal sediments

There is a necessity for further assessing the ecology and survival of FIOs and pathogens in sediments and sediment-associated transport in order to fully characterise potential risks to water quality and public health [28, 81]. Pathogen persistence has been generalised by many authors as being a first order inactivation constant [82], however the exact value of the constant varies considerably between species, and the ambient temperature and nutrient availability [82].

The persistence of faecal coliforms is increased in sediments compared to the overlying water [77, 83, 84], to longer than 68 days for *E. coli* [28]. Sterile eluent from sediments also supports population growth, as does non-sterile sediment or seawater, albeit temporarily [77]. Sediment-laden waters also allow for greater persistence of faecal coliforms compared to water alone [85]. An extended study by Ashbolt et al. [86] and Grohmann et al. [87] observed FIO numbers in sediments remained constant after outfalls were decommissioned, and FIO levels in the water column decreased to a safe level, presenting case-study evidence of increased persistence in sediments compared to overlying water [28]. Many sediment properties have been identified to affect the survival of faecal coliforms in sediments, including organic carbon [11], nutrient availability [88], particle size [11, 89], bulk density, acidity, exposure to light, temperature and the native microbiota [90].

Fecal bacteria have demonstrated the ability to reproduce in environmental conditions [77], therefore the question arises, is a pathogen population in the environment replicating, or are the same cells persisting? Genetic fingerprinting found that in Lake Michigan sediments relatively few isolates were replicates, indicating that *E. coli* were more likely to persist in that environment than replicate [91]. The native environment for faecal coliforms is the gastrointestinal tract of warm blooded animals. During environmental phases of transmission prior to colonising new hosts, cells are likely to experience unfavourable conditions for a considerable time [92]. Although these conditions are not optimal for the growth of faecal bacteria, they will not necessarily kill the cell, allowing for environmental persistence and cross infection. As discussed by Rozen and Belkin (2001), environmental conditions that support growth may not be the optimum conditions for persistence [93].

1.8 Abiotic factors affecting bacterial survival in intertidal sediments

1.8.1 Particle properties

The particle size of sediments has a significant effect on the survival of inoculated faecal coliforms, with the persistence being greater at smaller particle sizes [85, 89], and with lower temperatures [94]. It is suggested that this is because smaller particle size often comes with increased organic matter and nutrient concentrations [88]. Sediments have been shown to contain nutrient concentrations at least 4-6 times that in the overlying water [95]. At the solid-liquid interface there is likely to be a higher concentration of nutrients than the surrounding water, due to the adherence of nutrients to the surface, or other organisms degrading the surface, making resources available [96]. Bacteria associated with particles are also more metabolically active than their planktonic equivalents [97, 98].

In beach sands with differing particles sizes, inoculated *E. coli* O157:H7 was exposed to simulated tidal flushing, and sand with the smallest particle size yielded the largest recovery of cells after 5 days [99]. *E. coli* also preferentially adheres to soil particles of a diameter between 30 µm and 16 µm by almost 4 fold than any other size fraction in clay-loam soil (when adjusted for particle surface area) [100], with up to 99.2 % of *E. coli* reported to adhere to particles larger than 1 µm [101]. Mud-sediment has been demonstrated to support higher numbers of *E. coli* than sand, suggested to be due to the higher organic content and finer particles [89,

102]. It has been suggested that sediments with higher clay fractions support higher faecal coliform numbers because of the difference in particle charge and surface area [103].

The size and distribution of particles in a sediment effects cohesion, porosity, permeability, and chemical potential [104]. It has been shown that higher numbers of heterotrophic bacteria exist in sediments with high mud (silt and clay fractions) content, with 3.8 x 10^5 CFU g^{-1} of dry weight of sandy sediment compared to 6.0 x 10^5 CFU g^{-1} in mud [105]. Total bacterial production also positively correlates with organic matter inputs [106] that are usually associated with these finer sediments.

The mineralogy of the clay fraction (<63 µm diameter) also affects the cation exchange capacity and water retention of the sediment [107]. Clay mineralogy can affect bacterial metabolism, with the presence of montmorillonite increasing respiration rates in several species of bacteria [108]. The presence of clay in contaminated sediments may also prevent predation by protozoans by increasing 'protective microhabitats' for bacteria [109].

Coliform-containing secondary effluent passed through an 8 µm filter membrane (non-particle associated) was more sensitive to disinfection by UV compared to effluent not passed through (particle associated) the membrane [110], as was the case when ultrasonication was used to disperse bacteria from the UV protecting properties of particles in wastewater [111]. UV damage from sunlight to coliform cells is greater when associated with smaller particle sizes due to decreased shadowing compared to a larger particle [112]. This effect is greater when cells and particles are in suspension [113], as consolidated sediments give the necessary protection to cells from UV, therefore the damaging effect of UV on pathogens in sediments is likely to be less influential than other factors [99].

1.8.2 Salinity and pH

High salinity poses the threat of osmotic stress, but also specific ion toxicity to the bacterial cells [114]. Carlucci and Pramer [114] observed the persistence of *E. coli* to sharply decrease at salinities higher than ~9 practical salinity units (PSU), and survival at ~9 PSU was greater than in deionised water. Rapid increase of salinity is also more detrimental to the survival time of *E. coli* and *S. typhimurium* in sewage effluent stabilisation ponds compared to a gradual increase in salinity [115]. The survival of *E. coli* in seawater may also be dependent on the presence and activation of osmoregulatory genes that not all strains will possess [116], suggesting faecal

bacteria with the ability to survive in an estuarine environment are a proportion of the total load entering the estuary. The pH of seawater ranges from 7.5 to 8.5 [114] and is dependent on temperature, and microbial activity [117]. Higher survival rates of *E. coli* have been observed at lower pH (5 and 6) than 7 and above [114].

1.8.3 Temperature

Increased persistence of FIOs in sediment correlates with lower temperatures in estuarine water [17, 118] and sediments [77], with survival inversely related to temperatures between 1 °C and 28.2 °C [17, 119, 120]. This seems counterintuitive as it is well known that optimum growth conditions for enteric pathogens is the internal temperature of their preferred host, such as ~40.5 °C for *E. coli* strains [121]. Higher levels of coliforms were found in canal sediments during winter than in summer, attributed to an increase in die-off rates during summer [21], however, frequent flushing of sediments in winter caused higher coliform counts in summer than winter [122]. There was no seasonal variation detected in thermophilic *Campylobacter* in a study on English bathing waters despite higher abundance in the overlying water during the winter months [123], whereas a study on the same estuary revealed very strong seasonality of *Campylobacter* with higher abundance during the winter months, and negligible detection during summer [124].

1.8.4 Rainfall and hydrodynamics

Periods of high rainfall flushes FIOs from the land to surface waters [125-127] where flow will continue down-catchment to streams, rivers and eventually estuaries and the sea [128, 129]. The first rainfall after a dry period also has a 'first flush' effect, creating higher FIO counts for the expected rainfall volume [130]. Greater water discharge with increased rainfall also increases shear forces on the sediment increasing sediment bed erosion that resuspends bacteria from the sediment transporting them downstream. High rainfall events also redistribute available nutrients; a study on the Ythan estuary (Scotland, UK) showed a decrease in total organic nitrogen and silicates, and an increase in soluble phosphorus during high rainfall [131].

1.9 Biotic factors affecting bacterial survival in sediments

1.9.1 Macrobiota

Faecal coliforms can persist in the environment for at least 18 weeks [18], which is ample time for bacteria to be ingested by filter-feeding organisms. This can lead to marine mussels bioaccumulating *E. coli, V. cholera and E. durans* to concentrations of up to two orders of magnitude higher than the overlying water [132]. This suggests filter feeders could be a significant reservoir for pathogens within the estuarine environment [133], prolonging system contamination, and presenting a major risk to human health.

In freshwater sediments, macro-invertebrates serve as transport vectors of bacteria to [134], from [135] and through [136] sediments. Detritivores such as larval chironomids in freshwater acquire faecal coliforms and carry them through their instar stages to emergence as adults and could transfer the pathogens to uncontaminated areas [15]. This can be due to the unintended ingestion of bacteria by grazers or predators with their intended quarry [137] and their passage through the digestive system intact [138]. Invertebrate exoskeletons can also be colonised by a rich and diverse microbiota [139], which may be shed through abrasion with surfaces, or when the exoskeleton is shed [136].

Macroalgae such as *Cladophora* [140, 141] and samples of mixed species [142] have been identified as an environmental reservoir for *E. coli* and enterococci, and can support their growth [141]. This is of great importance as extensive beds of *Ulva* spp. occur seasonally in many estuaries, and after storm events where many pathogens may be resuspended, macroalgae often collect on beaches, creating a potential health hazard.

1.9.2 Indigenous microbiota

Many studies conclude that parasitism and predation are the most important factors involved in the decline in non-native bacteria in sediments [143]. Indigenous eukaryotes were found to have a negative effect on *E. coli* survival in compost slurry [144], and were also found to increase in abundance when *E. coli* populations decreased in estuarine water [119]. Protozoan predation rather than predatory bacteria however has been found to be responsible for the decrease in *E. coli* populations in estuarine water [145]. The presence of protozoan predators caused a net die-off of faecal coliforms in marine sediments, whereas their absence (through

addition of cycloheximide) allowed enhanced faecal coliform persistence and possibly allowed for growth [28].

1.9.3 Extracellular polymeric substances (EPS)

EPS are biosynthetic polymers exuded by bacteria, micro-flora and fauna that can aid in formation of microbial aggregates [146] when associated with surfaces or particles [147], and also increase erosion thresholds of sediments [148, 149]. EPS occur in many aquatic environments when bacteria are associated with detritus [150], sands [151], and fine sediments [152]. EPS production in bacteria can be a direct response to environmental stresses such as temperature [153] and light [154]. The primary function of EPS production is to maintain a constant environment for the cell and to protect it from environmental stresses rather than being an extracellular energy store [155]. However, EPS may be important in many ecosystems as it could have a key role in carbon cycling, acting as a carbon source for other microbiota and invertebrates [147, 156, 157]. The EPS produced by bacteria is usually higher in proteins than carbohydrates, whereas microalgae secrete mostly carbohydrates [158-161]. The carbohydrate composition of EPS and amount produced differs between diatom species, cell growth phase and nutrient availability [161], and the relative composition of these may influence the cohesive properties of EPS [162]. EPS is lost from sediments by erosion during the tidal cycle, and dissolution by its metabolism by heterotrophic bacteria [163]; bacteria dissolve EPS using hydrolases, but only assimilate a small fraction of the products [164]. Sediments containing high EPS concentrations may provide protection from environmental stresses to faecal bacteria, as well as possibly providing a nutrient source.

Many benthic diatoms produce EPS to facilitate movement into the photic zone of sediment to photosynthesise. They become submerged in sediment through deposition and mixing [161], and actively bury themselves during tidal immersion and low light conditions [149]. The increase of EPS causes diurnal changes in the cohesive strength of sediments. EPS production by diatoms also ‘armours’ sediment [165]; once at the surface of the sediment and photosynthesising, there is a lag period before sediment stability increases, suggesting EPS production continues after migration into the photic zone. This is assumed to be to increase sediment stability to reduce the chance of their suspension [165].

The physical state of EPS has been described as a continuum ranging from colloidal material to a gel-like state where molecules may form 'covalently crosslinked networks' [148] that can incorporate sediment particles as part of the biofilm. These networks of thread-like EPS have been suggested to contribute to the erosion resistance of intertidal sediments [149]. Addition of Xanthan gum (a substance emulative of diatom EPS) increases stabilisation of cohesive sediments through a strengthening and gluing action similar to that of EPS strands on particles [166].

1.10 Microbial biofilms

1.10.1 Microbial biofilm formation

Biofilms are a complex matrix of abiotic substances such as sediment grains, organic matter, and organisms such as diatoms, other algae, phototrophic and heterotrophic bacteria, fungi and protozoa [167] and of course, EPS [168]. Within biofilms, many interactions occur between the different groups of organisms [169]. Faecal coliforms are present in higher numbers in lotic biofilms than overlying water by 1-3 log units [170] as, similarly to particle-association, association with biofilms has many benefits to a bacterium including access to higher nutrient concentrations, protection from passive grazers and predators, and a medium for promoting quorum sensing [43]. Biofilms originating from microphytobenthos are found in the majority of photic-aquatic habitats [163, 171, 172]. In natural cohesive sediments, biofilms with epipelic diatoms as the dominant microbiota are common [168, 171, 173], especially with decreasing salinity [171].

The formation of biofilms by bacteria occurs in most environments where there is sufficient nutrient availability [56]. Biofilm creation is the default mode of bacterial survival within the environment [39] as they enable robust attachment and allow a habitable micro-environment allowing changes in the growth rate and gene transcription of the cell [52]. Enteric pathogens are also able to create biofilms to protect themselves from the immune system of their host [52].

1.10.2 Diatom biofilms

The relative abundance of bacterial species within diatom-associated populations is a direct consequence of the diatom species present and their physiological state, due to changing selection pressures to highly-adapted bacteria [174]. Diatom exudates form a phycosphere around the cell [175] that is colonised by marine bacteria because of increased nutrient levels [175] with the polysaccharide and glycoprotein-rich diatom EPS providing a significant carbon source for bacteria [176]. The specific community assemblage for a diatom biofilm is determined through a selection process between facultative bacteria [175] best adapted to the specific species of organic carbon exuded by the diatom [177]. A non-indigenous pathogen occurring in the foreign environment of a marine epipelic ecosystem will therefore experience great competition for resources in diatom dominated biofilms.

Extracellular secretions from bacterial cells have significant effects on the amount and contents of EPS produced by epilithic freshwater diatoms [178]. The effect is species dependant, with an increase of diatom EPS of up to 10 x with the presence of *Pseudostaurosira* sp compared to axenic cultures. The changing constituent concentrations affects EPS properties [179], in turn affecting biostabilisation. There are many different interactions between diatoms and bacteria [178, 180] that will affect the formation, composition and biochemical characteristics of diatom-associated aggregated material, and may depend on bacterial community composition [174], and varying temperature and light conditions [180].

1.10.3 Bacterial biofilms

Many bacteria are able to produce their own EPS in order to adhere to surfaces to remain in nutrient rich areas [39], facilitate movement, and protect themselves from environmental stress [39, 156]. Bacterial EPS has been suggested to have a biostabilisation role by stabilising established aggregates [174]. In microcosm studies, bacterial biofilms dominated nutrient poor systems when co-introduced with diatoms, yet diatoms were more successful in nutrient rich systems [181]. Biofilms reduce surface turbulence, reducing the erosive forces, therefore faecal bacteria incorporated into biofilms may be less likely to be eroded and transported by shear forces.

1.11 Sediment transport: the erosion, transport, deposition and consolidation (ETDC) cycle

Natural Cohesive Sediments (NCS) are a definitive feature of most estuaries [27]. NCS show cohesive properties due to electrostatic interparticle forces between particles of the mud fraction of the sediment, resulting in higher resistance to erosion than sediments with a larger particle distribution. Generally, sediments with >10 % fine particle (<63 µm) proportion will start to display cohesive properties [182]. Sediments are rarely formed from uniformly sized particles in a homogenous bed, and with an increasing mud fraction, the erosive properties of sand will differ. When the sediment consists of particle sizes >63 µm, the erosion threshold increases with particle size, but below 63 µm, erosion thresholds are inversely correlated with particles size (Fig. 1.2) due to increased packing, or consolidation of the sediment allowing for strong cohesive interparticle forces [27]. The relationship between increasing mud fraction and erosion threshold is complex and depends on many variables, presenting difficulties in predicting sediment erosion and transport.

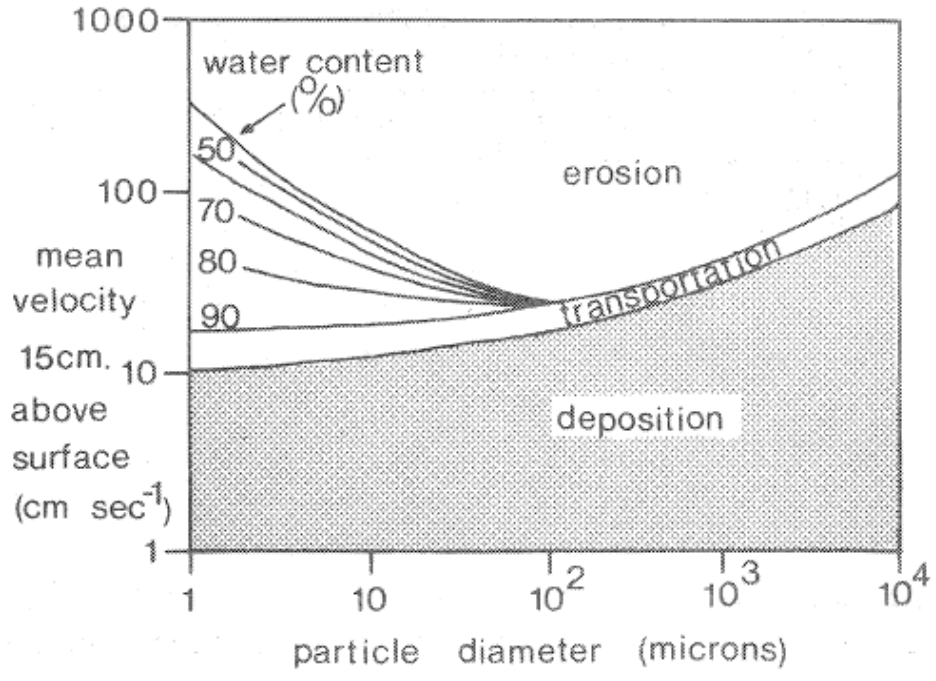

Figure 1.2 Mean water velocities at which erosion and deposition of sediment occurs at different particle sizes and water contents of sediment. From McLusky [27], after Postma [183].

Cohesive sediments in estuarine systems are exposed to processes of 'erosion, advection, dispersion, aggregation, settling, deposition, and consolidation', referred to as the erosion, transport, deposition and consolidation, or ETDC cycle [182] (Fig. 1.2). Water content (highly correlated with bulk density or consolidation) also affects the velocity needed to resuspend the smaller particle diameters. The erosion or entrainment of sediment is determined by the current shear forces, and the resistance of the sediment through cohesion. The lower the water content, the more interparticle forces dominate, creating cohesive sediment displaying erosive properties similar to larger particles.

Two mechanisms of cohesive sediment erosion have been described [184]. The first being surface erosion of 'floc-by-floc' entrainment of the uppermost layers of sediment into the water column. The second is larger scale mass-erosion where bed failure is in lower layers of the sediment, entraining all sediment above the shear plane. When sediment is entrained through disturbance or high shear force, for example during a storm event, high numbers of fecal bacteria are once again found in the water column and transported [51, 185]. They are then more likely to be ingested by bathers, or will settle in a new location, possibly in a high risk area such as a recreational beach, altering the exposure pathway to humans, and increasing the chance of pathogen ingestion and infection. As FIOs persist in marine sediments for longer periods compared to overlying water, detection of FIOs in water does not necessarily indicate recent contamination, rather it could indicate a resuspension event of contaminated sediment [105]. Considerable recent research has been performed on the resuspension of FIOs from sediments [126, 186, 187], and the dynamics of the process needs to be understood as it is the cycle of sedimentation and resuspension that prolongs water contamination and extends the risk to human health. Dredging, although an extreme resuspension event compared to that of shear from increased rainfall or wave action, demonstrates the extent of viable pathogen accumulation in sediments that can be resuspended into the water column and transferred to more high risk areas. Viable faecal coliform counts in the Mississippi river increased from 28 CFU 100 ml^{-1} to 170 CFU 100 ml^{-1} during dredging, with continued elevation of faecal coliforms levels 5 days post-dredging [188].

Knowing the erosion threshold of a sediment is vital to understanding the transport of pathogens. When sediment becomes entrained, it disperses within the water column and is transported, together with its bacterial load, affecting pathogen exposure pathways. Many factors affect the erosion threshold of cohesive sediments (Table 1.2), and they can be highly

interrelated, such as particle size and organic matter, but all have individual differences independent of other factors that may change the cohesion of the sediment. Historically, physical and geochemical factors were viewed as most important [189, 190] in controlling sediment dynamics, partly due to the difficulty in categorising and quantifying biogenic influences [191], but the influence of biology on sediment stability such as the actions of bacteria [151, 152] diatoms [192, 193], invertebrates [194], and macrofauna [195] has been demonstrated, and the importance of micro-organisms that mediate transport pathways, known as 'ecosystem engineers', was recognised [181, 196]. As previously discussed (1.10.3), EPS considerably increases erosion resistance and is one of the major driving forces in intertidal sediment stability.

Table 1.2 Factors effecting sediment erodibility, after Grabowski et al. (2011).

Physical Factors	Geochemical Factors	Biological Factors
Particle Size	Clay Mineralogy	Disturbance
Particle Size Distribution	Water Chemistry	Feeding and Egestion
Bulk Density/ Water Content	Organic Content	Biogenic Structures
Temperature	Salinity	EPS and Biofilms

Effects of macrobiota on sediment stability can be defined as stabilisation, destabilisation, or bioturbation (a change in sediment structure that can stabilise or destabilise the sediment) [197]. Stabilising influences include: sediment compaction and increased drainage as a cause of burrowing networks; increase in sediment EPS content; induction of skimming flow through extension of feeding tubes into the water column; deposition of sediment through faeces and pseudofaeces of filter-feeders; and flattening the surface of the sediment to reduce near-bed turbulence [197]. Destabilising effects include blistering, where air is trapped beneath a biofilm surface, giving it buoyancy that pulls it from the sediment surface, burrowing of invertebrates to loosen sediment, and the increase of bed roughness through surface disturbance that increases boudnary turbulence, increasing erosion [197]. Macrobiota can cause destabilisation through grazing [197, 198], and through increasing water content and predation of diatoms, and decreasing micro-topography [195]. Decreased populations of oligochaetes, *Nereis diversicolor*, and other meiofauna can cause a 300 % increase in sediment stability [195].

Sediment cohesion increases with increasing salinity, as does the stabilising effect of EPS due to the high ionic concentrations. Low salinities (<1 PSU) such as freshwater cause clay particles to be dispersed, whereas salinities occurring within estuaries and beyond (>2-3 PSU) cause particle flocculation [199] as the double layer of counterions are compressed allowing the repulsion force to be overcome by the attracting Van der Waals forces [200]. High salinity increases the cohesive effect of EPS through counterion compression [201] as the increase in ionic strength results in higher availability of cations for adsorption [202]. Rainfall also has direct influence upon sediment stability, with simulated rainfall reducing erosion thresholds through surface disruption, and changing biogeochemical properties such as electrolyte distribution, and chlorophyll and carbohydrate contents [203].

1.12 Study sites

1.12.1 Ythan estuary

The Ythan estuary is situated approximately halfway between the city of Aberdeen, and the town of Peterhead on the North East coast of Scotland (NK 00304 2621) (Fig. 1.4). The estuary has been described as a shallow, tidally driven, well mixed estuary [204]. The estimates of the flushing time of the estuary vary between 1.15 tidal cycles [204] 6.5 days [205], and 5-12 days [206]. The lower estimate of 1.15 days was justified by the low amount of freshwater entering the estuary compared to the strong tides encountered in the estuary [204].

The Ythan estuary catchment is estimated between 685 km^2 [207] and 760 km^2 [204] and is predominantly of mixed agricultural land, consisting of arable or grazing farmland, with areas of forestry [208]. The contribution of the Ythan River to the total freshwater discharge of the estuary is approximately 80 % [204], with an average flow of 8.1 $m^3 s^{-1}$ (mean of data collected 1984-2008) [208]. There are four major tributaries to the Ythan estuary excluding the main river channel. The largest of which is the Foveran Burn with a mean flow of 0.55 $m^3 s^{-1}$, followed closely by the Tarty and Forvie Burns at 0.4 $m^3 s^{-1}$, and the smaller at Auchmahoy Burn 0.23 $m^3 s^{-1}$ (figures calculated from the Low Flows 2000 model) [208]. There are no large feeder lochs in the catchment, so the water level of the river is heavily dependent on rainfall.

The area typically experiences 800 mm of rainfall which is relatively low for Britain, with an average summer temperature of 14 °C and an average winter temperature of 3.2 °C [209].

High wind speeds in excess of Gale Force 5 are common, and often from a southerly direction, which forces extra water inside the estuary creating conditions favourable to the resuspension of intertidal sediments and erosion of intertidal flats.

The area of the intertidal sediments has been estimated at 1.85 km^2, with the estuary typically being ~300 m wide, with the widest point being at the Sleek of Tarty at 620 m [204]. The tidal range in the Ythan estuary has been estimated to be between 8 km [204] and 10 km [207] from the mouth of the river, approximately up to the town of Ellon, but has been shown to vary with seasonal differences of rainfall [204]. To describe the estuary, it was divided into three distinct sections by Leach [204]; the lower ~1.5 km stretch is characterised by high salinities, high currents and intertidal sediments being dominated by sand and mussel beds. The middle ~5.5 km stretch between the Foveran Burn and 500 m upstream of the Forvie Burn is characterised by a variable salinities present and slower currents allowing large mudflats to develop. The Upper stretch of the estuary from 500 m upstream of the Forvie Burn upwards to the tidal reach is characterised by a narrower estuary boundary, with slow currents and low salinities.

The highest freshwater contributor of suspended sediments to the estuary is the Ythan River at 66 % of all freshwater inputs [205]. The highest contributing tributary of suspended sediments from freshwater is the Auchmacoy Burn at 13 %, followed by the Forvie Burn at 10 %, the Foveran Burn at 6 %, and the Tarty Burn at 5 % [205]. Particulate organic matter entering the estuary has been shown to be primarily of marine origin [204].

Sedimentation rates within the estuary have been reported to be over 4 g m^{-2} $hour^{-1}$ at sites in the lower estuary, and between 0.15 and 0.7 g m^{-2} $hour^{-1}$ at sites between Newburgh Quay and the Logie Buchan Bridge [205]. The higher rate of sedimentation at sites in the lower reaches of the estuary were due to the sediment settling being of a medium sand, compared to the finer sediments that settled in the upper estuary. The intertidal flats on the South bank of the estuary are much more extensive than the North bank. This has been reported to be a result of the hydrology of the estuary directing suspended sediments during the tidal cycle towards the South bank [205].

The catchment supports up to 50,000 waterfowl in winter, including ~17,000 Pink-footed Geese, ~5000 Eider ducks, and >1200 Terns of mixed species visiting a breeding site on the North bank near the estuary mouth each year [209, 210]. A large colony of ~1000 Grey and

Common Seals reside at the estuary mouth, with smaller sub-colonies inhabiting the lower reaches of the estuary on the North bank. As a result of the biodiversity found in the estuary and its surrounding area, the site is designated as a National Nature Reserve (NNR) of Scotland, a Special Area of Conservation (SAC), a wetland of international importance (RAMSAR site), a Site of Special Scientific Interest (SSSI), and a Special Protection Area (SPA) under the European Union Directive on the Conservation of Wild Birds [209]. The estuary is an important sea trout river, attracting ~200 day ticket anglers a year, and ~40 season ticket holders annually, and the area attracts 15,000-20,000 visitors each year, and is a regular dog walking site [209].

The Ythan Catchment was declared a Nitrate Vulnerable Zone (NVZ) under the EU Nitrates Directive in 2000 [208] and this continues to be in place in 2016. Considerable research has been performed on the nutrient distributions of the Ythan estuary [131, 206, 208, 211], with the work on the eutrophication of the estuary by the Raffaelli group at Aberdeen University [212-215] contributing significantly to the declaration of the NVZ and the subsequent protection of the estuary. Macroalgal blooms (Fig. 1.3) occur seasonally at both the Ythan and Eden estuaries. These blooms, that can be increased in frequency and severity by eutrophication [216], are traditionally viewed as imparting a negative effect on invertebrates [217, 218], specifically *Corophium* sp, inhabiting the mudflats. This in turn has a detrimental effect on the wildfowl feeding within the estuary [215]. However, as Lyons et al. (2014) discuss, the complete ecosystem effect of macroalgal blooms is uncertain as, depending on algal species and underlying habitat, they can sometimes increase abundance and species richness of organisms by increasing habitat complexity, creating shelter and providing sustenance for grazers [216].

Figure 1.3 Seasonal macroalgal bloom in the Ythan estuary.

There are many sources of possible faecal contamination within the Ythan catchment. There are 14 wastewater treatment plants in the extended catchment which, depending on their efficiency, may contribute to faecal indicator organisms present in the estuary. The Ythan catchment is a very rural area, resulting in many houses running private water supplies and therefore domestic sewage treatment systems. Again, depending on their efficiency, they may also contribute towards the total FIOs present in the estuary. There are also many sources of diffuse contamination within the Ythan catchment; 5.3 km^2 of farmland was spread with sewage sludge in 2009, with most of the fields draining directly into the Ythan estuary via the Tarty and Foveran burn tributaries [208]. The relatively high number of waterfowl, seals and dog-walkers visiting the estuary will all, albeit unavoidably, contribute to the load of faecal indicator organisms in the estuary. The closest regularly sampled SEPA-designated bathing water is Collieston, 5 km North of the mouth of the Ythan estuary, which was designated as a bathing water in the 2014-2015 report achieving a 'Mandatory' level of bathing water safety from SEPA (<2000 CFU faecal coliforms 100 ml^{-1}) [219], and a 'Good' (250-500 CFU *E. coli* 100 ml^{-1}) in 2016 [220]. Balmedie, to the south of the estuary between the Ythan estuary and Aberdeen City has achieved the 'Guideline' (<100 CFU faecal coliforms 100 ml^{-1}) or 'Mandatory' level over the last 11 years [219], with a 'Good' in 2016 [220].

The Ythan estuary has long been a study site for biodiversity and ecosystem ecology [131, 204, 211, 213, 221, 222] and as a result is 'one of the best-documented catchments in the UK' [223].

Figure 1.4 Study sites used in this thesis. Blue circle- Ythan estuary, Red circle- Eden estuary.

1.12.2 Eden estuary

The Eden estuary is situated approximately 120 km South of the Ythan estuary between the town of St Andrews and the City of Dundee (NO 48288 19319) and is located 10 km South of the much larger Tay estuary (NO 47738 29771) (Fig. 1.4). The Eden estuary has been described as a tidally-driven shallow estuary [224, 225]. The catchment is mainly agricultural land [201] and covers approximately 307 km^2 [225], with approximately 76 % of the catchment reported to be 'prime agricultural land' [226]. Under average flow conditions, the estuary is 'vertically homogenous', and partially mixed when under periods of high rainfall [225].

The tidal range of the estuary is approximately 7 km to the West of the mouth of the estuary, although the low tide channel meanders both North and South down the estuary to create a ~9 km long channel. At the widest point, the estuary is 2 km wide just inside the mouth of the

estuary. Further upstream there is a well-developed sandy spit forming a narrowing of 500 m in the estuary 3.5 km from the mouth, with the estuary widening again to 1 km. Five km from the mouth, the estuary narrows to a width of 80 m to 20 m at the tidal limit. The intertidal area of the estuary is comprised of approximately 8 km^2 of mudflats, and 0.11 km^2 of saltmarsh [225].

The mean freshwater input from the river Eden is approximately 2 m^3 s^{-1} [224], with high precipitation in winter increasing the discharge up to 5.5 m^3 s^{-1} [225]. Data collated by Eastwood (1977) [225] showed the contribution of freshwater to the estuary from the river Eden to be highly dependent on rainfall. There is one major tributary entering the Eden estuary. The Motray Water stream enters ~4.75 km from the mouth of the estuary at Guardbridge. The catchment for this tributary is approximately 52 km^2 [225]. Motray water had a mean contribution of freshwater to the estuary of 0.38 m^3 s^{-1} between October 1969 and September 1972 [225]. The closest weather station to the Eden estuary is at Leuchars. Between 1981-2010, the average annual rainfall was 691 mm [227].

The estuary can be divided into 3 sections [225]. The lower section from the sea to a small spit (Sanctuary Spit) on the North bank is characterised by open sandflats often exposed to high salinities and more severe weather from the open sea. The middle section from Sanctuary Spit to Guardbridge is more sheltered with extensive hard-packed mudflats and cockle beds with a large North facing spit known as Coble Shore (Fig 1.5). The upper section from Guardbridge to the tidal limit is very sheltered, with low salinities and mudflats with a high water content. At low tide, the river channel is approximately 100m wide in the middle part of the estuary, leaving almost 1 km of mudflats from both the North and South banks to the river channel. Generally, the south bank has sediments with a coarser grain size than the north bank as it is more exposed to prevailing weather [225]. The movement of sediment within the estuary is dominated by bedload transport, and has been shown to be seasonally-dependant, with higher suspended sediment levels in winter months corresponding to higher wave activity [224].

The estuary is designated as a SSSI, Local Nature Reserve (LNR), Special Area of Conservation (SPA) and a Special Protection Area (RAMSAR) site [228]. The area is also included in the Strathmore and Fife 'Nitrate Vulnerable Zone'. The West Sands beach, which forms the south bank of the mouth of the Eden estuary is the closest SEPA-designated bathing water to the estuary. In 2014-2015 it achieved the 'Guideline' level [219] and in 2016 achieved the 'Good' standard [220] from SEPA, however, it achieved only the 'Mandatory' level between 2011-

2014 [219]. Sources of possible faecal contamination are similar to that of the Ythan estuary, with the site being important for waterfowl and seals, although the absence of a sandy upper shore throughout the majority of the estuary restricts most visitors and dog-walkers to the outer estuary on West Sands.

Similarly to the Ythan estuary, the Eden estuary has historically been affected by eutrophication, with some research having been performed on its affects regarding seasonal macroalgal growth [228, 229]. The Eden estuary has recently been the focus of extensive research on the effect of macroalgal and microbial assemblages on sediment stability [181, 201, 230], and saltmarsh restoration as a coastal defence mechanism [231].

Figure 1.5 Looking North over the lower and mid-sections of the Eden estuary, with the Coble Shore spit in the foreground.

1.13 Thesis aims

As recognised by Burton et al. [88], difficulties in drawing comparisons between the large number of studies done on pathogen survival within the environment are encountered due to differences in physical, chemical and biological characteristics of the water, soils or sediments examined. This is still the case, with no widely accepted, validated method for bacterial enumeration of fecal bacteria or pathogens in different types of sediments, and many studies not analysing a full suite of sediment properties. Extensive field monitoring with comprehensive sediment and microbe analyses combined with focused laboratory experiments can help identify sediment-microbe associations and facilitate model development and water quality policy adjustments.

The erosion of cohesive sediments is surrounded by multifaceted mathematics [232], and is affected by many factors such as grain size, water content, salinity, pH, and porosity of the sediment [192], with strong correlations between sediment properties and cohesive strength often absent due to the complexity of the system [233]. This is further complicated with notoriously hard to quantify biogenic influences [197]. As Jamieson et al. [51] concluded, sediment-microbe interactions need to be monitored further and new data acquired so affects can be incorporated and developed into existing and new models, making them more useful as water quality monitoring tools.

In the first year-long field study, samples were collected from 4 distinct sediment types in the Ythan estuary every 4 weeks for 12 months. In the second field study, samples from estuary-long transects in the Ythan and Eden estuaries were collected seasonally. Samples from these two sampling campaigns were used to analyse the effect of environmental and sediment characteristics (Chapter 3) and changes in the native microbial community (Chapter 5) on *E. coli* abundance. The resuspension of *E. coli* due to low erosion resistance of sediments coinciding with high *E. coli* abundance was investigated in Chapter 4. The final experiment (Chapter 6) investigated the adhesion rates of *E. coli* to different types of suspended sediments to identify whether the prevalence of high *E. coli* abundance was partly caused by a preference of *E. coli* to adhere to certain types of sediments in suspension in higher abundance for these sediment types. The effect of *E. coli* strain characteristics on particle adhesion was also investigated in Chapter 6.

The aim of the research reported in this thesis was to increase understanding of the contribution of intertidal sediments to adverse water quality in terms of fecal bacteria

distribution in estuarine and coastal waters. This is achieved through year-long field studies of two estuaries, and a factorial laboratory experiment.

Questions addressed in this thesis:

1. Identify key physical, biogeochemical, biological and environmental factors influencing spatial and temporal variation in the abundance of faecal bacteria in intertidal sediments (Chapter 3).

   Hypotheses:

   a) **E. coli** ***abundance in the Ythan estuary can be predicted using sediment characteristics and environmental variables.***
   b) ***Explanatory models of the variation of*** **E. coli** ***with sediment characteristics and environmental variables are generic.***

2. Investigate whether intertidal sediments with a high risk of supplying a large number of faecal bacteria can be identified by combining erosion thresholds and *E. coli* abundance (Chapter 4).

   Hypotheses:

   a) ***Sediments that pose a risk to human health through easily-resuspendable faecal bacteria can be spatially and temporally identified by combining*** **E. coli** ***abundance and sediment stability measurements.***
   b) **E. coli** ***abundance in the overlying water will correlate with the abundance of*** **E. coli** ***in sediments.***

3. Determine whether or not *E. coli* abundance in intertidal sediments is affected by the native microbial community (Chapter 5).

   Hypotheses:

   a) The salinity gradient drives spatial variation in microbial species metrics (species abundance, diversity and evenness) in estuaries.
   b) Microbial community constituent composition is similar in the Ythan and Eden estuaries.
   c)* E. coli *abundance is affected by changes in microbial population metrics.
   d)* E. coli *abundance is affected by microbial community constituent composition.

4. Examine the role of zeta potential in the adhesion of *E. coli* to suspended intertidal sediments, and investigate how salinity, sediment characteristics and *E. coli* strain characteristics influence adhesion efficiency (Chapter 6).

   Hypotheses:

   a) ***Different* E. coli *strains will exhibit different zeta potential profiles over the salinity gradient.***
   b) ***Sediments will exhibit different zeta potential profiles over a salinity gradient***
   c) E. coli *strains will show different adhesion efficiencies with ionic strength (salinity).*
   d) E. coli *strains will show different efficiencies in adhesion to different sediment types.*
   e) ***The adhesion of* E. coli *cells to sediment particles can be explained by the zeta potential of the strain or sediment***.

2. Materials and methods

The methods defined here describe the materials, equipment and methodologies used in many of the sampling campaigns for this thesis. Methodologies relevant to specific chapters are described there in further detail.

2.1 Intertidal sediment collection

Sediment was sampled using a coring method similar to that of Lubarksy [234]. Twenty ml BD Discardit™ Eccentric Luer-Slip Two-Piece plastic disposable syringes (Fisher Scientific, UK) were cut off above the luer-slip tip (Fig. 2.1). 10 mm was measured from the end and marked. Polyethylene Snap Caps (Fisher Scientific, UK) were used to cap the syringe after a core was removed from the sediment surface. Syringe cores taken were 10 mm deep, and had a diameter of 20 mm, resulting in a core volume of 3.14 cm^3. Prior to sampling, the syringes and caps were machine washed, rinsed with 70 % ethanol and air-dried to ensure sterility for culture-based bacterial enumeration. Samples used for culture-based bacterial enumeration were stored at 4 °C before enumeration within 24 hours. Samples used for bulk density and subsequent analysis were stored at -20 °C.

Figure 2.1 Twenty ml cut-off syringe corers with caps. Each syringe contains 3.14 cm^3 of sediment sample ready for analysis.

Samples of a larger volume were required for the analyses of particle size distribution, colloidal carbohydrate and protein, organic carbon, total carbon and total nitrogen. Sediment to a depth of 10 mm was taken in a 50 ml centrifuge tube (Falcon™, Corning, NY, USA) and stored at -20 °C. Filled centrifuge tubes were defrosted slightly at room temperature before ejecting the contents into ziplock bags and stood upright in beakers and lyophilised for 48 hours.

2.2 Laser particle size analysis

Lyophilised samples were homogenised by hand inside the ziplock bag, and particle size analysis performed by laser diffraction with a Malvern Mastersizer 2000. Silica gel was used as a control with a median particle size of 220 μm. The sample was added to the water bath and sonicated for 30 seconds before the first analysis. Samples were analysed a minimum of twice, and repeatedly run until subsequent runs were satisfactorily alike. Particle size distribution was reported as proportion of fine particles (% fines), mean particle diameter (D (0.5)), and volume weighted mean particle diameter.

2.3 Organic and water content

Syringe cores were ejected into pre-weighed crucibles (Fig. 2.2). The crucibles were then weighed to allow calculation of bulk density (Equation 1). Crucibles were then oven dried at 105 °C for 24 hours and re-weighed to allow calculation of water content (Equation 2). The same crucibles were then ignited in a furnace at 450 °C for 12 hours and re-weighed to allow for calculation of organic content by loss on ignition (Equation 3). Except for the weighing of the initial core, samples were allowed to cool to room temperature in a desiccator before being weighed. Sediment cores were analysed in triplicate for each individual site.

Equation 1 $$\textbf{Bulk Density (g / cm}^3\textbf{)} = \textbf{Sed}_W \textbf{ / V}$$

Where Sed_W is the mass (g) of the wet sediment core and V is the core volume (3.14 cm^3).

Equation 2 $$\textbf{Water Content (\%)} = (\textbf{Sed}_W - \textbf{Sed}_D) / \textbf{Sed}_W) * 100$$

Where Sed_W is the mass (g) of the wet sediment core and Sed_D is the mass (g) of the sediment core post-drying.

Equation 3 $$\textbf{Organic Content (\%)} = (\textbf{Sed}_D - \textbf{Sed}_I) / \textbf{Sed}_D) * 100$$

Where Sed_D is the mass (g) of the sediment core post-drying and Sed_I is the mass (g) of the sediment core post-ignition.

Figure 2.2 Crucibles containing syringe corers after oven drying at 105 °C for 24 hours.

2.4 Total carbon, total nitrogen and organic carbon analysis

Lyophilised sediments were milled in grinding vessels with 2 zirconium milling balls loaded onto a Retsch Mixer Mill 200 (Retche, Germany) and milled at 60 % power (vibrational frequency ~900 min^{-1}) for 3 minutes. Samples were submitted to The James Hutton Institute Analytical Services for elemental analysis, and analysed using an Elemental Analyser FlashEA 1112 Series (Thermo Fisher Scientific, USA). Briefly, the amount of total carbon and total nitrogen were obtained by weighing 15 mg of milled sediment into a tin capsule dropped into a combustion reactor at 900 °C where a 'flash reaction' occurs raising the temperature to ~2000 °C. The products of the combustion are carried by a flow of helium through an oxidation catalyst, copper oxide and platinised aluminium oxide. CO_2, N_2, NO_x and H_2O are then carried into a reduction reactor containing copper wires at 680 °C, where NO_x is converted to N_2 and oxygen removed and then H_2O is removed by absorption by $Mg(ClO_4)_2$. A chromatographic column at 40 °C separates CO_2 and N_2, of which the amounts are determined with a thermal conductivity detector. To obtain the amount of organic carbon, a subset of samples were pre-treated with 0.5 M HCl and dried at 50 °C to remove calcium carbonate before proceeding with the same method as total carbon. The amount of the pre-treated sample subtracted from the un-treated sample to obtain the amount of organic carbon.

2.5 Extracellular polymeric substance (EPS) analysis

There is no singular established method of sediment sampling and storage for EPS analysis due to differences and preferences in sampling strategy, nor is there a single method of quantifying

all components of EPS. Samples analysed for this project were lyophilised, so both intracellular and extracellular carbohydrates and proteins are included in the measurement [156]. EPS that can be easily extracted from the lyophilised sediments using distilled water are termed colloidal carbohydrates [156]. Extraction with cation exchange resin [235] would extract more intracellular EPS and also that which is more tightly bound to sediment particles.

The Dubois, or phenol-sulphuric, assay [236] can only be used as a measure to show relative amounts of carbohydrate within sediment samples that can then only be expressed in relative terms to a single carbohydrate [237]. The assay detects not only carbohydrates that form part of the colloidal EPS, but almost every specie of mono-, di-, oligo-, or poly-saccharide [237] found in the sample. The carbohydrates are cleaved by the concentrated sulphuric acid and dehydrated to form furfural and hydroxymethyl furfural that then react with the phenol to cause a dark yellow product (Fig. 2.3A).

The Lowry procedure is a reaction based on the number of peptide bonds in protein, so can be used as an accurate measure of the amount of protein in a sample, expressed as bovine serum albumin equivalents. Peptide bonds in the proteins form a copper ion complex that, under alkaline conditions, creates reduced copper in a reaction known as the Biuret chromophore. The product of this reaction is then stabilised by $Na_2C_4H_4O_6$ [238]. This copper-peptide complex then reduces the Folin and Ciocalteu's reagent to create a blue product [239](Fig. 2.3B).

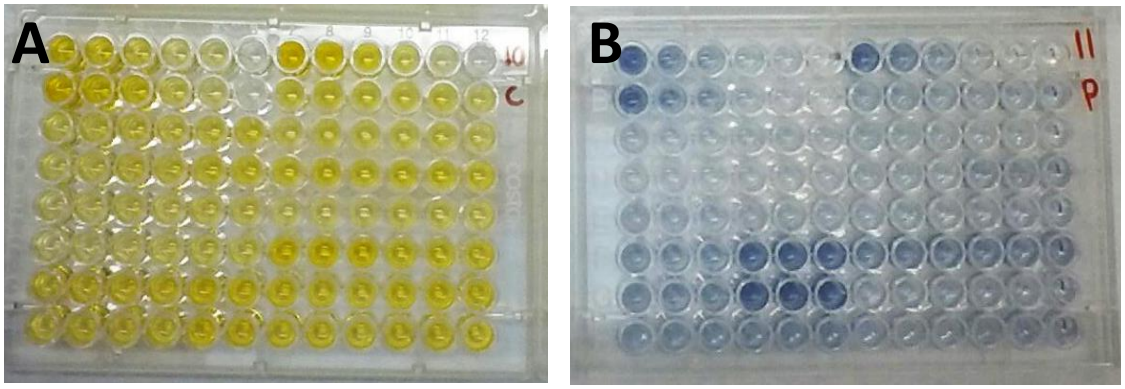

Figure 2.3 Optically clear 96 well plates containing completed reactions of the colloidal carbohydrate (A), and colloidal protein (B) analysis.

2.5.1 Colloidal EPS extraction

Six hundred µl of deionised (DI) H_2O was added to an accurately weighed quantity of lyophilised bulk sediment sample in a 1.5 ml Eppendorf tube. The quantity of sample depended on a visual analysis of grain size and therefore an EPS concentration estimate; approximate quantities used for each sediment type were 250 mg for fine grained mud, 300 mg for mixed samples, and 350 mg for sand. Samples with a larger particle size typically contained lower amounts of EPS. Samples were incubated for 30 mins at room temperature, vortexing thoroughly every 10 mins. Samples were then centrifuged at 6200 x g for 10 mins at room temperature (Eppendorf Minispin Plus, Eppendorf, Germany), and 400 µl of the supernatant containing the water soluble EPS was removed and stored in a clean 1.5 ml Eppendorf tube at 4 °C.

2.5.2 Standard curve construction

Standard curves were constructed from a group of standards run as part of each 96-well plate for both the carbohydrate and protein assays. For carbohydrates, the standard curve was created from 3 replicates of glucose (Fisher Scientific, UK, Cat. No G/0500/53) solutions. For proteins, 3 replicates of solutions of lyophilised bovine serum albumin (Sigma-Aldrich, UK, Cat. No A2153) were used. Standards of 0, 50, 100, 200, 300, 500 µg ml^{-1} in DI H_2O were used for both assays, created from a 1 mg ml^{-1} stock. A standard curve equation was constructed for each plate and the amount of carbohydrate or protein in each sample on the particular plate calculated from this using the following equation (Equation 4).

Equation 4 $$\textbf{Colloidal EPS (µg g}^{-1}\textbf{)} = \textbf{(((Abs-}B\textbf{) / }M\textbf{) / Sed}_D\textbf{) * 0.6}$$

Where colloidal EPS is colloidal carbohydrates and colloidal protein contents. Units of EPS are glucose and bovine serum albumin equivalents per gram of dry sediment, and Abs is absorbance at 486 nm and 750 nm for carbohydrates and proteins respectively. *B* is the constant, and *M* the gradient of the standard curve constructed for each individual plate. Sed_D is the weight of dry sediment used in the extraction procedure. The results were then multiplied by 0.6 to normalise sample data to the same numerical units as the standard solutions.

2.5.3 Colloidal carbohydrate analysis

The original method [236], modified by Taylor and Paterson [230] to produce the concentration and ratio of reagents used here, is further adapted for use in 96-well plates for high throughput of samples in a similar manner to Masuko et al.[240].

In an optically clear 96 well plate (Costar 3599, Corning, NY, USA), 35.7 µl of each sample supernatant or glucose standard was pipetted into triplicate wells. Then, column by column, 35.7 µl of 5% w/v phenol (Sigma-Aldrich, Cat. No. P1037) was pipetted via multi-channel pipette, immediately followed by 178.6 µl of concentrated sulphuric acid (BDH, UK) and mixed via pipetting. The plates were then incubated for 35 min at 30 °C and absorbance determined at 486 nm using a 96-well spectrophotometer (SpectraMax 190 Microplate Reader, Molecular Devices, CA, USA). Colloidal carbohydrate concentrations are presented as µg g^{-1} glucose equivalents per gram of dry sediment.

2.5.4 Colloidal protein analysis

The modified Lowry procedure of Raunkjaer *et al.* [241] was adapted for use in 96 wells plates, whilst the concentrations and ratio of reagents remained unchanged.

The working reagent was created by combining a 143 mM NaOH (Fisher Scientific, UK, Cat. No S/4920/53), 270 mM Na_2CO_3 (BDH, UK) solution with 57 mM $CuSO_4$ (Fisher Scientific, UK, Cat. No C/8600/50), and 124mM $Na_2C_4H_4O_6$ (Sigma-Aldrich, UK, Cat. No 71995) in a 100:1:1 ratio. Forty eight µl of each sample supernatant or standard was pipetted into triplicate wells of a 96 well plate. Forty eight µl of SDS 2% (Sigma-Aldrich, UK, Cat. No L3771) was added [235] and plates incubated for 15 minutes at room temperature in order to lineate the extracted proteins. After incubation, 134.5 µl of the working reagent was added to each well, followed by 19.5 µl of Folin and Ciocalteu's reagent (Sigma-Aldrich, UK, Cat. No F9252) (diluted 5:6 with DI H_2O) and mixed via pipetting. The plates were then incubated for 45 min at 30 °C and absorbance determined at 750 nm using a 96-well spectrophotometer. Colloidal protein concentrations are presented as µg g^{-1} bovine serum albumin equivalents.

2.6 Erosion resistance of sediments

2.6.1 Sediment stability: cohesive strength meter

The surface sediment stability was measured using the cohesive strength meter (CSM) (Fig. 2.4). The CSM was conceptualised as a device to determine the threshold of surface erosion by Paterson 1989 [192] and amended by Tolhurst et al. 1999 [242]. The device works on the principle that a more cohesive sediment is more resistant to erosion from a jet of water impacting the sediment surface, the force of which can be monitored and adjusted using the CSM interface.

The CSM head (Fig. 2.4), a watertight chamber 30 mm in diameter is placed on the sediment surface and held securely by a boss and clamp on a retort stand with the base removed, and the rod pushed ~20 cm into the sediment. The chamber is then filled with filtered seawater via a small opening on top of the chamber using a laboratory wash bottle. Filtered seawater is used as the ionic strength of water has implications for flocculation and cohesion of the sediment, the principles of which are discussed further in Chapter 1 (Section 1.11). Transmission of light is measured across the chamber, and this value is then used as a baseline for measuring the structural failure of the sediment surface. Filtered seawater is pressurised by the CSM unit, and pulses of water are jetted from the outlet inside the chamber towards the sediment surface. When the force of this jet is large enough to disturb the sediment surface, particles that are forced into suspension cause a decrease in the infrared light transmission across the chamber. When this declines below 10 % of the initial transmission, viewed as the critical erosion threshold, the force of the corresponding water jet to cause the surface failure is expressed as a stagnation pressure (N m^{-2}) at the sediment surface.

A calibration curve was constructed in order to convert the jet pressure to stagnation pressure [243]. The CSM head was suspended over a glass beaker on a balance. The Fine 1 programme was selected and executed, with the weight of each jet of water recorded using the balance. 5 replicates of the run were performed, and the average of each jet weight calculated. The average jet weight was calculated following the equation provided by Vardy et al. (2007).

Four replicate CSM measurements were taken at each individual sampling site. The most sensitive CSM programme, ‘Fine 1’, was used for the majority of the work to give the highest resolution at low cohesive strengths due to the thixotropic nature of some of the sediments involved. Several of the coarse grained sand sediments were too porous to enable filling of the

chamber so recordings were not taken. This can be overcome by removing sediment intact into a container and filling with water up to the sediment surface before performing the above method, but due to sampling time constraints this was not performed during this study.

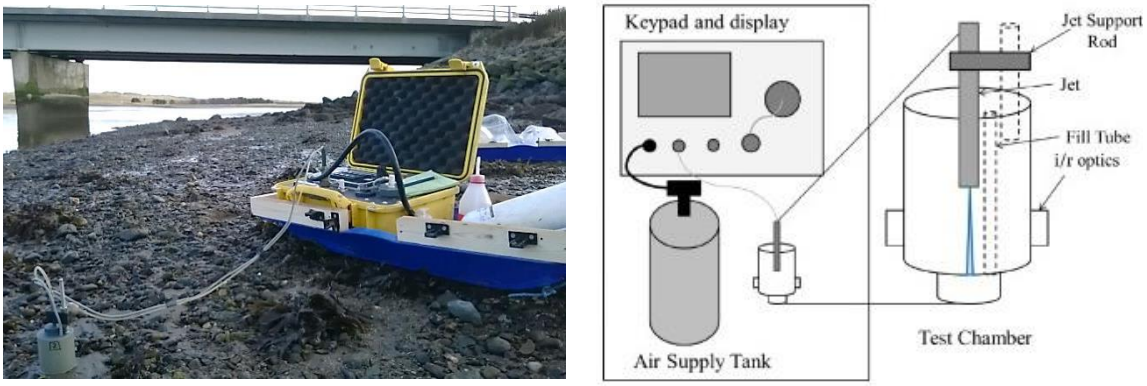

Figure 2.4 The Cohesive Strength Meter being used on a small area of cohesive sediment in the Ythan estuary (left), and a schematic of the CSM and test chamber components (right) from Singh and Thompson (2016) [244].

2.6.2 Sediment shear strength: shear vane

Sediment bed stability was measured using a handheld shear vane (Geonor, Augusta, New Jersey, USA). The widest vane available (50 mm x 12 mm) was used as low shear strengths were expected. The vane was pushed vertically into the sediment surface until the top of the vane was level with the sediment surface (depth of 50 mm). The handle was then turned clockwise at a rate of 1 rpm. When the sediment bed failed and the vane turned in the sediment, the reading on the collar of the shear vane was recorded and the collar reset. Four shear vane replicate measurements were taken at each individual sampling site and the results recorded in kPa.

2.7 Interstitial water pH and salinity

A compression method was employed in the field to separate the interstitial water phase from the sediment. Alternative methods such as centrifugation are available [245, 246], but as many samples must be taken in each sampling campaign, large weights of sediment would have to be retrieved to the laboratory. To combat any change to the porewater chemistry as a result of

oxygenation and light exposure from the method, samples were stored immediately on return to the laboratory in the dark at 4 °C, and the pH and salinity determined within 24 hours.

To sample the interstitial water of sediments, roughly 500 g of sediment was scraped with a clean pipette box lid to a depth of 10 mm. This was placed in a 0.25 mm aperture plastic mesh bag, and the bag squeezed by hand over a funnel draining into a 50 ml falcon tube. In sediment with standing surface water, the initial flow of water through the mesh was discarded. Multiple scrapes of sediment were necessary in sediments with low water content (i.e. sands) in order to fill the falcon tube to a sufficient volume for analysis (~25 ml). The pH and salinity of the interstitial water sample was determined using a Hach HQ40d multi-probe (Hach, CO, USA) within 36 hours.

2.8 Culture-based enumeration of FIOs from intertidal sediments

To determine coliform and *E. coli* concentration in sediments, 3 adjacent syringe cores were homogenised together to form a sample. On return to the laboratory, between 1 and 8 g were weighed into 100 ml sterile vessels. The quantity of sample depended on a visual analysis of grain size and therefore a coliform and *E. coli* abundance estimate; approximate quantities used were 1-3 g for fine grained mud, 2-6 g for mixed samples, and >6 g for sand. Seventy ml sterile Phosphate Buffered Solution (PBS) (137 mM NaCl (Fisherbrand, Fisher Scientific, UK), 2.7 mM KCl (BDH, UK), 4.3 mM $Na_2HPO_4.7H_2O$ (BDH, UK), and 1.4 mM KH_2PO_4 (BDH, UK)) was added, and the vessel hand shaken at the equivalent of a reciprocal shaker at 30 cm and 120 rpm for 1 minute. Vessels were left to settle for 1 h and 30 ml off supernatant removed via pipette. This was combined with 70 ml of fresh PBS and one snap-pack of IDEXX Colilert-18 reagent (IDEXX Laboratories, Westbrook, Maine, USA). Once the reagent had dissolved completely, the solution was poured into IDEXX Quanti-Tray/2000 (IDEXX), sealed with the Quanti-tray sealer (IDEXX) and incubated for 18-24 hours. After incubation, positive wells for coliforms (yellow) and E. coli (fluorescent under UV light) were counted and the IDEXX Quanti-Tray/2000 most probable number (MPN) table used to calculate MPN of colony forming units (CFUs) of coliforms and *E. coli* per 100 g of wet sediment using Equation 5. This value was then adjusted for 100 g dry weight sediment by using the mean water content for each sample location.

Equation 5 **MPN / 100 g Wet Sediment (CFU) = (((MPN / 30) * 100) / Sed_W) * 100**

Where MPN is the most probable number of coliform / *E. coli* CFUs per tray according to the IDEXX Quanti-Tray/2000 MPN table and Sed_W is the mass (g) of the wet sediment.

2.9 Retrieval of environmental data

Tidal amplitude data were retrieved from www.tidetimes.org, from data reproduced from the UK Hydrographic Office. Precipitation, air temperature and minimum grass temperature data were obtained from the Midas database held at the British Atmospheric Data Centre (BADC). The minimum grass temperature data were the lowest temperature read overnight by a thermometer touching short grass. This reading was incorporated into the analysis as the closest proxy for sediment surface temperature. For the Ythan estuary, sampling station 14887 at Esslemont House, Aberdeenshire, was used for precipitation data, and the air and minimum grass temperature from station 161 at Dyce, Aberdeenshire. For the Eden estuary, sampling station 15390 at St Andrews, Fife, was used for precipitation data, and temperature data from station 235 at Leuchars, Fife.

2.10 Field sampling designs

2.10.1 Intensively sampled sediments in the Ythan estuary

Several areas of the Ythan estuary were visually inspected to select areas with differing visual characteristics and that were known to be of a particle size distribution that remains consistent for long periods of time. Four sites were required, a sediment with high water content and consistently small particle size (mud), a sediment that had a small particle size, but with an element of larger particle sizes (mixed mud), a sediment with larger particle size distribution, yet still contained a proportion of smaller particles (mixed sand), and a sediment with large particle sizes akin to beach sand but was positioned well within the estuary (sand) (Fig. 2.5). Once suitable sites were located, a 15 x 15 metre box was centred over the site using ArcGIS (ArcMap, ed. 10.2.1. ESRI, CA, USA), and the 'create random points' programme within data management tools was used to create 6 random sampling points within the box with a minimum allowed distance of 2.5 metres between points to create 6 sampling sites for each

sediment type. The sampling sites were then located in the field and marked with a cane. Real Time Kinematic GPS, which has an accuracy of 3-4 cm, was used to position the sites as conventional handheld GPS would not allow the resolution needed to relocate sites in the case that site markers were removed by adverse weather conditions.

Figure 2.5 The location of the four intensively sampled sediment types in the Ythan estuary.

2.10.2 Seasonal transect sampling in the Ythan and Eden estuaries

Using ArcGIS (ArcMap, ed. 10.2.1. ESRI, CA, USA.), a line was traced over the MHWS and MLWS on the south side of the Ythan and Eden estuaries from the tidal extent to the mouth of the estuary. Both the MHWS and the MLWS was split into 13 equal segments using the split tool. The grid references of the 14 points created were exported and a new grid reference produced that was 20 % of the distance from each of the 14 points on the MHWS linearly towards the corresponding MLWS point. This created 14 sampling sites on each estuary that were roughly

evenly spaced down the estuary and were far enough from the MHWS mark to be in an area of sediment that would be covered by the tide during neap tides (maps of sites can be found in Chapter 5 (Section 5.3.3). The sites were then located in the field using GPS. No markers were left at the transect sites as several were in exposed positions, and as the sampling was conducted several months apart their continued presence could not be relied upon. The study of Zetsche et al. [207] at the Ythan estuary analysed light and temperature data every 2 weeks between May 2007 and May 2008 in order to determine season boundaries. The authors suggest the seasonal boundaries for the site were: spring- Mid-April to end of June; summer- July to Mid-September; autumn- Mid-September to Mid-November and an extended winter period of Mid-November to Mid-April. These seasonal boundaries are referred to throughout the thesis.

3. The effect of environmental and sediment characteristics on the spatial and temporal distribution of *E. coli* in intertidal sediments

3.1 Introduction

3.1.1 Current water monitoring

Current water quality monitoring, in accordance with microbial water quality regulations (focussed primarily on bathing waters), does not take into account the presence of pathogens and indicators of fecal contamination in river or estuarine sediments because samples are only taken from overlying waters. This is despite increasing evidence suggesting the resuspension or release of *E. coli* from underlying sediments influences waterborne concentrations [247]. Understanding FIO distribution in sediments could provide an improved understanding of microbial pollution, and it is important to ensure that sampling is effective and representative. Sediment characteristics need to be comprehensively analysed in combination with FIO loading as they will influence FIO distribution among depositional habitats between freshwater and coastal sites. There is a necessity for further assessing the ecology and survival of FIOs and pathogens in sediments and sediment-associated transport in order to fully characterise potential risks to water quality and public health [28, 81].

As discussed in Section 1.2, faecally-associated bacteria enter the environment through point sources and non-point (diffuse) sources. When faecal contamination is delivered to water it is transported down the catchment, ultimately reaching estuaries. The dynamic environment of an estuary presents many opportunities for sedimentation and resuspension of faecal bacteria, increasing contaminant persistence within waterways.

3.1.2 E. coli *abundance in intertidal sediments*

Sediments act as a reservoir for bacteria, including human pathogens, with freshwater and marine sediments containing up to 4 times the number of coliforms than overlying water [19-22] with faecal coliforms recorded at concentrations up to 1.6×10^5 MPN 100 ml^{-1} in brackish sediments [77]. Bacteria also adhere to particles in the water column as they provide a substratum increasing protection and enhancing their survival; numbers of human pathogens are enriched several-fold when associated with suspended flocculated particulates compared to the surrounding water [23].

Pathogen persistence has been generalised by many authors as being a first order inactivation constant [82], however the exact value of Kd^{-1} varies considerably between species, and is affected by temperature and nutrient availability [82]. Enteric bacteria have however been shown to reproduce in autoclaved seawater amended with autoclaved sediment [77], although genetic fingerprinting has shown that in the sediment and water system in Lake Michigan (IL, USA), *E. coli* were more likely to accumulate and persist rather than replicate in the environment [91].

Many studies have demonstrated the ability of faecal bacteria to persist in the environment for prolonged time periods of up to several weeks, despite multiple stressors [11]. This, and more detailed information on various physical and biogeochemical variables that affect faecal indicator persistence in intertidal sediments has been previously discussed (Chapter 1). Briefly, extensive research has shown the persistence of faecal bacteria to be greater in sediments compared to the overlying water [77, 83, 84]. Many environmental variables relevant to both the sediment and interstitial water have been shown to affect the survival of faecal coliforms, including salinity [114], organic carbon [11], nutrient availability [88], particle size [11, 89], bulk density, acidity, exposure to light, temperature and the native microbiota [90]. Several of these variables have been reported to drive the distribution of total bacteria in intertidal sediments [248]. Many properties of intertidal sediments co-vary [248-252], with sediments of a smaller particle size distribution often correlating with increased organic matter and nutrient content, in addition to providing 'protective microhabitats' from protozoan grazing for bacteria [109].

High salinities have been shown to decrease the survival time of *E. coli* [115, 119] with the extent of the effect dependent on genetic traits of the cell [116]. Notably, the study of Carlucci and Pramer (1960) found a salinity equivalent to 8.75 practical salinity units (PSU) to be the optimal salinity for persistence of *E. coli*, with a sharp decrease in survival in higher salinities. Increased survival rates of *E. coli* have also been observed at lower pH (5 and 6) than 7 and above [114].

Environmental variables such as temperature and rainfall also affect the persistence of FIOs. FIO persistence is greater at lower environmental temperatures of river water [120], estuarine water [17] and sediments [77], suggested to be a result of accelerated bacterial die-off at higher temperatures compared to that of lower temperatures [118]. Lower FIO abundance in freshwater sediments during summer months compared to autumn, winter and spring have

been reported [21, 253]. Submerged estuarine sediments of a subtropical estuary were found to contain more faecal coliforms in August, December and February than May. Estuarine sediments in Northern California were also reported to contain an order of magnitude more FIOs during winter and spring. Periods of high rainfall flush faecal bacteria from the land to surface waters [125-127] where it can continue downstream. The first rainfall after a dry period also has a 'first flush' effect, creating higher FIO counts for the expected rainfall volume [130].

Parasitism and predation from indigenous microbiota have been found to decrease survival of *E. coli* in estuarine water [119, 145] and remains to be one of the most important factors involved in the decrease in non-native bacterial population abundance in sediments [143]. Extracellular polymeric substance (EPS), produced primarily by native microbiota, in a sediment provide a protective biofilm from environmental stresses such as temperature and light [153, 154]. The effect of EPS is therefore complex, as large amounts of EPS in sediment may indicate high numbers of indigenous microbiota; however the EPS itself provides may facilitate the survival of *E. coli*.

The sediment particle size of riverine and estuarine sediments has been reported to be one of the main drivers of spatial variability of FIOs, where abundance directly correlates with increasing proportions of finer particles [78, 247, 254-256]. However, it has been suggested that finer particle sizes may reduce water flow through bacterial biofilms in sediments [257], impeding biofilm production [258] and therefore exposing FIOs to environmental stress. Sediment particle size increases, with minor perturbations, towards the mouth of the estuary [27], therefore FIO abundance in estuaries is generally inversely correlated with the salinity gradient. This creates difficulties in separating the effect of particle size and the effect of salinity stress and dilution of FIOs by sea water.

3.1.3 Models predicting **E. coli** *abundance*

For local governing bodies to monitor FIO abundance in intertidal sediments, direct enumeration of FIOs is both time consuming and requires access to hazard category II laboratories in order to culture FIOs. The creation of a model based on easily measurable sediment characteristics and widely available online environmental data that effectively

predicts FIO abundance in intertidal sediments would allow for low-cost, fast-turnaround assessment of bathing water safety risk.

Models concerning the effect of aquatic sediments in the transport and die-off of FIOs were extensively reviewed by Pachepsky and Shelton (2011). The widely utilised Soil and Water Assessment Tool (SWAT), a watershed-scale model primarily used for assessment of hydrological and diffuse-pollution based problems [259], has been modified to incorporate modelling of FIO die-off rates in soil and water in order to predict FIO abundance in water [260]. It has been further modified to integrate a bacterial transport submodel concerning the release and deposition of FIOs from streambed sediments, however uncertainty of FIO abundance in sediments were suggested to limit the performance of the model [261]. Further modification to the submodel incorporated the effect of solar radiation on FIO die-off rates [262], and a critical temperature parameter to introduce season-dependant growth and die-off of bacteria [263].

Several difficulties arise when predicting the contribution of FIOs from underlying sediments to the overlying water. The settling and resuspension of particles and associated *E. coli* is dynamic with several processes contributing, as well as the currently unexplored flux of *E. coli* to the water column without resuspension of the sediment [247]. In addition, predicting the concentration of *E. coli* resuspended from sediment during an erosion event is challenging, with no current model accounting for the spatial distribution of *E. coli* within sediments and the resulting differential release into the water column.

The key to prediction of waterborne *E. coli* abundance may lie in successfully predicting the load of *E. coli* in sediments, combined with the likelihood of sediment resuspension (Chapter 4).

3.1.4 Aims and hypotheses

The overall aim of this chapter was to identify key driving factors that influence the spatial and temporal variation in the abundance of faecal bacteria in intertidal sediments. This was achieved through the enumeration of *E. coli* in conjunction with a wide range of physical, biogeochemical, biological and environmental variables over several sampling regimes. Using these variables, models were constructed to predict *E. coli* abundance in intertidal sediments without the necessity for culture based enumeration. Site-specificity of the models was also investigated to evaluate the relevance of models to other estuarine systems.

The following hypotheses were tested in this chapter:

a) **E. coli** ***abundance in the Ythan estuary can be predicted using sediment characteristics and environmental variables.***

b) ***Explanatory models of the variation of*** **E. coli** ***with sediment characteristics and environmental variables are generic.***

3. 2 Materials and methods

3.2.1 Sediment collection and analysis

Samples from the field sampling designs introduced in Section 2.10 were analysed in this chapter. Sampling of the 'intensively sampled sites' (Section 2.10.1) was performed every 4 weeks commencing on 9.12.2013, and finishing 18.11.2014. Sampling of the seasonal transects (Section 2.10.2) were performed roughly every 13 weeks commencing 10.2.14, and finishing 1.12.14. Due to weather and tidal regime constraints, sampling was often performed over two, and, rarely, 3 consecutive days. The materials and methods used for all sediment analyses and retrieval of environmental data have been described in Chapter 2.

3.2.2 Statistical analyses

Data were prepared using Excel (Microsoft 2010, v14), and statistical analysis was performed in GenStat (VSN International, v17.1) unless otherwise stated.

Correlations between variables: Spearman's rank correlation coefficients were calculated for each pair of variables within each sampling regime in SPSS (v.22, IBM corporations). No data transformations were necessary for this non-parametric analysis. Significant correlations (p <0.05) were designated as: Rho= 0.000- ±0.249- weak; ±0.250- ±0.499- moderate; ±0.500- ±0.749- strong; ±0.750- 1.000- very strong.

Data transformation: In order to meet the assumptions of ANOVA and multiple linear regression, the data for colloidal carbohydrates, colloidal proteins, organic carbon, total carbon and total nitrogen were square root transformed. Total nitrogen data values below the detection limit (0.03 % w) was adjusted to 0.5 x minimum detection limit (0.015 % w).

Outliers: Suspiciously high CSM data for one data point was removed. The cause of this was likely to be a shell or debris preventing resuspension of sediment. Two data points were removed from water and organic content, assumed to be caused by the presence of macrofauna or errors made during the analysis.

Analysis of variance (ANOVA): One-way ANOVAs were performed for each variable using all site and season as factors individually. The one-way ANOVAs for site were blocked by season, and ANOVAs for season were blocked by site. Fisher's *post-hoc* protected LSD test was used to determine significant differences between treatments.

Two-way ANOVAs were performed for each variable using both site and season as factors. Missing data (< 5%) was estimated by using the general ANOVA function in Genstat. Estimated data values were inspected to ensure they were realistic and fitted the seasonal trend for the site. Means plots (performed in SigmaPlot 13.0, Systat Software Inc., CA, USA) of the two-way were plotted alongside the maximum-minimum least significant difference (max-min LSD) between means (calculated using Fisher's *post-hoc* protected LSD test). Due to imbalance in the dataset the LSD varies slightly between treatments, so a difference in treatment means only slightly larger than the max-min LSD may not indicate a significant difference, however, differences much larger than the max-min LSD are likely to be significant.

Best subsets and multiple stepwise linear regression models: Best subsets models were performed using the 'all-subsets regression-linear models' function. The response variate was *E. coli* abundance. The maximal model was limited to selected variables due to a maximum variable number constraint. Variables selected were those that had been observed in preliminary analyses to significantly explain variance in *E. coli* abundance individually, or performed well in preliminary best-subsets models within variable categories. 'All possible methods' of variable selection was used. The first and second best models for each number of terms are displayed in Table 3.3.1.

Multiple stepwise linear models were performed using the 'generalised linear models' function. The response variate was *E. coli* abundance. The maximal model included all variables (within categories for individual category models) except CSM measurements due to a high proportion of missing data for sediments with a large particle size. Stepwise selection was performed using adjusted R^2 as the selection criteria, leaving the model free to reject variables as a next step rather than only adding subsequent terms. Additional terms were not added to the model when the term was not significant (p= <0.05). Factorial site, season and site x season variables were added after the optimal model for each dataset was obtained in order to assess the success of the model to explain seasonal and site variation.

Model success: The models were compared by how much of the variability of *E. coli* abundance was explained (adjusted R^2). As the aim of the thesis was to investigate the effects of relatively easily obtained sediment characteristics and environmental variables, a model explaining variability >90 % (adjusted R^2= >0.90) is unlikely as there are other factors present that will affect *E. coli* variability. These include hydrodynamics that, especially in estuarine systems, constantly change due to differing tidal forces and input flow speeds and volumes.

Also, variation in the sources of *E. coli* for example due to farming practices and migratory wildlife will affect the total load of *E. coli* entering the estuary, and its relative distribution between tributaries. Therefore, a model that explains >70 % of the variability of *E. coli* within intertidal sediments can be viewed as useful as it demonstrates that these easily obtained variables give significant insight to the distribution of *E. coli.* Even models that explain 50 % of the variance demonstrate that sediment type heavily influences the distribution of *E. coli,* but half of the variability was not successfully captured with the variables measured, which may be improved by the incorporation of other sediment characteristics, or other external factors. Models that explain 30 % of the variability of *E. coli* do not satisfactorily explain the variability of *E. coli* abundance. However, if the model has overall significance, it does still indicate that the variables play a fairly major role in the distribution of *E. coli*, but further investigation is necessary to identify other factors to explain the larger proportion of unexplained variability. Models where specific categories of variables have been excluded, such as the physical variables model, will inherently have a lower adjusted R^2 than models where variables have not been intentionally excluded, and they should be interpreted as such. Where an adjusted R^2 of 0.20 would initially appear as a poor predictive model, it still explains 20 % of the variability using just these limited variables and therefore sheds insight into the variability of *E. coli* distribution.

Model efficiency: Trends within the predicted vs observed values were identified by simple scatter plots in SigmaPlot. The 1:1 line of equal predicted vs observed values was overlaid to identify whether observed data points were under or over predicted. Prediction of *E. coli* abundance using model parameter values for alternative datasets was performed within Excel, and the predicted and observed values then exported into Genstat where simple linear regression was performed to investigate the ability of models to predict *E. coli* abundance in different datasets.

3.3 Results

3.3.1 Seasonal and spatial trends of environmental and sediment characteristics

3.3.1.1 Physical sediment characteristics

The organic content and water content of sediments followed a similar trend with the greatest quantities of organic content observed at the Mud (M) site, followed by Mixed Mud (MM) > Mixed Sand (MS), and Sand (S) (p= <0.001; Table A2), with water content M > MM > S > MS (p= <0.001; Table A2). The highest bulk density was observed at MS followed by S and MM, followed by M (p= <0.001; Table A2), but the site effect was not as strong as for organic and water content (Table A2). Mud had a significantly smaller median and volume weighted mean particle size than MM followed by MS < S (p= <0.001; Table A2). The proportion of fine particles inversely followed this trend with significant differences between each site (p= <0.001; Table A2). The effects of site for the physical variables were stronger than all other variables (Tables A1-A4).

Sediments contained a greater organic content during autumn than spring, and a greater quantity during spring than winter and summer (p= <0.001; Table A6). Water content was also highest during autumn, however there was no difference between winter, spring and summer (p= <0.001; Table A6). The bulk density of all sediments was highest during spring, followed by winter, then autumn and summer which were similar (p= <0.001; Table A6). Sediments contained a higher proportion of fine particles during summer, autumn and spring than winter (p= <0.001; Table A6). The mean particle diameter and volume weighted mean particle size were higher during winter than other seasons, and lower during summer than spring and winter (both p= <0.001; Table A6). The effect of season was much weaker than site for all physical variables (Tables A2 and A6), therefore the variation of physical characteristics between sites was more consistent and of greater magnitude than between seasons. The interaction between site and season was significant for all physical variables (Table A10, Fig. A1), but the effects were relatively weak and similar in strength to that of season alone.

There was moderate positive correlation at M, MM and MS between sediment organic content and water content, with a strong positive correlation when combining data from all sites (Figs. A5-A9). An increase in both organic content and water content were strongly correlated with particle size variables favouring a smaller particle distribution, and moderately correlated with lower bulk density when data from all sites were combined. However there were only weak to

moderate correlations between the same variables for individual sites, with the exception of MS where the above correlations between particle size variables and organic content were strong. There was a very strong positive correlation between organic content and water content with the elemental variables of organic carbon (C), total C and total nitrogen (N) over all sites, with moderate to weak positive correlation (where significant) at M, MM and MS. At S however, there was a moderate negative correlation with water content and the elemental variables. There was only weak positive correlation between bulk density and the particle size variables in the combined site data, with very weak or non-significant correlation within sites.

3.3.1.2 Biogeochemical sediment characteristics

There were significantly greater concentrations of colloidal proteins at M than MM, whereas there was no significant difference between these sites for colloidal carbohydrates (both p= <0.001; Table A3). S contained significantly greater colloidal carbohydrates than MS, and there was no significant difference between the sites for colloidal proteins. M and MM contained significantly greater colloidal carbohydrates and proteins than S and MS. M contained the higher organic C, total C and total N followed by MM > MS > S (all p= <0.001; Table A3). The effect of total carbon/total nitrogen (C/N) ratio between sites was relatively weak but still significant (Table A3). The C/N ratio was higher at MS than MM and S but not MM, and S was significantly lower than M and MS but not MM (p=0.004). The highest C/N ratio was MS at 17.05 ± SD 8.79, and the lowest was S at 12.07 ± SD 3.93. There was low variability of pH between sites, with the highest in S at 7.64, and the lowest in MS at 7.31, however pH at S was significantly higher than all other sites, and MS lower than MM, and neither MM nor MS were significantly different from M (p= <0.001; Table A3). The salinity at MS was significantly higher than M, which was higher than S and MM which were similar (p= <0.001; Table A3).

There were more colloidal carbohydrates and proteins during spring and summer than autumn and winter, although carbohydrates during autumn were not significantly different from spring and summer (both p= <0.001; Table A7). Organic and total carbon and total nitrogen were higher in summer than winter, with no significance between the other seasons (p= 0.001, p= 0.009, p= 0.002 respectively; Table A7). The C/N ratio was not significantly different between seasons (p= 0.147; Table A7). pH was highest during winter, followed by autumn and summer which were higher than spring (p= <0.001; Table A7). Salinity was highest during spring, followed by autumn and summer which were greater than winter (p= <0.001; Table A7).

The interaction between site and season was significant for all biogeochemical variables except total nitrogen content and the C/N ratio (Table A10), but the effects were relatively low compared to the one-way analyses (Table A7).

There was a strong positive correlation between EPS variables (colloidal carbohydrates and colloidal proteins) within each site and over all sites combined (Figs. A5-A9). Within sites M, MM, MS and over all sites combined, there was moderate to strong positive correlation between EPS and the organic content of the sediment. There was also a weak positive correlation between EPS and water content in MS and over all sites combined. There were moderate to strong correlations between finer particle distributions and increased concentrations of EPS and elemental variables over all sites combined, and within individual sites with the exception of S where correlations were weaker or non-significant. The elemental variables were all moderately or strongly positively correlated with one another within and over all sites combined. There were only very weak or non-significant relationships between EPS and bulk density over all sites combined and within sites except M where there was moderate positive correlation.

Correlation between the C/N ratio and a finer particle distribution was positive but very weak over all sites combined, however the correlation was slightly stronger and negative at M and MM. Correlations between EPS, and elemental variables were all positive and varied in strength, with weak and non-significant correlations at M and S, and moderate to strong correlation at MS, MM and over all sites combined. Only at M and MM were relationships between the C/N ratio and EPS and elemental variables more than weakly correlated, with a lower C/N ratio corresponding to increased EPS and increasing elemental variables. There was a moderate to strong negative correlation between the interstitial water pH and salinity within and over all sites combined.

The relationship between pH and EPS and elemental variables differed in strength, with some weak to moderate negative correlation within sites, and weak or very weak negative correlation over all sites combined. There was also positive correlation between salinity and EPS concentration within sites, with the strongest correlations with colloidal carbohydrates at MS and S. There was no discernible trends of correlation between pH and salinity, and physical sediment characteristics, except at M and MM and over all sites combined there was weak to moderate correlation between decreasing pH or increasing salinity with a shift towards a finer particle distribution. This was very weak or non-significant over all sites combined however.

3.3.1.3 Environmental variables

The minimum grass temperature was significantly lower in winter than summer and spring (p= <0.001; Table A8). Autumn was not significantly different from any other season. Minimum air temperature in winter was lower than summer and spring (p= <0.001; Table A8). Summer was higher than autumn and winter but not spring. The maximum air temperature showed better distinction between seasons with summer and spring being higher than autumn followed by winter (min. grass temp.: p= <0.001, min. air temp: p= <0.001, max. air temp.: p= <0.001; Table A8). Sea temperature showed the best distinction between seasons (p= <0.001; Table A8), with summer temperatures higher than autumn and spring which were higher than winter. Precipitation the day before sampling (Precip. 1) or cumulative precipitation before sampling was not significantly different between season (p= 0.897, p= 0.445, p= 0.078 for 1, 2 and 5 day precipitation respectively; Table A8), however the strength of the effect increased with more days added to the cumulative precipitation value.

There were only non-significant or very weak correlations between any environmental variables and physical sediment characteristics (Figs. A5-A9). There was weak positive correlation with increasing temperatures and EPS, with maximum air temperature correlating with EPS more strongly than the minimum temperature variables and sea temperature. Higher air temperatures also correlated weakly with a decrease in pH and an increase in salinity however these correlations were stronger for maximum air temperature than for sea temperature. There was a weak negative correlation with 5 day cumulative precipitation and colloidal carbohydrates, colloidal proteins, organic C and total C. The strength of the negative correlation between precipitation and minimum temperature variables increased when more days of cumulative precipitation were added, with a moderate negative correlation for 5 day cumulative precipitation.

3.3.2 Spatial and temporal variability of FIOs

There were significantly greater numbers of coliforms present at M and MM than S, which contained significantly more than MS (p= <0.001; Table A1). M and MM had a mean abundance over 1 log unit greater than MS. The mean *E. coli* abundance was roughly 1.2 log units less in each sediment type than total coliforms. The order of significant differences of abundance of *E. coli* between sites was the same as for total coliforms (*E. coli*; p= <0.001; Table

A1). The difference between the greatest number of *E. coli* in MM and the least in MS was 1 log unit.

During autumn there was greater abundance of coliforms in all sediments than summer, followed by winter, then spring (p= <0.001; Table A5). *E. coli* was in highest abundance during autumn, followed by summer and winter, then spring (p= <0.001; Table A5). The effect of site on total coliform abundance was stronger than that of season suggesting sediment type was more important than seasonal changes, however the effect of site on *E. coli* abundance was weaker than that of season (Table A5).

The two-way interaction between site and season was significant for coliforms (p= <0.001; Table A10), but the effect was weaker than that of site or season individually (Table A1, A5 and A10). Almost all S and MS sampling events were significantly lower than M and MM during all seasons (Fig. 3.3.1A). Spring and winter at MS and spring at S were significantly different from each other and significantly lower than all other treatments. During autumn, M and MM were significantly higher than all other treatments except MM during summer. The two-way interaction effect between site and season on *E. coli* abundance was, as for coliforms, much weaker than in the one-way analyses (Table A1, A5 and A10). A similar pattern was also observed in the significant groups (Fig. 3.3.1B), with MS and S being usually being significantly lower than M and MM with the exception of S during autumn being exceptionally high compared to other S and MS treatments, and M and MM during spring being lower than the general trend.

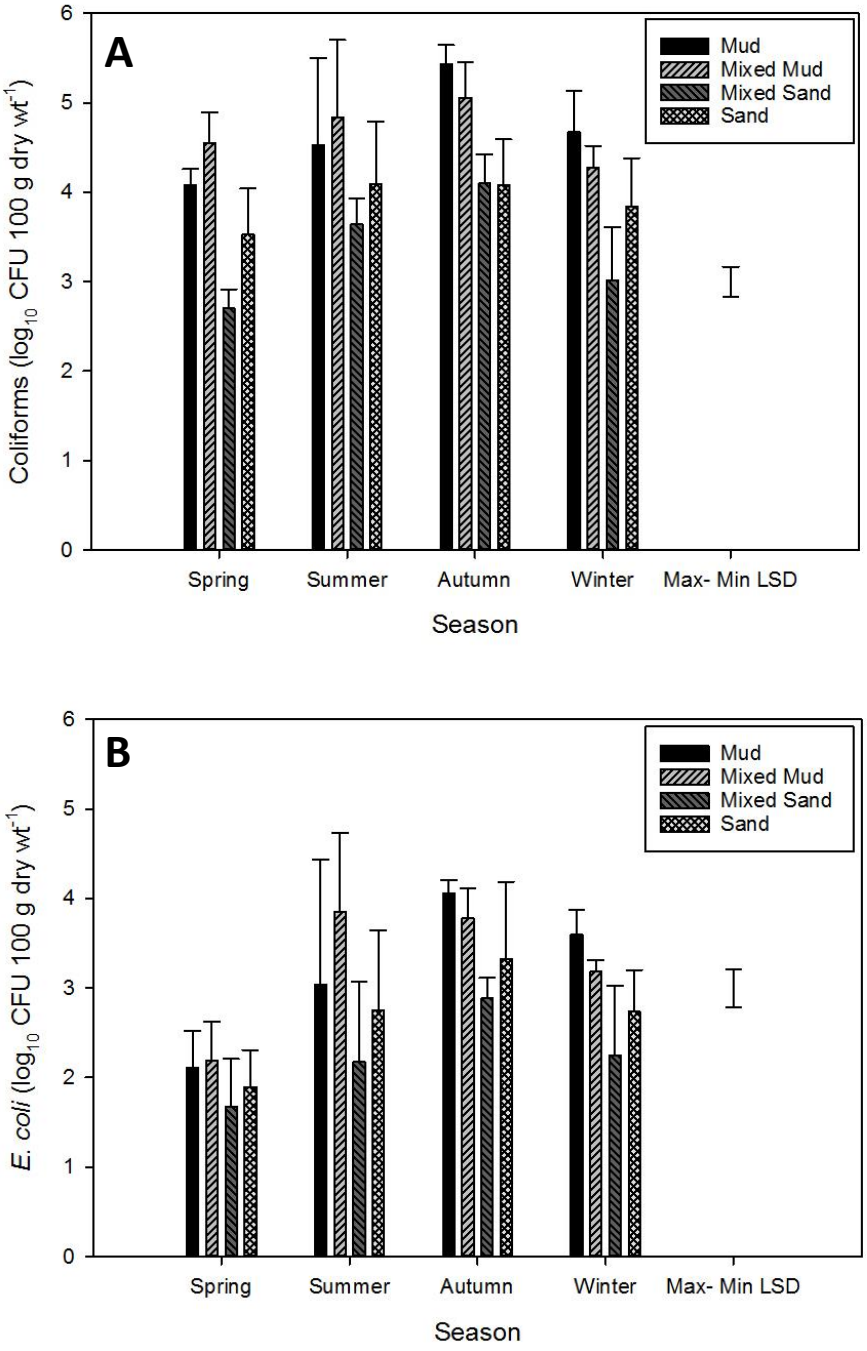

Figure 3.3.1 Mean values of coliform (A) and *E. coli* (B) abundances at four intertidal sediments during each season. Solid fill bars- Mud; light-grey dashed bars- Mixed Mud; dark-grey dashed bars- Mixed Sand; hatched bars- Sand. Error bars indicate standard error from the mean. Floating bar represents maximum – minimum least significant differences (LSD) (due to unequal number of samples within treatments) at p= 0.05 level. Difference between treatment means larger than the LSD bar generally indicates a significant difference.

3.3.3 Co-variance of FIOs with sediment characteristics and environmental variables

Over all sites combined, and at M, MS, and S individually there was a very strong positive correlation, and at MM a moderately strong positive correlation, between coliform and *E. coli* abundance in sediments (Figs. A5-A9). Over all sites combined (Fig. A9), there were moderate positive correlations between coliform abundance with several variables including organic and water content, an increase in finer particle proportion, and organic C and total C. There were also weak correlations between an increase in coliform abundance and a decrease in bulk density, salinity and sediment shear strength, and an increase in EPS and total N. Within individual sites, the direction of correlation between coliforms and the other variables was the same as over all sites combined, with the exception of MS and S showing a moderate negative correlation for both EPS variables, respectively, and the correlation with salinity at MS being non-significant. There was also a moderate negative correlation between coliform abundance and the C/N ratio at MM, and a weak positive correlation with sediment stability that was not significant at any other site or over all sites combined.

The relationships between *E. coli* and other variables were generally similar to that of coliforms. Notable differences over all sites combined include weaker positive correlations between *E. coli* abundance and EPS and elemental variables, and also weaker correlations with all of the physical sediment characteristics. There was an increased strength of correlation between *E. coli* abundance and salinity, however, with moderate to strong negative correlation at all sites and over all sites combined, with the relationship being slightly weaker at MS. At S, MS and over all sites combined there was also a weak positive correlation between *E. coli* and pH, and between *E. coli* and the C/N ratio at MS. At MS there was also weak negative correlation between *E. coli* and sediment shear strength, but only very weak negative correlation over all sites combined for sediment shear strength or sediment stability. There was a weak negative correlation between *E. coli* and maximum air temperature over all sites combined, with only very weak or non-significant correlation between *E. coli* and other environmental variables

3.3.4 Development of models to explain **E. coli** *abundance*

Best subsets model

Best subsets models were run (Section 3.2.2) using variables giving good significance in preliminary multiple stepwise linear regressions, and variables that featured significantly in preliminary best subset models using combinations of all variables. The variability of *E. coli* abundance explained by the optimal 2-term model was 54.55 % (Table 3.3.1). This increased slightly with each additional term until the 7-term model. The variance explained increased in very small increments after the optimal 4-term model, and Mallow's Cp value increased with additional terms after the 7-term model. Five-day cumulative precipitation was included in the second best model in the 3, 4 and 6-term models, and in the optimal 5 and 7-term models. Water content was the second best 1-term model, but did not feature in subsequent models. Proportion of fine particles featured in the second best 2-term model, and did not feature in any optimal model. The second best 4-term model substituted 5-day cumulative precipitation for bulk density with little change in the adjusted R^2 value. Likewise the substitution in the second best 5-term model removed 5-day cumulative precipitation for colloidal proteins without introducing a non-significant term. The variables selected in the optimal multiple stepwise linear models; salinity, organic content, sediment shear strength and bulk density featured heavily in the optimal multi-term models (Table 3.3.1, see below).

Table 3.3.1 Best subsets models with *E. coli* $\log_{10}$ CFU 100 g dry wt^{-1} as the dependant variable. † denotes square root transformed variables.

Terms (n)	Sample Units (n)	Adjusted R^2	Mallow's Cp	Regression d.f.	Fine Particles (% 0-63 µm)	Bulk Density (g cm^3)	Colloidal Carbohydrates† (µg g^{-1})	Colloidal Proteins† (µg g^{-1})	Organic Content (%)	Water Content (%)	Salinity	Sediment Shear Strength (Kpa)	Precip. 5 Day (mm)
1	275	37.3	176.7	2	-	-	-	-	-	-	<.001	-	-
1	275	24.5	268.3	2	-	-	-	-	-	<.001	-	-	-
2	275	54.6	54.2	3	-	-	-	-	<.001	-	<.001	-	-
2	275	52.3	70.3	3	<.001	-	-	-	-	-	<.001	-	-
3	275	57.2	36.3	4	-	-	-	-	<.001	-	<.001	<.001	-
3	275	56.0	44.7	4	-	-	-	-	<.001	-	<.001	-	.002
4	275	59.5	21.1	5	-	<.001	-	-	<.001	-	<.001	<.001	-
4	275	58.3	29.6	5	-	-	-	-	<.001	-	<.001	<.001	.005
5	275	60.2	17.3	6	-	<.001	-	-	<.001	-	<.001	<.001	.019
5	275	60.1	17.5	6	-	<.001	-	.021	<.001	-	<.001	<.001	-
6	275	61.3	10.4	7	-	<.001	.003	<.001	<.001	-	<.001	<.001	-
6	275	60.4	16.5	7	-	<.001	-	.104	<.001	-	<.001	<.001	.091
7	275	61.7	8.2	8	-	<.001	.001	<.001	<.001	-	<.001	<.001	.040
7	275	61.3	10.9	8	.216	<.001	.002	<.001	<.001	-	<.001	<.001	-

Intensively sampled sediments in the Ythan estuary

Multiple stepwise linear regressions were run (Section 3.2.2) using all available variables for the individual means for the 6 sampling locations within each sediment type for each sampling event (all replicates model), and for the means of each sediment type for each sampling event (replicate means model).

When all replicates within each site were included, interstitial pore water salinity of the sediment explained 37.1 % of the variability of *E. coli* abundance. The optimal model (all variables excluding sediment stability, organic C, total C, total N and total C/N ratio due to limited sample number) was salinity, organic content, sediment shear strength, bulk density, and 5-day cumulative precipitation, with an overall adjusted R^2 of 60.0 (Table 3.3.2). When the dataset was limited to biogeochemical variables, salinity and organic carbon explained 61.8 % of the variability (Table 3.3.3). The residual d.f. of the model were greatly reduced due to a limited number of samples being processed for elemental analysis. Physical variables alone were only able to explain 23 % of the variability of *E. coli* abundance (Table 3.3.4). When season was added as a factor to the optimal model the variability explained increased to 47 %. Environmental variables alone accounted for 17.7 % of *E*. *coli* variability (Table 3.3.5). In this model, maximum air temperature had a negative effect, and sea temperature had a positive effect on *E. coli* abundance. This was the only model where the added effect of site as a factor to the optimal model resulted in a larger increase of variability accounted for than season. When the mean for the replicates at each site for each sampling time point were used (data excluded as in all replicates model), the variables included were the same as the 'all replicates' model, however 5 day precipitation was not included (Table 3.3.6). The variation of *E. coli* abundance explained was higher in this model at 71 % than compared to single replicates. Over all successful models, there was a small increase in the variability explained when site was added as a factor to the optimal model, and a slightly larger increase when season was added, and again when both season and site were added.

Response values from the optimal stepwise linear regression model for all replicates were plotted against fitted values to identify trends of over or under prediction. Samples taken during autumn and summer were frequently predicted lower than the observed values (Fig. 3.2A), and samples during spring and winter predicted slightly higher than the observed values. There was no discernible trend to prediction inaccuracy between sites (Fig. 3.2B).

Table 3.3.2 Multiple stepwise linear model with *E. coli* $\log_{10}$ CFU 100 g dry wt^{-1} as the dependant variable. Model uses all variables except sediment stability based upon data including all site replicates.

Step		1	2	3	4	5	Added Individually		
Term added	*E. coli* ($\log^{10}$ CFU 100g dry wt^{-1})	+ Salinity	+ Organic Content (%)	+ Sediment Shear Strength (Kpa)	+ Bulk Density (g cm^3)	+ Precip. 5 Day (mm)	+ Site	+ Season	+ Season + Site
Adjusted R^2	-	37.1	54.4	57.2	59.3	60.0	63.4	68.7	70.5
Residual d.f.	262	261	260	259	258	257	254	254	251
Regression F- statistic	-	155.28	157.59	117.65	96.48	79.58	57.67	72.99	57.9
Regression Significance	-	<.001	<.001	<.001	<.001	<.001	<.001	<.001	<.001
Significance of Last Term	-	<.001	<.001	<.001	<.001	0.021			
Term Estimate (Final model)	Constant: 4.205	-0.057	0.226	0.043	-0.557	0.010			

Table 3.3.3 Multiple stepwise linear model with *E. coli* $\log_{10}$ CFU 100 g dry wt^{-1} as the dependant variable. Model uses biogeochemical sediment characteristics based upon data including all site replicates. Dagger (†) denotes a square root transformation of the variable prior to analysis.

Step		1	2	Added Individually		
Term added	*E. coli* ($\log^{10}$ CFU 100g dry wt^{-1})	+ Salinity	+ Organic Carbon† (% dry wt)	+ Site	+ Season	+ Season + Site
Adjusted R^2	-	46.9	61.8	64.4	69.3	71.7
Residual d.f.	84	83	82	79	79	76
Regression F- statistic	-	75.26	69.04	31.33	39.01	27.56
Regression Significance	-	<.001	<.001	<.001	<.001	<.001
Significance of Last Term	-	<.001	<.001			
Term Estimate (Final model)	Constant: 3.157	-0.057	1.106			

Table 3.3.4 Multiple stepwise linear model with *E. coli* $\log_{10}$ CFU 100 g dry wt^{-1} as the dependant variable. Model uses physical sediment characteristics based upon data including all site replicates.

Step		1	2	Added Individually		
Term added	*E. coli* ($\log^{10}$ CFU 100g dry wt^{-1})	+ Water Content (%)	+ Bulk Density (g cm^3)	+ Site	+ Season	+ Season + Site
Adjusted R^2	-	18.9	23.0	29.9	47.0	52.1
Residual d.f.	299	298	297	293	293	290
Regression F- statistic	-	70.60	45.53	26.80	54.23	41.74
Regression Significance	-	<.001	<.001	<.001	<.001	<.001
Significance of Last Term	-	<.001	<.001			
Term Estimate (Final model)	Constant: 3.599	0.025	-0.825			

Table 3.3.5 Multiple stepwise linear model with *E. coli* $\log_{10}$ CFU 100 g dry wt^{-1} as the dependant variable. Model uses environmental variables based upon data including all site replicates.

Step		**1**	**2**	**3**	**Added Individually**		
Term added	***E. coli*** ($\log^{10}$ CFU 100g dry wt^{-1})	**+ Max. Air Temp.** (°C)	**+ Sea Temp.** (°C)	**+ Precip. 1 Day** (mm)	**+ Site**	**+ Season**	**+ Season + Site**
Adjusted R^2	-	5.8	12.3	17.7	43.2	38.6	58.7
Residial d.f.	262	261	260	259	256	256	253
Regression F- statistic	-	16.22	19.42	19.76	34.24	28.42	42.40
Regression Significance	-	<.001	<.001	<.001	<.001	<.001	<.001
Significance of Last Term	-	<.001	<.001	<.001			
Term Estimate (Final model)	Constant: 2.652	-0.181	0.2035	0.0893			

Table 3.3.6 Multiple stepwise linear model with *E. coli* $\log_{10}$ CFU 100 g dry wt^{-1} as the dependant variable. Model uses all variables except sediment stability based upon data using mean for each site at each sampling event.

Step		**1**	**2**	**3**	**4**	**Added Individually**		
Term added	***E. coli*** ($\log^{10}$ CFU 100g dry wt^{-1})	**+ Salinity**	**+ Organic Content** (%)	**+ Sediment Shear Strength** (Kpa)	**+ Bulk Density** (g cm^3)	**+ Site**	**+ Season**	**+ Season + Site**
Adjusted R^2	-	45.6	63.2	66.0	71.0	75.5	77.2	79.7
Residual d.f.	46	45	44	43	42	39	39	36
Regression F- statistic	-	39.59	40.56	30.73	29.20	21.24	23.3	19.11
Regression Significance	-	<.001	<.001	<.001	<.001	<.001	<.001	<.001
Significance of Last Term	-	<.001	<.001	0.039	0.006			
Term Estimate (Final model)	Constant: 5.814	-0.063	0.197	0.064	-1.304			

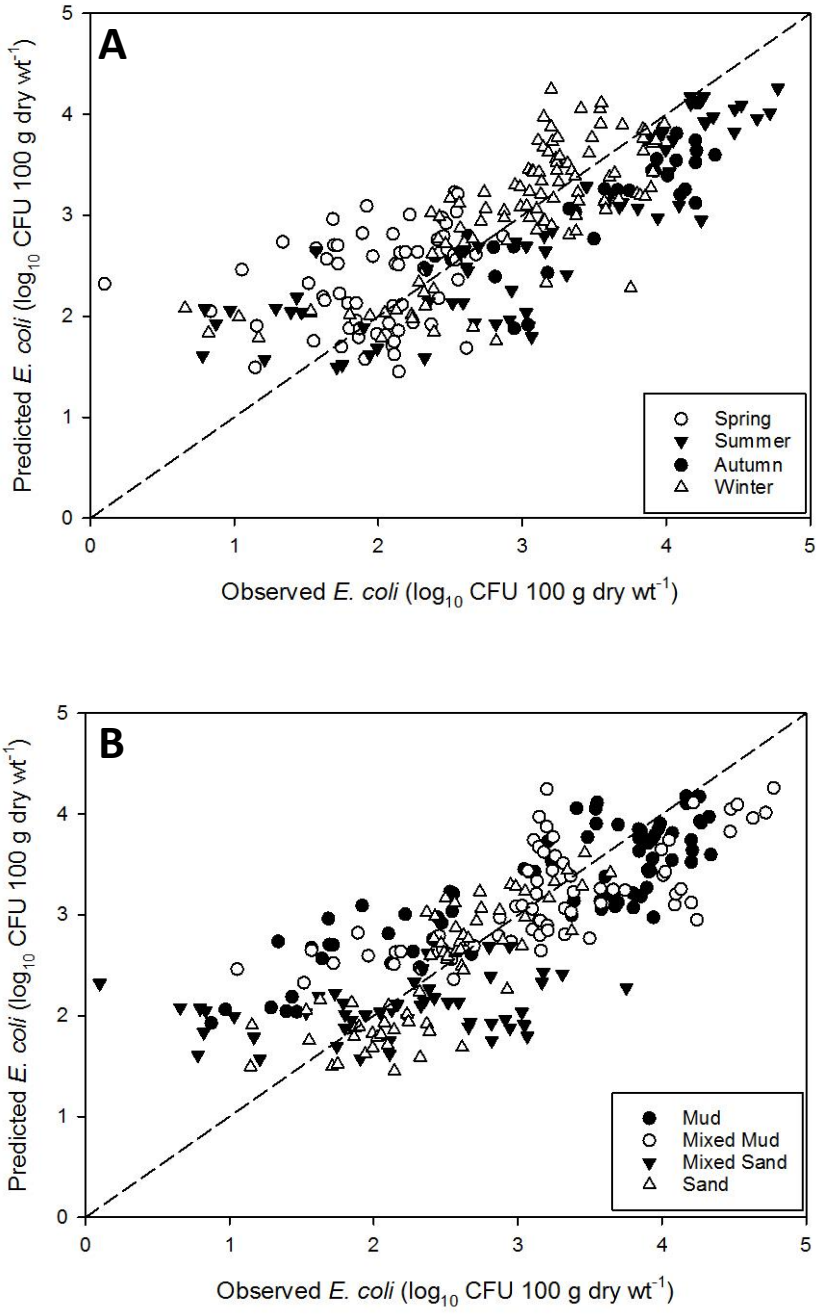

Figure 3.3.2 Scatterplots of observed vs. predicted *E. coli* abundance in intertidal sediments from the optimal multiple stepwise linear regression model using all variables except sediment stability based upon data including all site replicates. Plot A: hollow circles-spring; solid triangles- summer; solid circles- autumn; hollow triangles- winter. Plot B: solid circles- Mud; hollow circles- Mixed Mud; solid triangles- Mixed Sand; hollow triangles- Sand. Dashed line indicates 1:1 predicted vs. observed values.

Seasonal transects in the Ythan and Eden estuaries

Spearman's rank correlation tables were constructed for the Eden and Ythan estuary transect datasets (Figs. A10-A12). Generally, correlations between variables were very similar to that of correlations identified earlier for the combined intensively sampled sites dataset on the Ythan estuary, however there were several notable differences. There were fewer significant correlations between physical sediment characteristics and environmental variables in the transect datasets. Bulk density formed no significant correlations with any other variables in the Ythan estuary transect, and only weak correlations with organic content, water content and median particle diameter in the Eden estuary transect and the combined estuary transect datasets whereas there were several weak, but significant correlations in the intensively sampled dataset. Increasing salinity also correlated strongly with decreasing organic content and water content, decreasing EPS content and variables favouring a larger particle size distribution in the transect datasets, compared to negligible or non-significant correlations in the intensively sampled dataset. In the Eden estuary, there was no significant correlation of sediment shear strength with any variable, whereas in the Ythan estuary, it was significantly positively correlated with lower water content, higher bulk density, colloidal protein content and salinity, and variables favouring a larger particle size distribution. Sediment stability in the transect datasets was not significantly correlated with any physical sediment variables, as it was in the intensively sampled dataset, but was moderately to strongly correlated with increasing EPS content in the transect datasets.

The positive correlation between *E.coli* and coliform abundances was exceptionally high in the Eden estuary transect and correlations for the Ythan transect and combined transect data were higher than the correlation in the intensively sampled dataset (Spearman's rank correlation coefficients: Eden transect= 0.959, Ythan transect= 0.866, combined transects= 0.915, Ythan intensively sampled sites combined= 0.797; Figs. A10-A12). An increase *E. coli* abundance correlated moderately or strongly with all physical variables when both estuaries transects were combined, with the exception of the correlation of *E. coli* with bulk density in the Ythan estuary transect. *E. coli* correlation with EPS was stronger in the Eden estuary transect than in the Ythan estuary transect, and showed moderate to strong positive correlation when both transects were combined, compared to negligible or non-significant correlation in the intensively sampled dataset. There was also strong negative correlation of *E. coli* abundance with minimum grass and air temperatures at the Eden estuary, whereas this

correlation was much weaker in the Ythan estuary transect and the intensively sampled dataset.

The optimal multiple stepwise linear models for the Eden transect resulted in a very high adjusted R^2 value of 87.4 (p= <0.001; Table 3.3.7), compared to a relatively low adjusted R^2 of 49.8 for the Ythan transect (p= <0.001; Table 3.3.8). Several variables included in this model are similar to that of the best subsets and multiple stepwise linear models of the intensively sampled dataset (Tables 3.3.1 and 3.3.2). Salinity was included early in the Eden transect model as it was in the earlier models, however the proportion of fine particles, which does not feature in any of the intensive sampling regime models, was included as the first step of the model and alone accounts for an adjusted R^2 of 46.4 (p= <0.001; Table 3.3.7). Colloidal carbohydrates features in the model for the Eden transect, and featured in the later best subsets models for the intensively sampled dataset. Colloidal carbohydrates also features in the Ythan transect model (Table 3.3.8), which shares many variables with the Eden quarterly transect model. Both the individual transect models heavily utilise environmental variables compared to the intensive sampling models, with 4 of 8 of the explanatory variables in the optimal Eden transect model, and 2 of 5 in the optimal Ythan transect model. The optimal multiple stepwise linear model for the dataset combining both estuary transects has an adjusted R^2 of 48.7 (p= <0.001; Table 3.3.9), which is relatively low compared to other models. It does however utilise many of the common variables observed previously. Organic content and water content feature in the optimal model for the combined estuary transects, but are absent from the models for the estuaries individually.

Table 3.3.7 Multiple stepwise linear model explaining *E. coli* abundance in the Eden estuary transect dataset using all sediment characteristic and environmental variables available.

Step		1	2	3	4	5	6	7	8
Term Added	***E. coli*** (log^{10} CFU 100g dry wt $^{-1}$)	**+ Fine Particles** (% 0-63 µm)	**+ Salinity** (PSU)	**+ pH**	**+ Min. Air Temp.** (°C)	**+ Carbohydrates** (µg g $^{-1}$)	**+ Precip. 5 Day** (mm)	**+ Max. Air Temp.** (°C)	**+ Precip. 1 Day** (mm)
Adjusted R^2	-	46.4	55.0	63.9	67.3	72.8	77.4	84.6	87.4
Residual d.f.	47	46	45	44	43	42	41	40	39
Regression F- Statistic	-	41.62	29.77	28.74	25.17	26.22	27.81	37.83	41.81
Regression Significance	-	<.001	<.001	<.001	<.001	<.001	<.001	<.001	<.001
Significance of Last Term	-	<.001	0.003	0.001	0.023	0.003	0.004	<.001	0.003
Term Estimate (Final Model)	Constant: 10.66	0.017	-0.036	-1.220	-0.458	0.063	0.024	0.261	0.108

Table 3.3.8 Multiple stepwise linear model explaining *E. coli* abundance in the Ythan estuary transect dataset using all sediment characteristic and environmental variables available

Step		1	2	3	4	5
Term Added	*E. coli* (log^{10} CFU 100g dry wt $^{-1}$)	+ Salinity (PSU)	+ pH	+ Max. Air Temp. (°C)	+ Carbohydrates (μg g^{-1})	+ Min. Air Temp. (°C)
Adjusted R^2	-	30.7	33.8	41.2	45.6	49.8
Residual d.f.	49	48	47	46	45	44
Regression F- Statistic	-	22.66	13.49	12.44	11.27	10.74
Regression Significance	-	<.001	<.001	<.001	<.001	<.001
Significance of Last Term	-	<.001	0.078	0.011	0.035	0.034
Term Estimate (Final Model)	Constant: 12.63	-0.031	-1.137	-0.189	0.035	0.138

Table 3.3.9 Multiple stepwise linear model explaining *E. coli* abundance in the combined dataset from the Eden and Ythan estuary transects using all sediment characteristic and environmental variables available.

Step		1	2	3	4	5	6	7
Term Added	*E. coli* (log^{10} CFU 100g dry wt $^{-1}$)	+ Salinity (PSU)	+ pH	+ Fine Particles (% 0-63 μm)	+ Max. Air Temp. (°C)	+ Organic Content (%)	+ Water Content (%)	+ Carbohydrates (μg g^{-1})
Adjusted R^2	-	24.6	34.7	37.8	41.6	43.8	46.8	48.7
Residual d.f.	97	96	95	94	93	92	91	90
Regression F- Statistic	-	32.68	26.8	20.63	18.26	16.14	15.23	14.13
Regression Significance	-	<.001	<.001	<.001	<.001	<.001	<.001	<.001
Significance of Last Term	-	<.001	<.001	0.020	0.009	0.032	0.015	0.042
Term Estimate (Final Model)	Constant: 16.25	-0.027	-1.620	0.013	-0.098	0.279	-0.038	0.027

3.3.5 Efficiency of models across the different datasets

The optimal model for the Eden transect model performed very well, with little discernible trend away from the 1:1 line (Figs. 3.3.3A and 3.3.3B). The optimal model for the Ythan transect however demonstrated a tendency to over-predict samples at the mouth of the estuary where the lowest *E. coli* abundances were observed (Figs. 3.3.3C and 3.3.3D). The optimal models for the combined dataset of both estuaries demonstrated a tendency to under-predict the abundance of *E. coli* in the Eden estuary samples (Figs. 3.3.3E and 3.3.3F). In addition, similarly to both individual models, the model over-predicted samples where the observed *E. coli* abundance was below 1 log_{10} CFU. There was no strong trend of model inaccuracy between seasons in any of the transect models.

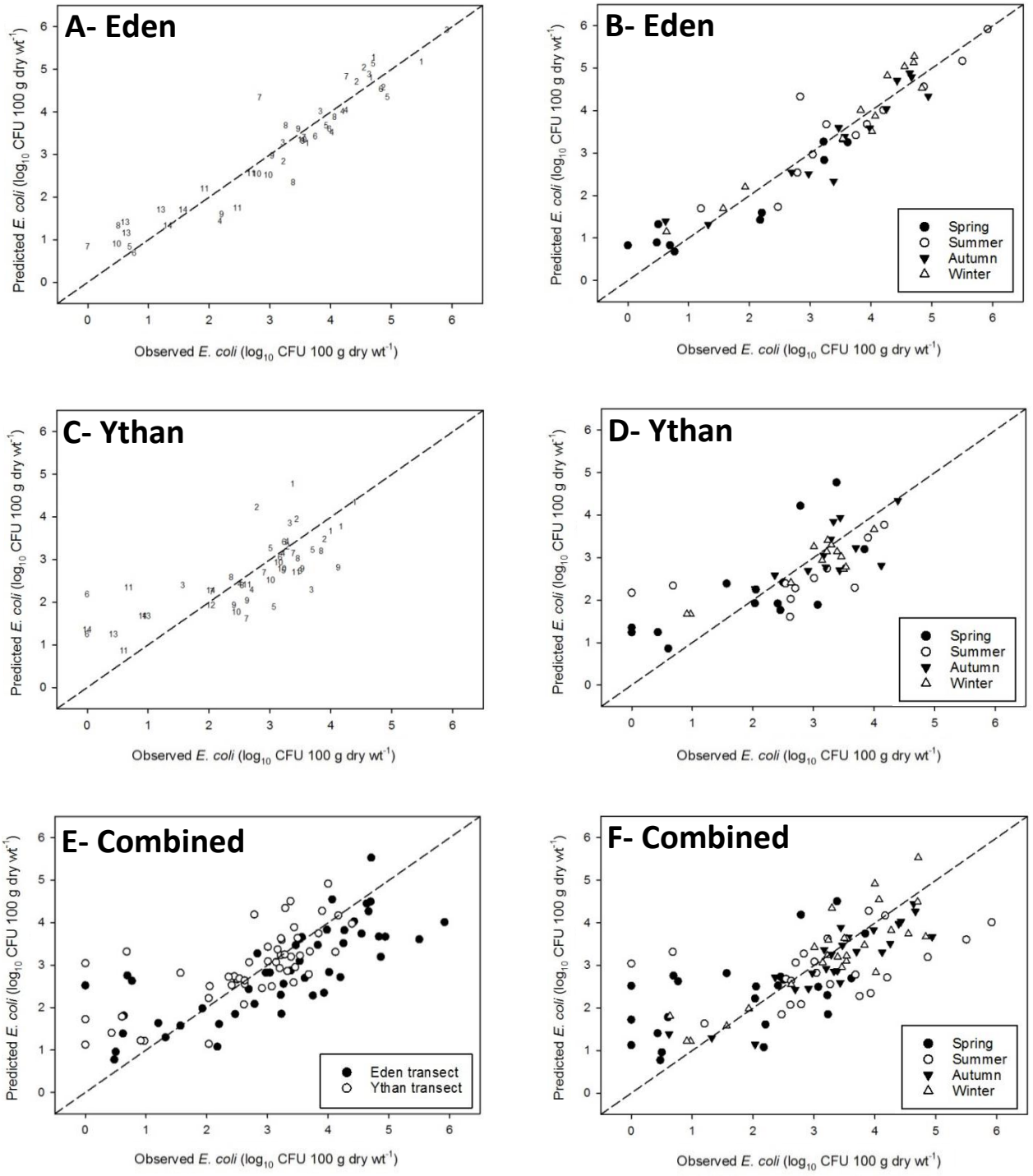

Figure 3.3.3 Scatterplots of observed vs. predicted *E. coli* abundance in intertidal sediments. A, B: Eden estuary dataset and model; C, D: Ythan estuary dataset and model; E, F: combined estuary transects dataset and model. A, C: numbers denote sampling position within the estuary. B, D, F: solid circles- spring; hollow circles- summer; solid triangles- autumn; hollow triangles- winter. E: solid circles- Eden estuary; hollow circles- Ythan estuary. Dashed line indicates 1:1 predicted vs. observed values.

Simple linear regressions between observed values and predicted values using alternative models revealed that the optimal model for all site replicates from the intensively sampled dataset was more effective at predicting the Eden transect samples than the Ythan transect samples and both transects combined (Adjusted R^2: Eden= 32.0, *p*= <0.001, Ythan= 22.8, *p*= <0.001, Combined= 28.8, *p*= <0.001; Table 3.3.10). There was a clear pattern once again of the samples with low observed *E. coli* abundance being over-predicted by the model (Fig. 3.3.4), however there was no clear trend of model inaccuracy between seasons, or between the estuaries for either model constructed on the Ythan intensive sampling regime. A similar pattern emerged for the model constructed from the means of the sampling events from the intensive sampling, albeit with lower adjusted R^2 values (Table 3.3.10, Fig. A13).

Table 3.3.10 Simple linear regressions and their statistical significance between observed and predicted datasets using models constructed on the same dataset, and models created on alternative datasets.

Input Dataset	Model Used	Residual d.f.	F-statistic	*p*-value	Adjusted R^2
Both Estuary Transects	**Both Estuary Transects**	96	40.17	<0.001	28.8
Eden Transect	**Ythan Intensive All Reps**	46	23.15	<0.001	32.0
Ythan Transect	**Ythan Intensive All Reps**	48	15.51	<0.001	22.8
Both Estuary Transects	**Ythan Intensive Rep Means**	96	37.63	<0.001	27.4
Eden Transect	**Ythan Intensive Rep Means**	46	20.75	<0.001	29.6
Ythan Transect	**Ythan Intensive Rep Means**	48	13.93	<0.001	20.9
Ythan Intensive All Reps	**Both Estuary Transects**	273	85.85	<0.001	23.6
Ythan Intensive All Reps	**Eden Transect**	263	37.00	<0.001	12.0
Ythan Intensive All Reps	**Ythan Transect**	275	68.42	<0.001	19.6
Eden Transect	**Eden Transect**	46	394.00	<0.001	89.3
Ythan Transect	**Ythan Transect**	48	58.57	<0.001	54.0
Both Estuary Transects	**Both Estuary Transects**	96	105.52	<0.001	51.9
Eden Transect	**Ythan Transect**	46	20.73	<0.001	29.6
Ythan Transect	**Eden Transect**	48	6.63	0.013	10.3

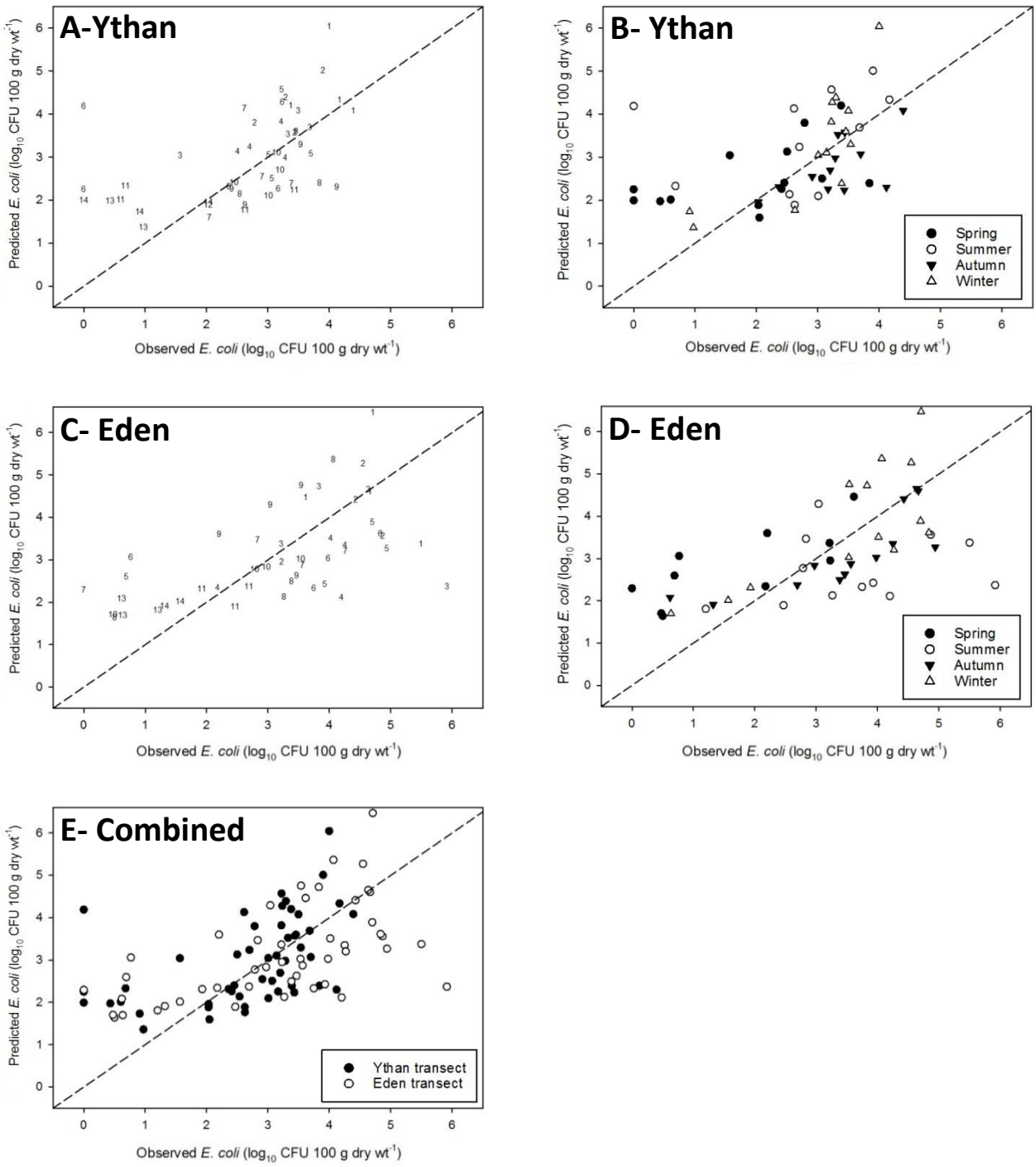

Figure 3.3.4 Scatterplots of observed vs. predicted *E. coli* abundance in intertidal sediments using the model constructed on data from intensive sampling on the Ythan estuary on the estuary transect datasets. A, B: Ythan estuary; C, D: Eden estuary; E- combined estuary transects dataset. A, C: numbers denote sampling position within the estuary. B, D: solid circles- spring; hollow circles- summer; solid triangles -autumn; hollow triangles- winter. E: solid circles- Ythan estuary; hollow circles- Eden estuary. Dashed line indicates 1:1 predicted vs. observed values.

The optimal model from the transect sampling regimes from either estuary, or both combined performed poorly in predicting the intensive sampling datasets (Table 3.3.10), with the highest adjusted R^2 observed for the model constructed from both estuary transects combined at 23.6 (p= <0.001). The model constructed from data from both estuary transects tended to over-predict samples from spring and under-predict samples from summer and from site S (Figs. 3.3.5A and 3.3.5B). The model constructed from the Ythan transect dataset was very poor in predicting samples above 3.2 $\log_{10}$ CFU 100 g dry wt^{-1} (Figs. 3.3.5C and 3.3.5D), therefore many samples from M and during autumn were almost entirely under-predicted. Samples during spring were also over-predicted. The model constructed from the Eden transect dataset performed very poorly on the intensively sampled data with very high predicted values for MM during autumn, and M, MM and S during winter (Figs. 3.3.5E and 3.3.5F).

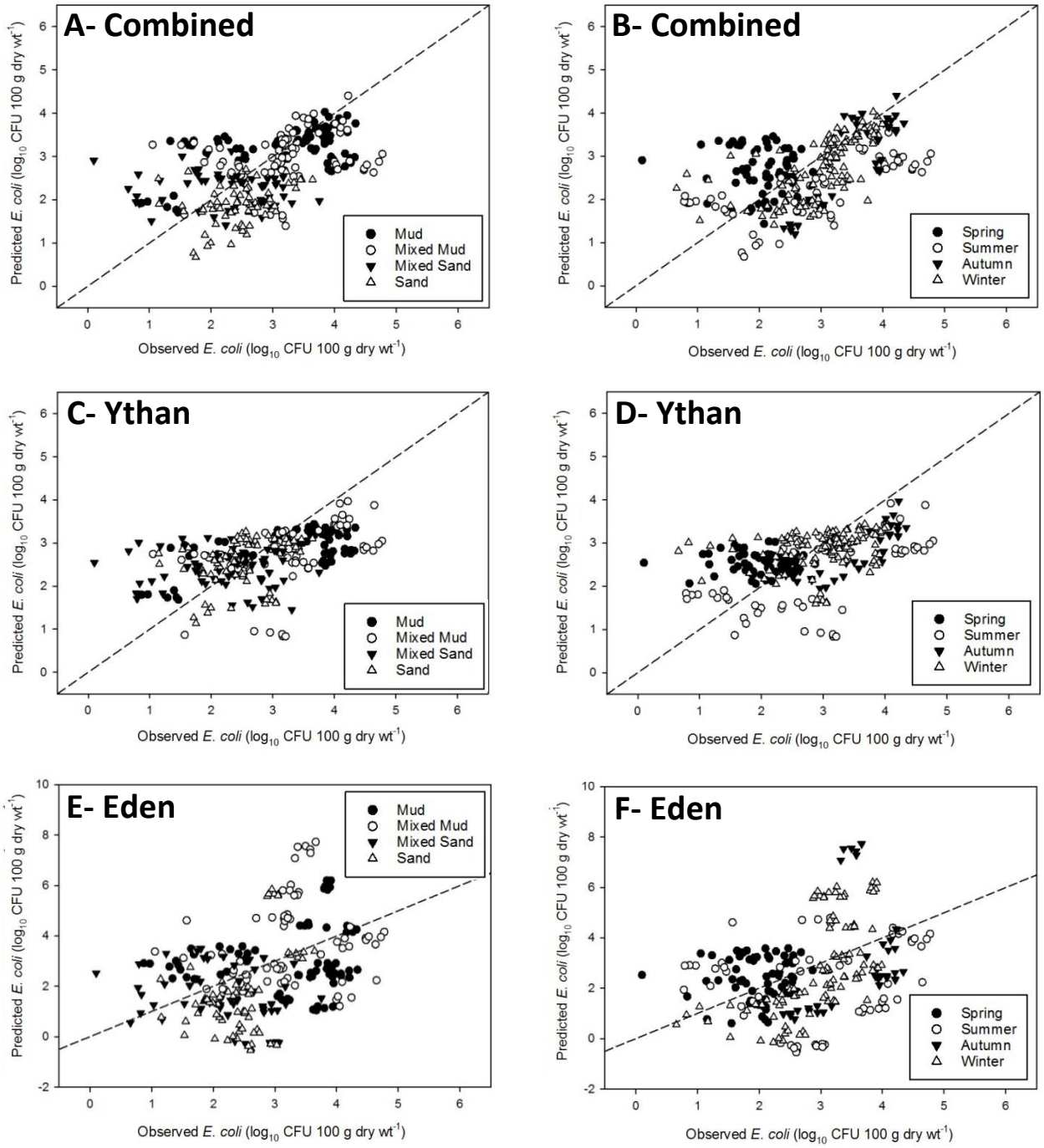

Figure 3.3.5 Scatterplots of observed vs. predicted *E. coli* abundance in intertidal sediments using the models constructed on the estuary transect datasets on the intensive sampling data from the Ythan estuary. A, B: Combined estuary transects dataset model; C, D: Ythan estuary model; E, F: Eden estuary model. A, C, E: solid circles- Mud; hollow circles- Mixed Mud; solid triangles- Mixed Sand; hollow triangles- Sand. B, D, F: solid circles- spring; hollow circles- summer; solid triangles-autumn; hollow triangles- winter. Dashed line indicates 1:1 predicted vs. observed values.

3.4 Discussion

3.4.1 The influence of sediment characteristics and environmental variables on the spatial and temporal distribution of E. coli

The results from the intensive sampling on the Ythan estuary are discussed in detail in Section 3.4.1 with focus on the co-variation of variables, and the effect of variables on the abundance of *E. coli* and their possible mechanisms. The co-variation of variables and the effects on *E. coli* abundance from the analysis of the transect datasets for the Ythan and Eden estuaries are discussed briefly in Section 3.4.2.3. The models constructed on the transect datasets are discussed in more detail in Section 3.4.3 when discussing the estuary-specificity of the models.

3.4.1.1 Physical sediment characteristics

High co-variation was observed between the different particle size variables, resulting in the redundancy of median particle diameter and volume weighted mean particle size as the proportion of fine particles displayed the highest correlation with *E. coli* abundance. This resulted in the inclusion of proportion of fine particles in the second best best-subsets model, and frequently featured in the multiple stepwise linear regression models (hereby termed regression models). Of all physical sediment characteristic variables, water content correlated most with salinity and was absent from best subsets models when salinity was also present. The inverse correlation between water content and salinity may be caused by evaporation of surface water raising the salinity of the interstitial pore-water, however lack of correlation within individual sites except MS suggests a more general relationship of sediments higher up the salinity gradient having a lower water holding capacity because of the physical nature of the sediment.

As discussed earlier (Section 1.8.1), *E. coli* abundance in intertidal sediments has been shown by many authors to be dependent on variables that typically co-vary with particle size distribution, in addition to smaller particle sizes favouring *E. coli* persistence in sediments and soils as smaller pore sizes may exclude larger predators [264, 265]. The data here shows particle size distribution does not vary greatly throughout the year within sediment types, so variables demonstrating good distinction between the sites were likely to perform well in the model. Physical variables demonstrated a higher distinction between sites than other

categories, suggesting one or more of them would frequently feature in the constructed models, however they do not incorporate seasonal changes as much as other variables.

Organic content correlated highly with the nutrient concentration variables of organic C, total C and total N. Of these variables, organic content showed the highest correlation with *E. coli,* confirming previous work suggesting both organic matter [89, 266] and nutrient concentrations [267] were beneficial to *E. coli* persistence in soils and sediments. For example, enteric bacteria are unable to compete with indigenous microflora at low nutrient concentrations [268]. Organic content features heavily in the best subsets model, and is the second step in the optimal regression model where variables are not limited. As mentioned earlier, organic content correlated highly with water content, particle size variables and nutrient content, so serves as a successful proxy for these variables in their effect on *E. coli* abundance. The effect of site was much stronger than season for organic content, indicating variability in organic content was a site-specific effect. Combined with the effect of salinity, these variables account for both seasonal and site-specific variability, resulting in a high variance accounted for of 54.4 % for these two variables in the optimal regression model when all sites were included. Sediment water content and organic content were positively correlated, but water content correlated more highly with salinity than organic content, possibly caused by surface-water evaporation. Organic content did not feature in the physical variables regression model, and was replaced by water content in the absence of the salinity variable and it discriminates better between seasons and has a higher correlation with salinity. Likewise, in the biogeochemical variables model in the absence of organic content, salinity was followed by organic carbon which correlated highly with organic content and particle size variables.

The presence of organic content increases the persistence of *E. coli* in the environment [77, 89] and has been found to be a significant factor explaining distribution of faecal indicator organisms in estuarine sediments [266] suggested to be a cause of the associated increase in nutrient availability [77]. Organic content at M and MM during summer was unusually low compared to the other seasons which did not coincide with reduced *E. coli* abundance, unusually low water content, or a change in particle size, leading to a possible reduction in strength of organic matter in the models. This reduction of organic content may be a result of increased macrofaunal abundance. Macrofaunal invertebrates such as *Corophium volutator* feed by grazing organic matter [269] and appear in great abundance in muddier sediments in

the mid-upper reaches of the Ythan estuary, with their abundance peaking in August and September [270]. Macrofauna were removed from sediment cores prior to measurements, so assimilated organic matter was effectively removed from the analysis.

3.4.1.2 Biogeochemical sediment characteristics

Colloidal carbohydrates and colloidal proteins were highly correlated, and consistently significantly correlated with almost all physical sediment characteristics except bulk density. Both measures of EPS correlated poorly with *E. coli* abundance however, so were unlikely to feature heavily in the models despite significant differences between both sites and seasons. The C/N ratio observed throughout the year in all sites was fairly consistent at around 13, with some higher results observed at MS possibly caused by increased algal biomass.

Salinity was the optimal 1-term model, and was consistently the first term added to the regression models when available. There was good discrimination of salinity between sites, primarily as a cause of dilution of the seawater further up the estuary. There was also significant discrimination between seasons with higher salinity in sediments in the warmer months than winter presumably caused by longer sunlight hours and higher temperatures increasing evaporation of surface water on the sediments, increasing the interstitial pore-water salinity. The interaction of salinity with *E. coli* abundance is therefore two-fold. The first is the clear effect of seawater (containing a negligible *E. coli* load) mixing with river water entering the estuary from the main river channel or tributaries the further down the estuary, diluting the *E. coli* load in the water [271] and reducing the density of *E. coli* available for sedimentation. The second, identified through the seasonal response is that *E. coli* persistence is reduced by high salinities [114, 115, 119]. All sediments contained an interstitial pore-water salinity higher than 8.75, demonstrated to be the salinity above which *E. coli* persistence in seawater is significantly reduced [114]. In addition, an increase of salinity has been demonstrated to induce the 'viable but non culturable' (VBNC) state in *E. coli* [272, 273], a reversible state where cells are not able to be recovered using traditional media-based enumeration. This results in lower abundance counts than are actually present in the sample. Therefore, the effects of salinity on the abundance of *E. coli* observed here may be underestimated [99]. Some authors argue that the state of VBNC does not occur in river water and soils [274] as cells are not able to be resuscitated, however, some species and strains adopting the VBNC state can remain virulent [275].

Low salinity at MM during summer highlights the importance of salinity as this coincided with unusually high *E. coli* abundance for the season. Hyper-saline conditions were observed occasionally during spring and summer at MS (data not shown) resulting in two of the lowest *E. coli* abundances throughout the year. High salinity at MS however also suggests higher dilution factor by seawater during low river flow conditions. In the regression model where variables were limited to biogeochemical only, salinity alone explains 46.9 % of the variance of *E. coli*. This result is based on a much reduced dataset caused by missing data for organic C, total C and total N analysis; however, the model does highlight the importance of the distinction between sites provided by particle size variables, and the distinction between seasons from salinity. The sand site selected in the Ythan estuary for the intensive sampling regime is unusually low down the salinity gradient for the particle size distribution, resulting in the non-significant correlation between salinity and particle size for the combined intensively sampled Ythan estuary sites. However there was significant and moderately strong positive correlation between salinity and particle size distribution in the estuary transects.

3.4.1.3 Environmental sediment characteristics

As expected, temperature variables correlated highly with one another, as did the precipitation variables. Temperatures were lowest in winter, followed by autumn, whereas the lowest *E. coli* abundance was during spring and winter, with the highest observed abundance during autumn. Minimum air temperature and minimum grass temperature were not as strongly correlated to *E. coli* abundance as maximum air temperature (MAT), however MAT was not included in any regression model for the intensive sampling dataset, as there was a stronger effect of salinity between seasons, in addition to the strong distinction between sites provided by salinity. There was also a significant discrimination of *E. coli* abundance between seasons, but the effect was not caused by direct variation in temperature alone, hence its absence in the regression model.

Sediment shear strength was originally measured in order to identify the erosion potential of sediments (discussed further in Chapter 4). It became clear however that there was significant negative correlation between *E. coli* abundance and sediment shear strength over all sites, especially at MS. MS demonstrated the greatest variation in particle size throughout the year as it was positioned near the mouth of the estuary where intertidal sediments are more dynamic as they are more vulnerable to wave and tidally driven accretion and erosion. Shear

strength is positively correlated with the increase in consolidation of the sediment which reduces water content and increases bulk density [276, 277], so intuitively, lower water content and higher bulk density are likely to increase shear strength, an effect observed here in the correlations between these factors. Sediment shear strength was frequently featured in the models as it provides very good distinction between sites, however the relationship it has with sediment properties is complex, and the effect between seasons was not as strong as that of site. Bulk density was correlated with many of the same variables as shear strength, but bulk density correlates more strongly with particle size variables. The magnitude of difference between sites for bulk density was smaller than that for shear strength. The higher variation within seasons for shear strength than bulk density, and its earlier inclusion in the regression model suggests it explains more small-scale variability of *E. coli* within sites. *E. coli* abundance was shown to be highly seasonal, therefore the optimal regression model utilising only physical variables only explained 23 % of the variance of *E. coli* abundance.

3.4.2 Analysis of best subsets and multiple stepwise linear regression models explaining the spatial and temporal distribution of E. coli *at four intensively sampled sites in the Ythan estuary*

3.4.2.1 Intensively sampled sediments in the Ythan estuary

In the best subsets models, the substitution of variables between the best and second best models were often between very highly correlated variables, such as salinity and water content, organic content and fine particle proportion. The remaining substitutions involve 5-day cumulative precipitation that, although only having weak correlations with most physical and biogeochemical sediment characteristics, followed the same trend between seasons as *E. coli* abundance with the highest values during autumn, and lowest during spring. 5-day cumulative precipitation was also included as the final term in the all replicates regression model, and had a very low, but significant effect. In all cases, including the Eden estuary transect model, increased precipitation always had a positive effect on *E. coli* abundance. Increased rainfall introduces higher levels of *E. coli* into the estuary via increased surface run-off from land [125-127] creating higher concentrations available for flocculation with suspended particles. EPS and nutrient concentrations were significantly inversely correlated with rainfall which may have negated the effect of sustained rainfall that raises *E. coli* concentrations through increased run-off. Rainfall on exposed intertidal sediments has been

shown to destabilise intertidal cohesive sediments [278], with the authors suggesting a mechanism of this could be caused by a dissolution of EPS components that would decrease both EPS and nutrient concentrations in the sediment. This destabilisation may have resulted in lower *E. coli* abundances as surface sediments containing higher numbers of *E. coli* [255] had been recently resuspended, negating the impact of high rainfall to increase *E. coli* abundance. Furthermore, at lower salinities *E. coli* can desorb from sediments [24] leading to their resuspension (the mechanisms of which are discussed further in Chapter 6) which has been suggested to be a cause of high abundance of faecal coliforms in suspension following high rainfall [79].

When comparing predicted and observed values from the regression models, samples with very low observed *E. coli* were often predicted at a higher abundance, and samples with a very high observed abundance were often predicted lower. The model struggled to predict *E. coli* abundance at densities less than ~1.3, and higher than ~4.2 $\log_{10}$ CFU 100 g dry wt^{-1}. This may be because the model struggles to incorporate inactivation rates of *E. coli* within the sediment. There may be a threshold of unfavourable conditions for *E. coli* persistence that is reached and die-off is faster than in sediments with more favourable conditions, resulting in the over-prediction of *E. coli* abundance. Likewise, there may be an upper threshold that, when exceeded, allows *E. coli* to thrive in extremely favourable conditions resulting in the model predicting *E. coli* abundance at a lower value than observed.

The model for all replicates at each sampling event explained 60 % of the variance of *E. coli* abundance in intertidal sediments. This 5-term model can therefore be viewed as fairly successful, confirming the first hypothesis, despite shortfalls of model accuracy at the extremes of observed values. When the model is based upon means of the replicates the model accuracy improves to 71 % despite the loss of 5-day cumulative precipitation variable. However, by taking the mean of the replicate sampling points, resolution of small-scale variability is lost. This small-scale variability is important to understand the variation of *E. coli* within sites, but also variability of the erosion potential and sediment characteristics. Terms included in the models were all variables that served as a more complex proxy for one or more other possible variables, demonstrating that in order to predict *E. coli* abundance it is not necessary to measure many sediment characteristics, but only a select few that may co-vary with others.

These models will only be useful for estuarine environments, as coastal sediments out-with estuaries will not experience such variable salinity. However these coastal sediments are likely to be sandier sediments with a higher grain size and contain lower *E. coli* abundances. Models excluding salinity and environmental variables based on all replicates explain 38.4 % of *E. coli* variance in a 4-term model using water content, pH, bulk density and sediment shear strength (data not shown), which shows promise for the construction of reliable models of *E. coli* abundance in fluvial, lacustrine and coastal sediments.

Many of the variables discussed here as affecting *E. coli* abundance and distribution were similar to those affecting the spatial distribution of total bacteria at the Petpeswick Inlet, Nova Scotia [248]. Very strong positive correlations between total bacteria number and lower particle size distributions, organic carbon, and organic nitrogen content were identified, in addition to the strong correlation found here between organic carbon and organic nitrogen with smaller particle size distributions. Furthermore, the similarity of variables affecting distribution of total bacteria to those affecting *E.coli* suggests a more general accumulation of bacteria including FIOs, rather than a sediment-type dependant separation of the two. Sediment specific characteristics and environmental variables may then differentially affect the persistence of *E. coli*, leading to variation in abundance in different sediment types. The interaction of the native microbial community with *E. coli* is discussed further in Chapter 5.

3.4.2.2 Site and season-specific effects

In all regression models, the addition of site increased the overall variance explained in each model, but the increase was not as great as adding season individually. The combined effect of adding both site and season as factorial terms was always greater than adding season alone, but the variance explained only increased slightly. This can be observed in the predicted vs. observed values scatter plots where site nor season were added (Fig. 3.3.2), as there was season-specific variation around the 1:1 line, whereas samples within sites were more evenly distributed around the 1:1 line.

Adding season to the regression model for all replicates and averaged replicates improves the variance explained by roughly 10 %. This is a significant increase in the accuracy in the model, which suggests the variables measured here do not satisfactorily explain the seasonal variation

in *E. coli*. Furthermore, the effect of season had a weaker affect than site for all variables, whereas the effect of season was stronger than site for *E. coli*.

When the second hypothesis is considered; the small increase in variance explained when adding site as a factor is negligible, showing the model performs well regarding spatial variation of *E. coli* abundance. The increase in variance explained when adding season however is larger, suggesting further consideration of appropriate variables to be included to explain seasonal variation of *E. coli* abundance in the models is required. The regression model for individual replicates explains the site factor more successfully than the regression model constructed from the site means, perhaps caused by the individual replicates model explaining small-scale spatial variability between replicates more successfully, and this resolution is lost when using site means. As a result of the significant increase in the accuracy of the model after including the season factor, the second hypothesis cannot be accepted.

The environmental variables included in the model were expected to account for the seasonal variability of *E. coli.* Maximum air temperature and average sea temperature were both significantly inversely correlated with *E. coli* abundance, supporting research indicating that environmental persistence of *E. coli* is enhanced at lower temperatures [17, 77, 120]. However, the lowest abundance of *E. coli* (during spring) did not coincide with the lowest air or sea temperatures, which likely compromised their effects in the models. Sediment temperature was initially measured as part of the dataset but was removed from the analysis because of high fluctuation of several °C throughout the sampling day (data not shown). Average sediment temperature data may perform better in the models than maximum air temperature and sea temperature, as these would affect sediment temperature differently throughout the year and perhaps explain more of the seasonal variability.

Favourable conditions in the sediments during summer and autumn may allow accumulation of *E. coli* in all sediments, such as the high organic content, and low bulk density as a result of the accretion of fine particles during more settled environmental conditions. There could then be a delayed die-off during colder temperatures until spring where more frequent storm events over winter erode surface sediments also gradually decreasing the sediment-associated bacterial load. It is also worth noting that water-borne *E. coli* is highest during autumn (see Chapter 4), which would increase the concentration of *E. coli* attached to particles available for sedimentation. Faecal bacterial abundance in water has been shown to be highly seasonal and will influence the accumulation of *E. coli* in sediments. Fewer pathogens were isolated during

winter than spring, summer and autumn in lakes and rivers of south-west Finland [279], and there were significantly higher *E. coli* and enterococci concentrations in stream waters of Pennsylvania (USA) during summer than spring [280]. In addition to seasonal variation of shedding rates of pathogens [280], seasonal variation in the flow of run-off and streams will effect waterborne concentrations through differential resuspension and transport rates and subsequently influence the number of *E. coli* entering the estuarine system [247]. In addition, low temperature (at low salinities) has been shown to induce the VBNC state (as discussed earlier) in *E. coli* [281] that may have resulted in underestimated abundance during colder months.

The extent of deposition and erosion was not measured in this study. This may have explained some seasonal variation if there was net erosion of sediments during spring as *E. coli* abundance decreases with sediment depth [255]. If surface sediments had been recently eroded during late winter and spring, *E. coli* abundance in the new surface layers would have been reduced. In Northern estuaries, there is generally increased erosion and transportation of intertidal sediments during the winter months [282]. There are factors that influence net erosion or deposition of sediments that were not measured in this study, including disturbance events such as high current speeds and wind-driven wave action. However, many sediment properties that affect sediment erodibility were measured, such as particle size, organic content and EPS content [283], in addition to the cohesive strength meter and shear vane directly measuring erosion potential. The problem with using the erosion potential in explaining *E. coli* abundance is that the measurement is taken after the event, so erosion potential of the new sediment surface layers will not reflect what has been eroded. Sediment shear strength correlated well with *E. coli* abundance, and was featured frequently in the models, which is more likely a cause of its high correlation with particle size variables.

3.4.2.3 Estuary transect models

The regression model constructed on the datasets for the estuary transects had a resemblance to those constructed for the intensively sampled sites. Salinity was an important variable once again, presumably as it gives insight to the spatial trends of sediment characteristics such as particle size distribution down the estuary, as well incorporating fluctuations in temperature as discussed earlier. In the Eden estuary however, proportion of fine particles was the first term included in the regression model, but is still indicative of the salinity gradient as particle size

variables correlated well with salinity. pH did not appear in the regression model or the best subsets models for the intensively sampled datasets, but was included in the Eden transect, Ythan transect and the combined transects regression model. pH correlated strongly with salinity in the intensively sampled sites in the Ythan estuary, however there was no significant correlation between the two variables in the transect datasets, despite there being correlation between more basic pH and larger particle sizes. There was a significant moderately strong correlation between pH and *E. coli* abundance in the transect datasets, suggesting sediments with an interstitial water of a more neutral pH provide a survival advantage compared to a slightly basic pH. pH has been demonstrated to heavily influence survival of *E. coli* in seawater, with 19.4 %, 2.5 % and 0.4 % survival after 48 hours at pH 6, 7 and 8 respectively [114]. Variability of pH in sediments may be a result of the pH of the incoming river water, the pH of the river Ythan varied between 6.6 and 7.9 in 2012 – 2013 [284], and between 7.5 and 8.2 in the river Eden [285]. Also, pH variation in estuarine water can be a result of biological activity from different trophic groups [286], and in algal mats photosynthesis can increase pH to around 10 during the day, whilst respiration at night can decrease pH to around 5.5 [287].

Colloidal carbohydrates were included in all estuary transect regression models, but were absent in the models for the intensively sampled dataset. Higher levels of EPS are indicative of the extent of biofilm formation in the sediment, and *E. coli* has been shown to be in higher abundance in natural river [170] and marine [288] biofilms than the surrounding water. The interaction between colloidal carbohydrates and enterococci was investigated by Piggot et al. (2012), and was discovered to be a non-linear relationship. The authors suggest that moderate biofilm presence enhances enterococci persistence through the protective micro-environment provided by the biofilm, however at high biofilm presence, enterococci are out-competed by native biota, thus decreasing their abundance [289], consistent with other studies identifying out-competition by native microbiota [290]. EPS variables may not have been influential enough to be included in the models for the intensively sampled dataset as a result of this complex relationship.

Temperature variables were included in the optimal transect regression model for both estuaries whereas they were absent in the regression model for the intensively sampled datasets (with the exception of the environmental variables only model). Increasing minimum air temperatures had a negative effect in the Eden estuary model whereas maximum air temperature, added later in the model, had a positive effect. This relationship was inverted in

the Ythan estuary model, and when the estuary datasets were combined, only a negative effect of maximum air temperature was included. This implies a complex relationship with the various temperature variables used in the analysis, further suggesting that average sediment temperature may reveal a more explicit relationship.

3.4.3 Efficiency of constructed models predicting **E. coli** *abundance in other estuaries*

The optimal regression model for the Eden estuary transect dataset was more predictive than the Ythan estuary. More terms were included in the model for the Eden estuary, specifically the proportion of fine particles, and precipitation variables. It is possible that with a larger sampling effort these variables may be significant in the Ythan estuary also, increasing the model accuracy, although as only 4 sampling events were conducted (seasonally), much of the effects of precipitation and other environmental variables may not have been successfully captured. However, only 5-day cumulative precipitation was added to the optimal regression model where samples were taken monthly, and added as a final term with negligible increase in variance of *E. coli* accounted for, so the effects of precipitation may be site or sediment type-specific within the estuary.

A common shortfall in all the models constructed in this study was that *E. coli* abundances below 1.5 $\log_{10}$ CFU 100 g dry wt^{-1} were not predicted accurately. Over prediction of these values will have been a major factor in decreasing the variance accounted for by the regression model. This abundance of *E. coli* equates to roughly 1 CFU in 3 g of dry sediment, which could be argued as a non-hazardous sediment, as when even large amounts of sediment is resuspended, it would have a negligible impact on waterborne *E. coli* concentrations compared to other sediment types. CFU counts at this abundance in sediment will also be highly variable between samples taken only several centimetres apart, especially if FIOs originate from sources directly introduced on the sediment such as bird faeces. The distribution of organisms in sediment is also known to be 'patchy' compared to overlying water [83]. In order to produce more accurate predictions for such sediments, a high number of replicate samples should be analysed in order to produce a more accurate measure of abundance which may result in better model prediction. Furthermore, as these sediments contain such a low abundance of *E. coli*, it would increase the predictive power of the models if *E. coli* abundances under a certain threshold were discounted from the model. An abundance of 2 $\log_{10}$ CFU 100 g dry wt^{-1} is suggested as the models were more accurate above this level and this equates to 1 CFU 1 g dry

wt^{-1}, which can still be viewed as a relatively non-hazardous sediment, especially as some sediment types in both estuaries often exceeded 4 log_{10} CFU 100 g dry wt^{-1}. If the 'Poor' EU bathing water quality classification [7] is converted from 100 ml^{-1} of water to 100 g dry wt^{-1} sediment, it would equate to 2.6 log_{10} CFU 100 100 g dry wt^{-1}. This would result in many sediments in the Eden and Ythan estuaries exceeding the 'Poor' classification. However, this conversion is suggested with caution as, presently, there are no sediment microbial quality classifications, and they are unlikely to be directly transferrable in this way due to differences in exposure and infection pathways.

The optimal regression model for both estuaries combined explained only slightly less of the variance of *E. coli* than the regression model for the Ythan estuary only, suggesting there is potential for successful models that can apply to several sites rather than being estuary-specific. This is relevant to the second hypothesis, although previously rejected, the combined estuary model contains variables that can successfully predict *E. coli* abundance across different estuarine systems. This only shortfall in the success of the optimal models to be generic is that of seasonal specificity. However, only 48.7 % of the variance of *E. coli* abundance is explained by the combined estuary model, suggesting there may be variables not measured in this study that could further enhance the model accuracy in addition to solving the issue of sediments with very low abundances.

The number and flow volume of tributaries entering the estuary was not accounted for in this study. Tributaries may carry elevated FIO loadings depending on their sub-catchment, and would influence *E. coli* abundance in nearby sediments. Proximity of sediments to input sources of pollution has been shown to be a significant driver of spatial distribution of faecal coliforms in freshwater sediments when the source was sewage outfall [21] and waste water treatment plant effluent [22]. Also, incorporating an average tidal exposure may be beneficial. The longer a sediment bed is exposed, the longer *E. coli* from diffuse sources such as animal faeces will have to form irreversible attachment to sediment particles, whereas they would be transported away from the site if the sediment bed is submerged. Conversely, the longer sediments are submerged, the more sedimentation of particles in the water column and any associated *E. coli* could occur, increasing the abundance in the sediment. *E. coli* in wave-exposed freshwater sandy beach sediment was shown to increase towards the water line [291], however at seawater beaches in Hawaii, abundance of enterococci further from

backshore sediment was often of higher abundance to that of fore and near-shore sediments [292], a trend also observed in sandy beaches in Florida [289].

Furthermore, the combined estuary regression model over-predicts many Ythan estuary samples and under-predicts many Eden estuary samples. To resolve this, an estuary-specific constant could be included in a model applicable to multiple estuaries that accounts for a general shift in *E. coli* abundance. This value may originate from existing data on waterborne *E. coli* concentrations entering the estuary from the main river, or may be only applicable after preliminary sampling if *E. coli* originates from other sources, such as wildfowl numbers or livestock within the direct estuary catchment.

3.4.4 Conclusions

It is accepted that the models constructed here using selected environmental and sediment characteristic variables will not explain 100 % of the variation in *E. coli* abundance, as there were many other contributing factors. The proportion of *E. coli* variation explained was 87.4 % and 49.8 % for the individual Eden and Ythan estuaries respectively, and 48.7 % for both estuaries combined. It was the aim of this chapter to identify the driving factors influencing variation in the abundance of faecal bacteria in intertidal sediments. The models presented here not only demonstrate to what extent *E. coli* abundance is dependent on sediment characteristics and environmental variables within and over multiple sites, but also indicate which variables were most influential. Prior to this investigation, the cumulative effect of sediment characteristics on the variability of *E. coli* abundance was largely unknown; therefore there was an inherent uncertainty when incorporating resuspension from sediments in water quality models. A model that can predict *E. coli* abundance in intertidal sediments of different estuaries very accurately, such as >90 % of the variability, combined with models concerning resuspension and release of *E. coli* to the water column would be a powerful tool in the regulation of bathing water safety allowing for improved accuracy of real-time water quality prediction.

The data presented here provide a valuable insight into the complex relationships between sediment characteristics and *E. coli* distribution that will aid future predictive modelling of *E. coli* abundance in estuarine sediments and their subsequent effects on water quality. *E. coli* abundance in 4 distinct sediment types was successfully explained using multiple stepwise

linear regression models. Biogeochemical variables were more important than other variable types, with salinity being the most important individual variable. There were weaknesses in the final models however, as the factorial effects of site and season were still apparent, in addition to inaccuracies of predicting *E. coli* abundance at the extremities of the ranges observed. A combination of selected physical, biogeochemical and environmental variables can be used to predict *E. coli* abundance in different estuarine systems, but the variance explained is not as high as models constructed for specific sites. The addition of an estuary specific constant may be of use to increase accuracy of further models across multiple estuaries.

The first hypothesis: E. coli *abundance in the Ythan estuary can be predicted using sediment characteristics and environmental variables* was confirmed as the regression model for the intensively sampled sites explained 60.0 and 71.0 % of the variability for the 'all replicates' and 'replicate means' models respectively. These models were viewed as successful as they explained a larger proportion of the variability that may be explained by other variables, though weaknesses were identified which could be corrected to improve model accuracy.

The second hypothesis: *Explanatory models of the variation of* E. coli *with sediment characteristics and environmental variables are generic* was rejected as the variance explained by the model increased when adding the factorial terms to the optimal regression model. This indicates that the variability of *E. coli* in intertidal sediments explained by sediment characteristics (site) and environmental factors (season) was not entirely captured by the variables measured. However, the models were successful in explaining variability of *E. coli* across multiple sites. Although the optimal regression model for both estuaries combined explained only 48.7 % of the variability of *E. coli* abundance, it was almost as successful as the model explaining variation in abundance in Ythan estuary alone. Also, several variables featuring in the individual estuary regression models were common between the Ythan and Eden estuaries.

4. Assessing the resuspension risk of FIOs from intertidal sediments

4.1 Introduction

4.1.1 Resuspension of FIOs from intertidal sediments

Faecal bacteria in estuarine sediments do not pose significant risk to human health until they are resuspended into the water column. This can be through a) mass erosion where sediment beds are eroded during storm conditions, or b) small scale erosion from tidal or current shear forces entraining the uppermost layers of the sediment [293, 294]. Whatever the erosive mechanism, the risk of disease increases once faecal bacteria are resuspended as there is more likely to be human contact with pathogens in surface waters than deposited sediments. Once in the water column, tidal currents may transport suspended bacteria away from contaminated sites to areas where the likelihood of human contact is increased, such as bathing waters and sandy beaches. However, predicting this erosion is problematic since the stability of intertidal sediments can be site- specific [294], with many driving factors including the hydrodynamic setting, sediment characteristics such as particle size and bulk density [283, 295, 296], plus biological factors such as EPS content, macrofaunal activity, and biofilm formation [197].

4.1.2 Factors affecting the stability of intertidal sediments

The physical characteristics of sediment heavily influence sediment stability. Estuarine sediments can be divided into two groups with very different erosional behaviour: cohesive and non-cohesive sediments. The erosion dynamics of natural cohesive sediments is discussed in more detail in Chapter 1 (Section 1.11). Briefly, in sediments consisting of particle sizes >63 µm particle size becomes less critical than inter-particle cohesion. Whereas in sediments with particle sizes <63 µm stability increases with smaller particle sizes. If there is a >10 % fraction of fine particles (<63 µm), sediments start to display these cohesive properties resulting in higher sediment stability [182].

The measurement of sediment properties related to stability is complex, and two properties are often measured: the shear strength and surface stability [296, 297]. Sediment shear strength is a measure of the internal strength of the sediment, often measured as the internal resistance to torque, and is used as an indicator of its susceptibility to mass erosion. The

surface stability is the resistance of sediments to small scale erosion that is regarded to be the dominant form of sediment transport within tidal waters [192]. It is worth noting however that cohesive and non- cohesive sediment can both be susceptible to mass and small- scale erosion. Shear strength typically increases in sediments with increased packing and consolidation, and therefore increased bulk density, and a related decrease in water content [296, 298]. Shear strength has been shown to be affected by increase in sediment tidal exposure time, and high evaporation of near-surface interstitial water that results in a 'hardening' in the surface layers [299]. Biological variables also affect shear strength, but perhaps to a lesser degree; extracellular polymeric substances (EPS) have a significant effect on the shear strength of sediments [296], the mechanisms of which are discussed in more detail below. Also, burrowing by macrofauna can compact sediments and increase water drainage, increasing sediment stability [197].

A comprehensive review of variables affecting the stability of cohesive sediments was provided by Grabowski et al. [283], where a number of physical, biogeochemical and biological variables were discussed, and their relative importance found to be site-specific. Briefly, sediment stability increases with an increase in median particle size [300] and an increase in clay content [301]. However, above 30-50 % clay content, sediment stability is assumed to decrease due to a decrease in bulk density [283]. Sediment organic content, despite often directly correlating strongly with water content and a decrease in bulk density [302], can also be a key driving factor, with dissolved organic matter increasing particle-particle adhesion [283]. An increase in organic content may also represent an increase in EPS [303]. Organic matter can also provide a physical barrier on the surface of sediments [304]. Salinity has been demonstrated to increase sediment stability in estuarine sediments [305], by enhancing the cohesive attraction between particles and EPS molecules [306].

Previously, physical and geochemical factors were viewed as most important in influencing sediment stability [189, 190], partly due to the difficulty in categorising and quantifying biogenic influences [191]. More recently the influence of biology on sediment stability such as the actions of bacteria [151, 152] diatoms [192, 193], invertebrates [194], and macrofauna [195] has been demonstrated, and the importance of micro-organisms recognised [181, 196]. The effects of macrofauna can be described as 'bioturbation, biostabilisation or biodestabilisation' [197], but the impact of an individual organism can differ depending on population numbers, individual size, activity, and interaction with the rest of the community

[283]. Perhaps the most widely researched factor affecting the stability of sediments is that of EPS [168, 181, 197, 234]. Microalgae are the primary source of EPS in intertidal mudflats [307], with diatoms supplying roughly 40 % of microalgal primary production [168]. Diatoms exude mainly carbohydrates, whereas many bacteria produce mostly protein [308], which together are the main constituents of EPS. The primary mechanism of stabilisation by EPS is that it forms a cohesive network by covering particles and spanning gaps between them with cohesive material [197], physically binding a sediment and increasing the erosion threshold [192].

4.1.3 Current modelling of resuspension of FIOs

Models predicting concentrations of waterborne *E. coli* have progressed to the inclusion of sub-models accounting for resuspension of *E. coli* from underlying sediments [247]. However, there is much uncertainty surrounding the issue. Current models utilise set parameters to simulate a critical shear stress that, when exceeded, account for the resuspension of bacteria from sediments. The value used for this parameter varies between 0.02 (for fine coastal bay sediments [309]) to 1.7 N m^{-2} (streambeds [185]). Yang et al. (2008) introduced a differential critical shear stress for cohesive and non-cohesive types of estuarine sediment to improve model accuracy for predicting enteric bacterial resuspension, however the critical shear stress for sediment erosion is based upon particle size without consideration of biological factors [310]. Erosion thresholds of intertidal sediments have been shown to vary both between [294] and within [296] sediment types and has been described as patchy, with high variability [191]. This presents problems for the modelling of sediment resuspension and transport [191], but furthermore, it results in great difficulty in combining the stability of sediments with the variability of *E. coli* abundance. However, if there is a strong relationship between *E. coli* abundance and stability, or at least identifiable trends within the variation, predicting the amount of *E. coli* resuspended into the water column using a combination of environmental and sediment characteristics may be more achievable. Otherwise, using current models, the number of *E. coli* resuspended into the water column from a particular sediment may be severely over- or underestimated.

A more simplistic means of informing bathing water regulation is to identify spatially and temporally explicit sediment types that combine high abundance of *E. coli* with a low erosion threshold, as they pose the highest risk of releasing faecal bacteria into the water column.

When these types of sediments arise or are identified, bathing in these waters can be advised against, or restricted.

4.1.4 Relationships between FIO populations in sediments and overlying water

Generally, the correlation between abundance of FIOs in sediments and the overlying water in a range of systems has been found to be weak [247]. This is perhaps intuitive because of the dynamic nature of the overlying water compared to relatively static sediment, as any resuspended sediment and associated bacteria are swiftly removed downstream away from the sediment origin. The genetic similarity of *E. coli* strains in the water column to those in spatially-corresponding sediments was observed to be lower at upstream sites than downstream sites in the Thomas Brook watershed (Nova Scotia, Canada), and a genetic similarity of 39 % was observed between *E. coli* at downstream sites and upstream sediments [311]. A similar pattern was observed in the Blackstone River watershed (MA, USA) by Wu et al. (2009) where, of the *E. coli* ribotypes of the strains at downstream sites that matched with upstream samples, 75 % matched with upstream sediments rather than the upstream water column. These studies highlight both the relevance of upstream *E. coli* abundance and stability of sediments, and the impracticality of using waterborne *E. coli* abundance to predict abundance in sediments.

4.1.5 Hypotheses and aims

In order to utilise the information gathered on the abundance of *E. coli* in intertidal sediments to predict abundance in the water column, the likelihood of the resuspension of the sediment and its associated bacterial load must be considered. Factors that influence spatial and temporal trends of *E. coli* abundance in intertidal sediments were investigated (Chapter 3), in this chapter, patterns between the erosion resistance of the sediment and FIO abundance in sediments and the water column are explored. The aim was to investigate whether intertidal sediments with a high risk of supplying a large number of faecal bacteria can be identified by combining erosion thresholds and *E. coli* abundance

The following hypotheses were tested in this chapter:

a) ***Sediments that pose a risk to human health through easily-resuspendable faecal bacteria can be spatially and temporally identified by combining* E. coli *abundance and sediment stability measurements.***
b) **E. coli *abundance in the overlying water will correlate with the abundance of* E. coli *in sediments.***

4.2 Materials and methods

The majority of methods used in this chapter are described in the general materials and methods (Chapter 2). Likewise, the statistical analyses performed for this chapter are described in Chapter 3 (Section 3.2.2). Other relevant methods are described here.

4.2.1 Culture-based enumeration of FIOs from water samples

To compare coliform and *E. coli* concentration in the water column to the concentration in sediments, water was sampled from the main estuarine channel at the shortest distance from the corresponding sediment sample. Water samples were taken in 250 ml sterile vessels at knee depth, with care taken to sample upstream as to not include sediment disturbed when entering the water. On return to the laboratory, a non-diluted 100 ml sample and a 1: 99 dilution with sterile water sample were enumerated using the IDEXX Colilert technique described in General Methods 2.7. Either the direct, or the diluted sample were readable in the IDEXX Quanti-tray/2000. Where the direct enumeration tested positive in all of the wells of the tray (above the maximum detection limit), the reading from the diluted sample was taken and multiplied by 100 to adjust the resulting concentration to CFU 100 ml^{-1}. Coliform and *E. coli* concentrations of the water column are expressed as log_{10} CFU 100 ml^{-1}.

4.2.2 Statistical analyses

Data manipulation, Spearman's rank correlations, analysis of variance and the plotting of treatment means were performed as described in Section 3.2.2.

Linear regression: Simple linear regression analysis was performed in Genstat (VSN International, v17.1) between *E. coli* abundance in sediments, and sediment stability and shear strength measurements in order to establish high-risk sediments. Linear regression was also performed on *E. coli* and coliform abundance in sediments against abundance in the water column. In order to identify sediments with high *E. coli* abundance and low erosion resistance, scatterplots were constructed in Sigmaplot (v13.0, Systat Software Inc., CA, USA) between sediment *E. coli* abundance and measures of erosion resistance.

4.3 Results

4.3.1 Spatial and temporal variation of sediment stability variables in the Ythan estuary

Sediment shear strength was greatest at MS followed by MM>S>M, all of which were significantly different from each other (p= <0.001; Table 4.3.1). Shear strength was also greater during spring and autumn than summer and winter (p= <0.001; Table 4.3.2). Shear strength at M and S did not vary widely throughout the year, but there was a general decrease from summer to winter (Fig. 4.3.1A). At MM, shear strength was significantly greater during autumn than other seasons, during which it did not significantly differ (p= <0.001; Table A10; Fig. 4.3.1A). Shear strength at MS was highly variable between seasons, with the greatest shear strength observed during spring, which was significantly greater than autumn, which in turn was greater than all other sediment-season combinations (p= <0.001; Table A10; Fig. 4.3.1A).

Sediment stability was greater at MS and MM than M (p= <0.001; Table 4.3.1). No sediment stability data was recorded at S because of the porous nature of the sediment. Data is also absent for MM during summer because of seasonal growth of macroalgae at this site that obscures the sediment. Sediment stability was greater during spring than winter and autumn, and stability during summer was not significantly different than any other season (p= 0.024; Table 4.3.2). Sediment stability at M was significantly greater during spring and summer than during autumn (p= <0.001; Fig. 4.3.1B), and at MM was highest during spring and autumn (Fig 4.3.1B). Sediment stability at MS was greater during winter than all other sediment-season combinations except MM during spring (p= <0.001).

Table 4.3.1 ANOVA summary table for the one-way analysis of the effect of site (blocked by season) on sediment shear strength and stability at four sediment types in the Ythan estuary. Significantly different groups obtained using Fisher's LSD test are displayed in brackets under the *p*- value. Single asterix (*) denotes analysis run with 'general ANOVA', allowing prediction of missing values.

		Mud	Mixed Mud	Mixed Sand	Sand	F- Statistic	*p*- Value
Sediment Shear Strength (kPa)	Group Mean	3.55	8.38	13.12	5.00	178.48	<0.001 (MS>MM >S>M)
	Group Standard Deviation	1.36	2.27	4.55	2.36		
	Replicates (n)	78	78	72	78		
Sediment Stability* (Nm^{-2})	Group Mean	11.16	18.63	23.35	-	12.85	<0.001 (MS,MM >M)
	Group Standard Deviation	9.63	16.34	20.08	-		
	Replicates (n)	78	78	78	-		

Table 4.3.2 ANOVA summary table for the one-way analysis of the effect of season on sediment shear strength and stability at four sediment types in the Ythan estuary. Significantly different groups obtained using Fisher's LSD test are displayed in brackets under the *p*- value. Single asterix (*) denotes analysis run with 'general ANOVA', allowing prediction of missing values.

		Spring	Summer	Autumn	Winter	F- Statistic	*p*- Value
Sediment Shear Strength (kPa)	Group Mean	8.63	7.14	8.43	6.36	10.19	<0.001 (Sp,A>Su, W)
	Group Standard Deviation	6.01	3.45	4.59	3.98		
	Replicates (n)	72	72	48	114		
Sediment Stability* (Nm^{-2})	Group Mean	21.63	19.82	12.15	15.39	3.24	0.024 (Sp>W,A)
	Group Standard Deviation	14.41	12.12	12.99	19.38		
	Replicates (n)	49	24	34	64		

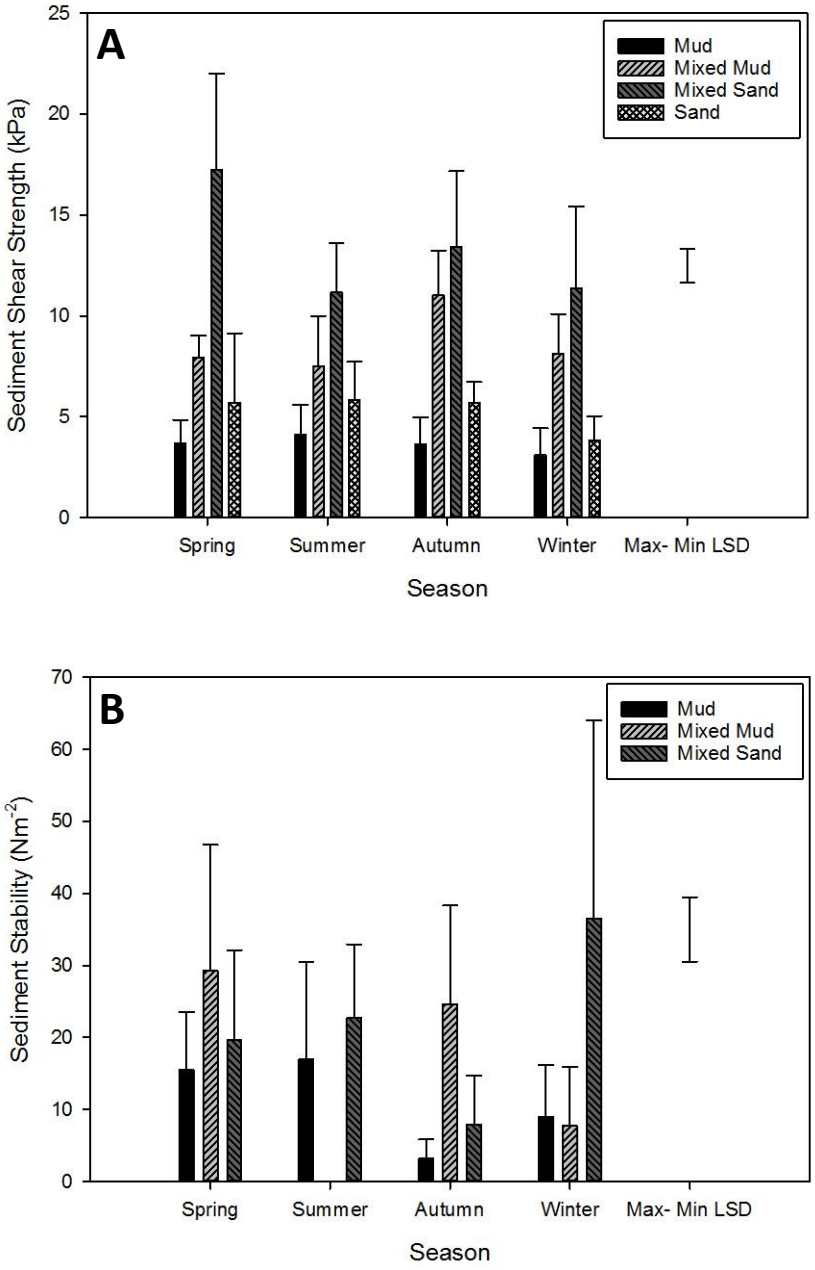

Figure 4.3.1 Means plot from the two- way ANOVA (Site x Season) for sediment shear strength (A) and sediment stability (B) at four sediment types in the Ythan estuary. Error bars denote standard error from the mean. In both: solid fill bars- Mud; light-grey dashed bars- Mixed Mud; dark-grey dashed bars- Mixed Sand; hatched bars- Sand. Sediment stability measures are absent in Mixed Mud during summer, and Sand during all seasons.

4.3.2 Co-variance of sediment stability variables and other measured variables in the Ythan and Eden estuaries

Sediment shear strength and sediment stability did not correlate strongly over all intensively sampled sites (Fig. A9), with only weak negative correlation at MS, and no correlation at M and MM and for the transect datasets (Figs. A7, A5 and A6 respectively).

Larger particle sizes and increased bulk density correlated significantly with an increase in shear strength and stability over all intensively sampled sites, as did particle size variables with shear strength in the Ythan estuary transect (Fig. A10), and both estuary transects combined (Fig. A12). Within individual sites, there was no correlation between sediment shear strength and particle size variables or bulk density at M and MS (Figs. A5 and A7 respectively), however at S, sediment shear strength increased with lower bulk density and increased proportion of fine particles (Fig. A8). Over all intensively sampled sites, water content and organic content were negatively correlated with shear strength and stability, however within site M, sediments demonstrated no correlation between shear strength and organic content, and at S, organic content was positively correlated with increasing shear strength, but decreasing stability. No significant correlations were observed at MM (Fig. A6), MS and the transect datasets.

Amount of colloidal carbohydrates was positively correlated with an increase in shear strength at M, MS and S, with no correlations in all other datasets. Colloidal carbohydrate was positively correlated with an increase in sediment stability at M, MM and for the Ythan and Eden (Figs. A10 and A11 respectively) transects individually. The pattern for correlations with colloidal proteins was different to that of colloidal carbohydrates, with positive correlation with an increase in shear strength at M and S, but a negative correlation over all intensively sampled sites, and the Ythan estuary transect. Colloidal proteins were positively correlated with sediment stability at MM, and for both estuary transects individually. Shear strength had a strong negative correlation with organic carbon, total carbon and total nitrogen at MM, whereas at S there was a moderately strong positive correlation with total carbon and total nitrogen. Over all intensively sampled sites, there was negative correlation between both shear strength and stability and all nutrient variables except sediment stability with total nitrogen (non-significant). At MS, there was a strong negative correlation between sediment stability and a lower carbon/ nitrogen ratio.

An increase in interstitial water pH was correlated with decreasing shear strength and stability of sediments over all intensively sampled sites, however within individual sites this was only observed in MM, and there was a correlation with shear strength only in MS. There was no significant correlation between pH and sediment stability variables in the transect datasets. Interstitial water salinity was positively correlated with shear strength at MS and S, over all intensively sampled sites, the Ythan estuary transect and both estuary transects combined. The relationship between salinity and sediment stability over all intensively sampled sites, within MM and the Eden estuary transect was a positive correlation, whereas over the Ythan estuary transect the correlation was negative.

There was only very weak or no correlations between environmental variables and sediment stability variables over all the intensively samples sites and the Ythan transect, however in the Eden estuary, sediment stability correlated with increased minimum air and grass temperature (Fig. A11).

4.3.3 Correlations between **E. coli** *abundance and sediment stability variables*

E. coli abundance and sediment stability variables only correlated significantly at MS, where the relationship between *E. coli* and shear strength was moderately negative, and over all intensively sampled sites, where both shear strength and stability were weakly negatively correlated. There was no correlation for the Eden estuary, but in the Ythan estuary transect there was a weak negative correlation with shear strength.

4.3.3.1 Intensively sampled sediments in the Ythan estuary

There was negligible linear correlation between sediment *E. coli* abundance and shear strength or sediment stability (sediment shear strength: Adjusted R^2= 0.075, p= <0.001; sediment stability: Adjusted R^2= 0.016, p= 0.053). However, sediments with high *E. coli* abundance and low erosion resistance were identified (Fig. 4.3.2). High *E. coli* abundance combined with low sediment shear strength and stability is observed at M sediments during autumn and winter, as at MM sediments during winter with low sediment stability. S sediments during winter exhibit low sediment shear strength and moderate *E. coli* abundance.

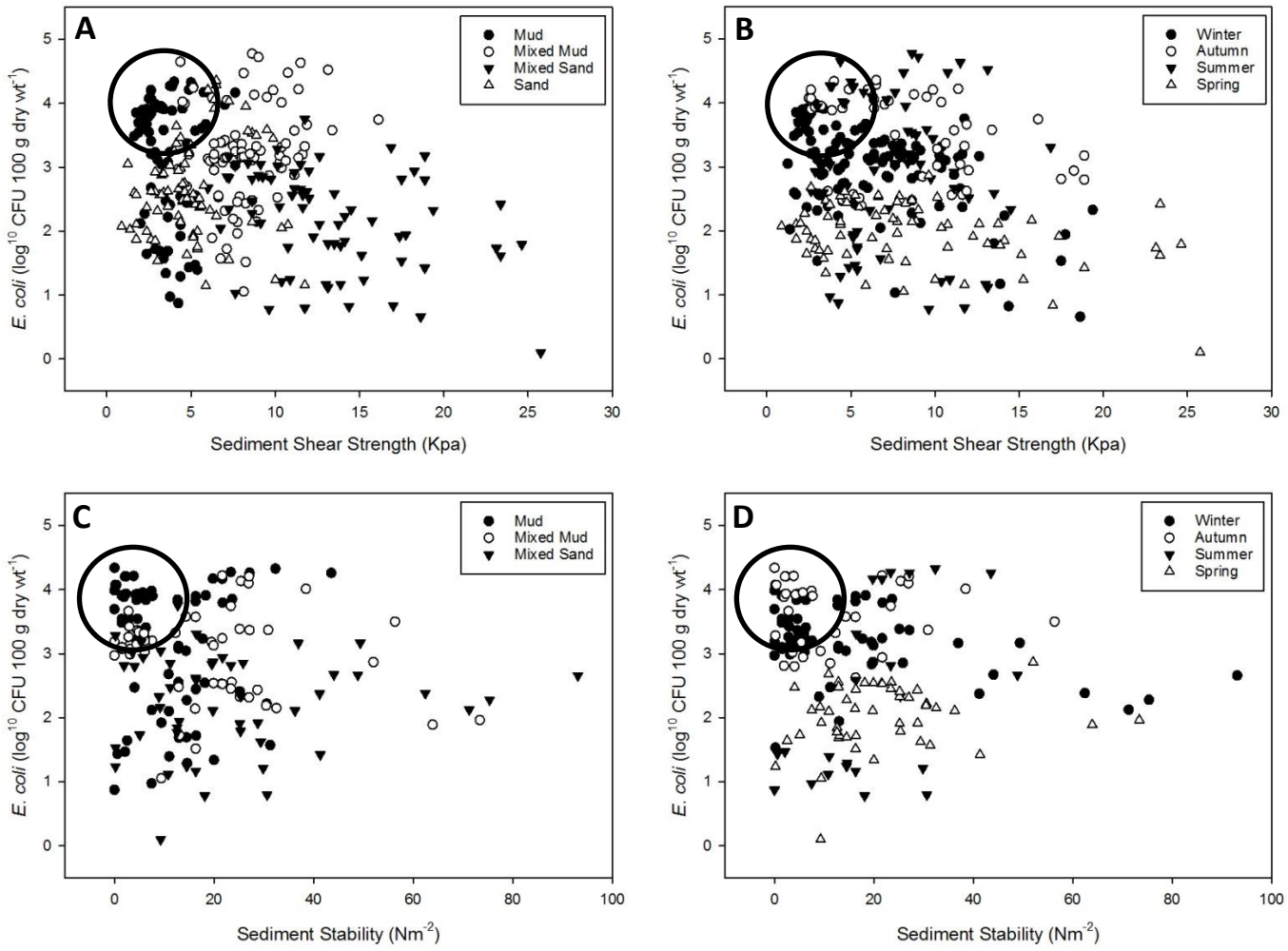

Figure 4.3.2 Scatterplots of observed *E. coli* abundance vs. sediment stability variables for intensively samples sites in the Ythan estuary. Plots A and C: solid circles- Mud; hollow circles- Mixed Mud; solid triangles- Mixed Sand; hollow triangles- Sand (plot A only). Plots B and D: hollow triangles- spring; solid triangles- summer; hollow circles- autumn; solid circles- winter. Circles highlight samples with high *E. coli* abundance and low erosion resistance.

4.3.3.2 Ythan and Eden estuary transects

Low shear strength and stability combined with high *E. coli* abundance was observed at upper-estuary sites (sites 1-3) in both estuaries, and most frequently observed during summer and autumn, with some occurrence of low sediment stability during winter (Fig. 4.3.3). In the Ythan estuary, sediments with a moderate *E. coli* abundance and low shear strength were distributed throughout the estuary, and observed during all seasons except winter. Sediments with low stability were distributed throughout the upper to mid-lower reaches of both estuaries, and

less frequently observed during spring than other seasons (Fig. 4.3.4). Sediments during spring typically demonstrated low sediment stability, but *E. coli* abundance was generally low.

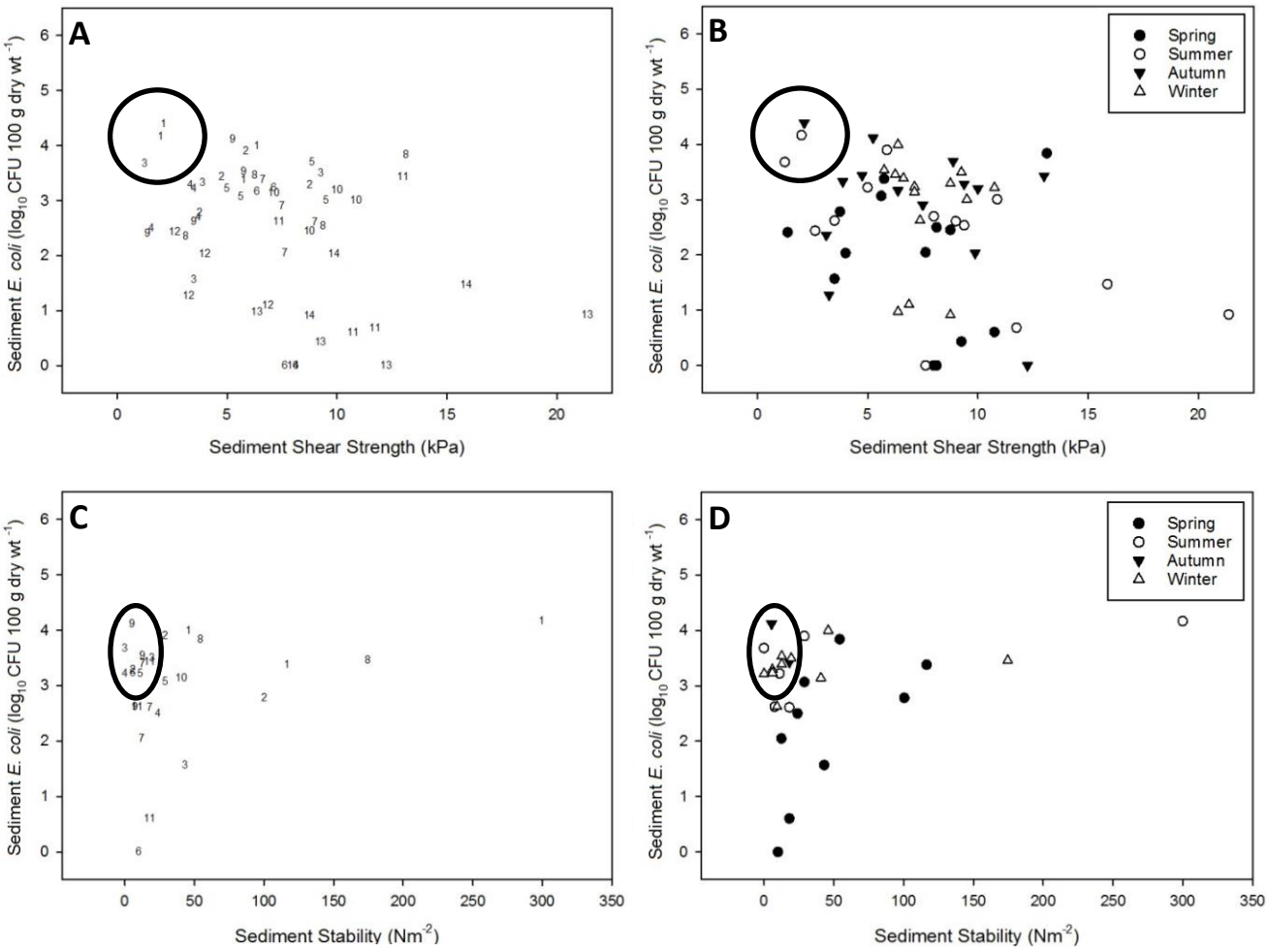

Figure 4.3.3 Scatterplots of observed *E. coli* abundance vs. sediment stability variables for the Ythan estuary transect dataset. Plots A and C: numbers denote sampling position within the estuary. Plots B and D: solid circles- spring; hollow circles- summer; solid triangles- autumn; hollow triangles- winter. Circles highlight samples with high *E. coli* abundance and low erosion resistance.

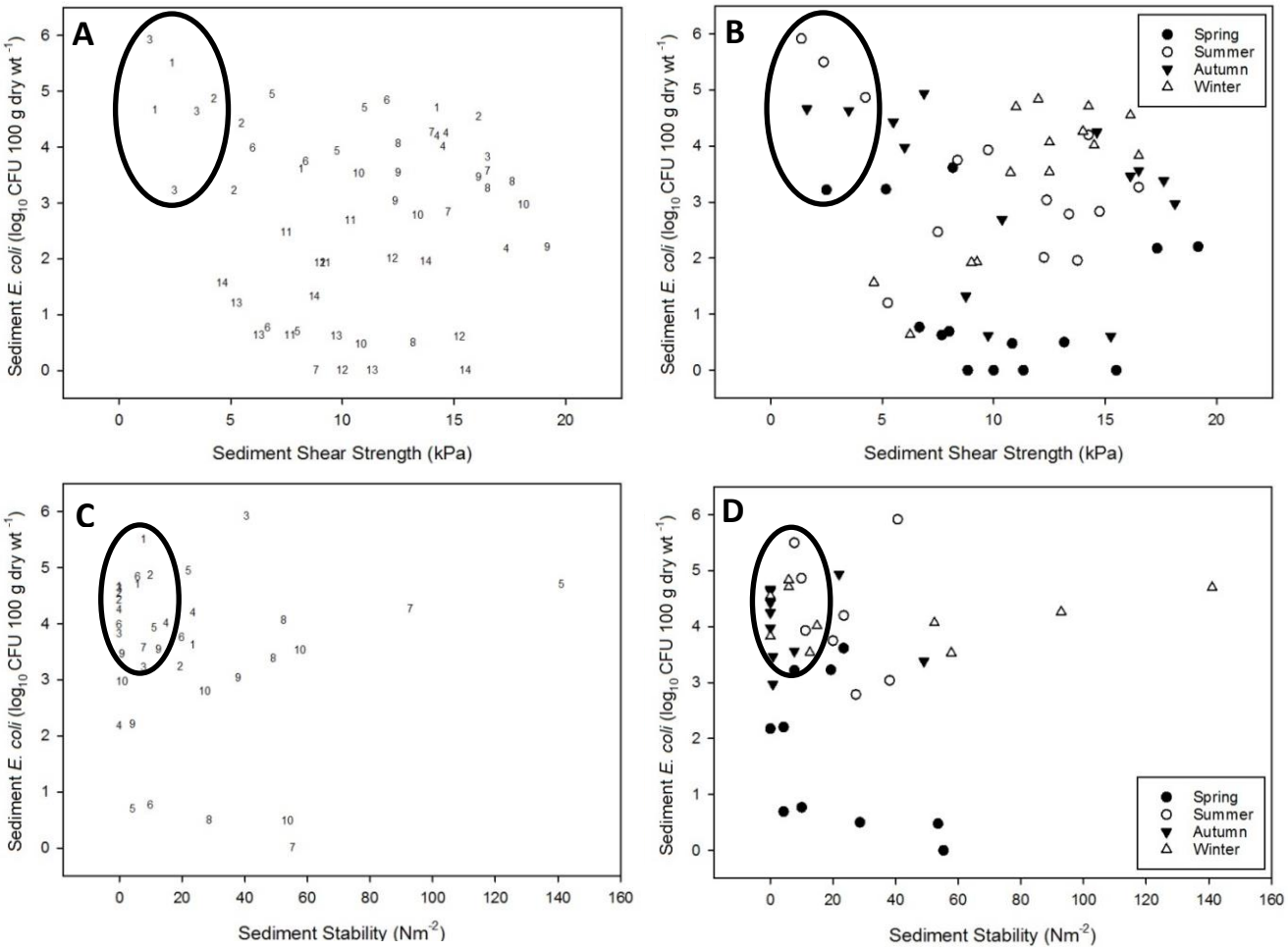

Figure 4.3.4 Scatterplots of observed *E. coli* abundance vs. sediment stability variables for the Eden estuary transect dataset. Plots A and C: numbers denote sampling position within the estuary. Plots B and D: solid circles- spring; hollow circles- summer; solid triangles- autumn; hollow triangles- winter. Circles highlight samples with high *E. coli* abundance and low erosion resistance.

4.3.4 Correlation of FIO abundance in sediments and the water column

Abundance of *E. coli* in waters throughout the Ythan estuary, and towards the head of the Eden estuary often exceeded the 'sufficient' classification standard for transitional waters of 500 CFU 100 ml^{-1} (2.69 log_{10} CFU 100 ml^{-1})[312] (Figs. 4.3.5A and 4.3.5B).

4.3.4.1 Intensively sampled sediments in the Ythan estuary

Counts of waterborne coliforms and *E. coli* were lower at MS than at all other sites (p= <0.001). Variance in the abundance of waterborne *E. coli* was not significant between seasons (p= 0.087), however waterborne coliforms were significantly higher during autumn than spring and winter (p= 0.024). Two-way ANOVA was unavailable due to the imbalance in the dataset. Simple linear regression between *E. coli* abundance in the water column and abundance in the underlying sediment revealed significant but weak positive relationship for both coliforms and *E. coli* (coliforms: Adjusted R^2= 38.8, p= <0.001; *E. coli*: Adjusted R^2= 33.5, p= <0.001). The slope of the regression was 0.72 for both coliforms and *E. coli*. However, there was no discernible pattern to seasonal variability around the trendline for either coliforms or *E. coli* (Figs. 4.3.5C and 4.3.5E). Samples from the MS site demonstrated a higher ratio of sediment/water coliform and *E. coli* abundance than other sites, and samples from site S demonstrated a lower ratio than the majority of samples for both coliforms and *E. coli* (Figs. 4.3.5D and 4.3.5E)

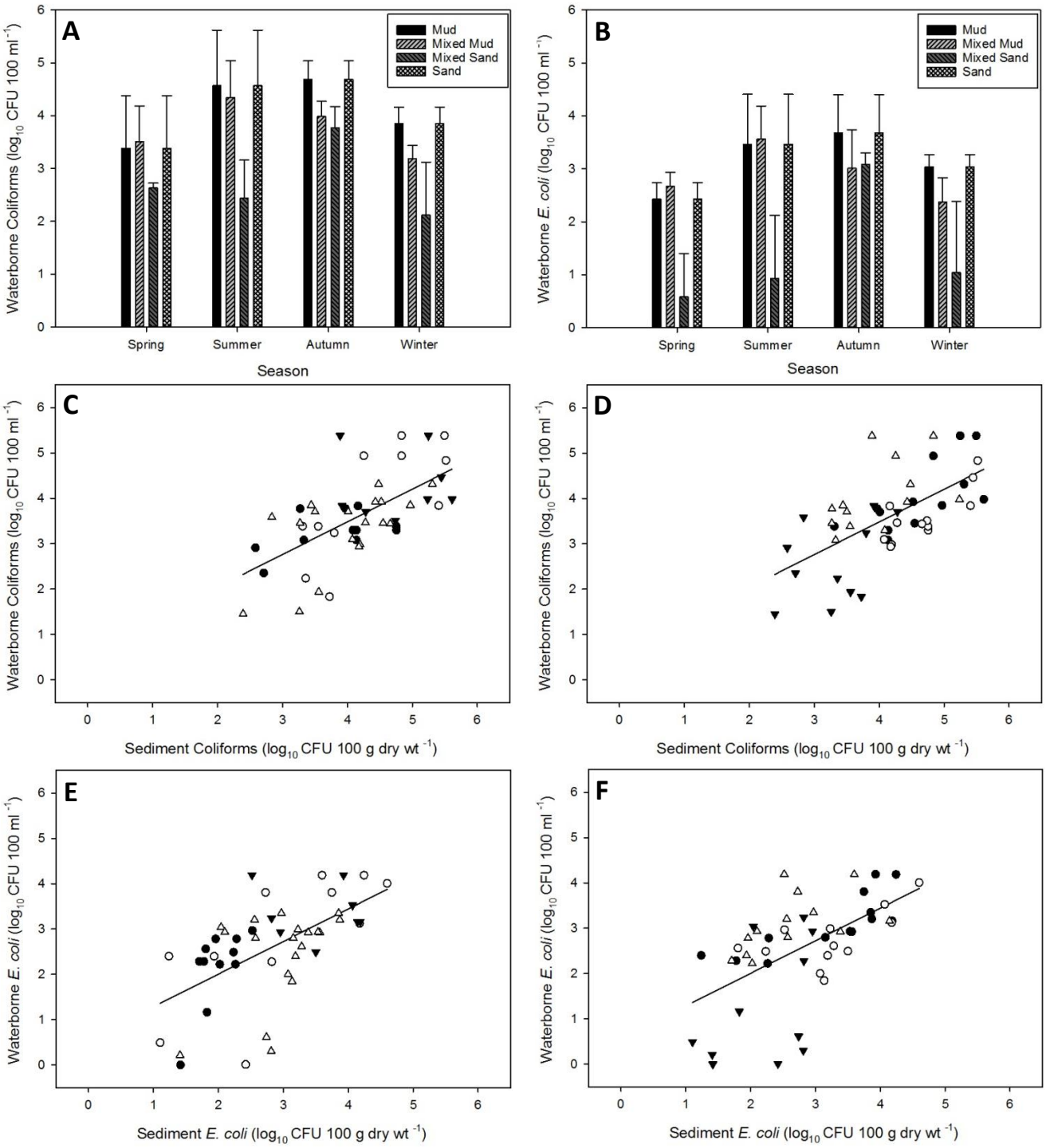

Figure 4.3.5 Plots A, B: Means plot of waterborne coliforms (A) and *E. coli* (B) at the intensively sampled sites in the Ythan estuary. Plots C, D, E, F: Scatterplots of waterborne and sediment coliforms (C, D) and *E. coli* (E, F). Plots A and B: solid fill bars- Mud; light-grey dashed bars- Mixed Mud; dark-grey dashed bars- Mixed Sand; hatched bars- Sand. Error bars denote standard error from the mean. Plots C, E: solid circles- spring; hollow circles- summer; solid triangles- autumn; hollow triangles- winter. Plots D, F: solid circles- Mud; hollow circles- Mixed Mud; solid triangles- Mixed Sand; hollow triangles- Sand. Solid line represents the line of best fit. The regression equations were: C, D- y=0.72x + 0.60 (F=31.38, n=49); E, F- y=0.72x + 0.57 (F=25.16, n=49).

4.3.4.2 Ythan and Eden estuary transects

The highest abundances of waterborne *E. coli* in the Ythan estuary were only slightly lower than that of the Eden estuary, despite the much larger difference of highest abundance observed in sediments (Figs. 4.3.6A and 4.3.6B). In all cases there was a significant positive relationship between coliform and *E. coli* abundance in the sediment and corresponding water samples, with samples towards the head of the estuary containing both higher sediment and waterborne coliform and *E. coli* abundance than samples at the mouth. The relationship of waterborne and sediment *E. coli* was stronger in the Eden estuary than the Ythan estuary (Table 4.3.3). Corresponding water samples to sediment sampling sites at the Ythan estuary were accessible at almost all sampling sites and events, however at the mid-reaches of the Eden estuary, corresponding waters were up to 1 km from the sediment site, so were not sampled. This resulted in fewer water samples from the Eden estuary, and those taken were almost entirely from the upper reaches (sites 1-3) and sites 11 and 14 (Fig. 4.3.6B). Therefore, a strong relationship might be expected as water samples were of mostly either river water, or sea water, without intermediate salinities sampled representatively. However, the gradient of the relationship was similar to that of the intensively sampled sites at the Ythan estuary (0.76, 0.72 for Eden transect and Ythan intensive sites respectively; both p= <0.001). The gradient of the relationship at the Ythan transect was lower than in other datasets at 0.41 (p= <0.001). When combining all available datasets (gradient= 0.60 p= <0.001), a lower sediment/water abundance ratio was observed for the data from the Ythan intensively sampled dataset compared to the transect datasets (Fig. 4.3.6C).

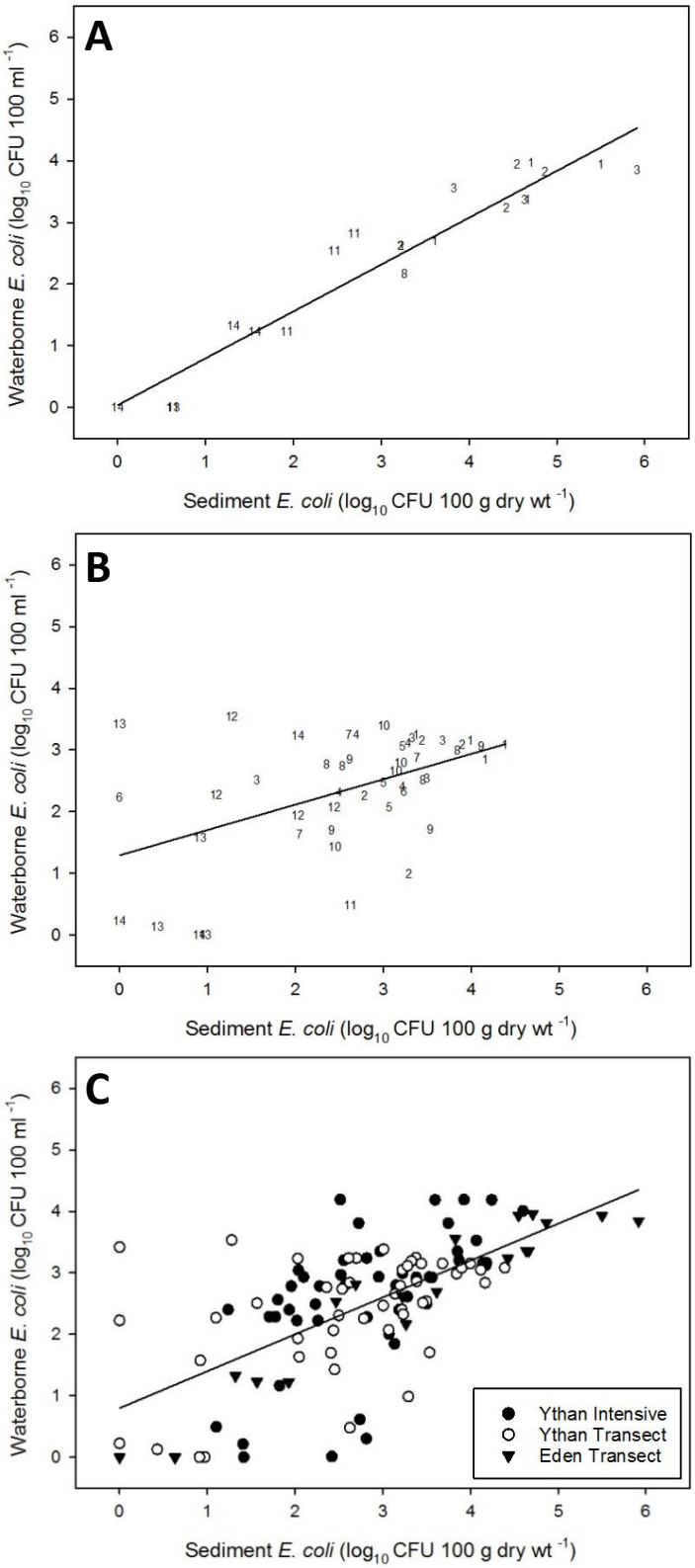

Figure 4.3.6 Scatterplots of waterborne and sediment *E. coli* for the Ythan transect (A), Eden transect (B) and both transects and intensively sampled site data combined (C). Plot C: solid circles- Ythan intensively samples sites; hollow circles- Ythan transect; solid triangles- Eden transect. Solid line represents the line of best fit. Regression equations were: A- y=0.41x + 1.29 (F=14.84, n=48) B- y=0.76x + 0.04 (F=201.75, n=21); C- y= 0.60x + 0.80 (F=87.03, n= 118).

Table 4.3.3 Summary of simple linear regression between waterborne and sediment *E. coli* abundance for the intensively sampled, transect and combined datasets.

Site	Sampling Regime	Residual d.f.	F- statistic	*p*- value	Adjusted R^2
Ythan	Transect	46	14.84	<0.001	22.7
Eden	Transect	19	201.75	<0.001	90.9
Ythan	Intensive	47	25.16	<0.001	33.5
Combined	All	116	87.03	<0.001	42.4

4.4 Discussion

4.4.1 Variation of sediment stability with associated sediment characteristics

As the relationship between sediment stability variables and particle size is non-linear and water content dependant [183], simple correlations and rank coefficients fail to fully explain the relationship between sediment stability variables and sediment characteristics over a range of sediment types. This was reflected in the estuary transects where relationships between sediment stability variables and any physical sediment characteristics were weak or non-significant. Several relationships were identified however and are discussed here.

Over all of the intensively sampled sites, the relationship of increasing sediment shear strength with decreasing water content and increasing bulk density was observed. Compaction, or consolidation, of sediment decreases the water content, and increases the bulk density, which has been demonstrated to increase erosion resistance in a range of sediment types [296, 298]. Likewise, sediment stability increased significantly with decreased organic content and water content, which were very strongly correlated to one another. Water content becomes more critical to the erosion threshold of sediments as particle sizes decrease below 100 µm [183]. This was evident where the sediment with the finest particles (mud) was the only sediment type to demonstrate this significant correlation. In similar muddy sediments with a mean particle size 7.8-62.5 µm, sediment stability has been demonstrated to increase with increasing organic content (colloidal carbohydrates) and decreasing water content [296].

Of all sampling events, the lowest sediment shear strength was consistently observed at M and S, suggesting these sediments were at greater risk of large-scale resuspension. However, this assumes that all sites were exposed to identical hydrodynamic stress, which was not the case. The M and MS sediments were situated in embayments and therefore probably not exposed to as much hydrodynamic force as sediments situated close to the main estuary channel such as S. It must be remembered that *in situ* erosive forces were not measured in this study, and the relative erosion risk of sediments is based upon only sediment stability measurements. Low sediment stability was also observed at M suggesting sediments of this type are also more prone to frequent small-scale erosion. Sediment stability was very high in MM and MS due to their mixed nature increasing sediment bulk density and resistance to surface shear stress [296, 298]. Sediment stability data was absent for MM during summer as a result of macroalgal growth (predominantly *Ulva* spp.), that is known to prevent sediment resuspension by

reducing sediment exposure to shear forces by forming a protective covering over the bed [313].

Environmental conditions during winter generally result in a net erosion of intertidal sediments in northern estuaries [282]. Shear strength of sediments increases with depth [298], so as surface layers of sediments are eroded the shear strength of the new surface layer can be higher, an effect observed previously on the Severn estuary [296]. This effect can be changed by bioturbation however. The highest shear strength was observed during spring, which may be a result of erosion during late winter/ early spring, however similarly high shear strength was observed in sediments during autumn, which cannot be reliably attributed to erosion events.

Sediment shear strength and stability was highest in spring and lowest in winter, coinciding respectively with the highest and lowest EPS content over all sediments respectively. Correlation between increased EPS content and increased shear strength and stability was evident within individual sediment types, and with sediment stability only over both estuary transects, confirming previous assertions that EPS is one of the important drivers of erosion resistance [149, 151, 168, 192, 303]. Over both estuary transects, and over all intensively sampled sites, EPS content increased in sediments in line with higher maximum air temperatures. Colloidal carbohydrates have been observed to increase with sediment surface temperature with a similar strength of relationship in sediments from the Severn estuary (Severn estuary: Rho= 0.40, p= <0.001) [296]. However, there was only a significant positive correlation between increasing temperature (minimum grass and air only) and increased sediment stability for the Eden estuary transect. Sediment at the mud site contained very high EPS contents, especially during spring, but failed to show high erosion resistance. This was probably caused by the very high water content observed at this site resulting in a gelatinous surface layer with very little cohesive strength, in addition, there was also a relatively high presence of *Hydrobia* sp. occurring seasonally at this site which may have led to the lower stability through surface bioturbation and grazing [198].

The correlation between increasing pH and decreasing erosion resistance was only evident over all intensively sampled sites at the Ythan estuary, a relationship demonstrated experimentally in pure kaolinite sediments within a relatively narrow pH range of between 5.6 and 8.2 [314]. However, there was no correlation between pH and sediment stability in the estuary transects, and pH co-varied strongly with particle size variables at the intensively

sampled sites. Thus, this apparent correlation between erosion and pH may be an artefact of the effect of varying particle size. The effect of salinity on sediment stability was more apparent, correlating directly with increasing shear strength in many cases. Salinity was consistently negatively correlated to water content, and the effect of decreasing water content on increase in bulk density and subsequent erosion resistance has already been discussed. In addition, higher salinity increases the cohesive effect of EPS [306], but salinity also directly correlated to increasing particle size that correlated with higher shear strength over most sediment types.

There was no significant correlation between sediment shear strength and stability over the two estuary transects, or within intensively sampled sediment types except mixed sand. This may be expected because, as discussed above, different variables affect each measure of sediment stability, for example over both estuary transects, shear strength is governed by physical sediment characteristics, and sediment stability by EPS content. However, within finer sediment types, a moderately strong positive correlation between shear strength and stability was observed [296]. As a result of the lack of correlation observed here it is suggested that, when incorporating erosion potential thresholds into models predicting resuspension of *E. coli* into the estuarine water column, both large-scale (shear strength) and small-scale (stability) resuspension parameters should be considered.

4.4.2 Relationships between **E. coli** *abundance and sediment stability variables*

Shear vane results observed here are consistent with values obtained from similar sediment types at the Bay of Fundy (New Brunswick/ Nova Scotia, Canada) [299]. Likewise, sediment stability results are in line with those obtained using the CSM on similar sediment types at the Severn and Eden estuaries (UK) [294, 296], suggesting the results here may be widely applicable.

Plotting *E. coli* abundance against sediment stability variables revealed little correlation, however it highlighted sediments of specific types and times of year that posed a higher risk of resuspending high levels of *E. coli* into the water column. Sediments at the mud site during winter and autumn, and to a lesser extent sediments at the sand site during the same period were designated as sediments that pose a high risk of releasing the highest levels of *E. coli* into the water column through large-scale resuspension. Small-scale resuspension of high levels of

E. coli is likely to occur from mud sediments during winter and autumn, as well as mixed mud sediments during winter. Some of the highest *E. coli* abundance observed during summer and autumn at the mixed mud site can be regarded as being at a relatively low-risk of resuspension due to high sediment shear strength and stability.

Sediments with the highest risk of large-scale resuspension of high *E. coli* levels occurred mostly during summer and autumn, and were located in the upper reaches of the Ythan and Eden estuaries, which generally had smaller particle sizes and high water content. Sediments with a high risk of small-scale resuspension of high *E. coli* loads occurred in every season except spring, and were distributed more widely across the both estuaries, however the conditions still occurred more frequently in the upper and mid-reaches of the estuaries.

As samples with high *E. coli* abundance and low sediment shear strength and stability were identified to be of specific sediment types during certain seasons, the first hypothesis can be confirmed. However, using this information to inform decisions regarding bathing water regulations and human safety is challenging as there were no definitive trends to the clustering. There was a larger and more discrete difference of sediment stability variables between sites than seasons, so it would seem sensible to discourage human contact with the water in areas where the sediment type frequently demonstrate high erosion potential. Conveniently, less human activity is likely in these areas due to the muddy nature of the sediments at the mud, mixed mud and upper estuary sites, with bathers and beach users preferring sandier areas. However, as discussed earlier, when faecal bacteria are resuspended into the water column, tides and currents will transport them away from the source sediment and possibly towards more heavily used areas. In estuarine systems this is especially relevant, as there are more visitors to the lower reaches of the Ythan and Eden estuaries where there are sandier sediments that can be walked upon, and kite surfers use the lower-mid reaches of the Ythan estuary. The underlying sediments at these sites are less likely to resuspend faecal bacteria, but high risk sediments upstream may be resuspended and the associated bacterial load transported down-stream with the river current and receding tide to these sites. Although ideally water users in such areas should be discouraged during summer, autumn and winter, these are peak times for bathing water usage and therefore it may be more appropriate to advise bathing to periods of incoming tide where contaminated waters will be forced up the estuary and diluted with the incoming seawater. Water users likely to resuspend sediments beneath them by wading, such as anglers, should be made aware of site-season specific risks

of high *E. coli* abundance in the sediment as sediment stability measurements are not as relevant when sediments are exposed to anthropogenic disturbance.

The data presented here has implications for the modelling of the resuspension and subsequent transportation of *E. coli* from intertidal sediments. Absence of a linear trend between erosion and *E. coli* abundance in sediments, and significance in the two-way interaction of site and season for both shear strength and stability highlights the site-specificity of temporal variability of *E. coli* resuspension potential. Therefore it may be necessary to perform sediment stability measurements at several sites within an estuary before applying differential erosion potential parameters in order to predict resuspension of *E. coli* into the water column, in addition to differentially accounting for large-scale and small-scale resuspension.

4.4.3 Relationship between FIO abundance in the overlying water and sediment

The abundance of FIOs in intertidal sediments exceeded that of corresponding water samples by up to almost 3 orders of magnitude. This is in line with previously reported data from estuaries [19, 21, 78, 79], rivers [122] and lakes [315, 316]. Correlations between waterborne and sediment *E. coli* abundance were generally weak, with the exception of the Eden estuary. This weak correlation has been observed to be the case in several different aquatic systems [247]. This relationship could be expected here as water samples corresponding to intertidal sediments were often taken several hours after the tide had receded from the site, and at a distance of up to ~50 m away. Therefore, the corresponding water sample may not bear a close relationship to the water that overlies the sampled sediments with the incoming tide. The abundance of waterborne *E. coli* can also be highly heterogeneous across a horizontal estuary transect [317], and the pattern and extent of this spatial variation will change as currents and tidal forces change during the tidal cycle.

There was a statistically significant positive correlation between the abundance of waterborne and sediment *E. coli* in all cases, which allows for confirmation of the second hypothesis. However, despite being statistically significant, the relationship was generally weak and of a lower strength than the relationships between sediment characteristics and sediment *E. coli* abundance observed in Chapter 3. Therefore, sediment characteristics provide a more useful model for the prediction of abundance of *E. coli* in sediments than the abundance in the

overlying water. This substantiates the need for the monitoring of underlying sediments in addition to the overlying water in order to assess risk of faecal contamination to bathing waters. Although not statistically significant between seasons, waterborne *E. coli* concentrations were highest during autumn and lowest during spring and winter which follows the same trend as *E. coli* abundance in sediments. This suggests that supply to the sediments by waterborne *E. coli* may have contributed to the seasonal variation in the sediment that could not be explained by any variables in the explanatory models in Chapter 3. Including waterborne *E. coli* in the explanatory models of Chapter 3 however detracts from the purpose of these models to utilise only environmental and sediment characteristics.

Sampling locations towards the mouth of the both estuaries (Ythan: MS, Ythan transect sites: 11-14) often demonstrated higher sediment/water *E. coli* abundance ratios than sites further up the estuary. This suggests that the beneficial association with sediment may be more influential at higher salinities due to osmoprotective properties of the sediment [318]. Therefore, for bathing waters at higher salinities it may be more important to monitor underlying sediments, as their resuspension may have a greater influence on increasing FIO abundance in the water column than at freshwater bathing sites. Furthermore, the difference between abundance of *E. coli* in sediments and in corresponding water samples increased as the abundance in sediments increased. This was evident in all cases as the gradient of the regression was below 1, especially in the intensively sampled dataset at the Ythan estuary. This is attributable to the persistence of *E. coli* being enhanced when in association with sediments compared to the overlying water (Section 1.7), resulting in an accumulation of *E. coli* within the sediment.

4.4.4 Conclusions

This chapter demonstrates the spatial and temporal variation of intertidal sediment shear strength and stability, and identifies specific spatial and temporal patterns for sediments that pose a high risk of resuspending large numbers of *E. coli* into the water column. Furthermore, it suggests that the measurement of both shear stress and surface stability of sediments are necessary factors to be included in future work predicting the resuspension of *E. coli* into the water column. It has also been shown that only a weak relationship exists between the abundance of *E. coli* in sediments and corresponding water samples, therefore further work is

necessary to elucidate the dynamics of the exchange of fecal contamination between the sediment and overlying water in order to reliably inform bathing water regulations.

The first hypothesis: *Sediments that pose a risk to human health through easily-resuspendable faecal bacteria can be spatially and temporally identified by combining* E. coli *abundance and sediment stability measurements,* was confirmed as high risk sediments were clearly spatially and temporally identified.

The second hypothesis: E. coli *abundance in the overlying water will correlate with the abundance of* E. coli *in sediments,* was confirmed as there was statistically significant correlation between the abundance of waterborne and sediment *E. coli*. However, this relationship was weak, and waterborne *E. coli* did not explain as much of the variability of sediment *E. coli* as using sediment characteristics as in Chapter 3.

5. The effect of changes in the native microbial community on *E. coli* abundance in intertidal sediments

5.1 Introduction

5.1.1 Native microbial communities of intertidal sediments

In the microbiome of intertidal sediments, eubacteria, cyanobacteria and algae co-exist [181], and these groups form the majority of the microbial community. Benthic microalgae account for up to 50% of total primary production of shallow estuaries, with production being higher in sediments of relatively small particle size [171]. Diatoms, a form of microalgae, alone have been estimated to provide 40 % of global primary production [319, 320]. Changes in the microbial community of intertidal sediments can have positive and negative effects on higher trophic levels [321]. For example, an increase in the primary production of algae increases food supply for surface deposit feeders [322] and oligochaetes [323], however blooms of cyanobacteria can increase mortality in grazing herbivores [321].

The majority of bacterial community analysis in estuaries is focussed on waters [324], but the relationship of microbial community shift with variables such as salinity are likely to be different for benthic communities as they may be exposed to greater fluctuation of salinity compared to planktonic organisms moving with water mass [325]. However, sufficient EPS content in sediments is known to buffer salinity fluctuation of interstitial water [148], so in sediments where EPS is present, it could be expected that microbial communities are less vulnerable to fluctuations in salinity and demonstrate community shift in a more similar manner to the planktonic community.

Several studies have reported planktonic estuarine microbial community shift as the mixing of communities of freshwater and marine sources [326, 327], however many have also reported distinct estuarine communities in brackish waters [328-331], suggested to occur when community doubling times are faster than the water flushing times [328]. Therefore, it is reasonable to assume that, as benthic organisms are not susceptible to flushing from the estuary on a time scale similar to that of planktonic organisms, there will be distinct estuarine bacterial communities that are more complex than the simple mixing of freshwater and marine species.

There are many variables that have been demonstrated to correlate with shift in microbial communities of estuaries, with many studies focussing on the effect of salinity and nutrient concentration gradients (Table 5.1). It is difficult however to individually investigate effects of salinity and nutrients in field experiments [332] as they often negatively correlate within estuarine systems [333, 334].

Table 5.1 Examples of studies that identify important variables that correlate with microbial community shift in estuaries.

Community	Phase	Variable	Reference
Bacteria	Water	Salinity	[326, 330, 331, 335, 336]
Bacteria	Water	Seasonality	[328, 335, 337]
Bacteria	Water	Nutrients	[326, 336, 338, 339]
Bacteria	Water	Light attenuation	[336]
Bacteria	Sediment	Salinity	[340, 341]
Bacteria	Sediment	Particle size	[342, 343]
Bacteria	Sediment	Nutrients	[340, 341]
Bacteria	Sediment	Dissolved oxygen	[342-344]
Bacteria	Sediment	pH	[341]
Algae	Sediment	Salinity	[332, 345, 346]
Algae	Sediment	Seasonality	[332, 346, 347]
Algae	Sediment	Particle size	[348]
Algae	Sediment	Nutrients	[332, 346]
Algae	Sediment	Grazing	[347]
Cyanobacteria	Sediment	Salinity	[332]
Cyanobacteria	Sediment	Particle size	[348]
Cyanobacteria	Sediment	Nutrients	[321, 332]
Cyanobacteria	Sediment	Grazing	[321]

5.1.2 Variables contributing to changes in native microbial communities

The salinity gradient is responsible for large changes in the biodiversity of estuaries (Fig. 5.1). Total species of macroinvertebrates decrease at a salinity between 5 and 8 PSU, known as the 'Artenminimum zone' [349], later referred to as the 'horohalinicum' by Kinne [350]. It occurs because marine species do not inhabit lower salinities and riverine species do not inhabit the higher salinities primarily due to the osmotic stresses incurred, therefore species are divided on their osmoregulatory abilities [351]. Deaton and Greenberg [352] argued however that the ionic composition only slightly changes within this salinity range, and an explanation behind the lower abundance of species is due to a limited number of species developing the necessary physiology to deal with the specifics of the environment. The dynamic nature of the reaches of an estuary at this salinity results in stationary organisms, such as those dwelling in intertidal sediments, being exposed to highly fluctuating salinities beyond the 5-8 PSU range, therefore despite the ionic composition not changing dramatically within the horohalinicum, organisms are frequently exposed to salinities higher and lower than this and the argument of Deaton and Greenberg is likely to be more accurate.

This relationship of total species with salinity however does not apply to planktonic protists [353] (Fig. 5.1), instead, they achieve a maximum species abundance in the salinity range of the horohalinicum as they move with water mass and are not affected as much by salinity fluctuation. Planktonic protists occur at lower species abundance at the low and high extremes of the salinity range, with an increase at the horohalinicum [353]. It was not been reported however how benthic protists respond to salinity gradients of estuaries as, being stationary, they are exposed to fluctuation in salinity, but demonstrate the fast generation time and fast adaptation to osmotic stress of planktonic protists [353].

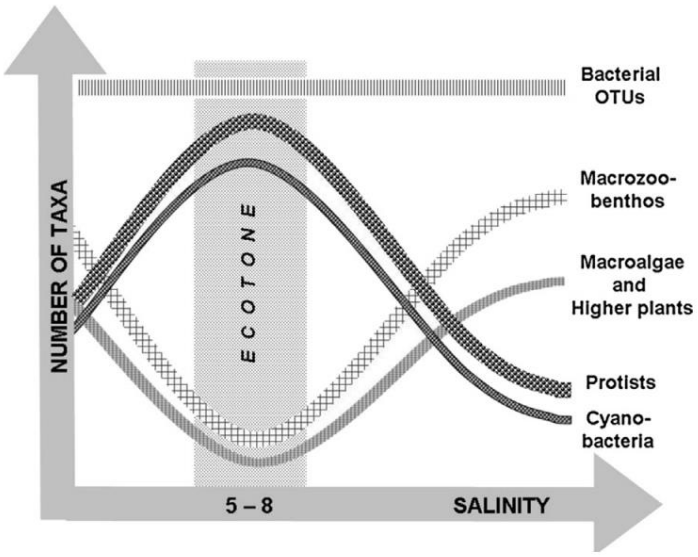

Figure 5.1 Theoretical taxa richness of planktonic micro-organisms and benthic macro-organisms over the salinity gradient. The 'Ecotone' refers to the range of salinities also referred to as the 'Artenminimum zone' or 'horohalinicum'. From Telesh et al. 2013.

Contrary to the above diagram, abundance of operational taxonomic units (OTU) of planktonic bacterial communities were observed to increase between salinities of 1.2 and 6.4 PSU at the Delaware Bay estuary (USA), with communities at lower and higher salinities demonstrating a similar abundance of lower than 50 % than the higher communities. OTU diversity was highest at 0 and ~31 PSU, with all salinities between these demonstrating diversity of less than 50 % of the highest and lowest salinities [336]. Likewise, salinity proved to be a key factor in the community shift of planktonic bacteria in the Changjiang estuary (China) [354], but there was no observed spatial variation of the bacterial community in sediments, however physical sediment characteristics were not investigated. There was however a seasonal shift in community structure suggested to be a result of season-specific particle transport, and bacterial diversity in sediments was observed to be higher at the mixing zone of the estuary at which salinity was recorded at 5.2 and 8.2 PSU than lower salinity samples. The diversity of bacterial communities has been demonstrated to be less diverse in water samples than the underlying sediments, in addition to the communities being clearly distinct with sediment bacterial communities primarily composed of Gamma- and Deltaproteobacteria, and water bacterial communities composed of Alphaproteobacteria and cyanobacteria [354].

In intertidal sediments, additional variables are introduced that effect microbial community composition. The most important perhaps being variation in particle size, shown to be a governing factor in bacterial community composition [342], and in the production and competition between diatoms and cyanobacteria, although dominance was also temperature dependant [348]. Changes in nutrient input to estuaries can also influence the relative composition of the different groups of organisms. Armitage and Fong [321] observed up to a 200 % increase of cyanobacteria and 400 % increase of purple sulphur bacteria in sandy sediments with the addition of nitrogen and phosphorus at concentrations of 88 mg N day^{-1}, 24 mg P day^{-1} for each 0.5 m x 0.5 m plot.

It has been suggested that marine diatom species are able to grow in salinities down to 4 PSU [173], however salinity has been found to be one of the main drivers of diatom distribution in estuaries [332, 345, 355]. Admiraal and Peletier [346] found that in individual cultures, the effect of salinity on photosynthetic ability was only slightly inhibited over a large range of salinities, however had a more profound effect on which species were the more dominant in mixed cultures. Shift in diatom community composition has also been shown to be highly seasonal and dependant on interspecific competition, vertical zonation, temperature, environmental stress and predation [347]

The effect of several physical, biogeochemical and environmental gradients in intertidal sediments on the relative abundance of several diatom and cyanobacterial taxa in a temperate estuary was investigated by Underwood et al. [332].The relative abundance of several diatom taxa was found to correlate with the salinity gradient of the overlying water, whereas only one species was found to correlate significantly with pore water salinity. There was also a significant response to the nutrient gradient caused by a sewage outfall, with some species increasing in abundance with increasing distance from the outfall. Water content of sediment was found to affect the abundance of a diatom and cyanobacteria taxa, and the abundance of two diatom species increased with an increase in EPS. Temperature was however identified as one of the principle driving factors in the shift in diatom community composition.

5.1.3 Interactions between the native microbial community and E. coli

One mechanism of interaction between the indigenous microbial community and *E. coli* is predation by protozoa, phages and lytic bacteria [356], with many studies concluding that

parasitism and predation are the most important factors involved in the decline in non-native bacteria in sediments [143]. Protozoan predation rather than predatory bacteria has been found to be responsible for the decrease in *E. coli* populations in compost [144] and estuarine waters [119, 145]. The presence of protozoan predators has been observed to cause die-off of faecal coliforms in both freshwater and marine sediments where their absence (through addition of cycloheximide) allows enhanced persistence and the possibility of growth of FIO populations [28, 132].

Although the abundance or diversity of predatory organisms are not targeted for analysis here, high bacterial prey diversity may suggest decreased predator performance [357] suggested to be a cause of defensive prey strategies such as microcolony formation, surface masking, toxin release, and digestional resistance [358]. Non-indigenous bacteria are not likely to demonstrate such functions when present in an alien environment and therefore may be at a higher risk of predation than indigenous bacteria, certainly, several studies have shown that *E. coli* is susceptible to predation in estuarine environments [145, 359]. Conversely, they may also benefit from these defensive strategies through incorporation into biofilms, which in a marine environment, have been shown to contain increased abundance of *E. coli* than surrounding water [288].

The second mechanism of microbial community on *E. coli* abundance is that of competitive exclusion. The generally accepted ecological theory is that with high biodiversity, it is more difficult for invading species to be successful, as ecological niches are occupied, and competition for resources is high [360]. Spatial and temporal shift in microbial community composition may leave vacant ecological niches that *E. coli* may benefit from. A decrease in microbial diversity may therefore affect the abundance of *E. coli* through decreasing its survival; likewise, a decrease in microbial diversity may lead to increased susceptibility of sediments to harbour increased abundances of faecal bacteria.

Much of the effects of indigenous microbiota on faecal bacteria abundance rely on whether the invading organism is an active part of the microbial community, or a senescent passenger. A study on the impact of 'urban microbial signatures' (microbial communities associated with sewage outfall and stormwater that typically contain faecal indicator organisms) found that these communities were present in waters further downstream from the sources, and that their presence correlated directly with increased rainfall. It was unclear however whether these organisms were active within the microbial community [361].

5.1.4 Aims and hypotheses

The aim of this chapter was to elucidate whether or not the indigenous microbial community affects the abundance of *E. coli* in intertidal sediments. This was investigated by identifying spatial and temporal variation in microbial population metrics (species abundance, diversity and evenness of the microbial community), and identifying shift in microbial community constituent composition within the Ythan and Eden estuaries with the use of terminal restriction fragment length polymorphism (TRFLP). Shift in microbial community constituent composition was then correlated to environmental and sediment characteristics in an attempt to identify important variables governing microbial community shift in estuaries. Relationships between *E.* coli abundance and the changes and shifts in the microbial community constituent composition were then investigated in order to better understand if and how the indigenous microbial community may affect the abundance of human pathogens in intertidal estuarine sediments.

The following hypotheses were tested in this chapter:

a) ***The salinity gradient drives spatial variation in microbial species metrics (species abundance, diversity and evenness) in estuaries.***
b) ***Microbial community constituent composition is similar in the Ythan and Eden estuaries.***
c) **E. coli *abundance is affected by changes in microbial population metrics.***
d) **E. coli *abundance is affected by microbial community constituent composition.***

5.2 Materials and methods

5.2.1 Sediment collection and analysis

Three of the 6 sampling sites for each sediment type for December 2013, February 2014, March 2014, May 2014, July 2014, September 2014 and November 2014 from the intensive sampled sediments described in Section 2.10.1 were used for DNA extraction. In addition, samples were taken from the 4 seasonal transects described in Section 2.10.2 sampled in February, May, August and November 2014.

5.2.2 Native microbial community constituent composition

To determine the native microbial community at each site, 3 adjacent 1 cm deep syringe cores (Section 2.1) were combined and homogenised to create a sample. All samples were snap-frozen in liquid nitrogen immediately on return to the laboratory and stored at -80 °C.

5.2.2.1 DNA extraction and quantification

DNA extraction was performed using the Powersoil® DNA Isolation Kit (MO BIO, CA, USA). The manufacturers protocol was followed, with the exception of the use of a Precellys 24 (Bertin Technologies, France) used at 2 x 6500 rpm for 15 seconds for the bead-beating stage, and an added incubation of 2 minutes at room temperature after the elution buffer was added to the spin filter membrane prior to centrifugation in order for the elution buffer to fully cover and adsorb to the membrane. A positive control for the DNA extraction was a Quality Control Mineral Soil (QCM) that had yielded high DNA concentrations in preliminary experiments, and a negative control of DI H_2O was used.

The concentration of DNA recovered was determined using the Qubit dsDNA HS (High Sensitivity) Assay kit (Invitrogen, Fisher Scientific, UK). The manufacturer's protocol was followed with 2 µl of sample used in the reaction.

To visualise the DNA, 4 µl sample was combined with 2 µl 40 % sucrose loading dye (40 % w/v sucrose, 0.25 % bromophenol blue (w/v in DI H_2O)) and loaded into a 15 cm x 15 cm 1 % agarose gel (1 % agarose (Bioline, UK) in TBE buffer (Tris base (Promega, UK), Boric Acid, (Promega, UK) Ethylenediaminetetraacetic acid (Sigma Aldrich, UK)). Four µl ethidium bromide

was added to the gel before pouring in order to stain DNA. The gel was electrophoresed in a running buffer of 1 x TBE at room temperature for 40 minutes at 70 V. 5 µl hyperladder 1 kb (Bioline, UK) was used to identify sample fragment sizes. The gel images were taken with the GeneSnap software (Syngene, UK) under UV light using the Genegenius Gel Documentation system (Syngene, UK).

5.2.2.2 Multiplex TRFLP (M-TRFLP)

The TRFLP method of Vinten et al. (2011) [362] was followed. The method consists of 3 separate PCRs: targeting the 16S rRNA gene of eubacteria and cyanobacteria and the 18S rRNA gene of algae (Table 5.2.1).

Eubacteria 16S rRNA PCR: DNA samples were amplified in separate reactions. The Eubacteria 16S genes were amplified using a 50 µl mixture containing of 5 µl 10x NH_4 Buffer (Bioline, UK), 20 nmol deoxynucleoside triphosphates (Bioline, UK), 100 nmol $MgCl_2$ (Bioline, UK), 20 µg Bovine Serum Albumin (Roche, UK), 10 pmol of both 63F-VIC and 1087R primers, 2.5 units of Biotaq (Bioline, UK), and 50 ng of template DNA in DI H_2O. The DNA extracted from the QCM was used as a positive control, and DI H_2O as a negative control. DNA extracted from QCM was used as a positive control, and DI H_2O as a negative control.

The PCR was performed in a DYAD DNA Engine Peltier thermal cycler (MJ Research, MA, USA), with the following conditions: an initial denaturation for 5 minutes at 95 °C; 30 cycles of denaturing for 30 s at 94 °C, annealing for 30 s at 55 °C, elongation for 1 min at 72 °C; with a final elongation for 10 min at 72 °C.

Algae 18S rRNA PCR: The Algae 18s genes were amplified using a 50 µl mixture containing of 5 µl 10x NH_4 Buffer, 20 nmol deoxynucleoside triphosphates, 100 nmol $MgCl_2$, 20 µg Bovine Serum Albumin, 10 pmol of both P73F-FAM and P47R primers, 2.5 units of Biotaq, and 50ng of template DNA in DI H_2O. DNA extracted from *Navicula pelliculosa* was used as a positive control, and DI H_2O as a negative control.

The PCR was performed with the following conditions: an initial denaturation for 5 minutes at 94 °C; 30 cycles of denaturing for 30 s at 92 °C, annealing for 30 s at 57 °C, elongation for 1 min at 72 °C; with a final elongation for 10 min at 72 °C.

Cyanobacteria 16S rRNA PCR: The cyanobacteria 16S genes were amplified using a 50 µl mixture containing of 5 µl 10x NH_4 Buffer, 20 nmol deoxynucleoside triphosphates, 100 nmol $MgCl_2$, 20 µg Bovine Serum Albumin, 20 pmol of both 359F-NED and 792R primers, 2.5 units of Biotaq, and 50ng of template DNA in DI H_2O. DNA extracted from *Anabaena flos-aquae* (UTEX-1444, UTEX, Austin, Texas, USA) was used as a positive control, and DI H_2O as a negative control.

The PCR was performed in with the following conditions: an initial denaturation for 5 minutes at 95°C; 30 cycles of denaturing for 30 s at 94 °C, annealing for 30 s at 58 °C, elongation 1 min at 72 °C; with a final elongation for 10 min at 72 °C.

Table 5.2.1 Primer name, label, target gene, PCR annealing temperature and product size, and primer sequences of those used in the TRFLP method. * denotes inaccuracy in reported fragment length discussed later in this chapter (Sections 5.3.1, 5.4.1).

Primer	Label	Target Taxa	Target Gene	Sequence (5' to 3')	Amplicon size (bp)	Annealing Temp. (°C)	Reference
63F	VIC	Eubacteria	16S	AGGCCTAACACATGCAAGTC	1024	55	[363-365]
1087R	None			CTCGTTGCGGGACTTAACCC			
359F	NED	Cyanobacteria	16S	GGGGAATYTTCCGCAATGGG	433	58	[362, 366]
792R	None			TCCCCTAGCTTTCGTCCC			
P73	FAM	Algae	18S	AATCAGTTATAGTTTATTTGRTGGT	400 (290-300*)	57	[367]
P47	None			TCTCAGGCTCCCTCTCCGGA			

5.2.2.3 PCR product purification

To determine the PCR success and amplicon size, each PCR product was visualised by gel electrophoresis as in Section 5.2.2.1. The PCR product was purified by washing excess PCR reagents using the Wizard® SV Gel and PCR Clean-Up System (Promega, UK). The manufacturer's protocol was followed, with all 50 µl of the PCR product being used in the system, and the cleaned PCR product being eluted in 50 µl of elution buffer. The Qubit Broad Range Assay Kit was used to determine DNA concentration, using 2 µl of sample.

5.2.2.4 PCR product concentration

The eluted DNA after PCR product purification was not concentrated enough for a multiplex digest, therefore DNA was concentrated by evaporating the cleaned PCR product in an Eppendorf vacufuge (Eppendorf, UK). Samples were dried at 30 °C until all moisture was removed from the sample leaving the DNA pelleted on the wall of the 1.5 ml Eppendorf tube. Fifteen µl sterile DI H_2O was added to each tube and left to incubate overnight at room temperature before vortexing gently to ensure resuspension of the DNA pellet. The Qubit Broad Range Assay Kit was again used to determine the DNA concentration, using 1 µl of sample.

5.2.2.5 Enzyme digest

Eighty ng of DNA template from each of the 3 purified PCR products were combined in a 10 µl reaction, along with 10 units of HhaI enzyme (New England Biolabs, MA, USA), and 1 µl of Cutsmart buffer (New England Biolabs, MA, USA). Samples were then incubated at 37 °C for 3 hours for digestion of the PCR products, and the enzyme then denatured at 95 °C for 10 mins. 2 µl was then transferred into clean 96-well plates and submitted for fragment size analysis.

5.2.2.6 Fragment size analysis

(Samples run by D. White, The James Hutton Institute, Aberdeen)

The length of the labelled terminal restriction fragments was determined using an ABI-3130xl Genetic Analyser (Applied Biosystems, Life Technologies, Paisley, UK). To each sample well of the 96 well plates, 12 µl of Hi Di Formamide and 0.3 µl of the size standard Liz 500 were added.

The plate seal was added and the plate centrifuged at 3000 x g for 10s. Samples were denatured at 95 °C for 5 min on a heating block and cooled on ice for 2 mins before loading into the capillary array.

Sequence files were imported into Genemapper (v.4.0, Applied Biosystems, Life Technologies, Paisley, UK). The analysis method was set to 'aflp default'. Peaks out-with 50-500 bp were excluded to avoid primer-dimers and to include pea ks only within the size standard range [365]. Size callings: 2nd order least squares, peak amp threshold: green= 20, yellow= 20, blue= 20 and the analysis performed.

Data were exported from Genemapper as a tab-delimited text file and imported into T-REX [368], an online program for processing and analysing TRFLP data. In T-REX, the clustering threshold was set to 0.99 and terminal restriction fragments (TRFs) that occur in less than 0.5 % of the samples omitted [365], and a data matrix created using peak heights. The data matrix was then exported into Excel and relative abundance of individual TRFs within each of the 3 dyes calculated as the individual peak height divided by the total peak height of the dye for the TRFLP profile for that sample.

5.2.3 M-TRFLP peak identification

TRFs with a correlation above 0.75 in the intensively sampled sediment dataset, and 0.65 for transect sampling regimes were submitted to peak identification using the online TRFLP Analysis (PAT+) of Microbial Community Analysis III (MiCA 3) [369] using the 16S bacterial rRNA database (eubacteria/ cyanobacteria), and the 16S/18S database (algae). The sensitivity was set to 0 mismatches, and the window size set to a forward match of ± 1 bp.

5.2.4 Data manipulation and statistical analysis

Microbial population metrics: TRF abundances for all dyes for each Individual replicate sample for the monthly data were analysed for total species (S), Shannon's diversity index (H') and Pielou's evenness (J') using DIVERSE in PRIMER6 [370]. Species numbers referring to data collected here refers to number of unique TRFs herein.

S= Total species of TRFs

H'= -Sum of TRFs (Pi*log e (Pi))

J'= H'/ log (S)

Where Pi= Number of individuals of species / total number of samples.

One and two-way ANOVAs were performed on the total species, Pielou's evenness and Shannon's diversity index data using Genstat (ed. 17.1, VSN International Ltd. Hempstead, UK). Simple linear regression was performed also in Genstat to analyse relationships between total species, Pielou's evenness and Shannon's diversity index, and *E. coli* abundance. Fisher's *post-hoc* protected LSD test was performed to identify significant differences between treatments where the effect was significant, and the LSDs were plotted alongside treatment means as in Section 3.2.2. There was no unbalance in the datasets in this chapter however, so LSDs plotted are true LSD values rather than max-min LSDs.

Microbial community constituent composition: A Bray-Curtis similarity matrix was constructed using the relative abundance data of the TRFs. Environmental data were normalised within PRIMER6, and a Euclidean distance matrix was constructed. nMDS plots were created using PRIMER6, and ANOSIM analysis performed with 999 manipulations in order to detect significant differences between the treatment groups of season, site and estuary. RELATE analysis within PRIMER6, that compares similarity matrices in a Mantel- type test, was performed using the Spearman's rank correlation method on both similarity matrices with 999 permutations. BEST analysis was performed within PRIMER6 using the BIOENV and Spearman's rank correlation method on the normalised environmental data and the similarity matrix of the TRFs with 99 permutations.

DistLM analysis, that analyses and models relationships between multivariate datasets and multiple predictor variables, was performed within PRIMER6 on the normalised environmental data and the Bray-Curtis similarity matrix of the TRFLP data using the stepwise selection procedure with the adjusted R^2 selection criterion with 99 permutations. Several dbRDA ordination plots were produced, where the ordination of samples are constrained to only variables included in the DistLM analysis. Symbols on the dbRDA plots represent *E. coli* abundance in order to visually identify trends of *E. coli* abundance with shift in microbial community constituent composition.

5.3 Results

5.3.1 TRFLP profiles

The amplicon length of the eubacteria and cyanobacteria 16S primer pairs were of the expected length, however the amplicon length of the algae primer pair P73-P47 was roughly 290-300 base pairs (bp) rather than the expected 400 bp (Fig. 5.3.1). *In silico* analysis of a wide range of diatom species revealed the absence of HhaI cleave sites in almost all species resulting in expected TRFs between 277 and 301 bp. The TRF for the positive control of *Navicula pelliculosa* was at 290 bp, confirming the lack of enzyme cleave sites observed *in silico.* A relatively high abundance of TRFs were observed for all samples between 270-320 bp, indicating a large proportion of amplicons were not cleaved by the enzyme. Un-cleaved samples in this range comprised 48.5 %, 61.0 %, 51.0 %, and 72.1 % of total TRFs for M, MM, MS and S sediments respectively. Similarly for the cyanobacteria amplicon, un-cleaved samples were evident between 405-421 bp, but in lower relative abundance between 9.3-21.3 %. This is not seen as problematic compared to the un-cleaved algae amplicons, as cyanobacterial TRFs between 347-349 bp comprised between 28.0-56.0 %. Un-cleaved amplicons were not observed in the eubacterial dataset as the amplicon was over the upper threshold of the internal control, and therefore excluded from the analysis, and the distribution of TRFs within the total TRF range was more evenly distributed than in the cyanobacterial and algal datasets. The high proportions of un-cleaved amplicons should be noted before the subsequent analysis as they form a bias in the algal and cyanobacterial datasets where many lineages are contained within one TRF. In addition to the absence of cleavage sites in algal TRFs, *in silico* investigation revealed consistent mismatches with the forward primer at positions 1 and 23 from the 5’ of the forward primer. Though both mismatches were present in the 18S gene of *Navicula pelliculosa* (Genbank ID AY485454.1) the amplicon was successfully amplified (Fig. 5.3.1), however the mismatches will have compromised PCR efficiency of diatom amplicons, introducing further bias to the algae dataset.

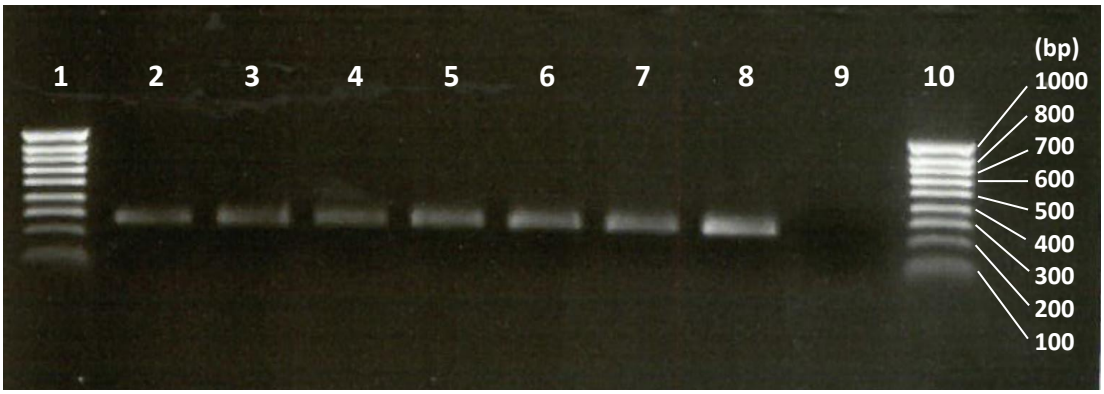

Figure 5.3.1 Gel electrophoresis of algal PCR products amplified from a range of intertidal sediments (lanes 2-7) *Navicula pelliculosa* (lane 8) and PCR negative (lane 9). Lanes 1 and 10 contain Hyperladder IV, (Bioline, UK). Fragment sizes (base pairs) of Hyperladder IV are displayed on the far right.

5.3.2 Spatial and temporal variation of microbial population metrics

5.3.2.1 Total species, diversity and evenness of TRFs across all sampling regimes

Between all sampling regimes, there were more total species of TRFs (S) observed for eubacteria than algae, followed by cyanobacteria (Table 5.3.1). There was little difference between total species of algae and cyanobacteria between sampling regimes, however there were less species of eubacteria observed in the intensively sampled sediments in the Ythan compared to the transect sampling regimes. This leads to the number of total species of all targets being slightly higher in the Eden and Ythan transects compared to the intensively sampled sites. The range of number of species observed over all targets in the Eden transect sampling regime was much greater than that of the Ythan sampling regimes. There was a larger range of species number of cyanobacteria observed in the Eden estuary transect than the Ythan estuary, and there was a narrower range of species number of eubacteria in the intensive sampled sediments in the Ythan estuary than the transect datasets. There were generally similar Pielou' evenness of TRFs (J') and Shannon's diversity of TRFs (H') for all targets over the three sampling regimes, with higher J' and H' observed for eubacteria than algae and cyanobacteria, which demonstrated similar J'. H' of algae was slightly higher than cyanobacteria for all sampling regimes.

Table 5.3.1 The mean ± SE, minimum, maximum and range of observed values for total species of TRFs (S), species evenness of TRFs (J') and species diversity of TRFs (H') of eubacteria, algae, cyanobacteria and all targets combined for the transects of the Ythan and Eden estuaries, and the intensive Ythan sampling T-RFLP datasets.

		All Targets			Eubacteria			Algae			Cyanobacteria		
		S	J'	H'	S	J'	H'	S	J'	H'	S	J'	H'
Ythan Transect	Mean ± SE	76.41 ± 1.63	0.74 ± 0.01	3.20 ± 0.04	34.30 ± 0.97	0.74 ± 0.01	2.58 ± 0.05	24.09 ± 0.87	0.65 ± 0.01	2.05 ± 0.06	18.02 ± 0.77	0.59 ± 0.02	1.66 ± 0.05
	Min. Observed	50.00	0.57	2.33	17.00	0.44	1.42	9.00	0.41	1.11	8.00	0.34	0.79
	Max. Observed	108.00	0.86	3.61	60.00	0.97	3.23	44.00	0.86	3.00	34.00	0.85	2.36
	Range (Min. - Max.)	58.00	0.29	1.28	43.00	0.53	1.81	35.00	0.45	1.90	26.00	0.51	1.57
Eden Transect	Mean ± SE	77.24 ± 3.11	0.73 ± 0.01	3.14 ± 0.05	34.07 ± 1.31	0.74 ± 0.02	2.57 ± 0.06	23.44 ± 0.98	0.61 ± 0.01	1.92 ± 0.06	19.73 ± 1.76	0.59 ± 0.02	1.65 ± 0.06
	Min. Observed	46.00	0.59	2.28	11.00	0.35	0.83	10.00	0.43	1.05	5.00	0.34	0.66
	Max. Observed	183.00	0.87	3.80	62.00	0.88	3.19	40.00	0.84	2.75	86.00	0.94	2.53
	Range (Min. - Max.)	137.00	0.27	1.52	51.00	0.54	2.36	30.00	0.41	1.70	81.00	0.60	1.87
Ythan Intensive	Mean ± SE	70.53 ± 7.74	0.76 ± 0.08	3.21 ± 0.35	29.63 ± 3.25	0.78 ± 0.09	2.62 ± 0.29	22.01 ± 2.40	0.63 ± 0.07	1.93 ± 0.21	19.06 ± 2.09	0.63 ± 0.07	1.81 ± 0.20
	Min. Observed	40.00	0.61	2.45	16.00	0.50	1.51	10.00	0.33	0.77	9.00	0.25	0.82
	Max. Observed	131.00	0.84	3.73	47.00	0.89	3.05	35.00	0.80	2.68	56.00	0.86	2.50
	Range (Min. - Max.)	91.00	0.22	1.28	31.00	0.39	1.53	25.00	0.47	1.91	47.00	0.60	1.67

5.3.2.2 Intensively sampled sediments in the Ythan estuary

Total species of TRFs for eubacteria were significantly fewer in M and MS than S and MM (p= <0.001; Table 5.3.2 and 5.3.3). Algal species were significantly fewer in S than MS and M, and greater in M than MM (p= <0.001). Number of total species of between seasons was only significant in eubacteria (p= 0.010) where during autumn and summer total species were fewer than winter.

Pielou's evenness of TRFs (J') for algae at S and MM was lower than M and MS (p= 0.032; Table 5.3.2 and 5.3.3). There was also significant differences of J' for algae between seasons, where summer was lower than autumn and spring (p= 0.032). J' for eubacteria during summer and winter was lower than during autumn (p= 0.036), and for cyanobacteria was lower at MS than all other sites (p= 0.013).

There was only significant difference of Shannon's diversity of TRFs (H') for algae between sites, where S and MM were lower than MS and M (p= 0.003; Table 5.3.2 and 5.3.3). The two way interaction of site x season was not significant for S, J' or H' over all targets or individually, with the exception of total algal species, where total species were greatest at M during spring, summer and autumn (Fig. 5.3.2). During this period at MM the number of total algal species were much lower, at a similar level to M during winter. Conversely, MM during winter had a higher number of total algal species than the rest of the year. Number of total algal species did not vary greatly throughout the year at MS and S.

Table 5.3.2 Summary of means ± SE of total species (S), Pielou's evenness (J') and Shannon's diversity (H') four sediment types in the Ythan estuary.

	All Targets			**Eubacteria**			**Algae**			**Cyanobacteria**		
	S	**J'**	**H'**	**S**	**J'**	**H'**	**S**	**J'**	**H'**	**S**	**J'**	**H'**
Mud	67.14 ± 2.23	0.77 ± 0.02	3.22 ± 0.07	25.86 ± 1.05	0.76 ± 0.03	2.47 ± 0.09	24.43 ± 1.03	0.65 ± 0.02	2.08 ± 0.09	16.86 ± 1.47	0.68 ± 0.03	1.80 ± 0.11
Mixed Mud	73.55 ± 3.24	0.75 ± 0.01	3.23 ± 0.07	33.20 ± 1.11	0.78 ± 0.02	2.71 ± 0.07	21.33 ± 1.28	0.60 ± 0.03	1.83 ± 0.10	18.86 ± 1.41	0.65 ± 0.02	1.86 ± 0.06
Mixed Sand	68.81 ± 1.96	0.76 ± 0.01	3.19 ± 0.05	27.10 ± 1.06	0.80 ± 0.02	2.61 ± 0.06	23.19 ± 0.89	0.66 ± 0.02	2.06 ± 0.06	18.52 ± 1.09	0.56 ± 0.03	1.61 ± 0.09
Sand	72.76 ± 3.79	0.75 ± 0.01	3.21 ± 0.03	32.52 ± 1.61	0.78 ± 0.02	2.70 ± 0.06	19.10 ± 0.77	0.60 ± 0.01	1.75 ± 0.03	21.14 ± 2.12	0.64 ± 0.02	1.89 ± 0.05

Table 5.3.3 ANOVA summary table for the two-way effects and interaction effect of site and season on total species, Pielou's evenness and Shannon's diversity of TRFs for the intensively sampled sediments in the Ythan estuary. *p*- values in bold denote significance lower than <0.05.

Ythan Intensive Sampling		Site		Season		Site x Season Interaction	
		F-statistic	*p*-value	F-statistic	*p*-value	F- statistic	*p*- value
All Targets	Total Species	1.36	0.263	2.00	0.122	1.81	0.083
	Pielou's Evenness	0.22	0.882	1.34	0.269	0.41	0.928
	Shannon's Diversity	0.08	0.973	1.46	0.234	0.57	0.815
Eubacteria	Total Species	11.25	**<0.001**	4.06	**0.010**	1.63	0.125
	Pielou's Evenness	0.47	0.707	3.02	**0.036**	0.45	0.905
	Shannon's Diversity	2.35	0.081	2.12	0.106	0.52	0.856
Algae	Total Species	6.40	**<0.001**	0.13	0.944	3.21	**0.003**
	Pielou's Evenness	3.11	**0.032**	3.11	**0.032**	1.12	0.364
	Shannon's Diversity	5.16	**0.003**	2.15	0.102	1.64	0.122
Cyanobacteria	Total Species	1.24	0.302	1.29	0.286	0.76	0.655
	Pielou's Evenness	3.84	**0.013**	0.05	0.985	1.02	0.431
	Shannon's Diversity	2.66	0.055	1.88	0.140	0.70	0.706

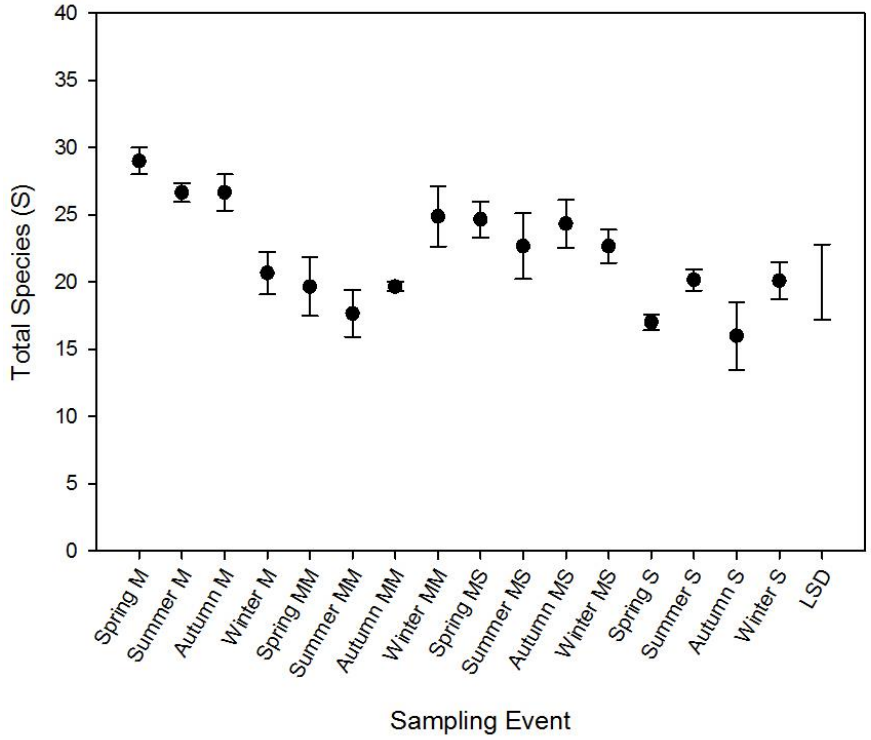

Figure 5.3.2 Means plot of total species of algal TRFs for the intensively sampled sediments in the Ythan estuary. Error bars indicate SE. n= 3 in all cases. Error bar on far right denotes max-min LSD for two-way interaction.

5.3.2.3 Seasonal samples from the Ythan estuary transect

There was only significant difference in number of total species for algae between sites (Table 5.3.4) with a slight decrease total species between sites 8-11 (Fig. 5.3.3). When including all targets and within each target independently, there were consistently significant differences between sites for both J' and H'. Over all targets, and all individual targets (Fig. 5.3.4), the general trend was that both J' and H' increased as sites progressed towards the mouth of the estuary up to site 7, where it decreased to around or below the level observed at the head of the estuary (site 1) until sandier sediments at the mouth of the estuary (sites 12-14) where levels similar to that of site 7 were observed. Site 9 over all targets, eubacteria and cyanobacteria was an exception to the decrease in evenness and diversity between sites 7 and 12 where levels similar to that of sites 7 and 12-14 were observed. There was no significant difference between S, J' or H' of different seasons for the Ythan transect sampling.

Table 5.3.4 ANOVA summary table for the one-way effects of site and season on total species, Pielou's evenness and Shannon's diversity of TRFs over a transect of the Ythan estuary. *p*-values in bold denote significance lower than <0.05.

Ythan Transect		Site		Season	
		F-statistic	*p*-value	F-statistic	*p*-value
All Targets	Total Species	1.61	0.121	1.09	0.363
	Pielou's Evenness	5.38	**<0.001**	0.09	0.964
	Shannon's Diversity	5.80	**<0.001**	0.21	0.890
Eubacteria	Total Species	0.78	0.677	0.61	0.612
	Pielou's Evenness	2.49	**0.013**	0.45	0.720
	Shannon's Diversity	2.42	**0.015**	0.64	0.593
Algae	Total Species	4.16	**<0.001**	0.64	0.591
	Pielou's Evenness	2.30	**0.021**	0.48	0.695
	Shannon's Diversity	3.57	**<0.001**	0.31	0.818
Cyanobacteria	Total Species	1.09	0.390	1.76	0.167
	Pielou's Evenness	5.08	**<0.001**	0.69	0.561
	Shannon's Diversity	2.72	**0.007**	0.09	0.965

.

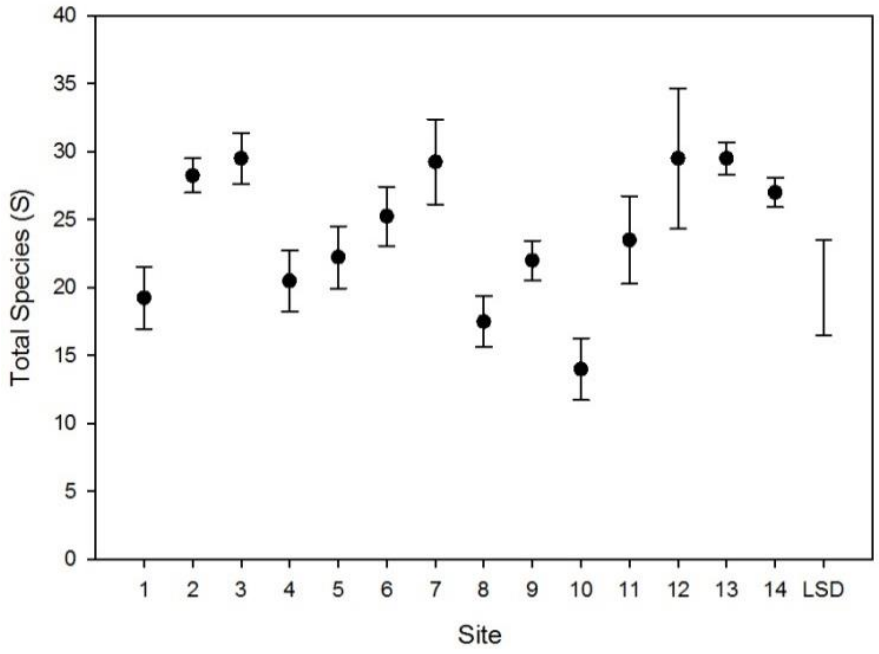

Figure 5.3.3 Total algal species for the Ythan Transect sampling regime. Error bars indicate SE. n= 4 in all cases. Error bar on far right denotes LSD for one-way effect of site.

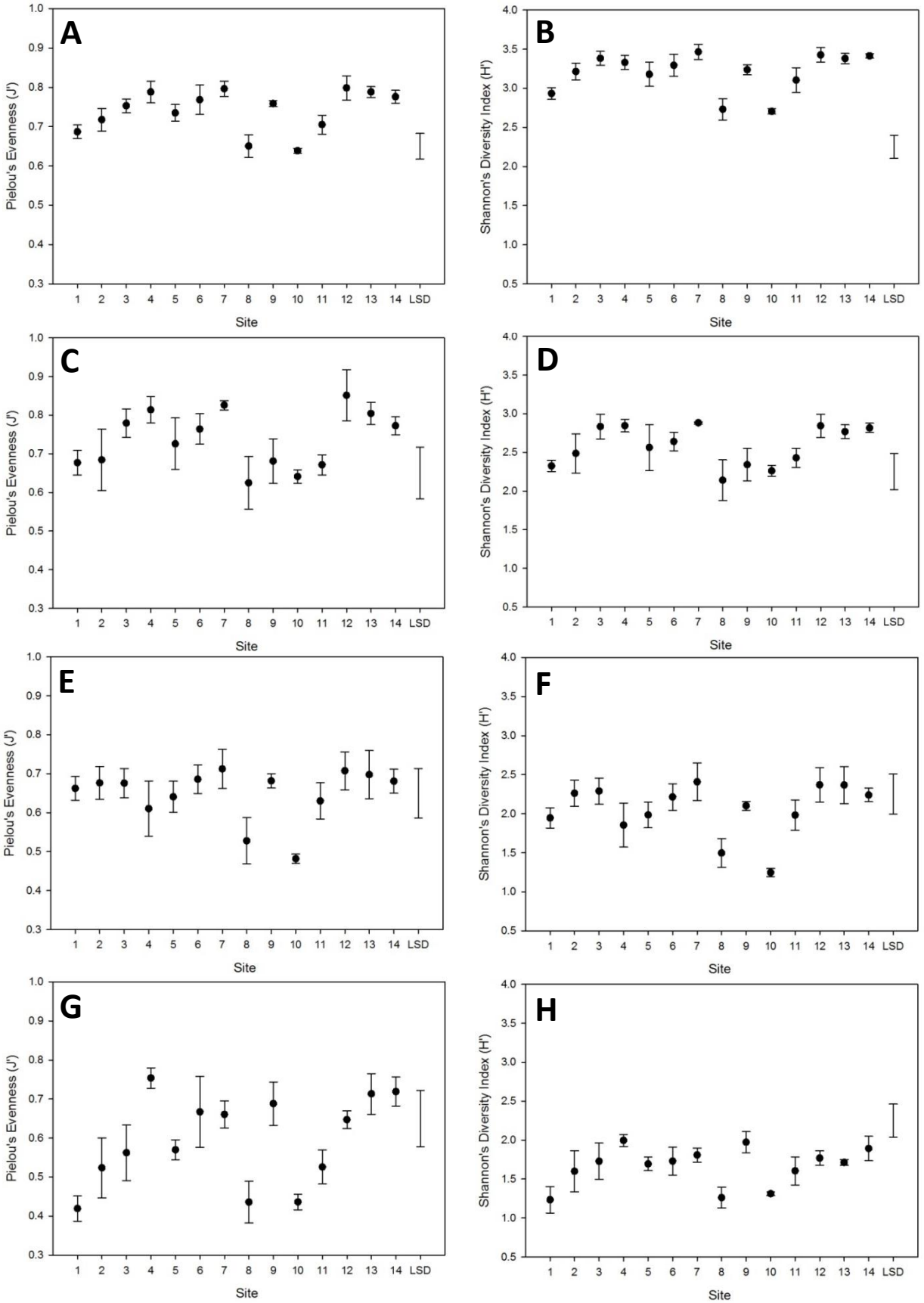

Figure 5.3.4 Pielou's Evenness and Shannon's Diversity Index for the Ythan Transect sampling regime. A,B= All targets, C,D= Eubacteria, E, F= Algae, G,H= Cyanobacteria. Error bars indicate SE. n= 4 in all cases. Error bar on far right denotes mean LSD for one-way effect of site.

5.3.2.4 Seasonal samples from the Eden estuary transect

There was only significant difference in number of total species between sites within algae (Table 5.3.5) with a slight trend of lower total species between sites 7 to 12 inclusive (Fig. 5.3.5). There were significant differences between sites for both J' and H' for both algae and cyanobacteria, and over all targets (Fig. 5.3.6). The general trend over all targets, algae and cyanobacteria was a general decrease of both species evenness and diversity from the head of the estuary (site 1) to site 10. Evenness and diversity at the same level as the head of the estuary was observed in the sandier sediments at the mouth (sites 11-14). Temporal variation was not as strong as spatial variation (Table 5.3.5), but there were significant differences of total species between seasons when including all targets, where total species at S was higher during spring than autumn and summer (means: autumn: 68.08 ± SE 2.18, summer: 72.50 ± SE 4.09, winter: 81.58 ± SE 7.65, spring: 84.08 ± SE 3.99; p= 0.049). The J' for eubacterial species was significantly lower during winter than spring and autumn (means: winter: 0.66 ± SE 0.04, summer: 0.72 ± SE 0.04, spring: 0.75 ± SE 0.02, autumn: 0.80 ± SE 0.02; p= 0.020).

Table 5.3.5 ANOVA summary table for the one-way effects of site and season on total species, Pielou's evenness and Shannon's diversity of TRFs over a transect of the Eden estuary. *p*-values in bold denote significance lower than <0.05.

Eden Transect		Site		Season	
		F-statistic	*p*-value	F-statistic	*p*-value
All Targets	Total Species	0.58	0.854	2.80	**0.049**
	Pielou's Evenness	3.30	**0.002**	2.28	0.091
	Shannon's Diversity	3.15	**0.003**	1.52	0.221
Eubacteria	Total Species	0.73	0.727	2.14	0.106
	Pielou's Evenness	1.08	0.402	3.57	**0.020**
	Shannon's Diversity	0.90	0.559	2.60	0.062
Algae	Total Species	3.89	**<0.001**	1.00	0.399
	Pielou's Evenness	2.72	**0.007**	1.40	0.253
	Shannon's Diversity	4.16	**<0.001**	1.25	0.303
Cyanobacteria	Total Species	0.70	0.752	2.65	0.059
	Pielou's Evenness	4.16	**<0.001**	0.78	0.511
	Shannon's Diversity	3.43	**0.001**	0.22	0.884

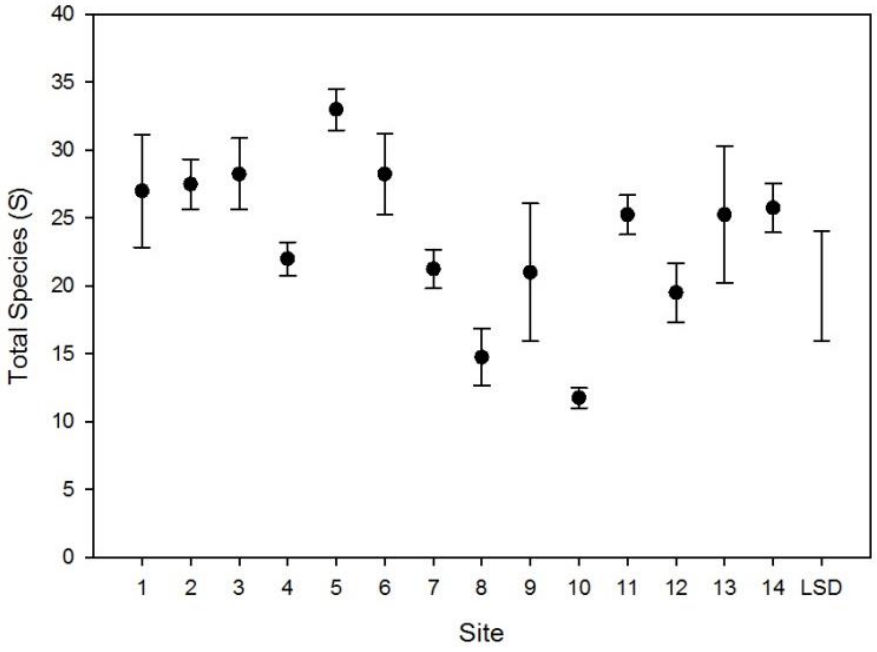

Figure 5.3.5 Total Species for Algae for the Eden Transect sampling regime. Error bars indicate SE. n= 4 in all cases except site 5 where n=3. Error bar on far right denotes mean LSD for one-way effect of site.

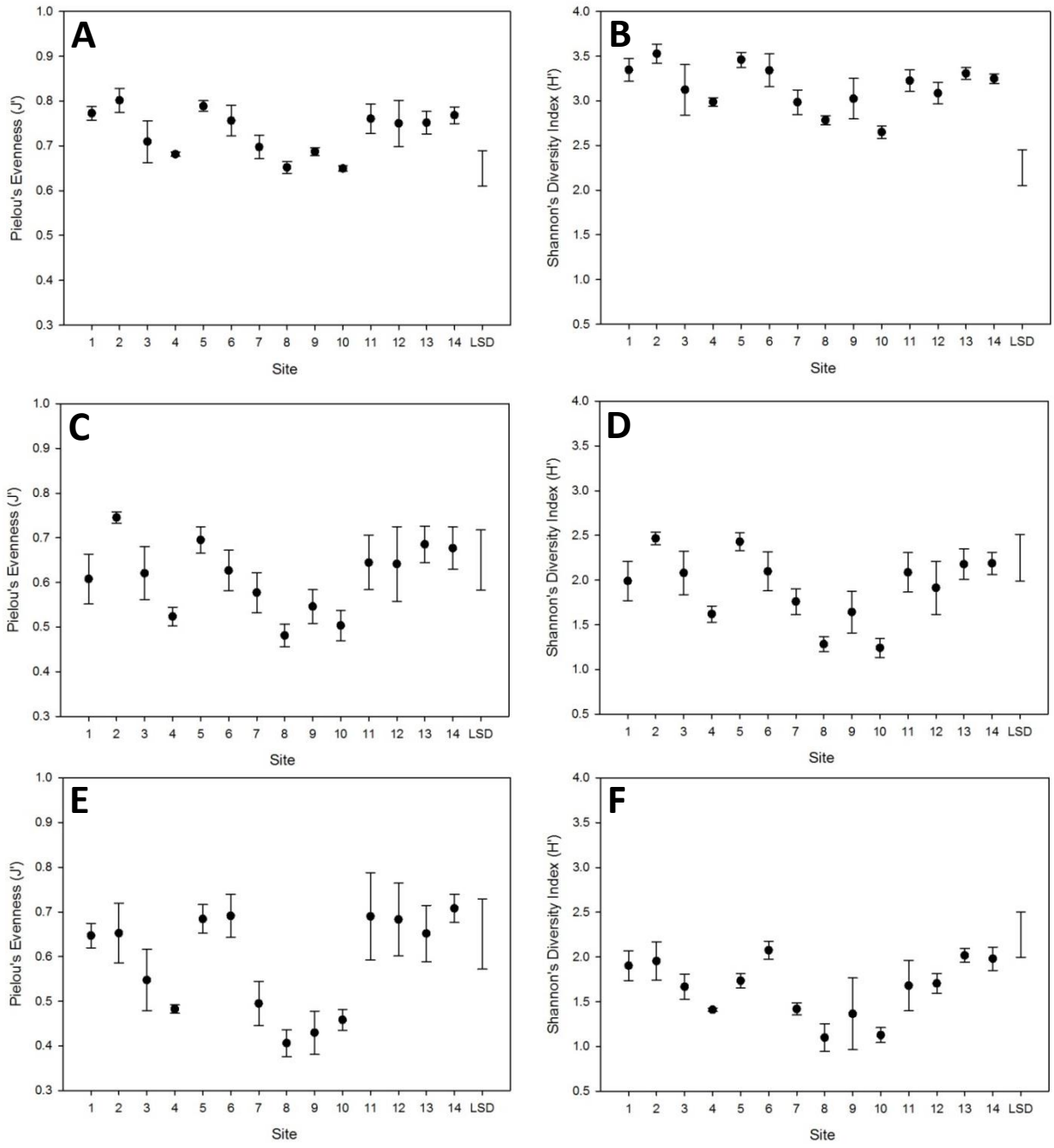

Figure 5.3.6 Pielou's Evenness and Shannon's Diversity Index for the Eden Transect sampling regime. A,B= All targets, C,D= Algae, E, F= Cyanobacteria. Error bars indicate SE. n= 4 in all cases except site 5 in A,B where n=3. Error bar on far right denotes mean LSD for one-way effect of site.

5.3.3 Relationship between **E. coli** *abundance and microbial population metrics*

Overall abundance of *E. coli* was generally greater in intertidal sediments during summer, autumn and winter than spring in both the Ythan and Eden estuaries, with abundance generally decreasing towards the mouth of the estuaries (Figs. 5.3.7 and 5.3.8 respectively). Sites at the mouth of both estuaries (12-14) contained similar abundances of *E. coli,* however at the head of the estuaries the Eden estuary typically demonstrated higher abundances than the Ythan. At both estuaries during winter, although sites at the head of the estuary were not the highest observed throughout the year, high *E. coli* abundance was sustained further down the estuary to site 10. *E. coli* abundance at the head of the estuaries were higher during summer and autumn, but decreased rapidly down the estuary between sites 4 and 6 in the Ythan estuary, and sites 7 and 8 in the Eden estuary. Sites in the mid- reaches of the Ythan estuary (6 and 7) often contained a lower abundance of *E. coli* than sediments towards the mouth of the estuary, which is especially evident during autumn (Fig. 5.3.7D). This was also observed to a lesser degree in the Eden estuary, where sediments at site 9 during spring and summer contained a higher abundance of *E. coli* than site 7 (Figs. 5.3.8B and 5.3.8C).

There were only extremely weak or non-significant linear regressions between *E. coli* abundance and total species, species evenness, and species diversity of TRFs for both the intensively sampled sediments and transect sampling regimes (data not shown). Linear regressions were significant when grouped by transect site, however within group regressions were non-significant.

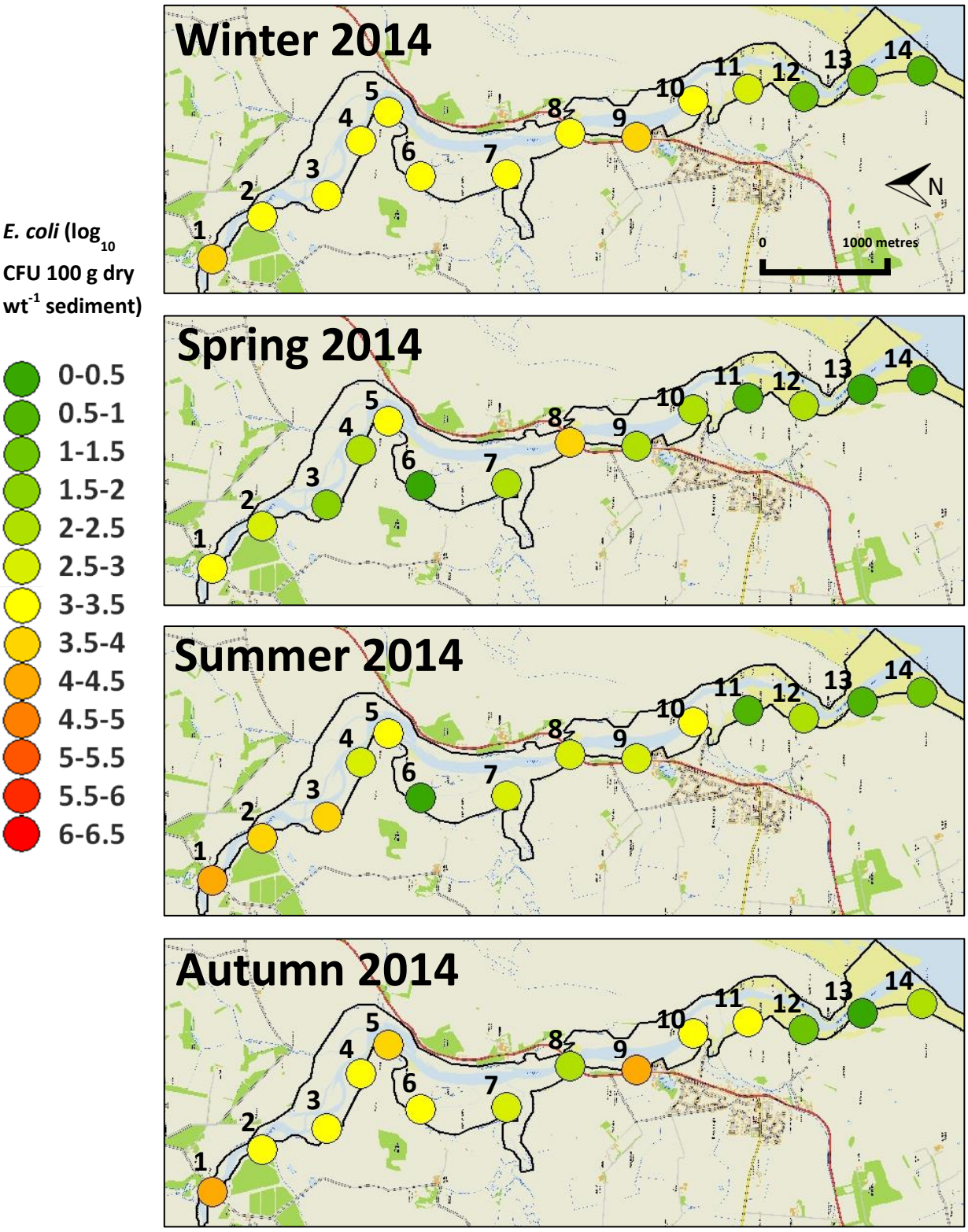

Figure 5.3.7 *E. coli* abundance in the Ythan estuary during winter, spring, summer and autumn 2014. Numbers denote Site ID. Symbol colour denotes mean *E. coli* abundance (log_{10} CFU 100 g dry wt^{-1} sediment).

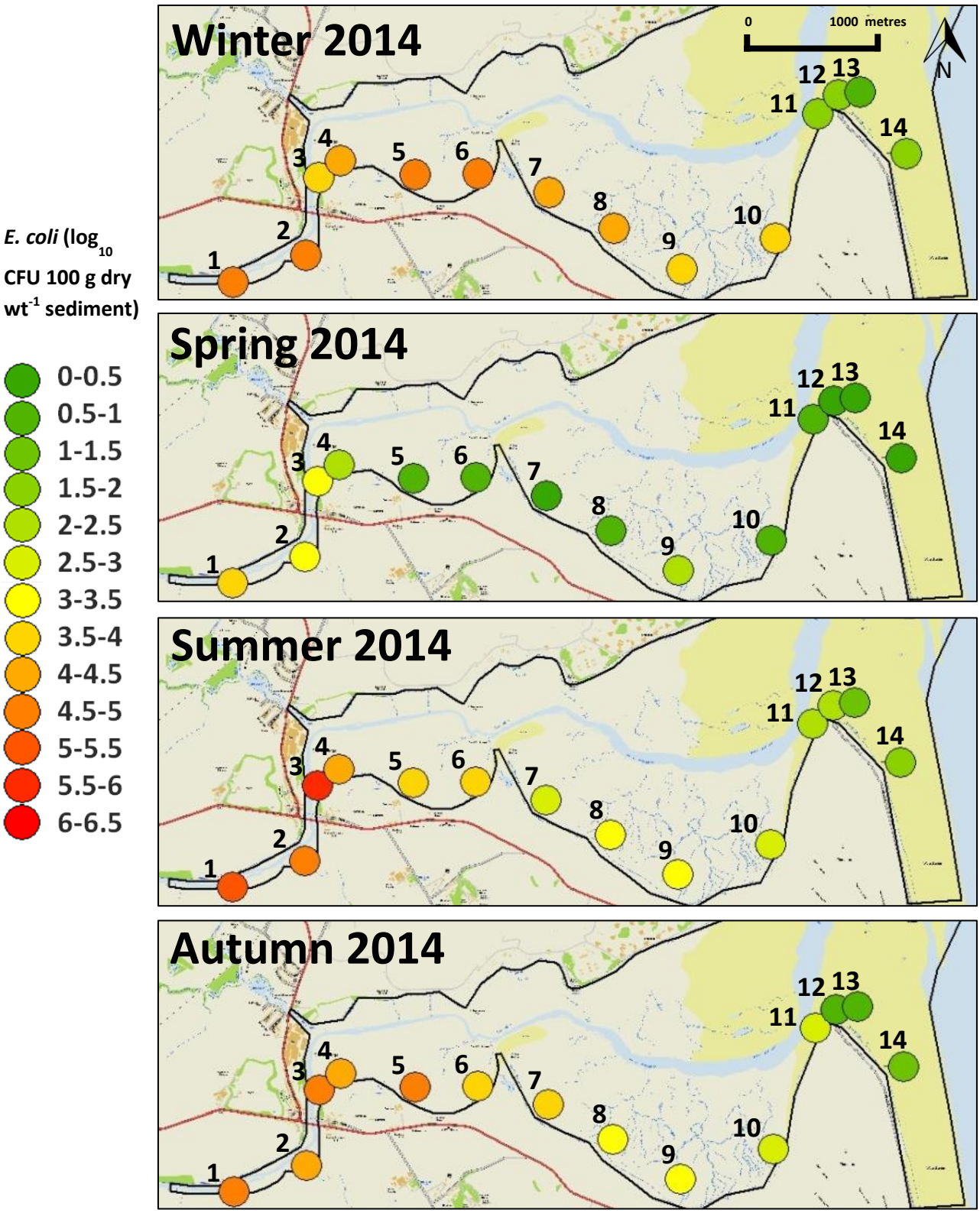

Figure 5.3.8 *E. coli* abundance in the Eden estuary during winter, spring, summer and autumn 2014. Numbers denote site ID. Symbol colour denotes mean *E. coli* abundance (log_{10} CFU 100 g dry wt^{-1} sediment).

5.3.4 Spatial and temporal shift in microbial community constituent composition

The stress values of the nMDS ordinations ranged between 0.13 and 0.18 (intensive Ythan sampling and combined estuary transect regimes respectively), and although quite high are not deemed suspect due to the number of samples plotted. Several of the overlaid TRF vectors are common to all datasets, and were of algal, eubacterial and cyanobacterial TRFs (TRF suffix- B, G and Y respectively; Figs. 5.3.9, 5.3.10 and 5.3.11).

The nMDS ordinations of the T-RFLP data demonstrated distinct spatial patterns of community composition along the estuary transects (Table 5.3.6). There was no significant difference in microbial communities with season in any sampling regime, however site was a significant factor in separating microbial communities in the intensive sampling regime on the Ythan estuary, and within the individual estuary transects, and within both estuary transects combined (Table 5.3.6). Sites near the mouth of the estuaries (Ythan= 13, 14; Eden= 12-14) were clearly clustered at the right hand side the ordinations (Figs. 5.3.9A and B respectively). TRFs 412Y, 271Y, 139Y and 189G were positively correlated, and 349Y, 68B, 291B were negatively correlated with this positioning in both the Eden and Ythan estuary, and appear to also correlate with the separation of sites at the mouth of the estuary and several sites in the mid-lower estuary located on the left hand side of both ordinations (Ythan= 8, 10, 11; Eden= 8-10). Sites at the head of both estuaries (Ythan= 1, 2; Eden= 1) were positioned at the top of both ordinations with an almost equal distance to the sites at the mouth, and mid-lower parts of the estuaries. In the Ythan estuary, sites further up the estuary correlate with the presence of the algal TRF 295B and the absence of algal TRF 68B.

There was considerable similarity between microbial communities of the Ythan and Eden estuaries at similar positions down the estuary (Fig. 5.3.10). The most distinct similarity is of sites at the mouth of the estuary sharing very similar communities, positioned at the right hand side of the ordination. Microbial community composition at the head of the estuaries were not as similar to one another however, with compositions at the head of the Eden estuary being more similar to the upper-mid section of the Ythan estuary, clustered in the centre of the ordination. Communities at the mid-lower reaches of the estuaries (8-10) were similarly composed between the estuaries, and positioned to the left of the ordination.

The microbial community compositions of the intensively sampled sediments in the Ythan estuary were very distinct between sediment types, with only slight overlap between M and MM (Fig. 5.3.11). There was no discernible trend with season, although samples within a

sediment type taken in the same season were positioned relatively closely compared to other seasons within the sediment type. The compositions of sand sediments seemed to be more similar to that of mixed mud, rather than mixed sand. MS sediments were positively correlated with TRF 349Y, and M sediments positively correlated with 81Y. Sediment types were separated horizontally in the ordination by predominantly algal and eubacterial TRFs.

Table 5.3.6 Summary table of the ANOSIM analysis. Numbers in bold represent significance <0.05.

Microbial Community	Factor	Global R	*P*- value
Ythan Transect	Season	0.008	0.336
Ythan Transect	Site	0.637	**0.001**
Eden Transect	Season	0.059	0.035
Eden Transect	Site	0.487	**0.001**
Combined Transects	Season	0.040	0.017
Combined Transects	Site	0.391	**0.001**
Combined Transects	Estuary	0.052	0.007
Ythan Intensive	Season	-0.047	0.733
Ythan Intensive	Site	0.771	**0.001**

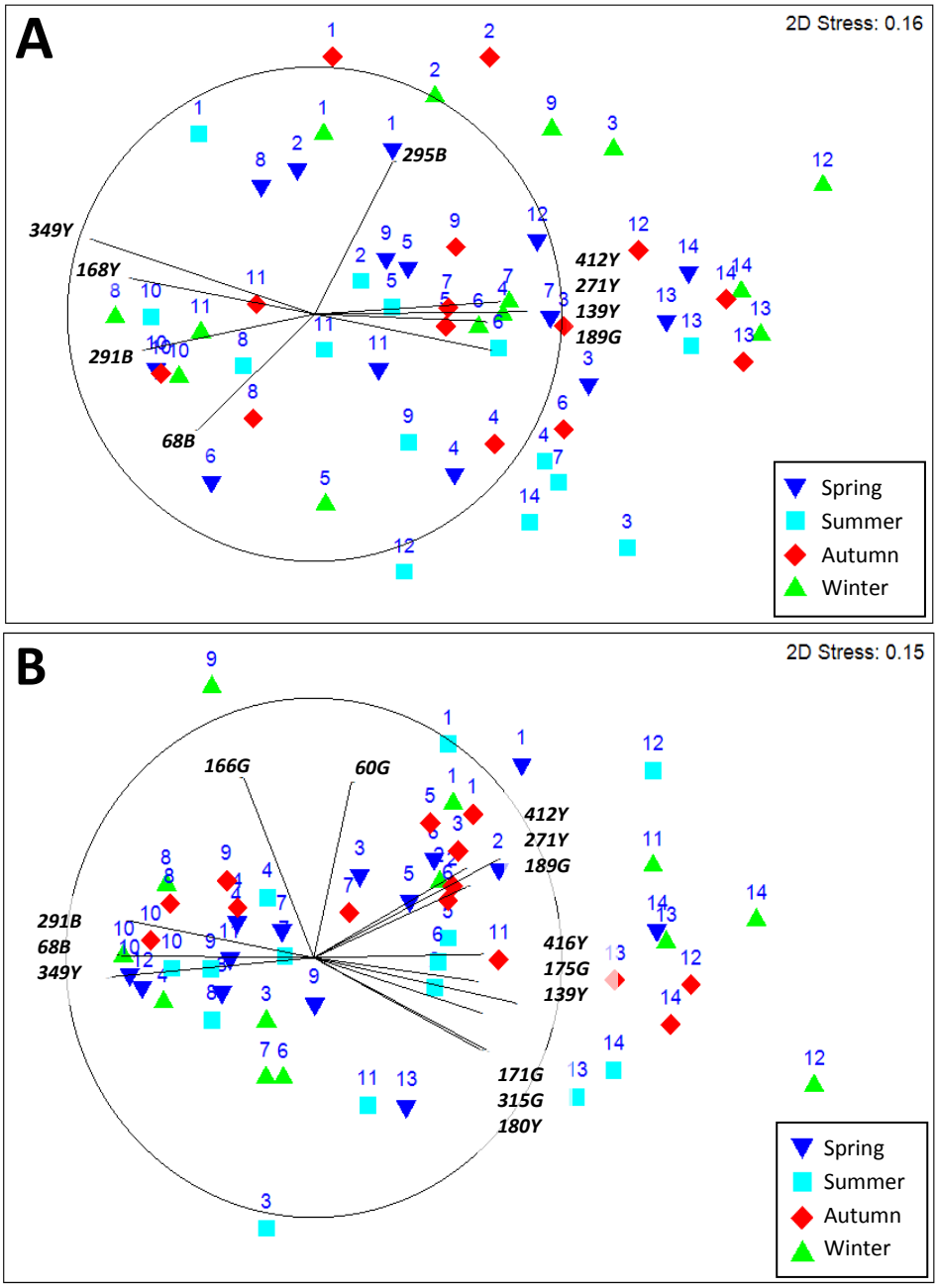

Figure 5.3.9 NMDS ordination of the TRFLP microbial community analysis of the Ythan (A) and Eden (B) estuary transects. Overlaid vectors are of TRFs that defined variables with a Pearson's correlation >0.65. Vector labels denote fragment length (bp), and target where G- eubacteria; B- algae; Y- cyanobacteria. Sample labels denote site ID. Blue triangles- spring; turquoise squares- summer; red diamonds- autumn; green triangles- winter.

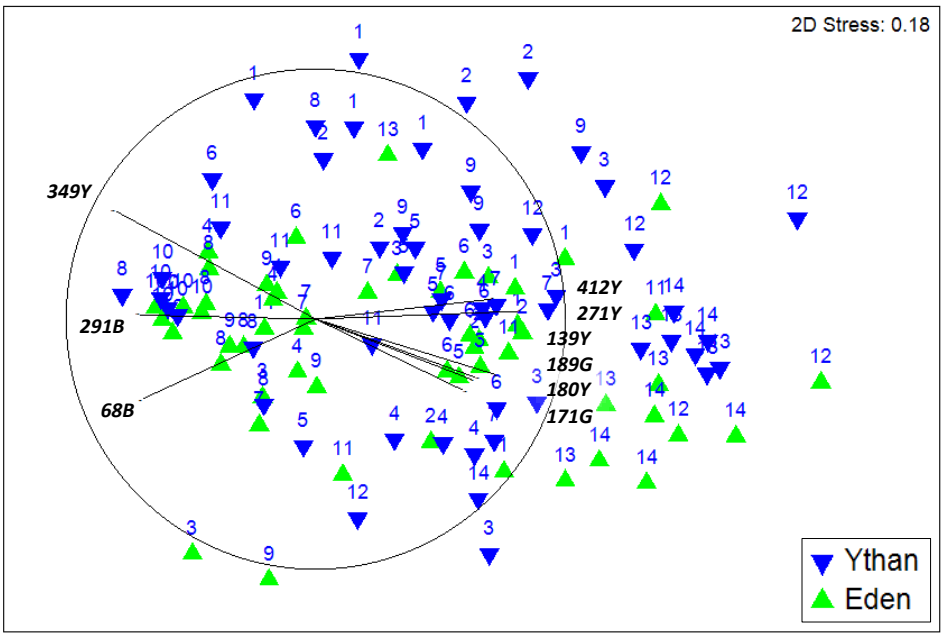

Figure 5.3.10 NMDS ordination of the TRFLP microbial community analysis of the combined Ythan and Eden estuary transects. Overlaid vectors are of TRFs that defined variables with a Pearson's correlation >0.65. Vector labels denote fragment length (bp), and target where G- eubacteria; B- algae; Y- cyanobacteria. Sample labels denote site ID. Blue triangles- Ythan estuary; green triangles- Eden estuary.

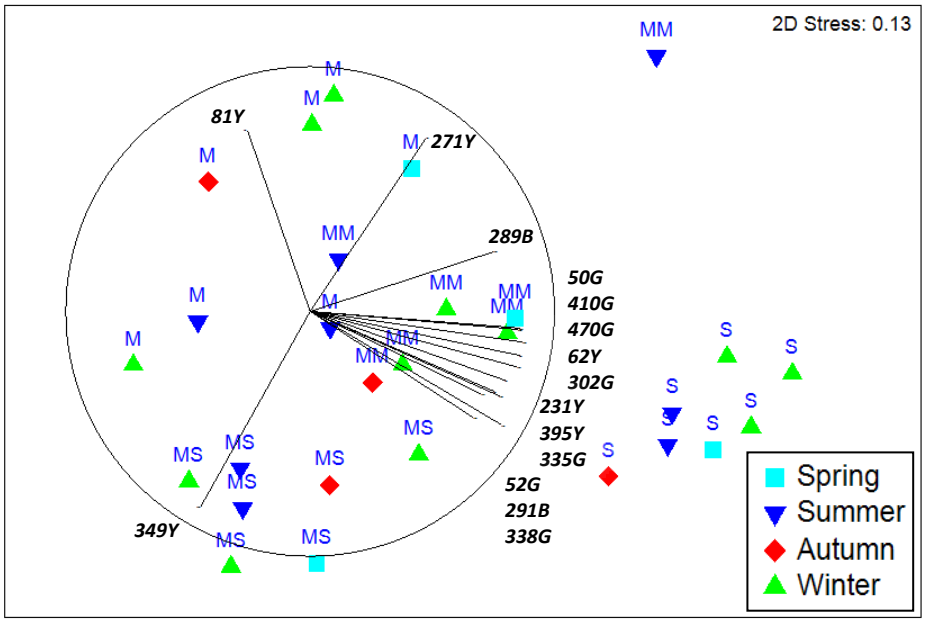

Figure 5.3.11 NMDS ordination of the TRFLP microbial community analysis of intensively sampled sediments at the Ythan estuary. Overlaid vectors are of TRFs that defined variables with a Pearson's correlation >0.75. Vector labels denote fragment length (bp), and target where G- eubacteria; B- algae; Y- cyanobacteria. Sample labels denote sediment type where M- mud; MM- mixed mud, MS- mixed sand, S- sand. Turquoise squares- spring; blue triangles- summer; red diamonds- autumn; green triangles- winter.

5.3.5 Identification of overlaid TRFs

Taxonomic resolution was very poor within the algal TRFs. There were no reliable or realistic positive identifications for TRFs 68B or 289B. TRF 291B however returned several positive identifications of Chlamydomonadales and Prasinophyceae, and TRF 295B was positive for a very wide range of freshwater and marine Chlorophyta (Table A11). Un-cut TRFs will also contribute to the 289B, 291B and 295B TRFs, which include almost all diatom species, therefore the correlation of these peaks may be indicative of diatom presence and absence. However, there was a major issue with the algal dataset, as TRFs 291B and 295B matched with many 18S sequences of a wide range of species within the fungal phylum of Basidiomycota.

Within the cyanobacteria, TRFs 231Y, 271Y and 349Y returned positive identifications (Table A11). TRF 231Y was primarily Oscillatoriales, though several Synechococcales and one species of Nostocales also matched the TRF. TRF 271Y was similar to 231Y, but with the absence of

Synechococcales and the presence of chrococcales. TRF 349 was comprised primarily of Nostocales, however there were matches with several other lineages (Table A11).

Within the eubacteria, there was one positive identification for TRF 50G that was for the Rhodospirillalas (Table A12). TRF 52G contained lineages of Alpha- Delta- and Gammaproteobacteria. 166G contained Alteromonadales only. TRF 171G matched primarily Gammaproteobacterial lineages, and Burkholderiales, and TRF 175G contained Gammaproteobacteria only. TRF 189G contained Alpha- and Gammaproteobacteria. 302G contained exclusively Rhizobiales. TRF 335G was the only TRF to contain Actinobacteria, but also Alpha- Beta- and Gammaproteobacteria, with Enterbacteriales being the dominant order. TRF 338G was similar to TRF 335G, but with the absence of Actinobacteria and betaproteobacteria, and presence of Deltaproteobacteria. TRF 470G contained Rhodobacterales (Alphaproteobacteria) and Alteromonadales (Gammaproteobacteria).

5.3.6 Correlations between environmental variables and microbial community constituent composition: RELATE and BEST Analysis

RELATE analysis revealed all datasets had a weak but statistically significant correlation between the Euclidean similarity matrix of the environmental variables and the Bray-Curtis similarity matrix of the microbial community T-RFLP data (Table 5.3.7). The microbial community constituent composition of the Eden estuary transect had a higher correlation with environmental parameters than the Ythan estuary transect (Global Rho: Eden: 0.366, p= 0.010; Ythan: 0.226, p= 0.001). BEST analysis based on the normalised environmental data and the Bray-Curtis similarity matrix of the microbial community revealed stronger correlations than the RELATE analysis as redundant variables were excluded (Table 5.3.7). The order of the correlation strength of the sampling regimes was the same as observed in the RELATE analysis. Colloidal carbohydrate content was the only variable included in both the Eden and Ythan transect analyses, however variables related to particles size that typically co-vary were included in both analyses, with proportion of fine particles (% fines), and median particle diameter (D (0.5)) included in the Ythan estuary transect subset, and volume weighted mean particle size included for the Eden estuary. Only one environmental variable was included (maximum air temperature) in the optimal correlation of sediment characteristics and community composition shift, and was only utilised in the Eden estuary transect and combined estuary dataset models.

Table 5.3.7 Summary table of the RELATE and BEST analysis. Variables marked with ✓ denote inclusion in the optimal BEST model to which the Global Spearman's rank (Rho) and associated significance refer. Rho and associated *p*- value are based on 999 permutations. *p*- values in bold denote significance <0.05.

	RELATE Analysis		BEST Analysis													
	Global Spearman's Rank (Rho)	Rho *P*- value	Global Spearman's Rank (Rho)	Rho *P*- value	Organic %	Bulk density	% Fines	D (0.5)	Vol. Weighted Mean	Carbohy-drate	Protein	Organic C	Total C	Max. Temp.	Shear Vane
Ythan Intensive Sampling	0.326	0.001	0.509	0.010	✓			✓	✓				✓		✓
Ythan Transect	0.226	0.001	0.352	0.010			✓	✓		✓	✓	✓			
Eden Transect	0.366	0.010	0.541	0.010	✓	✓			✓	✓				✓	
Both Transects	0.271	0.010	0.379	0.010	✓	✓		✓		✓				✓	

5.3.7 Modelling the effect of sediment characteristics on microbial community constituent composition: DistLM

Generally, sediment characteristics and environmental variables poorly explained shifts in microbial community constituent composition in the estuary transect datasets. The optimal DistLM model for the Eden transect dataset was more effective than the Ythan estuary transect at explaining the variance of the community composition (adjusted R^2= 0.41, 0.28; Eden and Ythan transects respectively) (Table 5.3.8), with the model for both estuary transects combined achieving a similar adjusted R^2 (0.27) as the Ythan transect model (Tables 5.3.9 and 5.3.8A respectively). The DistLM model for the intensive Ythan sampling regime was more successful with an adjusted R^2 of 0.59 (Table 5.3.10). The dbRDA ordinations (Figs. 5.3.12, 5.3.13, 5.3.14) generally showed similar separation of samples to the nMDS ordinations (Figs. 5.3.9, 5.3.10, 5.3.11), with clustering of sites at the mouth of the estuary, the mid-lower reaches, and the head of the estuary in the transect datasets.

DistLM analysis of the Ythan estuary transect dataset revealed that shift in community composition could be explained by colloidal protein concentration, water content, proportion of fine particles and salinity before the sequential terms added were non-significant (Table 5.3.8A). Likewise, the community composition of the Eden estuary were primarily governed by sediment shear strength, carbohydrate content, proportion of fine particles, sea temperature, water content and pH (Table 5.3.8B). Several variables measuring temperature were included in the models for both estuary analyses individually (Table 5.3.8), though only water content, proportion of fine particles, salinity and organic content were variables common to both individual analyses. Water content and proportion of fine particles were the only parameters common to both estuaries before terms were non-significant. The DistLM for the combined estuary transects contained parameters from both individual estuary models, in addition to water content and proportion of fine particles that were common to both estuaries (Table 5.3.9). The dbRDA ordinations indicate that community composition nearer the mouth of both estuaries were correlated with a decrease in proportion of fine particles, decrease in water and organic content, and increase in pH (Fig. 5.3.13). EPS content (colloidal proteins and carbohydrates for the Ythan and Eden estuaries respectively (Fig. 5.3.12)), primarily protein for the combined dataset (Fig. 5.3.13) was responsible for much of the separation along dbRDA 1 of both estuaries.

The DistLM analysis of the intensively sampled sediments in the Ythan estuary demonstrated that shift in community composition was governed greatly by particle size parameters up to an adjusted R^2 of 0.39 (Table 5.3.10). The position of sand sediment microbial communities in the dbRDA ordination were correlated with a larger particle size, and lower total carbon (Fig. 5.3.14). The microbial communities of the mud and mixed mud sediments correlated with higher water content and fine particle proportion, and mixed sand communities with higher salinity, bulk density and sediment shear strength.

5.3.8 Relationships between E. coli *abundance and microbial community constituent composition*

E. coli abundance demonstrated no obvious trends with shift in community composition between sites 1- 10 at both the Ythan and Eden estuaries (Figs. 5.3.12 and 5.3.13). However, lower *E. coli* abundance was observed to correlate with community composition of sites at the mouth of the estuaries (Ythan: 12-14, Eden: 11-14) which exhibited a distinct shift from the majority of the higher and mid-estuary samples. Similarly, in the intensively sampled sediments there were no overriding trends, however there was slightly lower E*. coli* abundance in microbial communities in sandier sediments that correlated with an increase in mean particle size, bulk density, shear strength and salinity (Fig. 5.3.14). Higher total species of all targets in the Eden estuary overall all sites during spring also coincided with the lowest *E. coli* abundance throughout the estuary (Table 5.3.5, Fig. 5.3.8).

Table 5.3.8 Summary table of the DistLM analysis of the microbial community of the Ythan estuary (A) and Eden estuary (B) transects. *p*- values in bold denote significance <0.05.

A

Step	Variable	Adjusted R^2	Pseudo F-statistic	*p*- value	Individual R^2	Cumulative R^2	Residual d.f.
1	**+ Protein**	0.09	5.60	**0.001**	0.10	0.10	48
2	**+ Water %**	0.14	3.90	**0.001**	0.07	0.17	47
3	**+ % Fines**	0.17	2.58	**0.010**	0.04	0.22	46
4	**+ Salinity**	0.18	2.01	**0.048**	0.03	0.25	45
5	**+ Precip. 1**	0.20	1.90	0.069	0.03	0.28	44
6	**+ pH**	0.21	1.52	0.130	0.02	0.31	43
7	**+ Sea Temp**	0.23	2.27	**0.030**	0.04	0.34	42
8	**+ Min. Grass**	0.24	1.45	0.191	0.02	0.36	41
9	**- Precip. 1**	0.24	0.90	0.512	0.01	0.35	42
10	**+ Organic %**	0.25	1.24	0.258	0.02	0.37	41
11	**+ Bulk density**	0.25	1.24	0.258	0.02	0.39	40
12	**+ Max. Air Temp**	0.25	1.21	0.285	0.02	0.41	39
13	**+ Min. Air Temp**	0.27	2.03	**0.050**	0.03	0.44	38
14	**+ Vol. Weighted Mean**	0.28	1.22	0.254	0.02	0.45	37

B

Step	Variable	Adjusted R^2	Pseudo F-statistic	*p*- value	Individual R^2	Cumulative R^2	Residual d.f.
1	**+ Shear Vane**	0.13	8.11	**0.001**	0.15	0.15	45
2	**+ Carbohydrate**	0.22	5.79	**0.001**	0.10	0.25	44
3	**+ % Fines**	0.28	5.05	**0.001**	0.08	0.33	43
4	**+ Sea Temp**	0.32	3.45	**0.004**	0.05	0.38	42
5	**+ Water %**	0.34	1.98	**0.037**	0.03	0.41	41
6	**+ pH**	0.36	2.17	**0.031**	0.03	0.44	40
7	**+ Min. Air Temp**	0.37	1.69	0.072	0.02	0.46	39
8	**+ Min. Grass Temp**	0.38	1.84	0.059	0.02	0.49	38
9	**+ Vol. Weighted Mean**	0.39	1.49	0.118	0.02	0.51	37
10	**+ Salinity**	0.40	1.78	0.057	0.02	0.53	36
11	**+ Organic %**	0.41	1.65	0.100	0.02	0.55	35

Table 5.3.9 Summary table of the DistLM analysis of the microbial community of the combined estuary transects.

Step	Variable	Adjusted R^2	Pseudo F-statistic	*p*- value	Individual R^2	Cumulative R^2	Residual d.f.
1	**+ Protein**	0.07	8.31	**0.001**	0.08	0.08	95
2	**+ Shear Vane**	0.14	9.12	**0.001**	0.08	0.16	94
3	**+ % Fines**	0.20	7.13	**0.001**	0.06	0.22	93
4	**+ Sea temp**	0.22	3.46	**0.001**	0.03	0.25	92
5	**+ Water %**	0.23	2.82	**0.010**	0.02	0.27	91
6	**+ pH**	0.25	2.88	**0.008**	0.02	0.29	90
7	**+ Salinity**	0.25	1.74	0.073	0.01	0.31	89
8	**+ Vol. Weighted Mean**	0.26	1.18	0.275	0.01	0.32	88
9	**+ Min. Grass Temp**	0.26	1.12	0.336	0.01	0.33	87
10	**+ Min. Air Temp**	0.26	1.37	0.193	0.01	0.34	86
11	**+ Precip. 1**	0.26	1.10	0.347	0.01	0.35	85
12	**+ Precip. 2**	0.26	1.16	0.308	0.01	0.35	84
13	**+ Max. Air Temp**	0.26	1.10	0.345	0.01	0.36	83
14	**+ Precip. 5**	0.26	1.24	0.226	0.01	0.37	82
15	**- Vol. Weighted Mean**	0.27	0.97	0.431	0.01	0.36	83
16	**+ Bulk density**	0.27	1.04	0.391	0.01	0.37	82
17	**+ Carbohydrate**	0.27	1.05	0.378	0.01	0.38	81

Table 5.3.10 Summary table of the DistLM analysis of the microbial community of the intensively sampled sites in the Ythan estuary.

Step	Variable	Adjusted R^2	Pseudo F-statistic	*P*-value	Individual R^2	Cumulative R^2	Residual d.f.
1	**+ Vol. Weighted Mean**	0.21	7.45	**0.001**	0.24	0.24	24
2	**+ % Fines**	0.33	5.61	**0.002**	0.15	0.39	23
3	**+ D (0.5)**	0.39	3.31	**0.002**	0.08	0.47	22
4	**+ Shear Vane**	0.45	3.29	**0.003**	0.07	0.54	21
5	**+ Sea temp**	0.48	1.98	**0.042**	0.04	0.58	20
6	**+ Total C**	0.50	1.83	0.056	0.04	0.62	19
7	**+ Carbohydrate**	0.52	2.03	**0.030**	0.04	0.66	18
8	**+ Bulk density**	0.53	1.48	0.148	0.03	0.68	17
9	**+ Salinity**	0.55	1.47	0.147	0.03	0.71	16
10	**+ Max. Air Temp**	0.57	1.81	0.074	0.03	0.74	15
11	**+ Precip. 2**	0.58	1.56	0.127	0.03	0.77	14
12	**+ Min. Air Temp**	0.59	1.16	0.343	0.02	0.79	13
13	**+ Water %**	0.59	1.16	0.314	0.02	0.81	12

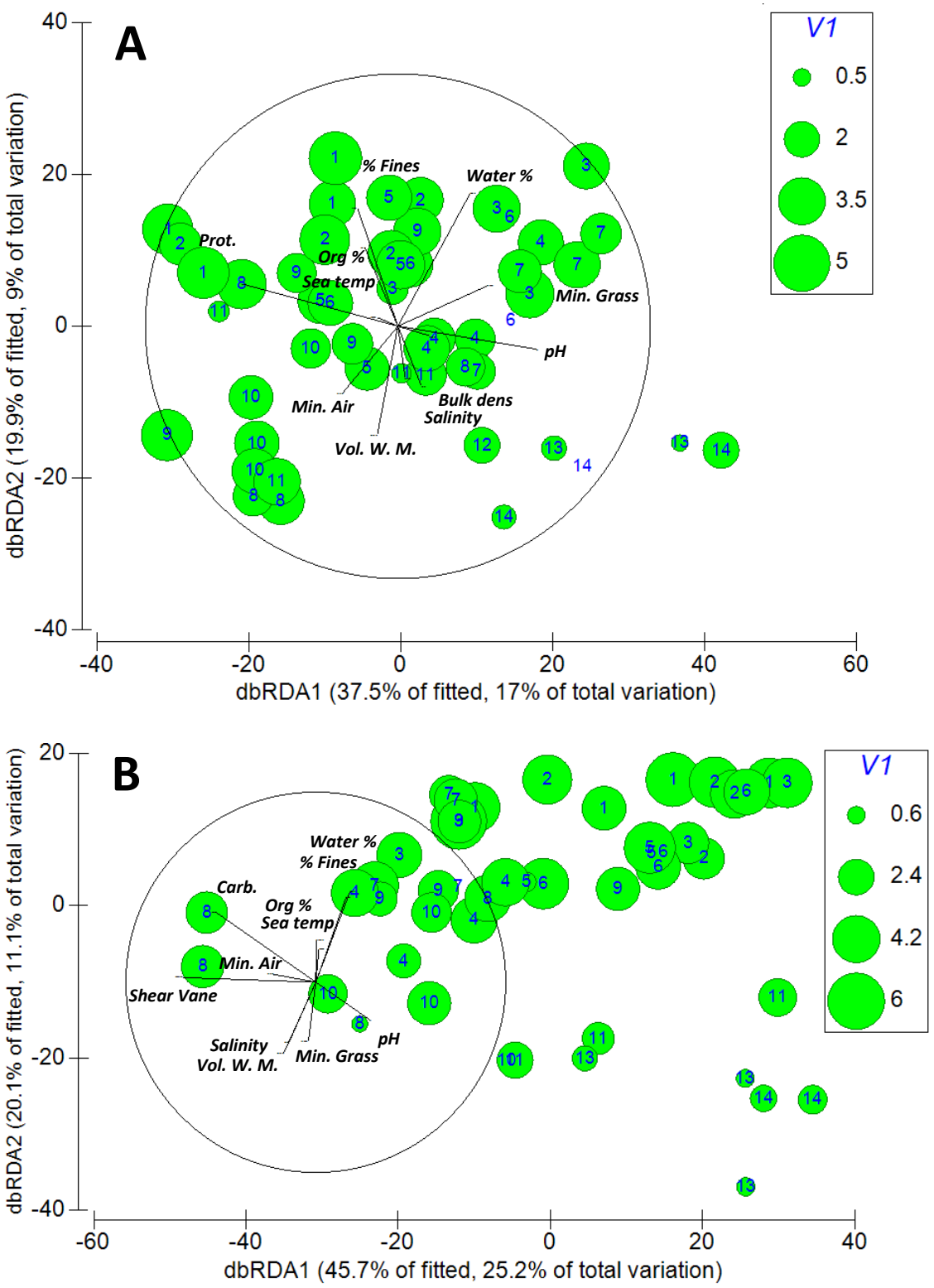

Figure 5.3.12 dbRDA ordination of the TRFLP microbial community analysis of the Ythan (A) and Eden (B) estuary transects. Overlaid vectors are of environmental variables that were included in the optimal DistLM model. Sample labels denote site ID. Size of symbol (V1) denotes *E. coli* $\log_{10}$ CFU 100 g dry wt^{-1} sediment according to the legend on each ordination.

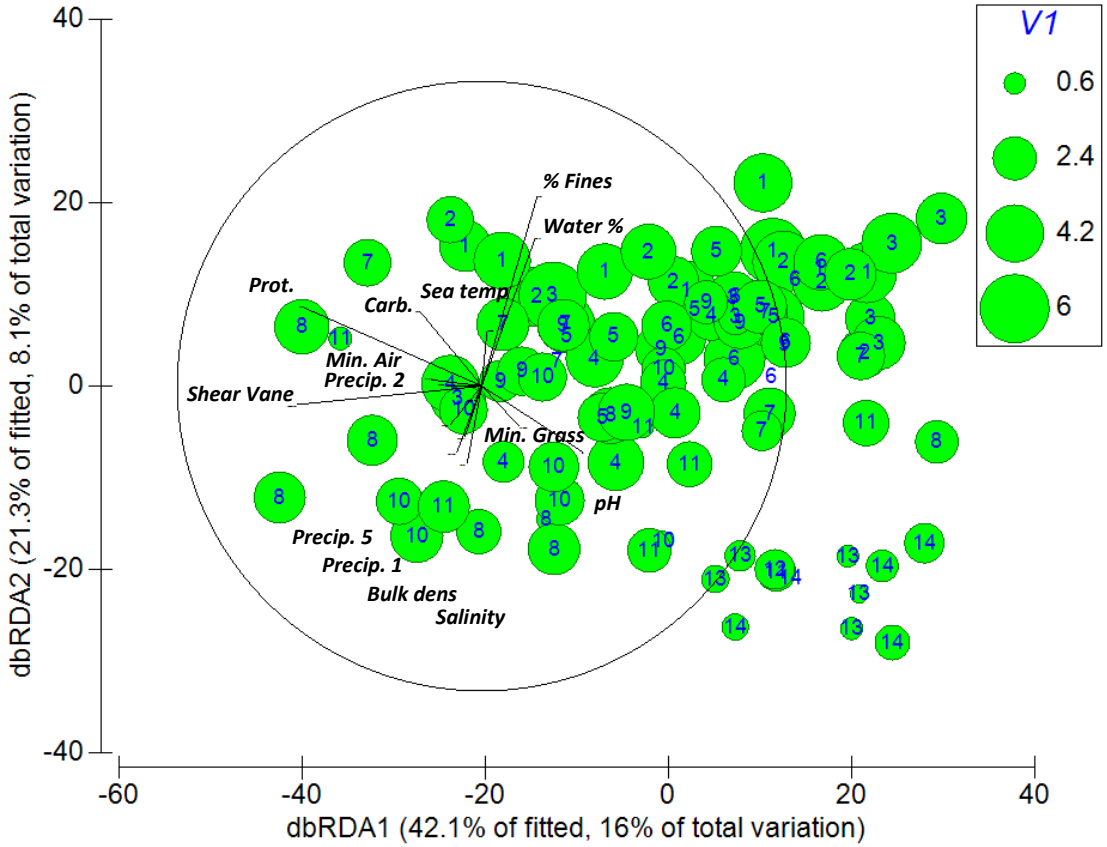

Figure 5.3.13 dbRDA ordination of the TRFLP microbial community analysis of the combined Ythan and Eden estuary transects. Overlaid vectors are of environmental variables that were included in the optimal DistLM model. Sample labels denote site ID. Size of symbol (V1) denotes *E. coli* $\log_{10}$ CFU 100 g dry wt^{-1} sediment according to the legend on the ordination.

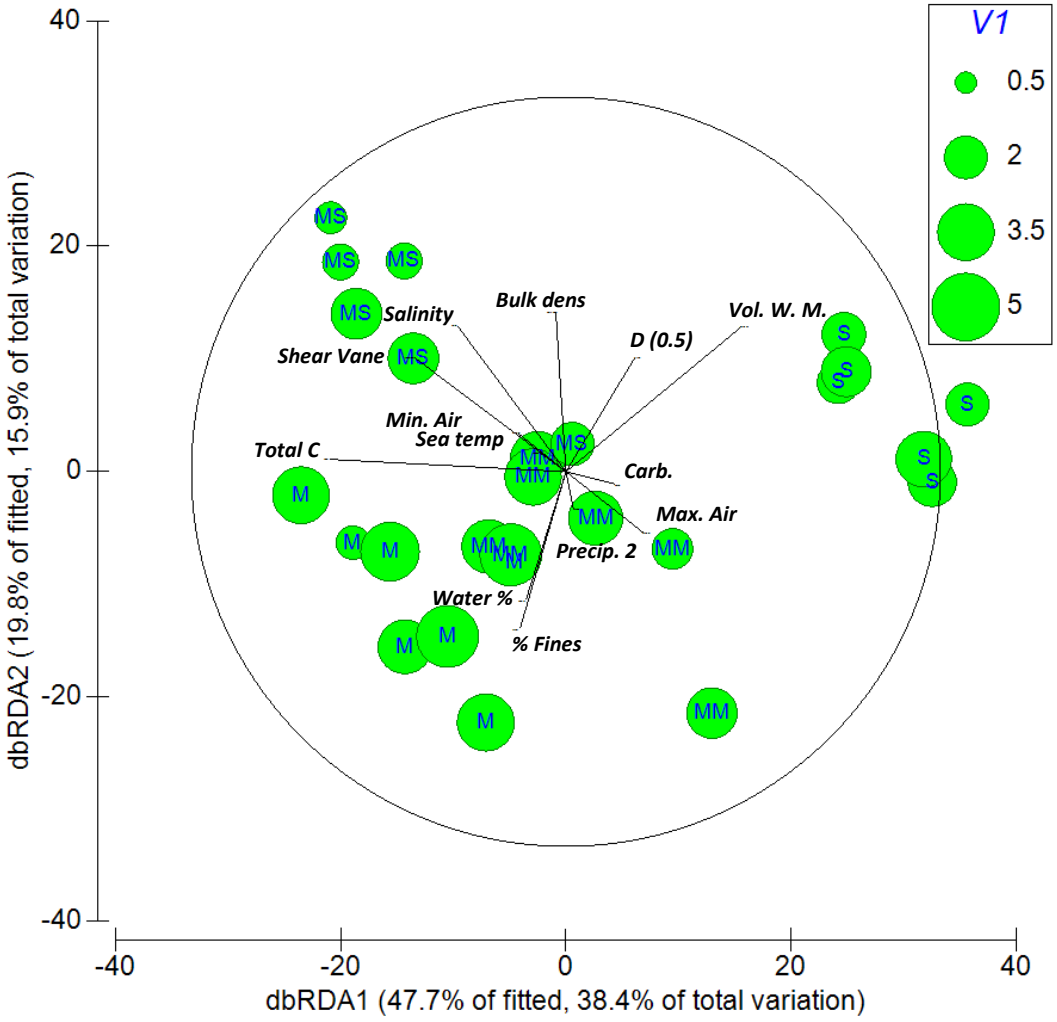

Figure 5.3.14 dbRDA ordination of the TRFLP microbial community analysis of the intensively sampled sediments in the Ythan estuary. Overlaid vectors are of environmental variables that were included in the optimal DistLM model. Sample labels denote site ID. Size of symbol (V1) denotes *E. coli* $\log_{10}$ CFU 100 g dry wt^{-1} sediment according to the legend on the ordination.

5.4 Discussion

5.4.1 M-TRFLP method analysis

The multiplex T-RFLP method outlined by Vinten et al. [362] was adapted here for investigating the microbial community of intertidal sediments rather than stream biofilms. The method here successfully identified changes in microbial community metrics and constituent composition of intertidal sediments, however, several improvements can be made to increase the value of the data obtained by the method. Identification of TRFs was suggested as a subsequent analysis in order to identify specific species or communities [362], and was attempted in this study. However, the taxonomic resolution of TRFs between different lineages of algae, cyanobacteria or eubacteria was poor. Attempts made here to match TRFs to groups of organisms failed as multiple lineages corresponded to a single TRF, in addition to a large proportion of un-cleaved amplicons of multiple lineages.

The PCR method of amplifying algal 18S genes of Bérard et al. [367] was found to have an amplicon size of 290-300 bp, smaller than the expected 400 bp [367]. The impact of this on the current study is negligible, however future studies using this primer set should be aware of this inaccuracy. The method proposed by Bérard et al. was to improve on a previous method of Dorigo et al. [371] by replacing the P45 primer with P73 to avoid amplification of fungal DNA. As demonstrated here by the peak identification, fungal DNA is still amplified, and furthermore, cleaved by the HhaI enzyme at identical TRF sizes to true algal TRFs leading to further ambiguity of peak identity. Despite the P73/P47 primer pair being designed to amplify diatom DNA, the original study did not successfully amplify any diatom DNA in soil samples [367], suggested to be a result of difficulty in destroying the strong frustules of diatoms. The DNA extraction method of Bérard et al. included a bead-beating stage, as included in the method used here, and DNA was successfully extracted from pure diatom culture controls but not environmental samples. In this study, whilst the DNA extraction method of the Mobio Powersoil kit provided adequate yield and quality of DNA from intertidal sediments, a bias against the isolation of diatom DNA may have occurred, as this method has proved to produce poor yields of DNA from pure diatom culture compared to other traditional and commercially available plant-targeting DNA extraction kits [372]. This may have resulted in the absence of diatom-specific TRFs being identified as TRFs that discriminated between microbial community types.

Diatom DNA may have also been poorly amplified from environmental samples as a result of the base pair mismatches in the forward primer P73. Primer mismatches are known to introduce bias in PCR efficiency, especially when mismatches are at the 3' end of a primer [373] as this interferes with the active site of the polymerase [374]. The effect of a mismatch on PCR efficiency is dependent on the mismatch type [373, 375] however, the mismatch at position 23 in the P73 primer for the positive control *Navicula pelliculosa* and other diatom species is a G:T mismatch, reported to only have a minor effect on PCR efficiency when positioned 3 nucleotides from the 3' end of the primer [375].

An accumulation of these factors may have resulted in poor representation of diatom species in the TRFLP analysis, however these issues can be resolved with the design of a new forward primer, with a second degenerate nucleotide at position 23, or preferably, a new sequence target site altogether that excludes the amplification of fungal DNA.

TRFLP relies on cleavage of amplified fragments with a restriction enzyme [376] to provide a fingerprint of multiple TRFs for an environmental sample. Restriction enzymes cleave DNA at specific nucleotide sequences, and by using computer simulations such as 'Cleaver' [377], the theoretical resolution of taxonomic groups for a particular enzyme on a database of sequences can be observed. These computer simulations can be used to optimise the restriction digest so that the required level of discrimination between taxonomic groups can be achieved. Here, the enzyme HhaI was used and failed to resolve TRFs below phylum and class level, but with further restriction digest design, it may be possible to improve the method to discriminate consistently at class level, in addition to finding a restriction enzyme that cleaves the high proportion of un-cleaved amplicons observed here. This could involve a digest using more than one enzyme or different enzymes for the algal, eubacterial and cyanobacterial amplicons to achieve optimal resolution within for amplicon. The literature however is unclear as to whether the HhaI provided the best taxonomical resolution of TRFs over all three amplicons with the view to compromise between the cost efficiency of a multiplex digest and optimal taxonomical resolution.

Another option to increase taxonomic resolution of TRFs would be to add a fluorescent label to both the forward and reverse primer, as when only one primer is labelled, additional cleavage sites within the sequence are undetected, whereas the first and last cleavage site in an amplicon are detected when both the forward and reverse primers are labelled. The disadvantage of additional dyes in this multiplex method however is that as three different

dyes are already included, each with a different peak emission wavelength, care must be taken when including additional dyes to avoid overlap of the emission wavelength spectra of the dyes. Singh et al. [365] suggested a maximum of four dyes could be used in multiplex T-RFLP, presumably to avoid emission spectra overlap.

5.4.2 Spatial and temporal variation of microbial species metrics

Blackwood et al. [378] warned of the bias and inaccuracies of estimates made using true diversity and evenness measures on T-RFLP data. They advise that inferences made using traditional ecological diversity measures should be referred to as changes in community composition, rather than a true diversity measure. Bias is introduced to these traditional measures when applying them to T-RFLP data as multiple species are represented by the same TRF [379], as observed in this study in the taxonomical identification of TRFs. Furthermore, in the routine data processing of T-RFLP data, a peak threshold is applied where peaks present in less than a certain percentage of samples are removed. As a result, rare species cannot be detected [378], despite these rare species possibly being pivotal to true diversity in microbial communities [380]. Blackwood et al. [378] proceed to demonstrate the accuracy of true diversity measures with various imposed thresholds, with higher correlations between true diversity measures and those based on T-RFLP data when lower thresholds are imposed, with correlations of 0.68, 0.97 and 0.80 for total species, Shannon's diversity and Pielou's evenness respectively for a threshold of 0.1 %, whereas a threshold of 1 % results in correlations of 0.15, 0.71 and 0.7 respectively [378]. In this study a threshold of 0.5 % is used, so correlation between Shannon's diversity and Pielou's evenness here is expected to correlate well with the true measures. Total species here is expected to be of low correlation to true species number present, and it should be noted that total species (S) in this study is referring to total TRFs above the 0.5 % threshold. Despite the higher correlation, it should also be noted that Shannon's diversity, and Pielou's eveness still only represent the diversity and evenness of the dominant eubacterial, algal and cyanobacterial TRFs.

Sediments at the head of the Ythan and Eden estuary (typically sites 1-4) experience greatly fluctuating salinity due to the tidal cycles and differential flow of the river. Salinities encountered are within and around the horohalinicum salinities of 5–8 PSU. It is difficult however to designate particular sites as being within this salinity range as the estuaries studied here are macrotidal and therefore intertidal sediments experience a large salinity range

throughout the tidal cycle. The species abundance and diversity of protists has been shown to increase in the salinity range of the horohalinicum of the Baltic sea [325], and size-group composition analysis by Telesh et al. [353] confirms that total planktonic algae species smaller than 20 µm increase in the salinity range of 4-12 PSU, and the presence of larger algae species dominate outside this range. This trend was evident and significant in the TRFs detected in the intertidal sediments of Eden and Ythan estuaries, but perhaps most obvious at the Eden estuary. It is worth noting however that the algal primers targeted all algae, and despite efforts made to remove macroalgae from the samples, environmental DNA from macroalgae may remain in the samples.

The phenomenon of increased species abundance at the horohalinicum does not apply to the total species abundance of eubacterial OTUs, which has been observed not to change with salinity [331], possibly attributable to the ability of bacteria to adapt relatively quickly to fill ecological niches compared to higher organisms [331]. This non-deviating trend of bacterial species abundance was observed here as there was no significant difference in the species abundance of bacteria in either estuary, however there were significant differences in the intensively sampled sites of the Ythan estuary. Cyanobacterial species abundance has been shown to follow the same trend as protists (including microalgae) [353], but this trend was not detected in the estuary transects or the intensively sampled sites in the Ythan estuary.

Algal and Cyanobacterial diversity and evenness followed the same pattern as algal species abundance at both the Ythan and Eden estuaries, with a decrease in diversity and evenness at sites in the mid-lower reaches of the Ythan and Eden estuaries, and there were significant differences between the intensively samples sites on the Ythan estuary. Also, eubacterial diversity and evenness followed this same trend at the Ythan estuary, but differences were not significant at the Eden estuary. Analysis of 16S rRNA bacterial diversity using DGGE in the Brunei estuary, Borneo, revealed a similar trend to that observed here, with a decrease in bacterial diversity (Shannon's diversity index) from the head of the estuary towards the mid-reaches, with similarly high values of diversity at the head and the mouth of the estuary [381].

Total species of algae were greater in sediments with the finest particle size (mud) than the coarsest sediment (sand), however mixed sand yielded a higher species abundance than mixed mud. However, the mixed sand sediments were further towards the mouth of the estuary than mixed mud, highlighting the importance of the spatial distribution of sediments down the estuarine salinity gradient and as well as physico-chemical sediment properties.

Sites at the mid-lower reaches of the estuary are likely to be the sites exposed to the highest change of salinity during the tidal cycle. This will decrease evenness of species as pure riverine and marine species are less likely to thrive in these conditions, leading to a dominance of species that can cope with the osmotic stresses of highly fluctuating salinity. The diversity index will reflect this trend, but also any decrease in total species (shown to be significant only in algal species) will magnify any decrease in diversity. The magnitude of the fluctuation of diversity down the estuary did not appear to be greater than that of evenness as a result of the non-significant change in abundance, so the results indicate that in the mid-lower reaches of the estuary, it is primarily evenness that decreases rather than diversity.

The increase of algal species abundance, and the diversity and evenness of all targets (except eubacteria at the Eden estuary) from the head of the estuary to the mid-reaches of the estuary at site 7 is explained by the horohalinicum hypothesis. Also, the subsequent decrease in evenness can be explained by the large salinity fluctuation likely to occur at sites 8-11. These metrics then increase at the mouth of the estuaries (sites 11-14), and could be a result of the microbial community being composed of primarily marine organisms, with the species present not having to cope with highly fluctuating salinity and benefit from a more stable habitat, therefore evenness and diversity is restored to a higher level as expected in true marine sediments.

Canonical correspondence analysis on 16S rRNA DGGE derived data from the Pearl River estuary, China, has demonstrated that pH and salinity are important in governing the distribution and diversity of bacteria in subtidal estuarine sediments [341], suggested to be partially caused by changes in the bio-availability of nutrients and trace metals. The Shannon's diversity index analysis of the DGGE data revealed a lower diversity of bacteria in sediments at an intermediate salinity of overlying water (17.0 PSU) compared to the head and mouth of the estuary (overlying water salinity: 0.2 and 30.3 PSU respectively). Lower diversity at the intermediate site however was observed mostly in sediments at a depth of between 4 and 22 cm, whereas surface sediments demonstrated a similar bacterial diversity as the other sites throughout the depth profile. The data collected here demonstrated a decrease in bacterial diversity in the surface sediments (0-1 cm) in the mid-lower reaches of the estuary, but without further details on the physical sediment composition coupled with the samples taken sub-tidally rather than intertidally, it is difficult to draw reliable parallels regarding the diversity index of bacteria.

Trends of species abundance, diversity and evenness of the microbial community were driven by the salinity gradient, and were similar between the Ythan and Eden estuaries. This confirms the first hypothesis, and suggests that trends in microbial species metrics identified here may be similar to multiple estuarine systems. Further sampling campaigns are necessary however to definitively correlate salinity with these metrics in intertidal sediments, where salinity is measured regularly over a tidal cycle to capture the precise fluctuations in salinity in the sediment environment in order to definitively attribute the effects of the horohalinicum and of highly fluctuating salinity. Salinity measurements taken here were measured on the interstitial water at the time of sampling that will be affected by recent rainfall, and at what stage of the tidal cycle samples were taken.

5.4.3 Spatial and temporal shift in microbial community constituent composition

Changes in the microbial community reflect the differences observed in the microbial population metrics down the Ythan and Eden estuaries. nMDS and dbRDA ordination of the constituent composition revealed a clear shift between sediments at the head to mid reaches of the estuaries (1-7), the mid-lower reaches (8-11), and the mouth of the estuaries (12-14) This spatial grouping was similar to that of the differences observed for the microbial population metrics. This allows confirmation of the second hypothesis as the microbial community constituent composition of similar reaches at the Ythan and Eden estuaries were more similar than the composition at other reaches of the same estuary.

Population metrics were discussed in terms of the salinity gradient, which did not prove to be the most significant variable in the DistLM analyses, rather, particle size variables correlating with the salinity gradient explained shift in constituent composition more successfully as the increasing salinity down an estuary often correlates with increasing particle sizes, however, there are some perturbations with sediments with a smaller particle size settling in bays and sheltered areas [27]. In addition, the effect of salinity on species diversity and evenness is non-linear over the salinity gradient with abrupt changes around the horohalinicum [325].

Microbial community constituent composition at the head of the Ythan estuary (sites 1-2), were correlated with the algal TRF 295B and increased proportion of fine particles, organic content and protein content. There were no single TRFs that correlated strongly with community composition at the head of the Eden estuary, but several cyanobacterial and

eubacterial TRFs and increase in proportion of fine particles (as at the Ythan estuary) correlated with the shift in composition. The combined estuary ordinations revealed less similarity between constituent composition at the head of the estuaries than those at sites 8-10 and 12-14. Sites 8-10 at both estuaries individually correlated with the same algal and cyanobacterial TRFs, but were not clearly defined by sediment characteristics, but a decrease in water content, fine particle proportion and increase in salinity were positively correlated with changes in the constituent composition in the combined estuary dbRDA ordination.

Sites at the mouth of both estuaries shared similarities in community constituent composition which is intuitive as they share a common marine environment at the mouth of the estuary. but the rivers entering the estuaries have different catchment characteristics and water chemistry, resulting in more different upstream microbial communities. Seaward communities correlated with a decrease in EPS components, and a decrease in sediment shear strength and proportion of fine particles typical of sandier sediments at the mouth of an estuary. Several TRFs that correlated with community compositions at mouth of the Ythan estuary also correlated with some communities at the upper reaches of the Eden estuary. It is unlikely this was the result of the presence of same organisms, and highlights the necessity to improve the TRFLP method to provide higher taxonomic resolution as closely related species. As an example, TRF 271Y correlated with both upstream and marine microbial communities, and matched nucleotide sequence data of Nostocales, Oscillatoriales and Synechococcales, which include freshwater and marine species. Despite this however, there was successful separation of microbial communities of upstream and downstream sediments.

The effect of high EPS content creating a protective microhabitat from adverse environmental stressors has already been discussed (Section 1.9.3). Therefore, regardless of position in the salinity gradient, microbial community composition may be more similar in the presence of high EPS content as species that cannot physiologically cope with the large salinity fluctuations are not excluded. This may explain why in the DistLM models, protein content was the first model added in the Ythan transect model, and carbohydrates in the Eden transect model. As discussed in Chapter 3, colloidal carbohydrates and proteins in the sediments of the transects at both estuaries correlate strongly, which is mirrored in the angles of their vectors in the same direction in the dbRDA ordination of the combined transect dataset. Therefore, either parameter of carbohydrate or protein content could be seen as reflecting the relative amount of colloidal EPS.

5.4.4 Relationships between **E. coli** *abundance and changes in the indigenous microbial community*

There is increasing evidence that *E. coli* can persist for extended time-periods in soils from several months [382] to several years [13, 383] and becomes part of the indigenous microbial community. It has also been suggested that the survival of naturalised *E. coli* is facilitated by anaerobic conditions [13], which are frequently occurring in estuarine sediments. The results here show no relationship of abundance of *E. coli* with native microbial population metrics, or with native microbial community constituent composition shift in sediments from the head to mid-lower reaches of the estuaries. Presence of any relationship would suggest that *E. coli* plays a role in, or gains benefits from specific microbial communities. Therefore, the third and fourth hypotheses should be rejected. The data suggests a more general accumulation of *E. coli* within the estuarine system with environmental and sediment characteristics directly influencing the persistence of *E. coli* reflected in its differential abundance, rather than naturalised *E. coli* forming part of specific indigenous microbial communities. This study however did not investigate changes in the diversity of *E. coli* strains with microbial communities or between sediment types. Different strains of *E. coli* have been shown to vary in their ability to persist in environmental conditions in soil [384, 385], and different strain characteristics may also facilitate naturalisation within the indigenous microbial community. Therefore despite no correlation observed here between abundance of *E. coli* and changes in the microbial community, there may still be an interaction where the persistence of pathogenic strains benefit from particular microbial communities.

When microbial diversity is high, more ecological niches are occupied reducing the ability of a non-native organism to thrive within an environment [360], demonstrated to be the case with *E. coli* [386] and *L. monocytogenes* [387] persistence in soils. Therefore, in sediments where native microbial diversity was lower, such as observed at sites 8-11 of both estuaries, it could be expected that this leads to an increase in *E. coli* abundance. This correlation was not observed in the data here, suggesting further that *E. coli* does not interact substantially with the microbial community, and its persistence is governed primarily by short-term stresses associated with salinity and sediment characteristic variables that encourage increased accumulation and persistence of *E. coli* as discussed in Chapter 3. There was however an apparent correlation between the shift in microbial community constituent composition at the mouth of the estuaries and a decrease in *E. coli* abundance, but this was most likely due to the environmental and biogeochemical sediment characteristics such as the high osmotic stress of

seawater and larger particle sizes that correlate strongly with decreasing *E. coli* abundance (Chapter 3), rather than shift in community constituent composition. Furthermore, in both estuaries there was a greater shift in microbial community between sediments containing similar *E. coli* abundance than the shift between sites at the head and the mouth of the estuary where the difference in *E. coli* abundance was greatest.

5.4.5 Conclusions

The aim of this chapter was to determine if *E. coli* abundance was affected by the native microbial community. Despite several weaknesses of the adapted M-TRFLP method, there were still significant trends of changes in the microbial community observed within the data, and it was possible to compare these trends to patterns in *E. coli* abundance. Further improvements to the method are possible, and will improve the taxonomic resolution of the results. TRFLP is currently becoming obsolete to the preference of next-generation sequencing (NGS) methods, however, the current cost of NGS and time-intensive nature of analysing a large number of samples, such as in this study, results in TRFLP remaining as a useful method in identifying changes in microbial community constituent composition for the time being [388].

The first hypothesis: *The salinity gradient drives spatial variation in microbial species metrics (species abundance, diversity and evenness) in estuaries,* was confirmed as trends of the microbial species metrics followed a similar pattern of decreasing species abundance, diversity and evenness in the mid and lower reaches of both the Ythan and Eden estuaries compared to the upper reaches and mouths of the estuaries.

The second hypothesis: *Microbial community constituent composition is similar in the Ythan and Eden estuaries,* was confirmed as the constituent composition was more similar in the same reaches of the different estuaries compared to other reaches within the same estuary.

The third and fourth hypotheses E. coli *abundance is affected by changes in microbial population metrics,* and E. coli *abundance is affected by microbial community constituent composition* were rejected as there was no apparent relationship between changes in the native microbial community population metrics of constituent composition and *E. coli* abundance further than their co-variation with the geochemical and physical gradients occurring in the estuary.

6. The role of cell and particle characteristics in the adhesion of *E. coli* to suspended intertidal sediments

6.1 Introduction

6.1.1 Cell-particle adhesion

The extent of pathogen transport to and within aquatic systems depends heavily on whether the bacterial cells are freely suspended or in association with suspended particles [29, 389, 390]. When *E. coli* enters the water column from any route (point or diffuse pollution, resuspension from underlying sediment, detachment from biofilms), cells may be adhered to particles or as free cells, however the majority of bacterial cells in freshwater and marine systems are freely suspended rather than particle-associated [389, 391, 392]. Freely suspended cells are likely to be transported downstream faster, where they reach higher salinities that has detrimental effects on pathogen survival [93] (Section 1.8.2). When bacterial cells are attached to sediment particles, they are more likely to sediment out of the water column [28, 247], increasing their retention time in the estuarine system, and providing the survival advantages of association with sediment (Chapter 1). According to Stokes' law, particles of different sizes have different settling velocities [26], which impacts how far particles may travel in an aquatic system before sedimentation. Intertidal sediments and their associated bacterial load are frequently resuspended and deposited during the tidal cycle [393], so understanding the mechanisms behind variation in pathogen adhesion to particles is essential to understand their abundance, persistence and fate within estuaries.

Bacterial adhesion to sediment particles has been widely reported to be dependent on particle size, with cells preferentially attaching to relatively small particles around the clay-silt range (<63 μm) [100, 394, 395]. Different species of fecal bacteria have also shown preference for different particle size ranges, with enterococci preferring to attach to particles 10-30 μm, and *E. coli* attaching to a wider range of 5-30 μm [389]. Furthermore, strains of bacteria of the same species (*E. coli*) have been reported to have different particle size class preference within the broad range described above [396]. Different strains of *E. coli* also vary in attachment efficiencies to both biotic and abiotic surfaces depending on the presence of a range of extracellular appendages (Section 1.5), with some traits likely to improve adhesion capabilities also associated with increased pathogenicity [68, 69]. These traits may also be applicable to

the adhesion of cells to suspended particles in the water column, and so different species and strains of pathogens will be subject to varying sedimentation rates and resuspension frequencies. In addition to adhesion to particles being affected by these cell specific traits, species and strains of bacteria and particle surfaces also exhibit variation in electrostatic charge.

6.1.2 Derjaguin-Landau-Verwey-Overbeek (DLVO) theory

Although primarily applied in the context of abiotic colloidal particles [45], DLVO theory can serve as a simple model for initial bacterial attachment to surfaces, including that of river sediment particles [46]. As almost all bacterial cells [397-400], and suspended particles in natural aquatic systems [48, 49, 401, 402] are negatively charged, therefore there is an electrostatic repulsion that counters the attracting Van der Waals forces [403]. In order for adhesion to occur the electrostatic repulsion has to be sufficiently low to allow close contact between particles where Van der Waals forces can dominate [404], or biotic factors can influence adhesion.

DLVO theory demonstrates that co-sedimentation of suspended clay particles and organic matter in estuaries can be a result of electrostatic instability of particles when freshwater mixes with the increased electrolyte concentrations of seawater at the head of an estuary [48]. Higher concentrations of electrolytes compress the double layer of counterions that surrounds particles [405] allowing particle-particle repulsion forces to decrease. This in turn allows more particle collisions to occur, which promotes the flocculation of particles and generation of larger particles that in turn leads to increased settling according to Stokes' law [26]. This is not however the only mechanism of sedimentation in estuaries, the spatial deposition of sediments is also largely governed by the hydrodynamics of the overlying water [27, 183, 406]. Desorption of cells from sediment particles can also occur when the salinity of the water decreases [54], such as the result of the dilution effects of storm events, though this also depends on whether or not the cell has already formed an irreversible attachment. Zeta potential can provide a useful and readily measureable surrogate for surface charge of both bacteria and particles.

6.1.3 Zeta potential

There are two layers of ions surrounding a particle (Fig. 6.1.1). Firstly, the Stern layer consists of closely bound ions that are closely associated to the particle surface. When the particle moves within a liquid medium due to gravity, closely bound ions move with it, unaffected by the shear force of the passing liquid. Beyond the Stern layer is the Diffuse layer, where ions are more loosely associated. When the particle moves due to gravity these ions do not move with the particle, rather they stay in position within the medium. The zeta potential is the electrostatic potential at the point beyond the Stern layer where ions no longer move with the particle when it moves due to gravity, known as the slipping plane [407] (Fig. 6.1.1). Particles that exhibit strong positive or negative zeta potentials are not likely to flocculate with one another due to electrostatic repulsion. Particles with a zeta potential more negative than -30 mV, or more positive than +30 mV are considered stable, and particles exhibiting a zeta potential between these values designated as unstable [407], with particles closest to 0 mV most likely to flocculate. The zeta potential is calculated by measuring the electrophoretic mobility of the particle in solution, and converting this to zeta potential using the Henry equation [408] and the Smoluchowski approximation [409, 410].

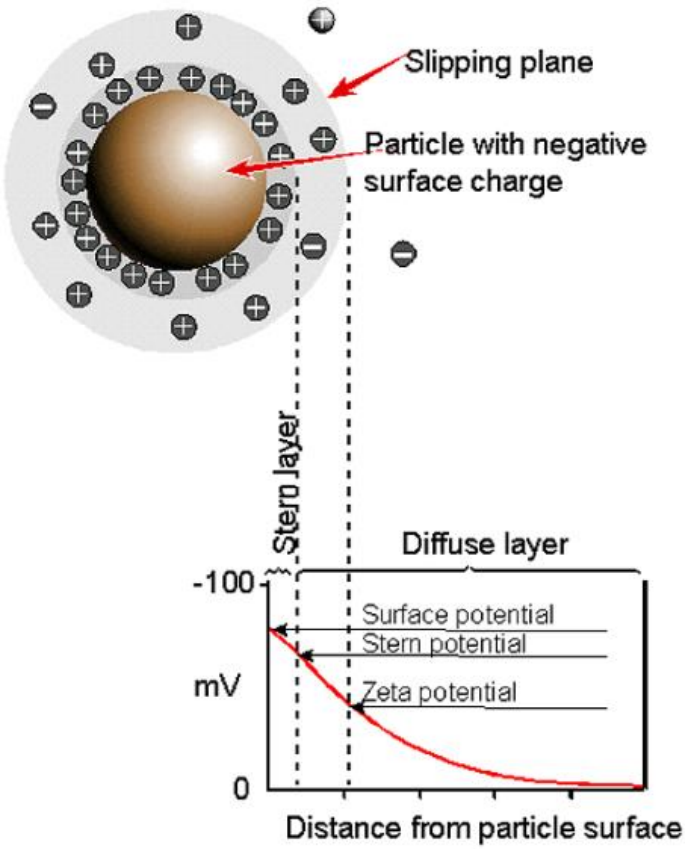

Figure 6.1.1 Schematic diagram of the location of the ion boundaries surrounding a particle in solution. From Malvern Instruments [407].

The electrophoretic mobility of particles is analysed by capillary electrophoresis, measuring the migration of particles within a capillary or cell whilst an electrical field is applied. The method used here utilises electrophoretic light scattering to measure the migration of particles. The Zetasizer nano (Malvern) by the M3-PALS technique, a combination of phase light scattering (PALS), and laser Doppler velocimetry [407]. The electrophoretic mobility measurement consists of two separate modes. The first is a fast field reversal, where the electric field is reversed many times per second avoiding the effect of the movement of the suspension (electro-osmosis), and measures only the movement of the particle (electrophoresis). The second is slow field reversal, where the field is reversed once per second which allows the sample flow to stabilise.

If hydrodynamics are momentarily overlooked, particles that reach a less negative zeta potential at lower salinities are more likely to flocculate higher up the estuarine system, and

those that exhibit a more negative zeta potential will not flocculate until higher salinities and will theoretically be found towards the mouth of the estuary. Particles of different mineralogy can also have different zeta potentials at a given ionic strength [411], however this can be masked by conditioning films [49], coatings of organic matter that are found over almost every substratum in aquatic environments [401], especially in high production environments such as estuaries.

6.1.4 Zeta potential of **E. coli** *cells*

The surface charge of bacterial cells is as important in affecting particle-sediment adsorption as that of environmental particles. The less negative the bacterial cell zeta potential, the greater likelihood of adsorption to a negatively charged sediment particle and then undergoing sedimentation whilst in association with the particle [28].

At environmental pHs, *E. coli* is negatively charged [412]. The degree of negative charge can vary depending on specific cell factors. For example, the zeta potential of *E. coli*, *Salmonella* and *Pseudomonas* sp. has been shown to vary with nutrient availability, starvation [50] and growth phase [413]. The zeta potential of *E. coli* has been demonstrated to vary between strains [414, 415], and can be due to differences in their membrane-bound proteins [397, 416].

As ionic strength is increases, the extent of attachment of bacterial cells to sediment particles should increase due to a less negative zeta potential. This has been shown experimentally to be the case with *E. coli* [415, 417]. Roper and Marshall (1974)[24] observed increased attachment of *E. coli* to sediment particles above a salinity of ~1.2 PSU. Gordon and Millero (1984)[418] also recorded an increasing attachment affinity of *Vibrio alginolyticus* to surfaces with increased solution ionic strength up to 0.1 M (equivalent to ~6.5 PSU seawater), but above this, found a decrease in attachment attributed to the concentration of cations rather than the ionic strength of the media. As seawater is a mixture of monovalent and divalent cations, with primarily monovalent (Cl^- and Na^+) cations, the effect of divalent cations on higher salinities is not expected to give the same decrease in bacterial attachment.

6.1.5 Aims and hypotheses

There is little research that demonstrates the effect of *E. coli* surface charge and sediment characteristics on bacterial adhesion to sediment particles *in situ* or using fresh sediments and environmental waters to construct an increase in ionic strength. The aim of this chapter was to determine whether these characteristics affect the adhesion efficiency of *E. coli* to minimally altered natural intertidal sediment particles in suspension. Different strains of *E. coli* were used to determine whether or not their adhesion to particles was an effect of cell phenotype. In addition, different sediment types were used to establish whether adhesion of bacteria to sediments was a function of zeta potential, particle size distributions, mineralogy and other characteristics.

The following hypotheses were tested in this chapter:

a) ***Different* E. coli *strains will exhibit different zeta potential profiles over the salinity gradient.***
b) ***Sediments will exhibit different zeta potential profiles over a salinity gradient***
c) **E. coli *strains will show different adhesion efficiencies with ionic strength (salinity).***
d) **E. coli *strains will show different efficiencies in adhesion to different sediment types.***
e) ***The adhesion of* E. coli *cells to sediment particles can be explained by the zeta potential of the strain or sediment***.

6.2 Materials and methods

6.2.1 Genotyping of E. coli *strains*

Intertidal sediments were collected in sterile falcon tubes (Fisherbrand, Fisher Scientific, UK) from three previously sampled sites on the Ythan estuary. Ten g of sediment was added to vessels containing 50 ml sterile Phosphate-Buffered Solution (PBS) (137 mM NaCl (Fisherbrand, Fisher Scientific, UK), 2.7 mM KCl (BDH, UK), 4.3 mM Na_2HPO_4 (BDH, UK), and 1.4 mM KH_2PO_4 (BDH, UK)) then hand shaken for 1 minute and left to settle for 1 hour. Five ml of supernatant was filtered through a sterile 0.2 µm membrane filter, and the filter paper placed onto MacConkey agar (Oxoid, Thermo Fisher Scientific Inc. UK) plates, which were inverted to avoid interference from condensation, and incubated overnight at 37 °C. An equal number of lactose fermenting colonies randomly selected from each site (pink coloured; total n=132, selected n=32) were picked and subcultured onto fresh MacConkey agar plates and then onto Simmons' Citrate agar (LabM, UK) and incubated as above to check for the inability to use citrate as the sole carbon source (putative *E. coli*). Strains showing no growth on citrate agar (n=24) were inoculated into 5 ml of tryptone water (Sigma Aldrich, UK) and incubated for 18 h at 37 °C in a shaking incubator at 150 rpm. Kovac's reagent (0.2 ml; Sigma Aldrich, UK) was then added and the appearance of a red/ pink layer at the top of the mixture demonstrated tryptophan utilisation, and therefore indicated that the isolate was *E. coli*. Positive strains (total n= 14) were then subject to DNA extraction and 16S rRNA sequencing to confirm the species identification (Fig. 6.2.1).

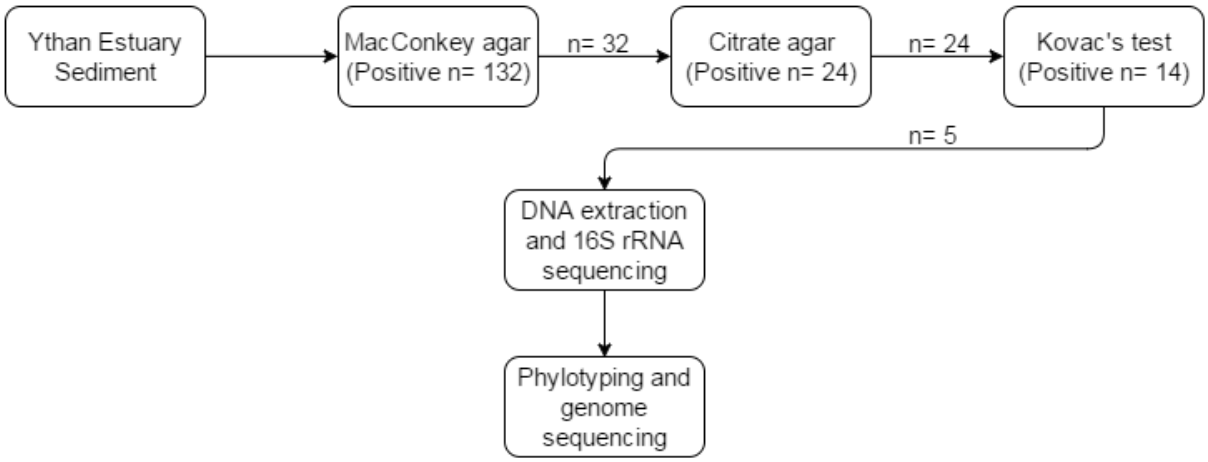

Figure 6.2.1 Schematic diagram of *E. coli* strain isolation and confirmation from Ythan estuary sediments.

6.2.2 DNA extraction

Suspected *E. coli* strains (n= 14) were cultured overnight in 5 ml Luria-Bertani (LB) broth media (Merck Millipore, MA, USA) in 15 ml falcon tubes (Fisherbrand, Fisher Scientific, UK) and cultured overnight at 37 °C in a shaking incubator at 150 rpm. DNA extraction was performed using the GenElute bacterial genomic DNA extraction kit (Sigma Aldrich, UK) following the manufacturer's protocol for gram-negative bacteria. A positive control of *E. coli* O157:H7, and a negative control of DI H_2O were used.

The concentration of DNA recovered was determined using the Qubit dsDNA HS (High Sensitivity) Assay kit (Invitrogen, UK). The manufacturer's protocol was followed with 2 µl of sample used in the reaction.

To visualise the DNA, the method described in (Section 5.2.2.1) was followed using 4 µl sample template combined with 2 µl loading dye and loaded into a 15 cm x 15 cm 1 % agarose gel with 4ul ethidium bromide alongside 5 µl hyperladder 1kb. The gel was electrophoresed for 40 minutes at 70 V.

6.2.3 PCR and sequencing

16S rRNA genes of each strain of putative *E. coli* isolated from the Ythan estuary were amplified using a 50 µl reaction mixture containing 5 µl 10x NH_4 Buffer (Bioline, UK), 20 nmol deoxynucleoside triphosphates (Bioline, UK), 100 nmol $MgCl_2$ (Bioline, UK), 20 pmol of both 27.F and 1392.R primers (Table 6.2.1), 2 units of biotaq (Bioline, UK), and 40 ng of template DNA in DI H_2O. DNA extracted from a Mineral Soil (Hartwood, N. Lanarkshire) was used as a positive control, and DI H_2O as a negative control.

The PCR was performed in a DYAD DNA Engine Peltier thermal cycler (MJ Research, MA, USA) , with the following conditions: an initial denaturation for 5 minutes at 94 °C; 30 cycles of 45 s at 94 °C, 45 s at 55 °C, 1 minute at 72 °C; with a final extension of 5 minutes at 72 °C. Gel electrophoresis was performed to confirm amplification of the 16S rRNA gene.

Table 6.2.1 Primers used in the 16S sequencing (27.F/1392.R) and PCR phylotyping of *E. coli* strains (remainder).

Primer	Target Gene	Sequence (5'-3')	Amplicon size (bp)	Annealing temperature (°C)	Reference
27.F 1392.R	16S	AGAGTTTGATCCTGGCTCAG ACGGGCGGTGTGTRC	1365	55	Primers [419] Conditions [384]
chuA.1b chuA.2	chuA	ATGGTACCGGACGAACCAAC TGCCGCCAGTACCAAAGACA	288	59	[420]
yjaA.1b yjaA.2b	yjaA	CAAACGTGAAGTGTCAGGAG AATGCGTTCCTCAACCTGTG	211	59	[420]
tspE4C2.1b tspE4C2.2b	tsp.E4C2	CACTATTCGTAAGGTCATCC AGTTTATCGCTGCGGGTCGC	152	59	[420]
AceK.f ArpA1.r	arpA	AACGCTATTCGCCAGCTTGC TCTCCCCATACCGTACGCTA	400	59	[420]

PCR products were purified using the Wizard SV gel and PCR clean-up system (Promega, UK). The manufacturer's protocol for PCR product purification was followed, with DNA eluted in 50 µl of sterile DI H_2O. Gel electrophoresis was performed as in Section 5.2.2.1 to confirm presence of the purified PCR product.

Purified PCR products (n=14) were sent to GATC Biotech for sequencing. The returned fasta sequences were submitted to the nucleotide Basic Local Alignment Search Tool (BLAST) [421] against the NCBI database (accessed July 2014) and the identity (%) and species of the resulting alignments recorded.

A selection of strains (n=5) from different isolation sites on the Ythan estuary that returned a positive for *E. coli* from the BLAST alignment were further subjected to a molecular phenotyping method to determine the phylo-group that the strains belonged to [420]. A multiplex PCR [420] was performed on the DNA extracted in Section 6.2.2. Genes for the arpA,

chuA, tsp.E4C2, and yjaA were amplified using a 25 µl reaction mixture containing 2.5 µl of 10x NH_4 Buffer (Bioline, UK), 10 nmol deoxynucleoside triphosphates (Bioline, UK), 50 nmol $MgCl_2$ (Bioline, UK), 10 pmol of each primer (Table 6.2.1), 1 unit of biotaq (Bioline, UK), and 60 ng of template DNA in DI H_2O. Positive controls of 3 *E. coli* strains of known phylo-types (Lys 5: group F, lys 13: group B1, Lys 15: group A) were used as they incorporated all 4 bands as positive results. A negative control of DI H_2O was used. Gel electrophoresis was performed to view PCR products and determine the phylo-group against profiles published by Clermont et al. [420].

6.2.4 Genome sequencing

The five *E. coli* strains isolated above (AW1, AW3, AW4, AW6, and AW13) and stock strains Deutsche Sammlung von Mikroorganismen ((German Collection of Microorganisms) DSM) 8698 and DSM 9034 (Table 1) were submitted for genome sequencing at the Oxford Genomics Centre. DNA was prepared in 1.5 ml Eppendorf tubes at a concentration of 20 ng/µl in 60 µl 10 mM Tris-Cl pH 8.5. To analyse the purity of samples, the 260/280 nm and 260/230 nm ratios were checked with a Nanodrop (Nanodrop ND1000, Thermo Scientific, UK).

Table 6.2.2 Summary information of the *E. coli* strains sent for genome sequencing.

Strain Name	Serotype	Strain Details	Origin	Date Isolated
AW1		Wild Type	Ythan estuary (Sand)	May-2014
AW3		Wild Type	Ythan estuary (Mixed Sand)	May-2014
AW4		Wild Type	Ythan estuary (Mixed Sand)	May-2014
AW6		Wild Type	Ythan estuary (Mixed Sand)	May-2014
AW13		Wild Type	Ythan estuary (Mixed Mud)	May-2014
DSM 8698	O111:H-	Enteropathogenic-Gastroenteritis in young children	DSMZ Culture collection, Human diarrhoea	1950 [422]
DSM 9034	O164:H-	Enteroinvasive	DSMZ Culture collection, Human diarrhoea	1947 [423]
Sakai	O157:H7	Enterohemorrhagic	Clinical Isolate, Human diarrhoea	1996 [424]

6.2.5 BLAST sequence extraction and alignment

In order to further investigate the genotypes of the strains used for the sediment adsorption experiment, a database in CLC Main Workbench (Qiagen, v7.6.3) was created using assembled contig files received from Oxford Genomics Centre. Reference sequences from *E. coli* K-12 MG1655 for 7 housekeeping genes (adk, fumC, gyrB, icd, mdh, purA and recA) of roughly 500 base pairs were used as a BLAST query to the created database with the following parameters: Low-complexity filter applied, E-value of 0.1, word size= 11, match/mismatch of 2/-3, gap cost

of existence= 5, extension= 2. Several *E. coli* genomes were subjected to the BLAST queries; *E. coli* O157:H7 str. Sakai (NC_002695.1), *E. coli* O 83:H1 str. NRG 857C (NC_017634.1), *E. coli* O 104:H4 str. 2011C-3493 (NC_018658.1), *E. coli* O127:H6 E2348/69 (NC_01161.1), *E. coli* O111:H- str. 11128 (NC_013364.1) and also an *E. fergusonii* reference genome str. ATCC 35469 (NC_ 011740.1) as an outlier for analysis.

Alignments were created in CLC sequence viewer (Qiagen, v7.6.1) for each of the BLAST hit sequences for each gene from the sequenced and reference strains. The following parameters were used for the standard progressive alignment function: Gap open cost= 10, gap extension cost= 1, end gap cost= as any other, and 'very accurate' alignment. Reverse compliment manipulation was performed where appropriate. Gaps arising at the beginning and end of the sequences from sequencing errors were trimmed until there was consensus in the first and last base of the sequence. A Basic Maximum Likelihood Tree (BLMT) was constructed on the concatenated gene sequences in Bionumerics V.7.5 (Applied Maths, NV).

6.2.6 Multi-locus sequence typing (MLST)

Trimmed sequences were imported into Bionumerics (Applied Maths, v7.5) for modelling of Minimum spanning tree analysis. Sequences that were trimmed beyond the typical MLST boundaries were submitted independently through the *E. coli* MLST database (http://mlst.warwick.ac.uk/mlst) for allocation of MLST numbers [425]. The 'closest resemblance' MLST was used for sequences that had been trimmed beyond the expected boundaries. Only reference MLST sequences that had 100 % identity with the query sequence were accepted.

BLAST queries were also performed for the genes targeted in the phylo-grouping PCRs. *E. coli* strain K12: MG1655 was used as a reference genome for the arpA, chuA and yjaA genes, and *E. coli* strain CFT073 for tsp.E4C2 as the gene is not present in K12: MG1655. Presence and absence profiles were compared to the Clermont typing method [420] as before.

A minimum spanning tree (MST) was created using the MST for categorical data function within Bionumerics V.7.5 (Applied Maths, NV) for the MLST numbers for each organism. Aligned sequences for each gene were concatenated to form one sequence for each organism. A tree was constructed for this using the standard maximum likelihood tree function also within Bionumerics.

6.2.7 Phenotypic analysis: biofilm assay

Biofilm formation potential was evaluated using the method of Merritt et al. (2011) which measures the mass of biofilm formed on the abiotic surface of a tissue culture plate by staining cells attached to the plate surface then measuring the absorbance of the eluted stain [426]. The *E. coli* strains used for this assay and subsequent experiments were AW1, AW13 (isolated from the Ythan estuary), DSM 8698 and DSM 9034, from the DSM collection, and a toxin-inactivated strain of Sakai (*E. coli* O157:H7).

E. coli strains were cultured overnight (18 hours) in 5 ml sterile LB broth media (Merck Millipore, MA, USA) in 15 ml sterile falcon tubes at 37 °C in a shaking incubator (Innova 4230 Refrigerated, New Brunswick Scientific, Enfield, CT, USA) at 150 rpm. Cultures were normalised to an OD600 of 0.5 using 70-850 µl disposable micro-cuvettes (Brand GMBH + CO KG, Germany) in a spectrophotometer (BioPhotometer 6131, Eppendorf). One µl of each normalised *E. coli* culture was inoculated into 4 replicate wells in a sterile tissue culture plate (Corning, NY, USA) alongside 4 wells containing media only controls. One hundred µl of fresh sterile LB broth media was added to each well. The plate was then covered with laboratory film to minimise evaporation, and incubated at 25 °C for 48 hours. After incubation, the plate was shaken over a waste tray to remove non-biofilm incorporated cells and spent media. The plate was then submerged in DI H_2O, shaken again over the waste tray and this rinse repeated a second time. One hundred and twenty-five µl of 0.1% (w/v) crystal violet in DI H_2O solution was added to each well and the plate incubated for 10 minutes at room temperature. The plate was rinsed twice as above in fresh DI H_20 and left to air-dry. When dry, 200 µl of an 80:20 ethanol: acetone solution [427] was added to each well and the plate incubated for 15 minutes at room temperature. The well contents were thoroughly mixed by pipetting and 125 µl transferred to the micro-cuvettes. The OD of all strain replicates and the media controls were measured at 600 nm against a blank of the ethanol: acetone solvent. The average OD value of the adsorption for the un-inoculated LB broth media wells was subtracted from that of the inoculated wells.

6.2.8 Phenotypic analysis: swarming assay

The extent of motility of the *E. coli* strains at 15 °C and 25 °C was analysed using a swarming assay adapted from Wolfe and Berg (1989) [428]. Overnight cultures *E. coli* were streaked on 1% LB agar plates using a sterile culture loop and the plates incubated overnight upside-down

at 37 °C. Thinly poured 0.4 % LB agar plates were air dried in a laminar flow hood in order to remove any surface water and stab-inoculated with single colonies picked from streak plates. Three replicate plates at each temperature were inoculated for each strain tested. Inoculated plates were inverted and incubated at 15 °C and 25 °C and the diameter of the growing colony measured with a ruler to the nearest mm every 24 hours for 19 (15 °C) and 13 days (25 °C). The experiments were terminated when plates begun to dry out causing the agar to split, deforming the swarming colony.

6.2.9 Sediment and water properties

Laser Particle Size Distribution analysis was performed as in Section 2.2. X-Ray Powder Diffraction (XRPD) analysis was performed by H. Pendlowski at The James Hutton Institute, Aberdeen. Briefly, lyophilised sediment samples were ground by hand in a mortar and pestle, then wet milled in ethanol (McCrone Mill, McCrone, IL, USA.) and spray dried. XRPD patterns were measured using copper Kα radiation.

Surface area analysis was performed by H. Pendlowski at The James Hutton Institute, Aberdeen. Surface area was analysed by the adsorption of nitrogen gas to the sample (Coulter SA 3100, Beckmann Coulter, UK) and calculated using the Brunauer, Emmett and Teller equation [429].

6.2.10 Measurement of zeta potential

For the zeta potential and adsorption experiments, samples and microcosms were resuspended in seawater diluted to a specific salinity with river water. Sea water was collected from Collieston Harbour (NK 04077 28493), and river water collected from the River Ythan beyond the tidal range (NJ 95672 30326). Each water was filtered through 0.45 µm filter paper (Merck Millipore, MA, USA). Stock solutions of 0, 1, 1.5, 2, 2.5, 3, 3.5, 4 and 5 Practical Salinity Units (PSU) were created using a salinity probe (Hach HQ40D, Hach Lange, UK). The pH of each seawater dilution was also recorded using a pH probe (Hach HQ40D, Hach Lange, UK). The true salinity of the river water was 0.11 PSU. The lowest salinity treatments constructed from pure river water are hereby referred to as the 0 PSU treatments for convenience.

Sediments were collected from the Ythan estuary at 3 previously sampled sites (Chapter 3): Organic Mud (Location- NJ 99064 29919), which had a high organic content and fine particle size distribution; Mud (NJ 99828 27145), which had a fine particle size distribution and less organic matter; and Mixed Sand (NK 00467 24815), which had a larger particle size distribution and lower organic content. Sediment for this experiment was taken from the Ythan estuary, from the ~4km stretch between the Sleek of Tarty and the Logie Buchan bridge where large changes in salinity are observed [211]. The equivalent of 2 g dry weight of each sediment was weighed into 50 ml falcon tubes. Sediments were suspended in 40 ml DI H_2O and centrifuged at 1450 x *g* for 15 minutes. The supernatant was removed, and 40 ml of fresh DI H_2O added. The centrifugation washing procedure was performed 3 times to remove existing pore-water from the sediment. Sediments were finally resuspended in 40 ml of the appropriate seawater dilution. Sediment suspensions were left to settle for 10-15 minutes and samples taken from the surface for analysis to reduce particle settling during the zeta potential measurement.

E. coli strains AW1, AW13, DSM 8698, DSM 9034 and Sakai were cultured in triplicate overnight as described in Section 6.2.7. Five hundred µl of overnight culture was washed, centrifuged (3000 x *g*; 5 minutes; 12 °C) and resuspended in 2.5 ml of the appropriate seawater dilution to remove any traces of the growth media. The final suspension was held at 12 °C for zeta potential measurement.

Measurements were performed on the Zetasizer Nano ZS (Malvern Instruments, UK) using the DTS 1070 cell at 12 °C. Samples were loaded into the cell using a disposable 20 ml Luer-Slip syringe (Fisherbrand, Fisher Scientific, UK). In order to protect sample integrity, automatic voltage selection, monomodal analysis only, and a 60 secs delay between measurements were used [430]. The Smoluchowski model was used [409], with a fixed F(ka) value of 1.5. The model parameters for viscosity and refractive index of the dispersant were calculated using the complex solvent builder in the zetasizer nano software (Table 6.2.3). Quality control was performed using a transfer standard (Malvern Instruments, UK) at the start and end of each session. Zeta potential measurements are referred to by describing a shift from -10 mV to -20 mV as increasing in negativity, and -10 mV to -5 mV as becoming less negative. As the samples used here are of a high conductivity, to avoid degradation of the sample, monomodal analysis was applied [430], where only the fast field mode is performed to give an accurate mean. This results in no zeta deviation being recorded, but avoids sample and cell degradation.

Table 6.2.3 Viscosity, refractive index and dielectric constant parameter values for the dispersants used in the Smoluchowski equation.

Salinity (PSU)	Viscosity (cP)	Refractive Index	Dielectric Constant
5	1.2507	1.333	83.4
4	1.2495	1.333	83.4
3.5	1.2488	1.332	83.4
3	1.2482	1.331	83.4
2.5	1.2475	1.331	83.4
2	1.2469	1.331	83.4
1.5	1.2462	1.330	83.4
1	1.2456	1.330	83.4
0	1.2430	1.330	83.4

Preliminary samples were run on lyophilised sediments from previous sampling campaigns to examine zeta potential distribution on mixed sediments. Mud and sand sediments collected from the Ythan estuary were used. Roughly 10 g lyophilised sediment was hand shaken for 2 minutes in 30 ml of deionised water and left to settle for 15 minutes before the supernatant being drawn off via syringe and loaded into the zetasizer measurement cell. Measurements were recorded as above, however modal analysis was performed with no delay between measurements.

6.2.11 Adhesion of E. coli *to suspended intertidal sediments*

Sediment microcosms were prepared by weighing the equivalent of 50 g dry weight fresh sediment (Table 6.2.4) into 700 ml centrifuge vessels. Sediments were suspended in between 200 and 300 ml of sterile DI H_2O and centrifuged at 1400 x *g* for 15 minutes (Falcon 6/300 refrigerated centrifuge, MSE, UK). The supernatant was removed, and the sediment resuspended again in 250 ml sterile DI H_2O. This was repeated for a third time, and the sediment finally resuspended in 500 ml of the appropriate seawater dilution in sterile 500 ml duran bottles. Each sediment suspension was sonicated for 5 minutes at 20 % with the microtip attachment (600 W Ultrasonic Processor, Sonics and Materials Inc., CT, USA). After

sonication, duran bottles were set on a stirring plate to keep the sediment particles in suspension, and 20 ml of the homogenous suspension was transferred to three replicate sterile 50 ml falcon tubes for each strain and seawater dilution combination. Additional replicate microcosms were prepared for non-inoculated controls and non-sediment microcosm controls (Fig. 6.2.2). Falcon tubes were held at 12 °C prior to inoculation with *E. coli* culture.

E. coli strains AW13, DSM 8698 and DSM 9034 were cultured in triplicate overnight as in Section 6.2.7 with the exception of DSM 9034 which was cultured in 50 ml LB broth in order to match the inoculum level of the other 2 strains due to a slower growth rate. To harvest the cells, cultures were centrifuged at 3000 x g for 5 mins (Allegra X-22R, Beckman Coulter, UK) and the supernatant discarded. The pellet was then resuspended in 5 ml of the 2.5 PSU seawater dilution before a second centrifugation, again discarding the supernatant. The centrifugation process was repeated 3 times. The pelleted *E. coli* was finally resuspended in 5 ml of the 2.5 PSU seawater dilution. Two hundred µl of the resulting *E. coli* suspension was aliquoted into the appropriate 50 ml falcon tubes containing the sediment suspension to give a final inoculum level of 10^7 colony forming units (CFU) ml^{-1}. Each strain replicate was inoculated into each seawater dilution for each sediment type, as well as the non-sediment control microcosms (Fig. 6.2.2).

Table 6.2.4 Water Content, Organic Content and wet sediment equivalent of 50 g dry wt of preliminary sampled sediments.

Sediment Type	Water content % (average ± SE)	Organic content % (average ± SE)	Wet sediment wt required for 50 g dry wt (g)
Organic Mud	67.36 ± 9.16	9.16 ± 0.08	153.17
Mud	63.75 ± 0.11	7.17 ± 0.06	137.92
Mixed Sand	28.00 ± 0.11	2.20 ± 0.03	69.45

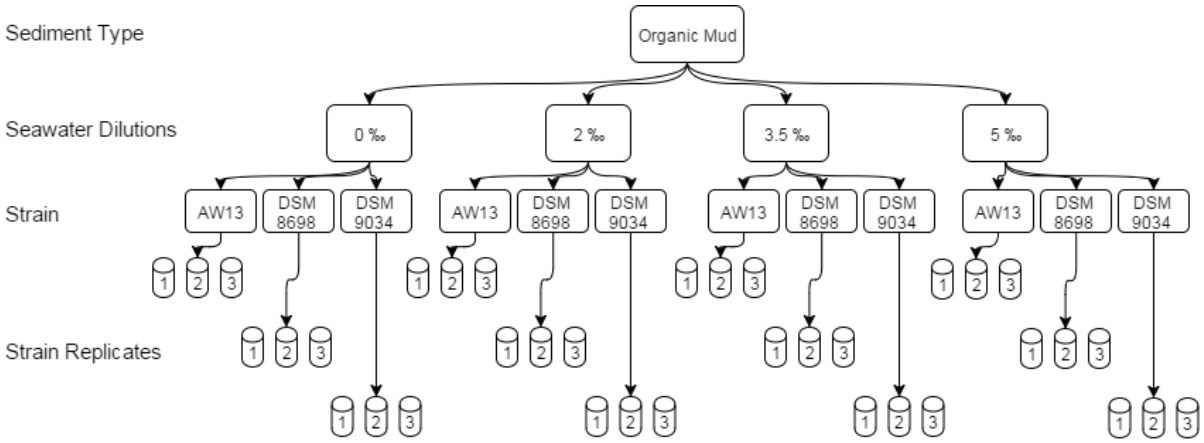

Figure 6.2.2 Experimental flow diagram for the adhesion microcosm experiment for the Organic Mud sediment (non-sediment and non-*E coli* controls are not shown).

Inoculated microcosms were secured in a shaking incubator (Innova 4230 Refrigerated, New Brunswick Scientific, Enfield, CT, USA) (Fig. 6.2.3) at 12 °C for 90 minutes. A shaking speed of 300 rpm was sufficient to keep sediment particles in suspension. Post-incubation, microcosms were centrifuged at 500 x *g* for 120 secs at 12 °C (JG-MI, Beckman Coulter, UK) to separate adhered and non-adhered *E. coli* [431]. This method, outlined in Goude et al. (*in prep*) [431], takes advantage of the lower particle density of *E. coli* cells at 1.16 g cm^{-3} [432], compared to 2.65 g cm^{-3}, the value commonly used to describe general soil particles [433]. This value is also close to the particle density of commonly found clays in intertidal sediments such as Kaolinite, Illite and Montmorillonite (2.6, 2.75 and 2.35 g cm^{-3} respectively) [434]. According to Stokes' law, particles with a higher particle density will descend quicker than similar sized particles with a lower particle density during centrifugation (Table 6.2.5). The density of the fluid medium is essential for the calculation of Stokes' Law (Equation 6.2.1). The density and viscosity of seawater alters with salinity, so the equation was adjusted accordingly. A centrifugation method was employed to distinguish between particle-associated and non-adhered *E. coli* cells. After centrifugation, samples will be taken 10 mm below the surface of the supernatant to gain a representative sample of non-adhered *E. coli* cells for enumeration. Supernatant samples taken at this depth separate non-adhered cells from those adhered to clay particles larger than ~1.55 µm (Table 6.2.5A). In order to calculate Stokes' law, the

acceleration of gravity (g) was set at 9.8 m/s^2. The density and viscosity of the fluid medium is essential for calculation of Stokes' law and zeta potential and varies with ionic concentration. Parameters were calculated for each diluent as appropriate using values for viscosity from Malvern Zetasizer software. The average temperature for Ythan river water at the head of the estuary between the months of May and October was 10.3°C and 11.2°C for 2012 and 2013 respectively [284]. A temperature of 12 °C was used to calculate Stokes' Law and also to run the adhesion experiments.

$$\textbf{Equation 6.2.1} \qquad V_{t=} \frac{\mathrm{g}d^2\,(P_{\mathrm{y}} - P_{\mathrm{m}})}{18\mu}$$

Equation 6.2.1 Stokes' Law, Where V_t= settling velocity (cm s^{-1}), g= acceleration of gravity (cm s^{-2}), d= particle diameter (cm), P_y= particle density (g cm^{-3}), P_m= medium density (g cm^{-3}), μ= medium viscosity (g cm s^{-1}).

Table 6.2.5 Summary of the parameters used for the calculation of settling velocity under centrifugation at 500 x *g* using Stokes' law for A) clay particles, and B) *E. coli* cells.

A

Salinity (PSU)	Particle Diameter (μm)	Particle Density (g cm^{-3})	Medium Density (kg m^{-3})	Medium Viscosity (cP)	Acceleration of Gravity (cm s^{-2})	Falling Velocity (cm s^{-1})	Distance Descended in 120 s (mm)
0	1.55	2.65	999.5	1.2430	4.9 $x10^5$	0.00868	10.42
2	1.55	2.65	1001.1	1.2469	4.9 $x10^5$	0.00865	10.38
3.5	1.55	2.65	1002.2	1.2488	4.9 $x10^5$	0.00863	10.36
5	1.55	2.65	1003.4	1.2507	4.9 $x10^5$	0.00861	10.33

B

Salinity (PSU)	Particle Diameter (μm)	Particle Density (g cm^{-3})	Medium Density (kg m^{-3})	Medium Viscosity (cP)	Acceleration of Gravity (cm s^{-2})	Falling Velocity (cm s^{-1})	Distance Descended in 120 s (cm)
0	1.3	1.16	999.5	1.2430	4.9 $x10^5$	0.00059	0.71
2	1.3	1.16	1001.1	1.2469	4.9 $x10^5$	0.00059	0.70
3.5	1.3	1.16	1002.2	1.2488	4.9 $x10^5$	0.00058	0.70
5	1.3	1.16	1003.4	1.2507	4.9 $x10^5$	0.00058	0.69

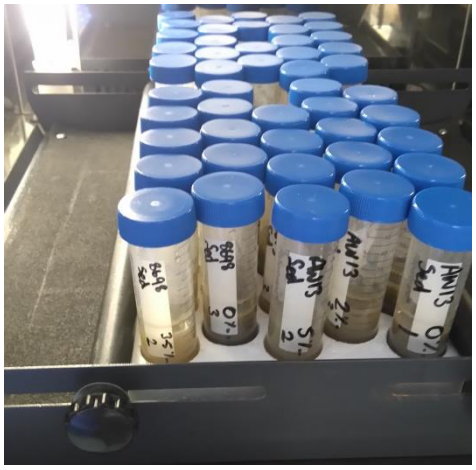

Figure 6.2.3 Prepared microcosms from the adsorption experiment secured for incubation.

6.2.12 Enumeration of E. coli

After centrifugation, microcosms were carefully removed from the centrifuge and triplicate aliquots of 20 µl of the supernatant were removed from each tube at a depth of 10 mm and transferred into separate wells in a 96-well PCR plate (Fisherbrand, Fisher Scientific, UK) containing 180 µl sterile DI H_2O. Serial dilutions to 10^{-8} were performed via pipetting 20 µl of the previous sample into 180 µl of sterile DI H_2O, mixing thoroughly at each stage with the pipette. Serial dilutions from 10^{-3} to 10^{-8} were plated following the drop-plate technique based on that of Miles and Misra [435]. Twenty µl was pipetted from a height of roughly 10 mm onto a pre-marked segment of a HiChrome Coliform agar plate (Sigma Aldrich, UK). Non-inoculated microcosms were analysed in order to enumerate any pre-existing *E. coli* in the sediment. Microcosms containing no sediment were also analysed in order to establish the recovery rate of viable *E. coli* after the centrifugation and harvesting process. The *E. coli* culture used to inoculate the microcosms was enumerated as above (but higher dilutions plated). Plates were inverted and incubated at 37 °C for 18 hours. The HiChrome agar distinguished *E. coli* positive CFUs with a dark blue colouration due to the presence of the β-D-glucuronidase and β-D-galactosidase enzymes. Coliform positive CFUs were distinguished with a red colouration due to the presence of the β-D-galactosidase enzyme. Non-coliform CFUs appeared colourless. This difference facilitated concomitant enumeration of *E. coli* and also of any coliforms and non-coliforms present on the natural sediments. *E. coli* positive colonies were counted at the appropriate dilution, i.e. where segments containing between 10 and 50 colonies where possible (Fig. 6.2.4).

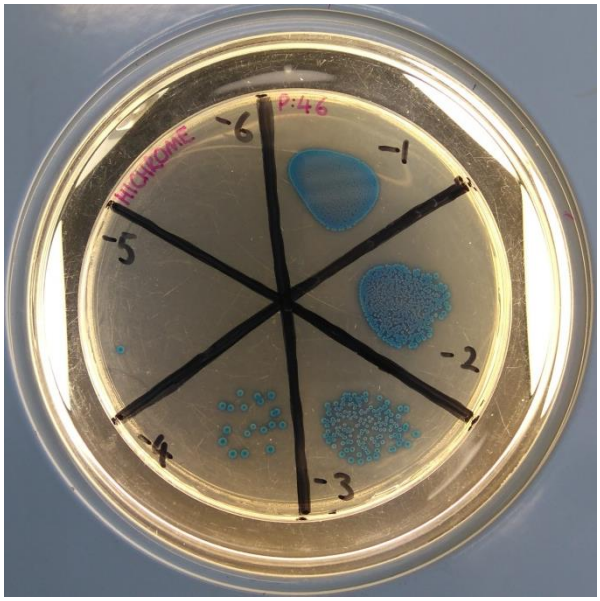

Figure 6.2.4 HiChrome agar plate after overnight incubation of serial dilutions from the *E. coli* inoculum culture for strain DSM 8698. In this case, colonies in segment "-4" (10^{-4}) were counted and used for data analysis. CFU density in segments "-1, -2 and -3" were designated too high for reliable enumeration.

6.2.13 Data manipulation and statistical analyses

Data were prepared using Excel (Microsoft 2010, v14), and statistical analysis was performed in GenStat (VSN International, v17.1).

Biofilm assay: The average absorbance value from the negative controls of the biofilm assay was subtracted from each sample absorbance. All data were then square root transformed to comply with the assumptions of ANOVA. A one-way ANOVA was then performed on the transformed data. Fisher's *post-hoc* protected LSD test showed significant differences between strains.

Sediment zeta potential: No data transformation was needed to meet the assumptions of ANOVA after checking for normality and heterogeneity. A two-way ANOVA was performed with sediment type and salinity as factors. Fisher's *post-hoc* protected LSD test was used to determine significant differences between treatments.

Strain zeta potential: No data transformation was needed to meet the assumptions of ANOVA. A two-way ANOVA was performed with strain and salinity as factors. Fisher's *post-hoc* protected LSD test was used to determine significant differences between treatments. Multiple linear regression was performed in Genstat to obtain the intercept and slope of lines for each strain replicate when plotted against salinity, and overall adjusted R^2 values for the average regression between zeta potential and salinity for each strain. The individual slope data were submitted into a one way ANOVA with strain as a factor.

Swarm assays: Data were analysed using a repeated measures residual maximum likelihood (REML) model. Parameters for the model were 'strain' as treatment, 19 days as equally spaced time points, autoregression order 1 as a correlation model, with additional uniform correlation within subject. Comparisons of overall means were performed using the 'vmcomparison' function. Comparisons of strain means was performed using Fisher's *post-hoc* protected LSD test. One-way ANOVA was used to compare between means at individual time points after bonferroni correction of the family-wise significance threshold to p= 0.002632 (original significance threshold= 0.05 / 19 comparisons).

Non-recovered *E. coli*: The data from the die-off experiment were analysed using a 2 way ANOVA using 'sediment type' and 'strain' as factors.

Adhesion experiment: The average value for the three replicate plates was converted to a value of CFU ml^{-1} after the subtraction of any *E. coli* counts in the sediment only treatments and adjusted to the starting inoculum. The average value for the three strain replicates was normalised to the starting density of 7 $\log_{10}$ CFU ml^{-1} and subtracted from the normalised inoculum after adding expected non-recoverable CFUs for each treatment to give the amount of sediment-adhered $\log_{10}$ CFU ml^{-1} for each treatment. Data were $\log_{10}$ transformed to meet the assumptions of ANOVA. A three-way ANOVA was performed with 'sediment type', 'strain' and 'salinity' as factors. Fisher's *post-hoc* protected LSD test was used to determine significant differences between treatments. Multiple linear regressions were performed to obtain the slope of lines of individual replicates and overall adjusted R^2 values for each strain against salinity with each of the three sediments. The individual slope value for each treatment was submitted into a 2 way ANOVA with 'sediment type' and 'strain' as factors.

The analysis of the strain zeta potentials and the application of DVLO theory gave rise to a suspicion that adhesion at salinities of 0 and 2 would be similar, and lower than that of 3.5 and

5, which would also be similar. To test this hypothesis, the contrasts function in ANOVA was performed. Further contrasts were also made between salinities of 0 and 5, and 2 and 3.5.

Linear regression: Simple linear regression was performed to analyse the strength of relationships between the extent of *E. coli* adhesion over all treatments and sediment suspension pH, sediment zeta potential, strain zeta potential.

6.3 Results

6.3.1 Genotyping of E. coli *strains*

The two bacterial strains AW1 and AW13, isolated from different sediment types from the Ythan estuary, tested positive for *E. coli* in the citrate utilisation and indole tests (Table 6.3.1). They were of different clades according to the Clermont PCR phylotyping method [420], and identity of *E.coli* confirmed by the Basic Local Alignment Search Tool (BLAST) results (Table 6.3.1). Strain AW13 did not show 100% BLAST identity with exclusively *E. coli*, but further genome sequencing showed high similarity with all other *E. coli* strains sequenced (data not shown).

Table 6.3.1 Results from culture and molecular based *E. coli* confirmation tests for strains AW1 and AW13. Culture based test outcomes (positive/ negative), 16S rRNA sequencing species matches and identity (%), individual outcomes for the phylotyping PCRs (positive/ negative), and phylogenetic clade according to Clermont et al. [420].

Strain Name	Citrate utilisation	Indole test	16S BLAST: Species and Identity	chuA	yjA	Tspe4c2	arpA	Clade
AW1	-	+	*E. coli,* 98 %	+	-	+	-	B2
AW13	-	+	*E. coli* , *Cronobacter, Shigella,* 96 %	-	-	+	+	B1

Sequence Type (ST) allocation (Table 6.3.2) revealed strains AW1 and AW13 were of high similarity to existing strains of *E. coli* in the Multi Locus Sequence Typing (MLST) database [425]. AW1 belonged to ST complex 131, and AW13 of ST complex 155. ST complex 131 comprised of 132 strains in the MLST database, almost all of which were isolated from human and companion animals worldwide and designated as pathogenic. ST complex 155 comprised of 27 strains isolated from a mixture of human, animal and soil sources worldwide, some of which were characterised as pathogenic and others non-pathogen strains [425].

Minimum Spanning Tree (MST) (Fig. 6.3.1) construction on the categorical ST data, and the Basic Maximum Likelihood Tree (BLMT) (Fig. 6.3.2) construction on the concatenated gene sequences successfully grouped the B1 and B2 clades from the Clermont phylotyping analysis. Strain DSM 8698 was placed within clade B1 in both analyses. The placement of the A and E clades differed slightly from Clermont et al. [420] presumably due to the low number of strains used. Low bootstrapping values are observed between groups at the AW1 and AW13 nodes, and between AW1 and O157:H7 and *E. fergusonii* nodes in the MST tree due to the low number of strains used. The expected differences between groups are displayed more clearly in the BLMT tree.

Table 6.3.2 Sequence types and complex types of the BLAST search results from 3 genome sequences (AW1, AW13 and DSM 8698) and several reference strains. Sequence types of reference strains were obtained from the NCBI database. * denotes match for all STs except mdh.

Strain ID	adk	fumC	gyrB	Icd	mdh	purA	recA	ST Complex
AW1	53	40	47	13	36	28	29	131
AW13	6	4	4	16	24	8	14	155
DSM 8698	6	4	3	7	7	7	6	20
O127:H6	15	15	11	15	18	11	11	None
O111:H-	6	4	12	16	314	7	12	9*
O104:H4	6	6	5	136	314	7	7	None
O83:H1	13	39	50	13	16	37	25	None
O157:H7 Sakai	12	12	8	12	15	2	2	11
K12:MG1655	10	11	4	8	8	8	2	10
E. fergussoni	431	654	167	532	136	40	339	None

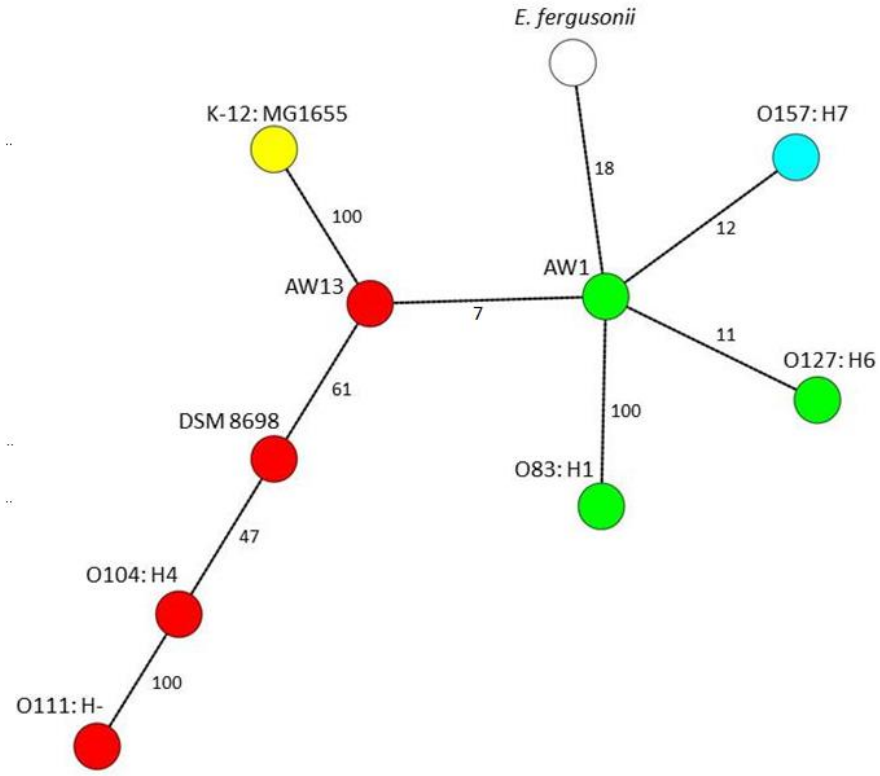

Figure 6.3.1 Minimum Spanning Tree based on Multi Locus Sequence Typing data. Node labels denote strain ID. Node colours denote strain clade (yellow nodes- A; red nodes- B1; green nodes- B2; blue nodes- E; white nodes- not applicable) Branch labels denote bootstrapping value from 100 permutations.

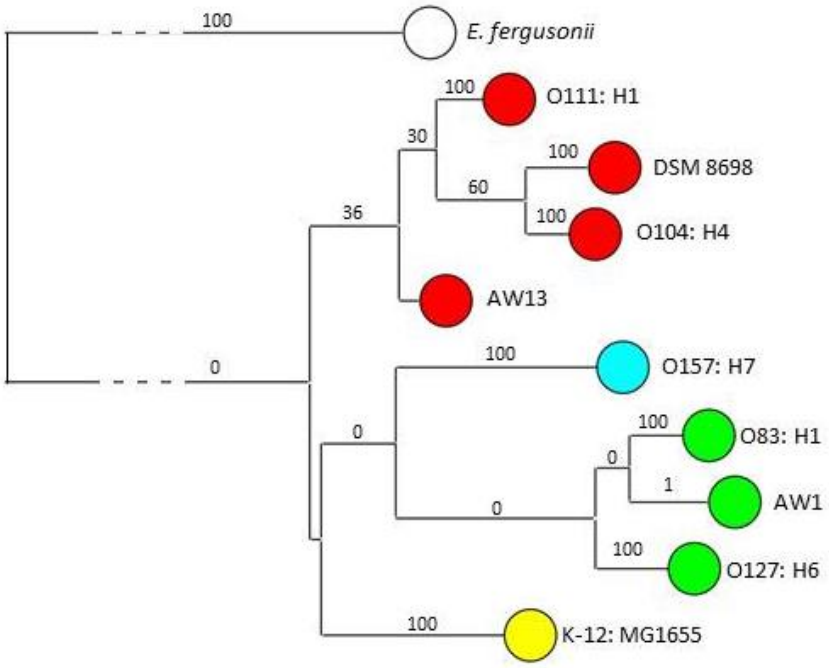

Figure 6.3.2 Basic maximum likelihood tree based on the nucleotide sequences of 7 concatenated housekeeping genes. Node labels denote strain ID. Node colours denote strain clade (yellow nodes- A; red nodes- B1; green nodes- B2; blue nodes- E; white nodes- not applicable) Branch labels denote bootstrapping value from 100 permutations.

6.3.2 Phenotypic analysis

There was no significant difference in biofilm production between strains AW1, DSM 9034 and Sakai, all of which showed poor biofilm formation in the context of the strains tested (Fig. 6.3.3). Strain AW13 produced a moderate amount of biofilm, over twice that of AW1, DSM 9034 and Sakai. Strain DSM 8698 exhibited high levels of biofilm formation, over ten times greater than AW1, DSM 9034 and Sakai (p= <0.001; Fig. 6.3.3).

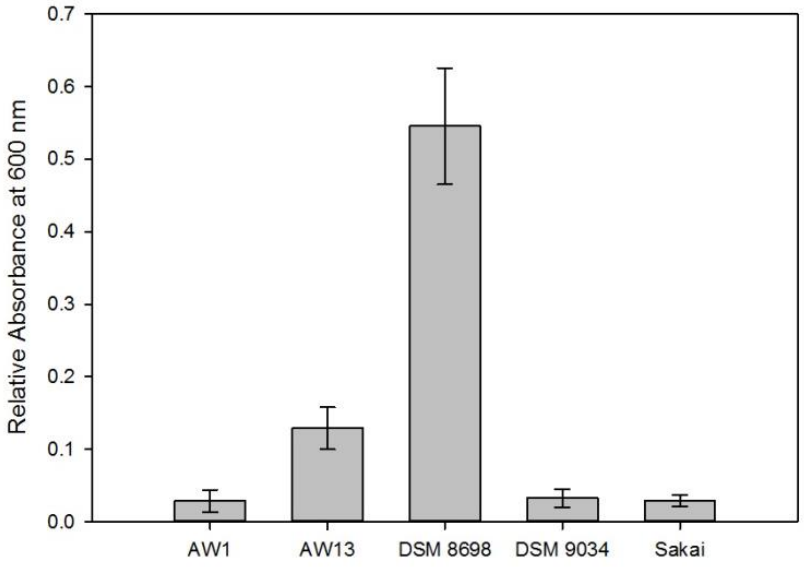

Figure 6.3.3 Extent of biofilm production after incubation for 48 hours at 25 °C in LB broth. Error bars indicate standard error from the mean (n=4).

For the colony motility assays carried out at 15 °C there was a fixed effect of the time and strain interaction (p= <0.001; Fig. 6.3.4A). The two sediment isolates (AW1 and AW13) demonstrated the most rapid growth at 15 °C, closely followed by Sakai and DSM 8698. DSM 9034 exhibited significantly less growth throughout, with colonies only reaching a diameter of 6 mm at the end of the experimental period compared with 12-18 mm for the other strains. Comparisons of treatment means at individual time points revealed no significant difference between strains until day 3 at which point the growth of AW1 and AW13 became greater than that of DSM 9034 (p= 0.001). By day 5, DSM 9034 was significantly lower than all other strains, none of which were different from each other (p= <0.001). Broadly, this pattern continued throughout the remainder of the experiment with some minor perturbations at days 6, 11 and 12.

All strains displayed higher motility at 25 °C than 15 °C (Figs. 6.3.4, B and A respectively). Strains DSM 8698, Sakai and AW1 reached the maximum colony size (>85 mm) in the 25 °C experiment within 6 days, demonstrating the largest increases in motility compared to motility at 15 °C. At 25 °C, DSM 9034 displayed the lowest motility as it did in the 15 °C experiment. Strain AW13 also displayed low motility compared to strains DSM8698, Sakai and AW1. Strains

DSM 9034, AW1, DSM8698 and Sakai demonstrated similar motility relative to one another at both temperatures. The motility of AW13 was poor at 25 °C, but the highest at 15 °C.

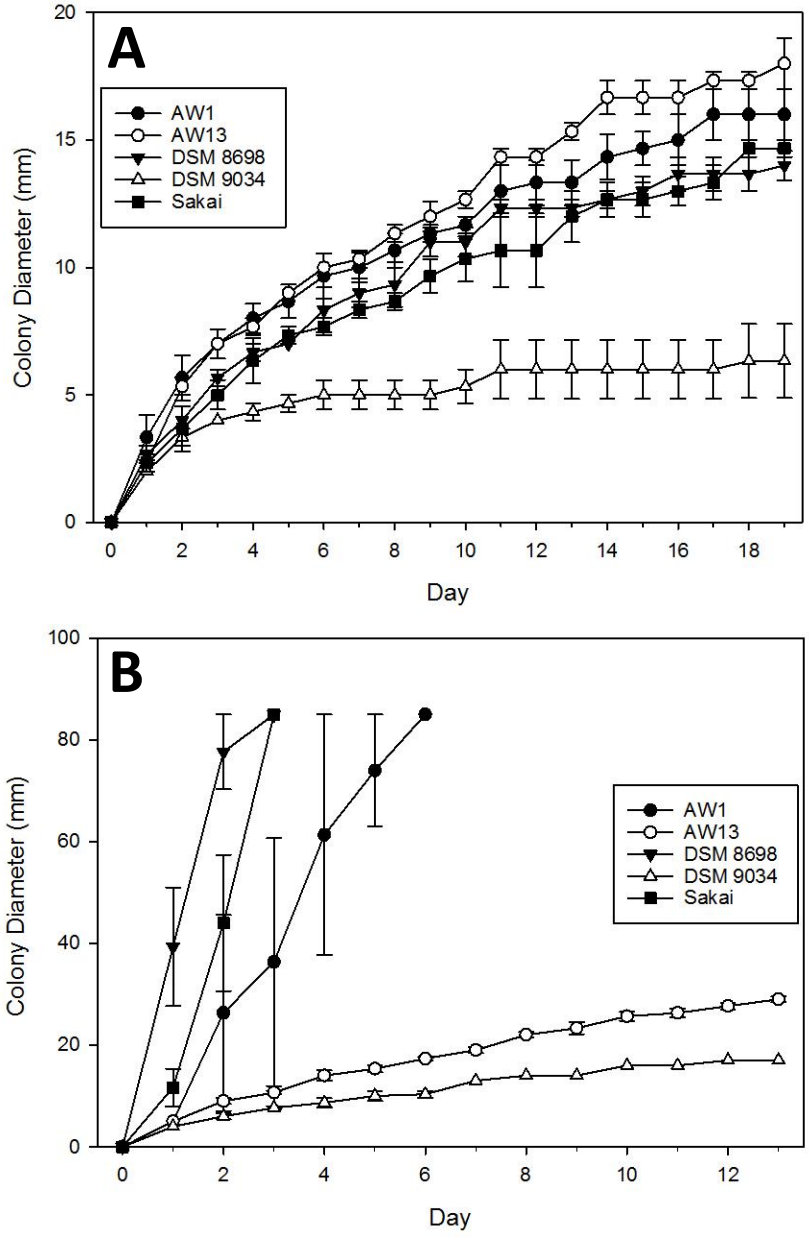

Figure 6.3.4 Swarming ability of *E. coli* strains on semi-solid agar at A: 15 °C, B: 25 °C. Maximum possible colony size was 85 mm. Not change of scale between fig A and B. Solid circles- AW1; Hollow circles- AW13; solid triangles- DSM 8698; hollow triangles- DSM 9034; solid squares- Sakai. Error bars indicate standard error from the mean (n=3).

6.3.3 Sediment and water properties

Organic Mud (OM) and Mud (M) sediments had similar physical characteristics, whereas the Mixed Sand (MS) contained more coarse particles, and had a higher bulk density, lower surface area and lower water and organic content (Tables 6.3.3 and 6.3.4). Mud had a slightly higher bulk density and lower water and organic content than OM. X-Ray Powder Diffraction (XRPD) bulk mineralogy analysis indicated a broadly similar abundance of minerals across all sediments, with MS having a greater quartz content (Table 6.3.5). The collected river water contained a lower NH_4 concentration than the sea water, but had a higher concentration of all other components analysed (Table 6.3.6). The chemistry of the river water used in this experiment was in line with the 2013 averages for the Ythan river as reported by SEPA [285].

Table 6.3.3 Sampling location and physical characteristics of sediments from the Ythan estuary used in the adsorption experiment.

Sediment Type	UK Grid Reference	Bulk Density (g cm^{-3} ± SE)	Water Content (% of core weight ± SE)	Organic Content (% of dry weight ± SE)	Surface Area (sq.m g^{-1})
Organic Mud	NJ 99064 29919	1.27 ± 0.01	65.42 ± 0.12	9.12 ± 0.12	7.101
Mud	NJ 99828 27145	1.38 ± 0.07	62.82 ± 0.26	7.00 ± 0.12	6.014
Mixed Sand	NK 00467 24815	1.95 ± 0.03	23.66 ± 0.17	2.16 ± 0.02	1.136

Table 6.3.4 Particle size distribution of the Organic Mud, Mud and Mixed Sand sediments used in the adsorption experiments.

	Volume in x µm- x µm fraction (%)								Diameter (µm)				
Sediment Type	**0.01-2**	**2-20**	**20-63**	**63-125**	**125-250**	**250-500**	**500-1000**	**1000 +**	**Vol. Weighted Mean D[4,3]**	**Surface Weighted Mean D[3,2]**	**D(0.1)**	**D(0.5)**	**D(0.9)**
OM	2.28	20.92	47.70	20.95	5.31	2.53	0.32	0	58.45	14.69	8.57	40.77	112.6
M	2.67	24.34	51.31	18.09	2.20	1.25	0.14	0	46.47	12.76	7.03	35.53	87.58
MS	0.97	9.11	21.17	11.93	16.27	33.55	6.99	0	211.55	31.44	19.76	192.3	461.1

Table 6.3.5 Bulk mineralogical analysis of the Organic Mud, Mud and Mixed Sand sediments used in the adsorption

Weight (%)

Sediment Type	**Kaolinite**	**Trioctahedral Clay**	**Illite/ Muscovite**	**Amphibole**	**Halite**	**Dolomite**	**Aragonite**	**Calcite**	**K-feldspar**	**Plagioclase**	**Quartz**	**Total**
OM	5.7	11.6	13.8	2.6	0	1.3	2.9	7.9	7.5	14.6	32.1	100
M	2.7	7.9	11.2	2.5	3.1	1.3	4.8	12.9	7.8	13.7	32.1	100
MS	0	2.2	3.7	2.2	2	0.7	1.8	5.7	8.4	15.2	58.1	100

Table 6.3.6 Sampling location and water chemistry of Ythan river water and sea water collected in Summer 2015.

Water Type	UK Grid Reference	Salinity (PSU)	NH_4-N (mg L^{-1})	PO_4-P (mg L^{-1})	NO_3-N (mg L^{-1})	Total Dissolved Nitrogen (mg L^{-1})	Total Dissolved Phosphorus (mg L^{-1})	Dissolved Organic Carbon (mg L^{-1})	Dissolved Organic Nitrogen (mg L^{-1})	Dissolved Organic Phosphorus (mg L^{-1})
River water	NJ 95672 30326	0.11	0.01	0.04	4.03	5.43	0.06	5.12	1.40	0.02
Sea water	NK 04077 28493	35.1	0.08	0.02	0.21	0.30	0.03	9.35	0.01	0.01

Sediment zeta potential correlated moderately well with salinity across all sediments (n= 36, Adjusted R^2= 0.642, *p*= <0.001; Fig. 6.3.5). The mean zeta potential for all sediments was more negative at 0 and 2 PSU than 3.5 and 5 PSU (*p*= <0.001; means: 0 PSU: -21.38 ± SE 0.35 mV, 2 PSU: -20.83 ± SE 0.03 mV, 3.5 PSU: -17.03 ± SE 0.09 mV, 5 PSU: -16.11 ± SE 0.08 mV). The mean zeta potential over all salinities also differed with sediment type, where OM was less negative than M and MS sediments (*p*= <0.001; means: OM: -17.30 ± SE 0.05 mV, M: -19.30 ± SE 0.10 mV, MS: -19.91 ± SE 0.28 mV).

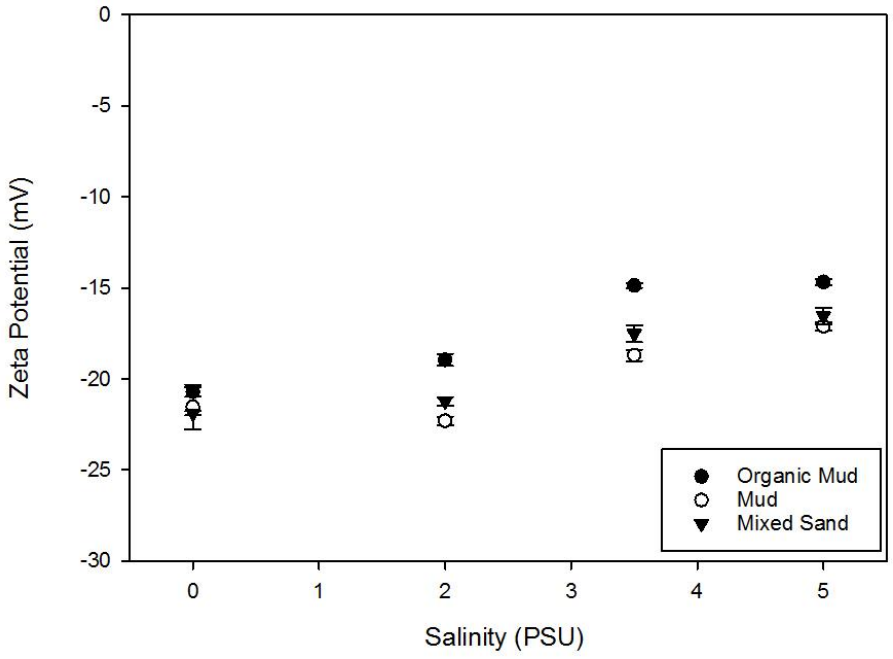

Figure 6.3.5 Zeta potential measurements of Organic Mud, Mud and Mixed Sand sediments at 0, 2, 3.5 and 5 PSU. Solid circles- Organic Mud; hollow circles- Mud; solid triangles- Mixed Sand. Error bars indicate standard error from the mean (n=3).

Strain and matrix salinity interacted to influence the zeta potential of *E. coli* strains (*p*= <0.001). The strains fell into two distinct groups (Fig. 6.3.6): The zeta potentials of DSM 9034 and Sakai were less negative than those of the other strains and changed minimally across the salinity gradient (means: -3.23 ± SE 0.07 mV, -3.70 ± SE 0.03 mV for DSM 9034 and Sakai respectively). There was no difference in zeta potential between these two strains except at the lowest salinity, where Sakai was slightly more negative than DSM 9034 (Fig. 6.3.6). In

contrast, the zeta potential of the other three strains ranged from -21.5 to -12.2 mV across the salinity gradient. Mean zeta potentials for these strains were -20.57 ± SE 0.55 mV, -18.01 ± SE 0.45 mV and -17.05 ± SE 0.56 mV for DSM 8698, AW1 and AW13 respectively. All three followed a similar pattern, remaining relatively stable up to 2.5 PSU and becoming increasingly less negative with increasing salinity thereafter.

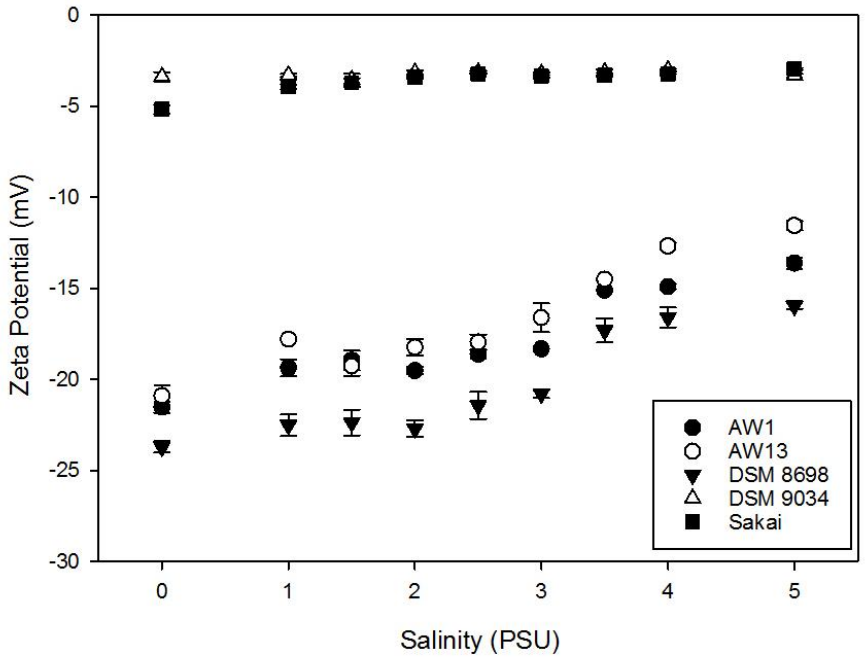

Figure 6.3.6 Zeta potentials of *E. coli* strain suspensions over a salinity gradient of 0 - 5 PSU. Solid circles- AW1; hollow circles- AW13; solid triangles- DSM 8698; hollow triangles- DSM 9034; solid squares- Sakai. Error bars indicate standard error from the mean (n=3).

6.3.4 Adhesion of E. coli *to suspended intertidal sediments*

There was no difference of recovery rate of *E. coli* between strain and salinity treatments of non-sediment microcosms (p= 0.899). Non-recovered *E. coli* ranged from -0.023 ± SE 0.086 $\log_{10}$ CFU ml^{-1} (AW13 at 3.5 PSU), to 0.180 ± SE 0.123 $\log_{10}$ CFU ml^{-1} (DSM 9034 at 2 PSU).

E. coli adhesion to sediment particles increased with sediment type in the order OM>M>MS. However only the difference between OM and MS was statistically significant (p= 0.007; Table 6.3.7). The number of *E. coli* cells adhering to sediment particles was significantly greater with

strain DSM 8698 than both AW13 and DSM 9034 (p= <0.001; Table 6.3.7). The adhesion of *E. coli* cells was significantly greater at 2 and 3.5 PSU than 0 and 5 PSU (p= <0.001; Table 6.3.7).

Table 6.3.7 General ANOVA summary table of the sediment x salinity x strain interaction. F-statistics and p- values are for single factor effects. Significantly different groups obtained using Fisher's LSD test are displayed in brackets under the p- value.

Sediment	**Organic Mud**	**Mud**	**Mixed Sand**		**F- statistic**	***p*- value**
Mean (log_{10} CFU ml^{-1})	0.334	0.299	0.272		5.34	0.007
SE (± log_{10} CFU ml^{-1})	0.020	0.034	0.029			OM>MS
Strain	**AW13**	**DSM 8698**	**DSM 9034**		**F- statistic**	***p*- value**
Mean (log_{10} CFU ml^{-1})	0.265	0.403	0.238		43.38	<0.001
SE (± log_{10} CFU ml^{-1})	0.027	0.030	0.019			DSM 8698> DSM 9034, AW13
Salinity (PSU)	**0**	**2**	**3.5**	**5**	**F- statistic**	***p*- value**
Mean (log_{10} CFU ml^{-1})	0.243	0.350	0.361	0.254	15.87	<0.001
SE (± log_{10} CFU ml^{-1})	0.020	0.044	0.031	0.026		2, 3.5>0, 5

There was no significant difference in adhesion between strains with OM (Table 6.3.8; Fig. 6.3.7A), however in MS, AW13< DSM 9034< DSM 8698 (p= <0.001; Table 6.3.8; Fig. 6.3.7C), and in M DSM 9034< AW13< DSM 8698 (p= <0.001), with the differences most apparent at 2 PSU (Fig. 6.3.7B). AW13 adhered greatest to OM, followed by M>MS (p= <0.001;Table 6.3.8; Fig. 6.3.7). The greatest adhesion for strain DSM 8698 was with M, which was significantly greater than MS and OM (p= <0.001). Conversely, the poorest adhesion for DSM 9034 was with M, which was significantly less than in MS and OM (p= <0.001). Over all strain and sediment interactions, the greatest adhesion was DSM 8698 with M (mean: 0.512 ± SE 0.047

log_{10} CFU ml^{-1}). The lowest adhesion was observed in DSM 9034 with M, and AW13 with MS (means: 0.114 ± SE 0.019 log_{10} CFU ml^{-1}, 0.166 ± SE 0.047 log_{10} CFU ml^{-1} respectively).

Adhesion of DSM 8698 was greater at 3.5 and 5 PSU than 0 PSU, and was much greater at 2 PSU (*p*= <0.001; Table 6.3.8; Fig. 6.3.7). Similarly, adhesion of AW13 is significantly greater by at least 2 fold at 3.5 PSU than at other salinities (*p*= <0.001; Table 6.3.8; Fig. 6.3.7). DSM 9034 follows a different pattern to the other strains, with the least adhesion at 2 and 3.5 PSU (Table 6.3.8), however adhesion between salinity treatments were not significantly different. The salinity dependant variation of adhesion of *E. coli* strains was consistent over all sediment types with only minor perturbations.

Table 6.3.8 Summary of E. coli adhesion (log_{10} CFU ml^{-1}) for treatment interactions

		Strain			Salinity (PSU)			
		AW13	**DSM 8698**	**DSM 9034**	**0**	**2**	**3.5**	**5**
Sediment	**Organic Mud**	0.356 ± 0.043	0.323 ± 0.042	0.323 ± 0.015	0.289 ± 0.021	0.356 ± 0.047	0.410 ± 0.051	0.281 ± 0.024
	Mud	0.272 ± 0.036	0.512 ± 0.047	0.114 ± 0.019	0.226 ± 0.040	0.341 ± 0.105	0.354 ± 0.061	0.276 ± 0.054
	Mixed Sand	0.166 ± 0.047	0.374 ± 0.053	0.275 ± 0.029	0.213 ± 0.037	0.350 ± 0.075	0.321 ± 0.051	0.204 ± 0.052
Salinity (PSU)	**0**	0.219 ± 0.024	0.251 ± 0.040	0.258 ± 0.039				
	2	0.198 ± 0.024	0.627 ± 0.043	0.223 ± 0.043				
	3.5	0.474 ± 0.049	0.379 ± 0.030	0.231 ± 0.050				
	5	0.168 ± 0.044	0.356 ± 0.042	0.238 ± 0.025				

When salinity was grouped to 0 with 2 PSU, and 3.5 with 5 PSU the factor effect of salinity became non-significant (non-grouped *p*= <0.001; grouped *p*= 0.453). However, when groups were 0 with 5 PSU and 2 with 3.5 PSU, the variance of the interaction effect of strain became stronger (grouped F-statistic= 47.03, non grouped F-statistic= 23.15, both *p*= <0.001).

DSM 8698 displayed the greatest range of adhesion of 0.580 log units (means: DSM 8698 x MS x 0 PSU: 0.159 ± SE 0.071 log_{10} CFU ml^{-1}, DSM 8698 x M x 2 PSU: 0.739 ± 0.076 log_{10} CFU ml^{-1}),

closely followed by AW13 with a range of 0.554 log units (AW13 x MS x 5 PSU: 0.020 ± SE 0.040 log_{10} CFU ml^{-1}, AW13 x OM x 3.5 PSU: 0.574 ± SE 0.073 log_{10} CFU ml^{-1}). Whereas the range of adhesion for strains DSM 9034 was only 0.293 log units (DSM 9034 x M x 2 PSU: 0.063 ± SE 0.031 log_{10} CFU ml^{-1}, DSM 9034 x OM x 3.5 PSU: 0.356 ± SE 0.051 log_{10} CFU ml^{-1}).

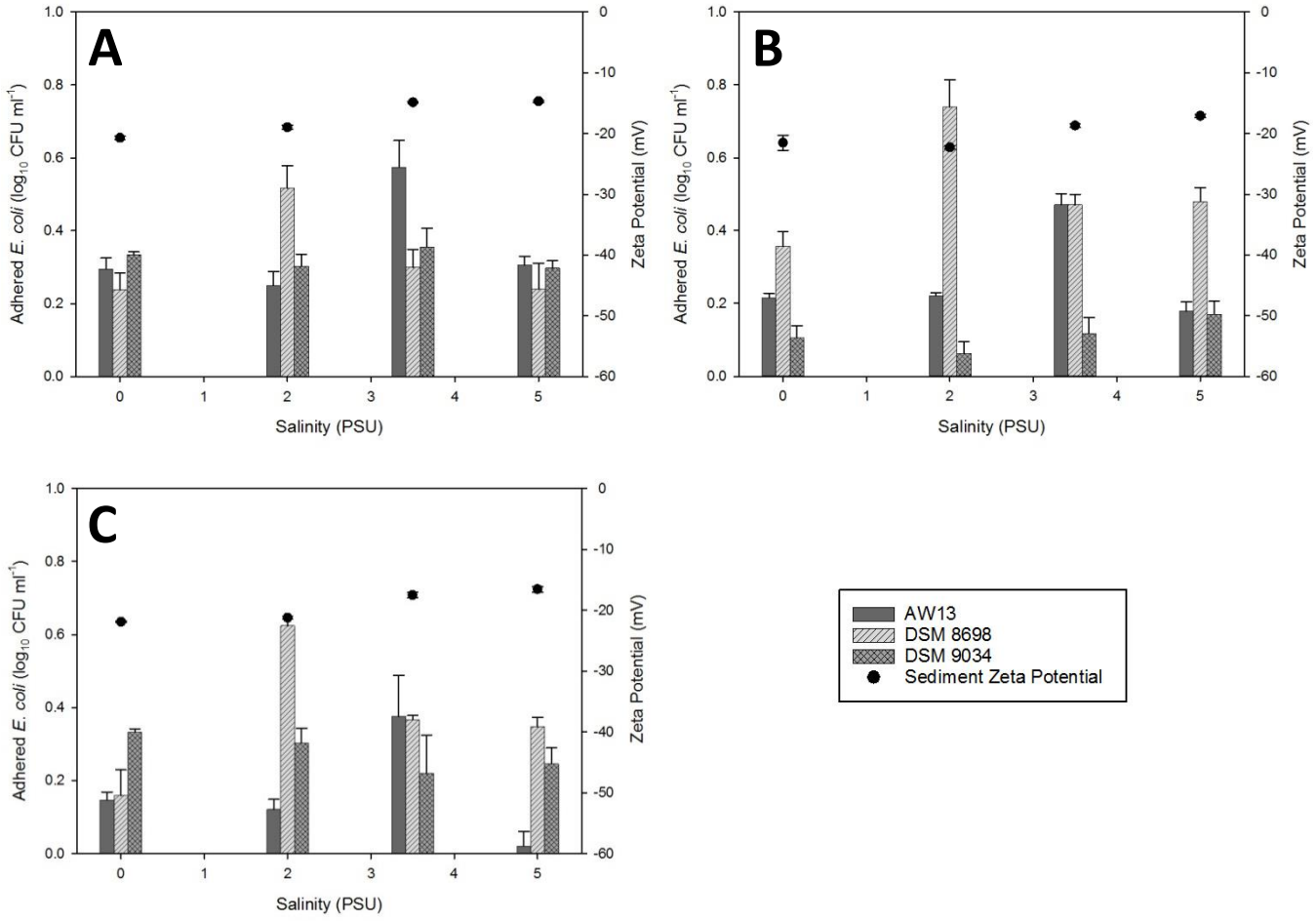

Figure 6.3.7 Number of adhered *E. coli* to sediment particles (bars) and zeta potential measurements of the sediment (solid circles) at 0, 2, 3.5 and 5 PSU. A- Organic Mud, B- Mud, C- Mixed Sand. Solid fill bars- AW13; dashed bars- DSM 8698; hatched bars- DSM 9034. Error bars indicate standard error from the mean (in all cases n=3).

There was a significant correlation between the decrease in negativity of sediment zeta potential with increasing pH (n= 12, Adjusted R^2= 0.66, *p*= <0.001; Fig. 6.3.8), despite the narrow range of pH values observed (Table 6.3.9). There was no significant relationship between sediment zeta potential and the amount of adhered *E. coli.* The relationship between strain zeta potentials and adhesion of *E. coli* was also tested, and showed a very weak, but significant relationship (n= 108, Adjusted R^2= 9.0, *p*= <0.001; Fig. 6.3.9).

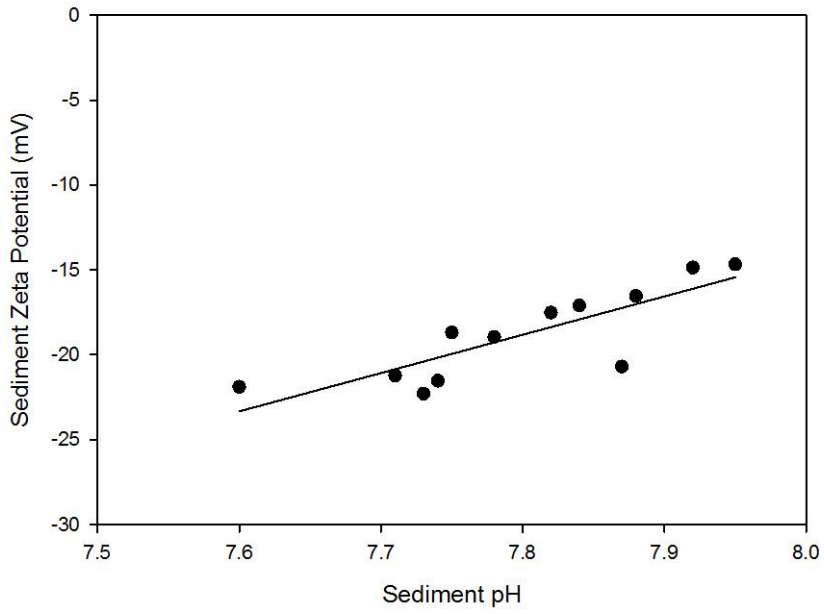

Figure 6.3.8 Linear regression between sediment zeta potential and pH of sediment microcosms. Regression equation: y=8.38x - 0.031 (F=22.23, n=12).

Table 6.3.9 pH values of sediment suspensions and water over the range of salinities tested.

Sediment Type	0 PSU	2 PSU	3.5 PSU	5 PSU
Organic Mud	7.87	7.74	7.60	7.60
Mud	7.78	7.73	7.71	7.72
Mixed Sand	7.92	7.75	7.82	7.82
Water Only	7.95	7.84	7.88	7.96

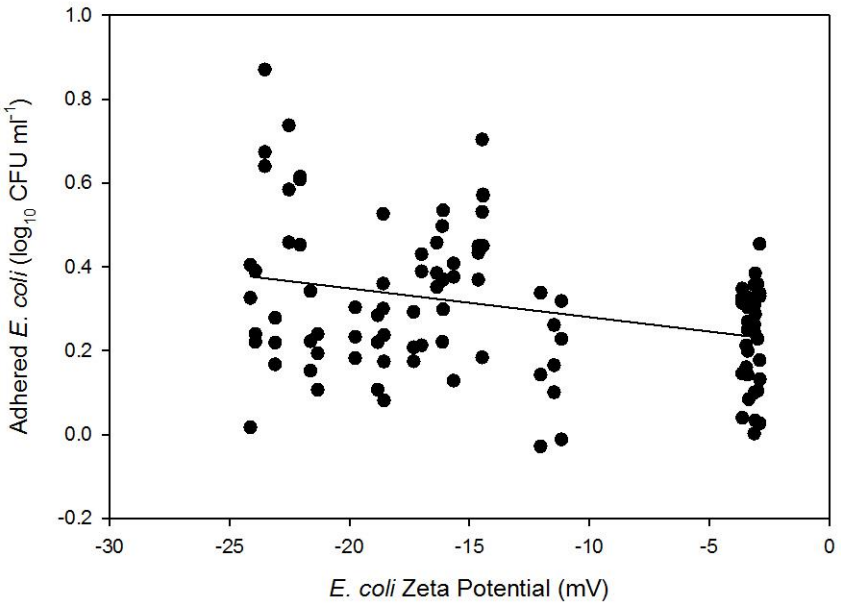

Figure 6.3.9 Linear regression between extent of *E. coli* adhesion to sediment particles and *E. coli* zeta potential (n=3). Regression equation: y=0.22x - 0.007 (F=11.52, n=108).

6.4 Discussion

6.4.1 Zeta potential of E. coli *strains*

All *E. coli* cell suspensions displayed negative zeta potentials, which is widely recognised to be the case for all bacteria in natural aquatic systems [397-400]. The zeta potential profiles of *E. coli* strains in this study formed two distinct groups: those which had a much less negative zeta potential, with the zeta potential not changing significantly over the salinity range tested (Sakai and DSM 9034); and those which displayed much more negative zeta potentials at low salinities, but became less negative as the ionic strength increased (AW1, AW13, DSM 8698).

The zeta potential of *E. coli* in artificial soil pore water of relatively low ionic strength has recently been shown to vary substantially between strains (n= 119, Mean= -26.5 mV, Range= -43.6 mV to -5.0 mV) [436]. Chen and Walker (2012) [414], found *E. coli* ATCC 12014 to have a negative zeta potential of -9.46 mV at 1 mM NaCl solution, with decreasing negativity of zeta potential until a slight positive charge of +1.77 mV at 100 mM NaCl. No strains exhibited a positive charge in this current experiment (Least negative: Sakai, 5 PSU= -2.95 mV), however the highest salinities tested here equates to ~71.4 mM NaCl which is lower than that of Chen and Walker [414]. The zeta potential profile of *E. coli* WH09 over increasing ionic strength of KCl obtained by Zhao et al. (2014) showed a similar trend to that observed here for strains AW1, AW13 and DSM 8698, with a sigmoidal curve plateauing at a zeta potential of -15 mV at 50 mM (~3.5 PSU) [415], and is explained by a limit on the compression of the double layer of counterions surrounding the particle [405]. The zeta potential of AW1, AW13 and DSM 8698 was unstable between 1 and 2 PSU, a trend observed by Carlsson (2012) in *E. coli* strain RNO4 (with a modified waaC gene) at 20mM of phosphate buffered solution [437].

Walker et al. (2004) investigated the zeta potential of three mutant strains of *E. coli* K12 that were known to display different lipopolysaccharide structures [397]. As observed in this study, the zeta potential of strains decreased became less negative with increasing ionic strength of KCl solution. The range of zeta potentials observed for 1 and 100 mM respectively were roughly -32 mV to -20 mV for strain JM109, -52 mV to -20 mV for D21f2, and -64 mV to -23 mV for strain D21. The less negative charge of strain JM109 compared to the other strains at 1 mM was attributed to a shielding effect from a long uncharged O-antigen on the outer membrane of the cell that was absent in the other strains indicating that extracellular appendages may alter zeta potential characteristics. Feng et al. (2014) investigated the zeta potentials of three

E. coli K12 mutants; ΔflgA, an assembly protein for ''flagellar basal-body periplasmic P ring'', ΔfimH, ''fimbrae adhesin unit'', and ΔcsgA ''curlin major unit'' [416]. All strains had previously shown reduced biofilm formation capabilities [438]. Zeta potential measurements show clear surface charge differences due to altered outer membrane proteins. The exhibited zeta potentials were -24.6 mV for the unaltered *E. coli* K12 WT, -27.3 mV for ΔflgA, -33.0 mV for ΔfimH, and -27.0 mV for ΔcsgA. Despite no significant difference in the zeta potentials between strains, in all cases the cell mutations caused the zeta potential to become more negative.

Further work is necessary in order to fully understand the causative mechanism for the difference in zeta potential between strains observed in this study, however the studies of Feng et al. (2014) [416] and Walker et al. (2004) [397] indicate there may be differences in the cell surface polysaccharide structure and membrane-bound proteins between the two distinct groups of zeta potential profiles. The advantage of expressing extracellular appendages such as flagellar and fimbrae that are beneficial in adhesion to surfaces, coupled with their presence possibly causing the zeta potential to become less negative resulting in lower electrostatic repulsion to surfaces may have a two-fold effect of increasing *E. coli* adhesion to sediment particles and other surfaces.

The results observed here confirm the first hypothesis as there were significant differences between zeta potentials of the different strains tested. The effect of salinity on the change in zeta potential profile was different between strains, with two distinct groups forming. It is necessary however to study more than the strains tested here to fully evaluate the relationship between phylogeny, genotype, phenotypic characteristics and zeta potential.

6.4.2 Zeta potential of sediment suspensions

As predicted with DLVO theory, the zeta potential of the sediments became less negative with increasing salinity; furthermore, the effect of salinity on the change in zeta potential was more apparent than any change due to sediment type. The trend of the sediment zeta potentials with increasing ionic strength of solution was a sigmoidal curve similar to that of the *E. coli* strains with a point of inflection between 2 and 3.5 PSU, the curve plateauing above 3.5 PSU. This plateau effect was also observed for soil coilloids in the work of Zhao et al (2014) [415] above 50 mM of KCl solution (~3.5 PSU). Furthermore, Zhao et al (2014) [415], also noted that

the change in sediment zeta potential with salinity was relatively small in magnitude, as observed during this current study. The authors proposed that this was due to the combination of variably and permanently charged minerals and organic matter present in the sample. A similar interaction between zeta potential and salinity was described by Hunter and Liss, (1982), where there was a decreasing concave curve in electrophoretic mobility (and therefore zeta potential) from 0 PSU, starting to plateau at ~5-7.5 PSU. This is in constrast with earlier studies where Pravdić (1970) [439] and Martin et al. (1971) [440] observed a reversal of the charge of marine sediments from a negative to positive charge even at just 2 PSU [439], although the assumption has been that later experiments were more reliable [48].

While the zeta potential of all sediments are similar at 0 PSU, the zeta potential of Organic Mud (OM) becomes less negative at 2 PSU, earlier than the change seen in other types of sediment, and also continues to be less negative than Mixed Sand (MS) and Mud (M) at the higher salinities, increasing the likelihood of flocculation and settling [26]. This confirms the second hypothesis as there are differences in the zeta potential profiles of the sediments. This may explain why constituents of the OM sediment were located higher up the estuary, as particles such as riverine-derived organic matter may settle out of the water column more rapidly on encountering the salinity of estuarine waters than downstream at where M and MS sediments are located.

The distribution of sediments within estuaries is dominantly caused by the hydrodynamics of the system, with lower tidal and current shear forces in bays and higher up the estuary allowing for the settling of smaller particles [183, 406, 441]. Sediments with a smaller particle size distribution (OM and M) demonstrated the previously observed relationships of increased organic content [88] and water content and a lower bulk density [442] than sediments of a larger particle size distribution (MS). The mineralogy present within the sediments seems to be controlled by the hydrodynamics of the estuary with deposition of smaller particle sized clay minerals (Illite/ Muscovite, Trioctahedral Clay and Kaolinite) at the sediments further up the estuary and therefore found in greater proportions in the OM and M sediments. The sediments used were generally similar in terms of mineralogical components present, suggesting a similar origin. All sediments contain the marine minerals calcite and aragonite, indicating a marine influence. It is difficult however to establish dominant origin of the sediment without further analysis such as isotope tracing [443]. The lower proportion of halite (sodium chloride) in Organic Mud sediments cannot be used to determine mineralogical

differences as its presence depends on the volume of freshwater run-off through the sediments, and the sampling time during the tidal frame as sea water recedes from the sediment.

OM and M had slight differences in mineralogy and it is known that mineralogy influences zeta potential at fixed pH and electrolyte conditions [411]. The difference in settling location may be from differences in the existing conditioning film surrounding particles, where breakdown of such conditioning films can lead to a more positive electrophoretic mobility [49] which is proportional to zeta potential. Conditioning films surrounding OM particles may exhibit a less negative zeta potential than other sediments and therefore flocculate at lower ionic strength and settle higher in the estuarine system [48]. It is also likely however that similar sediment particles settle out at the locations where OM and M were collected, but decaying organic matter from the extensive reed bed in close proximity to the OM sediments contributes to the high organic content, and creates a sediment environment that encourages development or change of a conditioning film on the particles that is of a less negative zeta potential than particles existing further downstream where the M sediments were collected. Throughout the year, OM sediments (Site: Ythan estuary, site 1) had a much higher concentration of EPS than M sediments (Site: Ythan intensive sampling, Mud site) (Chapter 3), which will contribute to differences in the conditioning film on the particles.

The zeta potential measurements of the different sediments suggest that zeta potential may explain some of the spatial distribution of sediments within the estuary. However, due to the subtle changes in zeta potential observed over the estuarine salinity range tested, and the similarity in mineralogy between the OM and M sediments, further work is necessary to investigate whether the zeta potential of a suspended sediment affects where it is deposited within an estuary.

6.4.3 Adhesion efficiency of E. coli *to suspended sediments*

There was no significant difference between any treatments in the recovery of *E. coli* cells in the absence of sediment, indicating there was little cell-cell adhesion at higher salinity treatments that may have caused lower CFU counts despite more individual cells being present. Previous studies investigating attachment of *E.* coli to soils and clays use inoculum concentrations of 10^6 CFU ml^{-1} [431](In Press), 10^7 CFU ml^{-1} [100] and up to 10^{10} CFU ml^{-1} [415].

For this experiment, a final inoculum concentration of 10^7 CFU ml^{-1} was used. A highly concentrated inoculum will mean the effect of binding will be hard to discern, and also lead to higher amounts of cell-cell binding. If the inoculum is too low, there may be interference from native bacterial activity and *E. coli* pre-existing in the collected sediments.

Phylotypic and genotypic analyses revealed a range of characteristics in the *E. coli* strains tested. The subset of strains AW13, DSM 8698 and DSM 9034 were selected for the sediment-adhesion assays as they represented a range of characteristics and included both clinical and environmentally isolated strains. DSM 8698 displayed prolific biofilm production and moderate swarming ability, AW13 displayed moderate biofilm production and very good swarming ability at 15 °C, and DSM 9034 displayed both poor biofilm production and poor swarming ability.

Over all sediment and salinity treatments, strain DSM 8698 showed the highest average adhesion, followed by strain DSM 9034, then AW13, with DSM 8698 being significantly higher than DSM 9034 and AW13. Strain DSM 8698 displayed a higher biofilm forming ability than AW13 and much higher than DSM 9034, which suggests DSM 8698 could have had an advantage over other strains to adhere successfully after contact with the particles compared to the other strains. Strain AW13 showed lower adhesion efficiency than other strains in the MS sediment treatments, but was only significantly different from DSM 8698. It could be that the two pathogenic strains DSM 8698 and DSM 9034 had an advantage over AW13 for adhering to sediment particle surfaces.

Pathogenic *E. coli* strains often have an increased presence of flagellar or fimbrae that increases their ability to attach to surfaces, and extent of biofilm formation is of key importance when studying the infectivity and risk with *E. coli* strains. Successful attachment to a surface is suggested to be down to several factors including the presence of extracellular appendages such as fimbrae [444] and flagellar [445], surface hydrophobicity and extent of EPS production [446]. The presence of flagellar is useful for providing motility to a bacterial cell to overcome the electrostatic repulsion of a substrate surface [446]. It is not essential however for the initial adhesion to a surface or for biofilm formation [447, 448], but strong adhesion factors may need to be present [56]. The presence of flagellar on bacterial cells may also enable the development of a more successful mature biofilm [449, 450]. The presence of fimbrae and related adhesins are widely considered to be important for non-specific binding and consequential production of biofilms on abiotic surfaces [56, 71, 451-455].

Strains Sakai, DSM 8698 and DSM 9034 were the pathogenic strains tested for biofilm production in this study, but only DSM 8698 showed significant biofilm formation. The regulation of genes controlling extracellular appendage production in these strains may be strictly limited to specific environmental conditions such as those involved in the regulation of curli fimbrae production by *E. coli* [445]. It may be that environmental conditions in this experiment were ideal for the upregulation of genes allowing for biofilm production in DSM 8698 but not Sakai and DSM 9034. The Sakai strain has been shown to have lower attachment efficiency than other *E. coli* O157:H7 strains on epithelial cells [456], so poor biofilm formation on an abiotic surface at sub-optimal growth temperatures may be expected. Difference in gene regulation could also explain the difference in biofilm formation between the two wild-type strains AW1 and AW13. Each strain showed different ranges of adhesion over all the treatments. DSM 8698 showed the largest difference between the highest and lowest adhesion at 0.58 log units, closely followed by AW13 with 0.55 log units, suggesting it they might have a tighter regulation of attachment facilitating genes, or greater sensitivity to environmental conditions. When conditions are ideal for their adhesion to sediment particles, they do so successfully. DSM 9034 shows a more conservative range of adhesion efficiency of 0.29 log units as they did not adhere as greatly in any treatment as DSM 8698 and AW13 did to the M and OM sediments respectively. The strict genetic control of pathogen attachment to different biotic surfaces is highlighted by Smith (1977) [457], and is quite possibly as stringent as the regulation of attachment to sediment surfaces. The constructed phylogenetic trees revealed strains AW13 and DSM 8698 to be in the B1 clade. These strains were the only ones to demonstrate biofilm formation, however not enough strains were tested to conclude that adhesion was linked to the phylogenetic grouping.

Wood et al. 2006 [458] found that high swarming ability correlated well with biofilm formation which is observed for strain DSM 8698. AW13 however was the only other substantial biofilm producer and only showed relatively good swarming ability at 15 °C and not at 25 °C, the temperature at which the biofilm assay was performed. The ability of *E. coli* cells to occasionally ‘tumble’ (spontaneously change direction) rather than a simple ‘run’ (move at a constant speed up a concentration gradient) allows formation of larger swarms [428]. Strains DSM 8698, Sakai and AW1 may have been demonstrating this ability in order to produce such rapidly expanding swarms at 25 °C, and may indicate why DSM 8698 adhered to sediments more successfully. The production of EPS and extent of chemotactic sensing ability have been suggested to be advantageous to swarming ability and biofilm formation respectively [459].

Strain DSM 9034 demonstrated minimal swarming ability at both 15 and 25 °C which may explain its relatively poor adhesion compared to DSM 8698, especially evident in M. Strain DSM 8698 demonstrated the high biofilm formation and swarming ability, especially at 25 °C which may be linked to its virulence characteristics of being a fairly aggressive pathogenic strain of *E. coli* [56]. At 15 °C, strains Sakai and DSM 8698 show a swarming ability weaker than wild type strains AW1 and AW13, whereas at 25 °C, they have the strongest swarming abilities of all strains. The swarming ability of Sakai seemed to have been upregulated at higher temperatures in a similar manner to DSM 8698. AW13, and the other environmental isolate AW1, demonstrated the strongest swarming ability at 15 °C of all strains. These strains were isolated from intertidal sediments so were likely to be already more adapted to surviving and thriving at lower temperatures that may explain its higher adhesion than DSM 9034 to M.

Pachepsky et al (2008) [396] found differences of *E. coli* strain preference to adhere to different sediment types. Clear clusters of *E. coli* strains were found to prefer sediment classes, where 80 % of strains adhering to silt particles were of one cluster, whereas no strains of the same cluster were found to adhere to fine sand. A second cluster was found to only adhere to fine, medium and coarse sand, and not silt or clay which demonstrates the existence of preference of *E. coli* strain to different particle sizes. The authors suggest that genetic variation could cause difference in strain preference to the same particle. This phenomenon was further indicated in the present study by the apparent preference of each strain for different sediments, such as higher adhesion of DSM 8698 to M, and likewise with OM for AW13 and DSM 9034. It is therefore appropriate to propose that within suspended sediments, the relative abundance of *E. coli* strains adhered to sediment particles will not be the same as the relative abundance of strains in the total number of cells in suspension. The precise relative abundance of adhered cells to suspended particles will depend on the characteristics of the suspended sediment, and the genetics of the *E. coli* strain [396].

Production of EPS is associated with good biofilm production [446], and was suggested earlier as the cause of DSM 8698 adhering more successfully over all treatments than the other strains. AW13 showed some biofilm forming ability, which may explain its higher adhesion than the remaining strains. Cao et al (2006) [460] suggest that cations in solution form bridges between EPS on the bacterial surface, and negatively charged sites on clay particles. The greater adhesion of DSM 8698 to the M sediment may have been a combination of the M sediment containing less EPS, exposing the negatively charged sites on the sediment particles,

coupled with the higher biolfilm EPS of the DSM 8698 cells resulting in bridges forming between the cell and particles allowing for greater successful adhesion.

6.4.4 E. coli *adhesion efficiency over the salinity gradient*

Over all sediments and strains, adhesion was greatest in the 2 and 3.5 PSU treatments. Further investigation is needed in order to determine why there was not at least equivalent adhesion in the 5 PSU treatments. Increasing salinity has been shown to be a cause of sub-lethal stress in *E. coli* [461], and it may be that there was lower metabolic activity in the higher and lower (due to hypoosmotic stress) salinities, so less cells than predicted may have overcome the initial electrostatic repulsion of the particle surface as a result of reduced motility [56]. It could be that adhesion between 0 and 3.5 PSU is in line with DLVO theory, but the 5 PSU treatment inhibited bacterial activity because of the osmotic stress, or ion-specific toxicity [114]. This effect is most apparent in the DSM 8698 and AW13 strains over all sediment types, displaying they may be more sensitive osmotic stresses, with a preference of ionic strength evident for strain DSM 8698 at 2 PSU, and AW13 at 3.5 PSU. It is also logical that strain AW13 has a higher salinity tolerance than DSM 8698 as it was isolated from the estuarine environment. This effect is not seen in the DSM 9034 treatments.

Strain DSM 9034 had a slight, non-significant, decreasing trend of adhesion with salinity, suggesting it may have been more sensitive to the increasing salt concentration rather than low osmotic stress. The only significant difference for strain AW13 in regards to different salinities was that adhesion at 3.5 PSU was higher than all other salinities, suggesting AW13 is more resilient to increasing salinity than DSM 9034, up to a threshold of between 3.5 and 5 PSU. When contrasts were made between the expected grouping of 0 and 2 PSU, and 3.5 and 5 PSU, there was no improvement of significance of the salinity effect, whereas when salinity was grouped as 0 and 5 PSU, and 2 and 3.5 PSU, the variance ratio increased for salinity, supporting the previous analysis where adhesion was greater at the mid ionic strengths of 2 and 3.5 PSU than the extremes.

On visual inspection of the microcosms for all sediment-strain treatments post-centrifuging, there is a clear decrease in turbidity due to an increase in the settling of smaller sediment particles with increasing salinity (Fig. 6.4.1) The pellet of sediment was clearly visible at the bottom of the microcosms. The decrease in negativity of the sediment zeta potential with

increased salinity has induced the effect predicted with DLVO theory that would cause increase particle-particle adhesion in the smaller fractions that would have otherwise stayed in suspension. With this in mind, and despite the experiment being designed as a short-term incubation to investigate only physical adhesion of *E. coli* according to DLVO theory, there seems to be a bacterial factor involved, otherwise greater adhesion would have been recorded in the 5 PSU treatments, rather than what is observed, with greater adhesion in the 2 and 3.5 PSU treatments only.

Figure 6.4.1 Visual inspection of the clarity of post-centrifuged microcosms. From left to right, treatments of 0, 2, 3.5 and 5 PSU for Mixed Sand with strain AW13.

The work on desorption of *E. coli* M13 from a mixed sediment (34.5 % coarse sand, 4.5 % silt, 49.4 % clay) of Roper and Marshall (1974)[24] showed a significant increase in desorbed cells below a critical salinity equivalent to ~1.22 PSU, with ionic strengths higher than this allowing for a strong adhesion of cells to sediment particles. This equates to theoretically lower concentrations of *E. coli* adhered to particles in this experiment in the 0 PSU treatment compared to higher salinities. This was observed in this study with significantly higher adhesion in the 2 and 3.5 PSU treatments, but not in the 5 PSU treatments which, as previously discussed may have been due to inhibitory mechanisms.

Abdulkarim et al [462] investigated the effect of increasing concentrations of NaCl and KCl on the growth of *E. coli* at 37 °C in modified nutrient broth. In the NaCl treatments, low growth was observed at low (0 mM NaCl) and high concentrations (257 mM NaCl). The highest growth was observed in the NaCl treatment at a concentration of 86 mM, equivalent of ~6 PSU seawater. Growth at 177 mM remained similarly high, and decreased to a similar abundance of the 0 mM treatment at 257 mM. In the KCl treatments, growth again was highest at the medium ionic strength of 67 mM, with the extent of growth decreasing at higher ionic strengths. The trend of *E. coli* growth at medium salt concentrations reflects the trend of increased adhesion at the medium salinities observed here, however the concentrations used by Abdulkarim et al. were higher than those of this experiment. The comparison is not directly applicable as the study used growth in nutrient broth at 37 °C, rather than investigating adhesion to particles in seawater at environmental temperatures. It does however indicate that *E. coli* cells have a preference for metabolic activity (in this case growth) at moderate salinities. It could be that *E. coli* are more sensitive to osmotic stress in low-nutrient seawater microcosms compared to growth media, so the effect here was seen at a lower salinity.

Carlucci and Pramer [114] also found increased respiration and survival of *E. coli* at a seawater concentration of 8.5 PSU compared to 0 PSU and salinities above 8.5 PSU. Again, this is a higher salinity than investigated in this experiment, but the temperature of the microcosms of Carlucci and Palmer were at 28 °C, rather than the 12 °C of this study which may have caused further stress to the bacterial cells. Increased survival at lower salinities was also observed by Anderson et al. 1979 [461]. To investigate whether the metabolism is truly reduced in the higher and lower salinities of seawater and if this could be the causative factor in the reduced adhesion, ATP could be measured using commercially available assay kits, or a method similar to that of Carlucci and Pramer 1960 [114] could be utilised where O_2 uptake is measured.

Adhesion efficiency did not increase with ionic strength over the entire range of salinities tested as expected. However, there were still significant strain-specific trends that influenced differing extents of adhesion of *E. coli* strains to suspended sediments, allowing confirmation of the third hypothesis.

6.4.5 E. coli *adhesion efficiency between sediment types*

All strains adhered more efficiently to the OM sediments than other sediment types, allowing confirmation of the fourth hypothesis. This increased adhesion may have been due to plentiful binding sites as a combination between the mineralogy and particle size of the sediment resulted in the largest surface area of all sediments and therefore most available surfaces for cells to adhere to. OM had the highest Adhesion efficiency of *E. coli* strains to M and MS also followed the trend of surface area and organic content. OM sediments have well-developed conditioning film evidenced by greater EPS concentrations typically found in OM than M and MS sediments (Chapter 3) which may have negated any strain specific advantage for adhesion to the particles, demonstrated by the lack of significant difference between strains adhering to OM. The typical sediment surface topography in MS is likely to be smoother as a result of the increased quartz presence, compared to smaller particles that have pits and layering that provide niches for adhesion through higher surface area, therefore initial adhesion would have been more challenging [463]. Phenotypic traits allowing greater biofilm and swarming abilities would have been more beneficial on smooth surfaces, possibly explaining why the pathogenic DSM 9034 and DSM 8698 strains adhered better to this sediment. As well as less surface area for cells to adhere to in MS, there were fewer particles, decreasing the likelihood of collisions between particles and cells that could result in successful adhesion.

Several studies have observed higher adhesion of *E. coli* to soil particles of smaller size fractions. Oliver et al [100] observed that the highest amount of *E. coli* bound to the 4-15 µm fraction of suspended soil particles, but the 16-30 µm fraction had almost 4 times the amount of adhered *E. coli* after adjustment for surface area. Muirhead et al. (2006) [464] also found most *E. coli* was being transported in overland flow in association with soil particles in the <20 µm fraction. Auer and Niehaus (1993) [465] also found >90 % of thermotolerant coliforms adhered to particles of the 0.45-10 µm fraction. In line with previous studies, the OM and M sediments had larger fractions of particles in the 0-63 µm range than the MS sediment and a greater *E. coli* adhesion, further indicating *E. coli* adheres in greater proportions to smaller particle sizes.

Roper and Marshall (1974) [24] observe the adhesion of smaller clay particles and organic matter to *E. coli* cells at all salinities. They determined the saturation point of this phenomenon is at a concentration of ~100 µg of colloidal montmorillonite per ml of suspension. This covering of smaller, dense particles of clay would increase the particle density

with relatively little increase in the particle size, increasing the settling rate according to Stokes' law. *E. coli* cells with a clay mineral coating, although not attached to larger particles, would be removed from the analysed supernatant by the centrifugation method used in this study. If the particle density increased by only 10%, the cells would descend 1.7 cm rather than the calculated 0.9 cm. This may have increased the number of *E. coli* enumerated as adhered when the cells are not actually adhered to larger particles. However, the increase in settling velocity incurred still means the cell is more prone to sedimentation than unadhered *E. coli*. The higher clay content of OM and M may explain why there was a higher mean of adhered *E. coli* to them compared to MS.

The zeta potential profile of OM was less negative than M and MS. In line with DLVO theory, there was more adhesion to OM compared to M and MS, despite similar physical characteristics measured between OM and M. However, the variation between *E. coli* strain and salinity treatments was greater than between sediments, suggesting sediment zeta potential was not the governing factor in *E. coli* adhesion to sediments. The differences between zeta potential profiles of strains were more dramatic, with DSM 9034 having a much less negative zeta potential than DSM 8698 and AW13. According to DLVO theory, this would result in greater adhesion of DSM 9034 than the other strains over all treatments, which again was not the case. Conversely, the average adhesion for strain DSM 9034 was much lower than strain DSM 8698. Results from the regression analysis show no significant relationship between the amount of adhered *E. coli* and the zeta potential of the sediment or the strain used.

The lack of correlation between recorded zeta potential profiles and adhesion could be attributable to the strain and sediment suspensions being similarly unstable. Zeta potentials between -30 mV and +30 mV are viewed as 'unstable', whereas zeta potentials lower or higher than this are viewed as 'stable' [407]. *E. coli* cells can reach zeta potentials lower than -30 mV (Avery, L. et al. Pers. Comm. 2016), but were not used in this study. Strains exhibiting a wider range of zeta potentials including those lower than -30 mV could be used in future studies to investigate the role of zeta potential on attachment of *E. coli* to sediments and surfaces in order to obtain clearer trends. The findings here support the conclusions of Rong et al. (2008) [466], that non-electrostatic mechanisms rather than electrostatic forces are more important in bacterial adhesion to particles. As a result of the lack of correlation between sediment or strain zeta potential and the amount of adhered *E. coli,* the fifth hypothesis was rejected.

6.4.6 Environmental implications

The results suggest that strain was the most important factor in determining the adherence of *E. coli* to sediment particles, but strain adhesion was also dependant on the sediment type and salinity. Strain DSM 8698 showed the highest adhesion across all strains, suggesting it is more prone to sedimentation than the other strains tested, indicating it would be more abundant in intertidal sediments, and therefore more likely to persist in the environment for longer periods of time, benefiting from the advantages of sediment association as discussed in Chapter 1. The large effect of strain in the analysis suggests that with different suspended sediment types, the relative abundance of adhered *E. coli* strains will be different, and this difference cannot be explained by variation in *E. coli* zeta potential. The characteristics of the sediments has shown to determine the extent of adhesion for *E. coli* cells to the sediment particles that may explain the relative distribution of *E. coli* within estuarine systems, depending on which sediment types settle out of suspension in certain areas of the estuary.

The salinity of the seawater suspension has a large effect on the adhesion of *E. coli* to suspended sediment particles. The data here shows that there will be less adhered *E. coli* at 0 and 5 PSU than 2 and 3.5 PSU leading to an increased abundance of *E. coli* in sediments higher up the estuary where seawater first meets incoming river water, reflecting *E. coli* distribution patterns discussed in Chapter 3. This applies also to areas in close proximity to tributaries entering the estuary, but these areas were not sampled intensively enough to draw any evidence-based conclusions. The intrusion of saltwater into an estuary will have a large impact on the distribution of *E. coli* settling out of suspension. Spring tides will mean river water will mix with seawater higher up the estuary, resulting in the adhesion of *E. coli* to suspended particles occurring higher up the estuary. In addition, the higher the tidal intrusion, the low shear forces experienced where tide meets river flow will be higher up the estuary, allowing for increased settling of sediment particles and associated *E. coli* higher up the estuary.

The data collected in this study on the zeta potentials of the different strains has implications for the electrostatic trapping of *E. coli* for decreasing bacterial contamination of drinking water [50]. Soni et al. 2007 [50] found that the zeta potential of pathogens changes with nutrient availability, but also highlighted the difference in zeta potential of different *E. coli* strains. Strains exhibiting less negative zeta potentials such as strain Sakai and DSM 9034 are less likely to adhere to positively charges surfaces used to trap bacterial cells than the other strains in this study.

The average suspended solids in the Ythan river are roughly 10 mg L^{-1} [285], however concentrations at the turbidity maxima, and in estuaries exposed to high shear forces such as the Severn estuary, Wales/England, can experience concentrations exceeding 300 mg L^{-1} [467]. The average percentage cells adhering to suspended sediments across all treatments for DSM 8698, DSM 9034 and AW13 were 57, 40 and 42 % respectively. The geometric mean for suspended *E. coli* in the water column at the head of the estuary over 2014 was 3.08 $\log_{10}$ CFU 100 ml^{-1}, and the average concentration for the Tarty Burn tributary entering the Ythan estuary at the Sleek of Tarty was 3.14 $\log_{10}$ CFU 100 ml^{-1}. This equates a geometric mean of *E. coli* adhered to sediment particles of 1.24 $\log_{10}$ CFU l^{-1} at the head of the estuary, and 1.97 $\log_{10}$ CFU L^{-1} at the Sleek of Tarty at higher concentrations of suspended sediment at 300 mg L^{-1}. When this sediment settles with the associated *E. coli*, it equates to 3.76, and 4.5 $\log_{10}$ CFU 100g dry wt^{-1} sediment for settling at the head of the estuary and the Sleek of Tarty respectively for water with high suspended solids. This contradicts the data from Chapter 3, with more *E. coli* present in the head of the estuary, but as shown in this chapter, the sediment characteristics located at the head of the estuary were more favourable for the adhesion of *E. coli.* These values do however generally represent the abundance of *E. coli* found in intertidal sediments (sampling site geometric mean for 2014: Mud= 3.20 $\log_{10}$ CFU 100g dry wt^{-1}, Mixed Mud= 3.17 $\log_{10}$ CFU 100g dry wt^{-1}, Mixed Sand= 2.12 $\log_{10}$ CFU 100g dry wt^{-1}, Sand= 2.63 $\log_{10}$ CFU 100g dry wt^{-1}). The values closely represent *E.coli* abundance in the sediments with high percentages of fine particles, such as those found at the head of the Ythan estuary (Chapter 3). The sediment sites of MS and S have less particles in the <60 µm range than the M and MM sites, which this study has shown will have increased concentrations of adhered *E. coli,* and as shown in Chapter 3, sediments of this type contain less *E. coli*. It is also likely that the values here for *E. coli* adhesion to particles are conservative, due to the high rotation speed during the incubation in this experiment that was necessary to keep particles in suspension. At lower shear forces, more adhesion is likely to take place as cells will not get sheared from the sediment particle surface after initial contact is made; only cells forming a strong adhesion quickly will have been associated with the sediment particles after incubation.

6.4.7 Conclusions

The aim of this chapter was to investigate the role of zeta potential in the adhesion of *E. coli* to suspended intertidal sediments. With the methods used here, clear trends in the zeta potential of different sediments and *E. coli* strains over a salinity gradient were demonstrated, and the adhesion experiment allowed this to be correlated to adhesion efficiency of *E. coli.*

The first hypothesis: *Different* E. coli *strains will exhibit different zeta potential profiles over the salinity gradient,* was confirmed as two distinct groups of zeta potential profiles over the salinity gradient were identified; those with a stable, less negative zeta potential, and those that demonstrated a larger range of zeta potentials. The second group of *E. coli* strains and the sediments demonstrated a sigmoidal curve of decreasingly negative zeta potential with increasing salinity, plateauing between 2 and 3.5 PSU.

The second hypothesis: *Sediments will exhibit different zeta potential profiles over a salinity gradient,* was confirmed as there were differences in the zeta potential profiles of the sediments, with a less negative zeta potential of the OM sediment at salinities greater than 0 PSU.

The third hypothesis: E. coli *strains will show different adhesion efficiencies with ionic strength (salinity),* was confirmed as there was greater adhesion of *E. coli* to sediment particles in the 2 and 3.5 PSU treatments.

The fourth hypothesis: E. coli *strains will show different efficiencies in adhesion to different sediment types* could be confirmed as adhesion of *E. coli* to the OM sediments was greater than other sediment types.

The fifth hypothesis: *The adhesion of* E. coli *cells to sediment particles can be explained by the zeta potential of the strain or sediment* was rejected as there was no obvious correlation between the number of adhered *E. coli* cells and the zeta potential measurements.

7. General discussion and future work

7.1 Summary of main thesis questions

Identify key physical, biogeochemical, biological and environmental factors influencing spatial and temporal variation in the abundance of faecal bacteria in intertidal sediments.

Explanatory models using sediment characteristics and environmental variables (Chapter 3) successfully explained a large proportion of the spatial and temporal variability of *E. coli* in intertidal sediments of the Ythan estuary. The models constructed on data from four intensively sampled sites on the Ythan estuary explained 60 % and 71 % of the variation of *E. coli* for the optimal 'all replicates', and 'replicate means' models respectively. The optimal models constructed on data from the Eden and Ythan estuary transects, and both estuary transects combined explained 87 %, 50 % and 49 % of the variability of *E. coli* respectively. Many of the factors that governed *E. coli* variability were common to both the Ythan and Eden estuaries, suggesting a likelihood of success for future modelling approaches predicting *E. coli* abundance across multiple estuarine systems. The optimal models however did not fully incorporate site-specificity within the Ythan estuary, or seasonal variation as the additional of factorial site and seasonal terms increased the variability of *E. coli* abundance explained by the models.

Investigate whether intertidal sediments with a high risk of supplying a large number of faecal bacteria can be identified by combining erosion thresholds and *E. coli* abundance.

Mud, mixed mud and sandy sediments during colder months at the Ythan estuary, and sediments in the upper reaches of the Ythan and Eden estuaries during summer, autumn and winter were identified as having a relatively high abundance of *E. coli* combined with a relatively low erosion resistance (Chapter 4). The correlation between *E. coli* in the water column and *E. coli* in intertidal sediments was also investigated, and it was discovered that abundance of waterborne *E. coli* did not explain the abundance of *E. coli* in the sediments as successfully as sediment characteristics and environmental variables, but there was a statistically significant positive correlation between *E. coli* abundance in sediments, and waterborne *E. coli*, suggesting a relationship does exist between the two phases.

Determine whether or not *E. coli* abundance in intertidal sediments is affected by the native microbial community.

It was identified that patterns of species abundance, diversity and evenness, and shift in native microbial communities were similar in both the Ythan and Eden estuaries (Chapter 5). These changes in microbial community had no apparent effects on the abundance and distribution of *E. coli* however, with the changes in both microbial community and *E. coli* seeming to co-vary with biogeochemical and physical gradients within the sediments of the estuaries.

Examine the role of zeta potential in the adhesion of *E. coli* to suspended intertidal sediments, and investigate how salinity, sediment characteristics and *E. coli* strain characteristics influence adhesion efficiency.

The zeta potential profiles of *E. coli* (Chapter 6) were found to respond to a salinity gradient in one of two ways; either becoming decreasingly negative as salinity increased, or being of an initial low negative zeta potential that did not change with increasing salinity. Intertidal sediment suspensions also became decreasingly negative with increasing salinity, but there was very little difference in zeta potential between the sediment types, and this did not relate to their relative location within the estuary. *E. coli* strains showed different adhesion efficiencies over the salinity gradient tested, with increased adhesion at 2 and 3.5 PSU compared to 0 and 5 PSU. Furthermore, *E. coli* strains adhered more successfully to the fine sediment with high organic content, and the extent of adhesion was strain dependant. These trends of more successful cell-particle adhesion at specific salinities and to specific sediment types could not be related to the zeta potential of the strains or sediment type or a combination.

7.2 E. coli *abundance in intertidal sediments*

Data collected in both field sampling campaigns have reinforced the belief that intertidal sediments are a significant reservoir of faecal bacteria within the environment [247]. The numbers of *E. coli* observed in the sediments of the Ythan and Eden estuaries were similar to those previously reported for similar sediments [78, 80], often exceeding 10^4 CFU 100 g dry wt^{-1}. The variability of *E. coli* within sediment types however was very large, to the extent that mud at the Ythan estuary could be designated as hazardous during autumn (10^2 CFU 100 g dry wt^{-1}), but abundances during spring could be viewed as relatively harmless (approximately 1 CFU g dry wt^{-1})).

It was suggested in Chapter 3 that a lower abundance threshold could be employed, where sediments with observed *E. coli* abundance below 2 $\log_{10}$ CFU 100 g dry wt^{-1} removed from the dataset, to allow for greater predictive power of models of *E. coli* abundance in sediment. Below this level, the risk of disease from direct contact with the sediment, or the contribution of the sediment to waterborne FIO concentrations would be negligible and the sediment could be deemed 'non-hazardous'. Quantitative risk assessment based on exposure risk and FIO levels could be performed on sediments in a similar manner to the bathing water advisory levels in order to advise the public to avoid direct sediment contact. Much of the uncertainty surrounding the prediction of *E. coli* in intertidal sediments of the Ythan and Eden estuaries in this study stemmed from the inaccuracy of the models of Chapter 3 at very low abundances of *E. coli*. If a lower threshold of FIO abundance in sediments is established where sediments are deemed non-hazardous, this would provide justification for excluding such sediments from future attempts to predict FIO abundance, therefore increasing the accuracy of the models in Chapter 3, and in future models explaining *E. coli* abundance in intertidal sediments.

A logical future study in the investigation of the effect of environmental and sediment characteristics on the distribution of *E. coli* within estuarine systems would be to conduct further sampling campaigns on multiple estuaries. Trends observed in Chapter 3 suggest this would be productive, as there were many similarities in the driving variables between the Ythan and Eden estuaries. One of the limitations of the sampling regimes conducted for this thesis was that not all sediment types and combinations of sediment types at different salinities were successfully examined as some sampling positions were over 650 metres apart. Future sampling efforts may not have to be as labour intensive as for the Ythan and Eden estuaries, as several variables did not show a significant relationship with trends in *E. coli*

abundance and could be excluded. If further sampling efforts are made, the creation of a model able to successfully predict *E. coli* abundances in multiple estuaries may be achievable, resulting in facilitated prediction of bathing water advisories for many sites, rather than site-specific models. In addition, the distribution of *E. coli* abundance in the estuaries observed in this study suggest that areas of high *E. coli* loading are relatively easy to identify, and therefore introducing advisories to the public to avoid such areas is a feasible, and sensible possibility in order to protect public health.

Current climate change observations [468] have noted a general increase in air and sea temperatures around the UK with fewer days of air frost. There has been an increase in the contribution of heavy precipitation events to total rainfall during winter and summer, with the exception of north- east England and northern Scotland which show a decrease (both the Ythan and Eden estuaries are situated within the east Scotland region). There has also been a significant increase in wave height in the south east, and in northern Scotland. These trends are forecasted to continue [469], with increase in temperatures and winter precipitation, and decrease in summer precipitation. These changes are more extreme in the south and western parts of the UK, with the highlands and north of Scotland least affected.

In Chapter 3 it was observed that during warmer months there was a decrease in the abundance of FIOs in the sediments. With a future increase in temperatures, the data here suggests that the abundance of FIOs may generally decrease. However, the effect of frost on the environmental persistence of fecal bacteria is relatively unexplored, and may serve to either inactivate them, or increase their persistence further during these colder months. Elucidating the effect of frost in different environments would be a worthwhile pursuit in order to aid the future forecasting of microbial pollution.

High rainfall was discussed earlier as being a cause of adverse microbial water quality because it flushes FIOs into watercourses. A future increase in heavy precipitation events during winter may transport higher levels of FIOs to downstream sediments faster than currently observed, which may increase the general abundance in estuarine sediments. However, higher rainfall also increases the shear force exerted on surface sediments in streams, rivers and estuaries, and therefore sediments containing a high abundance of FIOs may be more regularly resuspended. This will decrease the retention time of an FIO within a watercourse, reaching the inactivating influence of seawater more rapidly. Similarly, increased wave height is likely to promote resuspension of estuarine sediments, which would facilitate the remediation of

microbial contaminants despite possible short-term adverse water quality. Lower and less frequent rainfall during summer may also serve to increase the magnitude of the 'first flush' effect seen when rainfall following a dry period transports high amounts of FIOs into watercourses.

7.3 The importance of sediment characteristics to water quality

Current water quality monitoring does not take into account faecal bacteria residing in sediments. Consequently, there are inherent weaknesses in bathing water safety advice as certain conditions may lead to high abundance of faecal bacteria in sediments that may be resuspended putting water users at an unforeseen risk. The spatial and temporal distribution of *E. coli* in intertidal sediments was investigated in Chapter 3 and variability was found to be successfully explained by sediment characteristics and environmental variables. The patterns and trends of *E. coli* variability identified at both the Ythan and Eden estuary will form a useful basis upon which future modelling approaches of the prediction of the abundance of faecal bacteria in estuarine systems can build upon. Sediment characteristics that successfully explained large proportions of the variability of *E. coli* often co-varied with other variables; this co-variation reduces the need for extensive sediment characteristic monitoring in order to form a reliable prediction of FIO loading of sediments, rather, only several key variables identified here to be salinity, organic content, sediment shear strength, bulk density and particle size distribution of sediments need to be measured in order to support and improve upon accuracy of current bathing water safety advice. Site-specific models based on these variables can be incorporated into risk management tools such as 'quantitative microbial risk assessments' and 'hazard analysis and critical control point' assessments [2] to quantify potential risk of sediments and discourage bathing where areas of possible high faecal bacteria loading have been identified.

Understanding the flux of fecal bacteria between sediments and water, and their persistence within these phases are worthwhile in order to model and predict microbial contamination. Such sub-models that concern fine-scale dynamics are a complement to models such as the Soil and Water Assessment Tool [259] that provide in-depth modelling of the fate and transport of fecal bacteria throughout a catchment. Without wider-scale models of point and diffuse contamination inputs to the catchment system, fine- scale models explaining FIO persistence in estuarine sediments are not sensitive to variation of inputs from the catchment.

Conversely, the fine-scale models are also essential to the wider functioning of the catchment-based models, highlighting the complementarity of both approaches.

The recently published model of Feng et al. [470] predicted advisory levels of FIO loading in water at a success of 70 % and 90 % at knee and waist depth of water respectively. The model utilised an assumption that a linear relationship existed between wave energy and resuspension of FIOs to predict influx of FIOs from sediments to the water column. Incorporation of a sub-model to existing models such as that of Feng et al. [470] and the bacteria module in the modified Soil and Water Assessment Tool of Cho et al. [262] to predict more accurate loading of FIOs in the sediment based on sediment characteristics as in Chapter 3 would likely further increase their accuracy to predict bathing advisory levels.

Inclusion of a further sub-model including the differential erosion of sediments would also further increase accuracy of waterborne FIO predictions. In Chapter 4 it was observed that there was no strong relationship between *E. coli* abundance and the erosion potential of the sediment, suggesting this is not a simple linear function that can be included, but instead predictions of FIO loading in different sediment types would have to be incorporated into existing sediment transport models. Specific sediment types at the highest risk of resuspending faecal bacteria through high loading and low erosion resistance were identified successfully in Chapter 4, suggesting that there is scope and a necessity to predict the resuspension of these sediments in order to accurately predict bathing water advisories as these sediments can be viewed as contributing highly to adverse water quality.

One of the aims of Chapter 4 was to compare *E. coli* abundance in sediments to that of the water column. The sampling design used was not entirely appropriate to draw definite conclusions, as corresponding water samples at sediment sites were taken when the sediments were exposed by the tide. This resulted in the sampling of water that had probably not been in contact with the nearby sediment, and any suspended particles and bacteria in the water were likely to be of a source further upstream. Alternative sampling designs to those of Chapter 4 are necessary for future investigations of the relationship between *E. coli* in the sediment, erosion potential of sediments and *E. coli* in the water column. This could be performed by isolating channels on intertidal sediment beds where sediment *E. coli* can be enumerated and erosion potential of the sediment measured before the incoming tide. Water could then be sampled from the both ends of the channel when the tide has risen and erosion can take place, enabling the enumeration of *E. coli* in the water column that had been eroded

from the site of interest. This would also allow for the measurement of *in situ* shear forces. Investigations such as this are essential to understanding how *E. coli* is resuspended from intertidal sediments, and must be performed before the contribution of specific sediments to *E. coli* in the water column can be reliably estimated.

Current predictions of bathing water quality advisories in Scotland are created using rainfall and river flow data [8]. This generated a 69 % success rate of correct, and 99 % success of correct or precautionary water quality advisories at 23 locations in 2014 [219]. It is unclear however whether this success rate will be similar in areas susceptible to contamination arising from sediment resuspension such as those within and in close proximity to estuaries. The measurement of *E. coli* abundance in sediments for such sites may be critical to achieve an acceptable success rate of water quality prediction.

Anthropogenic disturbance of sediments has been recognised to affect microbial water quality [103, 188, 471, 472]. Predictive models involving erosion potential are not relevant in this context, as mechanical or anthropogenic disturbance exerts a much larger force that is likely to suspend large amounts of sediment, however data presented in this thesis can be used to facilitate prediction of FIO loading of sediments and therefore the potential effects on downstream water quality before dredging or other major disturbance events are undertaken.

The effect of the resuspension of sediment and associated bacteria by bathers could be incorporated into predictions of water quality advisories in addition to the predicted water-borne FIO loading. A calculation that incorporates the amount of sediment a bather suspends in a given time frame and the predicted FIO loading of the underlying sediment at designated bathing waters would provide a better prediction of the levels of FIOs a bather can expect to be exposed to, rather than the existing system that does not account for resuspension of sediment-associated FIOs by the bather.

The findings presented in this thesis also have implications for the aquaculture industry. Shellfish are known to be an environmental reservoir of FIOs [473] through the bioaccumulation in their somatic tissues [474], therefore presenting a possible hazard to human health when consumed. Shellfish beds are classed according to EC regulation 854/2004 [475], where shellfish with >230 *E. coli* 100 g^{-1} must be purified or relayed resulting in an increased production cost. Recently, Clements et al. (2015) observed no correlation between the total coliform and *E. coli* abundance in mussel (*Mytilus edulis*) tissues and spatially

corresponding surface sediments [476], therefore direct measurement or prediction of *E. coli* abundance in sediments directly underlying shellfish beds may be unlikely to be of use. However, knowledge of the potential for upstream or up-tide sediments to resuspend and release FIOs into the water column which then may accumulate in shellfish tissue through filter feeding is likely to be of interest to the industry in determining and identifying the causes of bioaccumulation of FIOs in shellfish.

In addition to loss of revenue through aquaculture, adverse microbial water quality can impact local economies through a loss of tourism. Meeting the 'Excellent' standard of microbial water quality is an explicit criterion to 'Blue Flag' beach status [477]. Failure to meet this requirement will result in the loss of the 'Blue Flag' status and may discourage tourists from visiting the area if they intend on visiting the bathing water. Loss of 'Blue Flag' status is often reported in the regional and national news and receives large amounts of media attention [478-481]. Therefore monitoring of bathing water quality and understanding causes of adverse water quality is of the upmost importance to areas reliant on tourism.

7.4 Relationship between FIOs and pathogens

E. coli was used throughout this project as an FIO. There are several other organisms that are commonly used as FIOs for microbial water quality, including faecal streptococci and enterococci [482]. There are doubts concerning the suitability of *E. coli* as an indicator organism, predominantly because studies have shown *E. coli* to be able to persist and even replicate in the environment [483], however *E. coli* was recommended by USEPA for use as an indicator of faecal contamination in freshwater systems as it demonstrated the highest correlation with swimming-associated gastroenteritis [484] and is currently one of the most frequently used and understood indicator organisms as it's detection is cost and time efficient, sensitive and specific [485]. The majority of models concerning microbial fate and transport are designed around indicator organisms rather than the pathogens themselves [486], and it is also worth bearing in mind that the relationship between the abundance of different FIOs in sediments is not a perfect correlation [78, 487, 488], therefore the choice of FIO can influence the success of fate and transport models for the prediction of pathogen abundance.

Differences between the ecology of pathogenic and non-pathogenic strains of the same bacteria also exist, further complicating the effectiveness of FIO monitoring to predict actual

pathogens present and therefore assess risk to public health. The study of Anderson et al [83] highlights this issue, where the persistence of *E. coli* in freshwater microcosms was observed to be dependent on the strain ribotype. The survival of *E. coli* O157 and non-O157 strains was also found to differ between soil types with individual strains affected by different soil properties, such as particle size distribution, pH, nutrients and salinity [385]. The soil characteristics that correlated with the differential survival of pathogenic and non-pathogenic strains in the study of Ma et al [385] featured frequently in the multiple stepwise linear regression models of Chapter 3 indicating there may be discrepancies between predictions of the abundance of total *E. coli* as an FIO, and the relative abundance of pathogenic *E. coli* made using these models.

Different strains of *E. coli* have also been demonstrated to attach to different particle size classes of sediment particles [396], which suggests possible differences in the subsequent transport and survival of pathogenic and non-pathogenic strains. This variation in different *E. coli* strain adhesion was investigated in Chapter 6. The experiment was initially designed to understand the role of electrostatic charge (zeta potential) of both cells and sediment particles on the adhesion of *E. coli* to suspended sediment particles, however adhesion was observed to be dependent on strain type and sediment characteristics rather than zeta potential. This indicates further that different strains of *E. coli* may have different survival potentials as strains more likely to adhere to sediments are likely to persist longer in the environment as they benefit from the survival advantages that sediments provide. In addition, the relative distribution of pathogenic and non-pathogenic *E. coli* may differ where strains demonstrate an affinity for attachment to different particle size classes and therefore settle out of suspension in particular areas of an estuary.

Studies such as this are vital to understanding the processes leading to adverse water quality, and necessary in order to be able to create accurate models to predict bathing water advisories based on FIO abundance. Ideally, the investigation into the ecology of individual pathogenic strains of organisms would be performed as it would provide better insight to the risk of disease. However, monitoring individual species and strains would be an inefficient use of time and money, and not possible in the environment due to their low abundance and the inability to release pathogenic organisms in order to monitor their survival. Rather, by using reliable correlations made between the abundance of FIOs and particular pathogenic

organisms, the successful prediction of FIO abundance can be used more efficiently to protect public health.

7.5 The native microbial community

The optimal explanatory models of Chapter 3 left a significant proportion of unexplained variability of *E. coli* abundance. It was hypothesised in Chapter 5 that changes in the native microbial community may affect the abundance of *E. coli* in intertidal sediments. The multiplex TRFLP method used in Chapter 5 revealed changes spatial in the microbial community, but these changes appeared to co-vary with environmental gradients, rather than explain any changes in *E. coli* abundance. Several suggestions were made that would improve the taxonomic resolution of this method in order to increase the value of the information gained. These improvements may elucidate finer variations in the microbial community, and identify changes in smaller taxonomic groups such as at class or order level. It could be argued that techniques such as TRFLP are becoming obsolete to high-throughput Next Generation Sequencing (NGS) techniques. This may be the case, however due to the current significant increase in cost associated with NGS, an optimised TRFLP may still prove useful in situations such as this where large numbers of samples are required for analysis.

7.6 Final conclusions

To summarise, this thesis has demonstrated the importance of monitoring sediment characteristics in order to inform bathing water regulations and protect public health. Intertidal sediments are a significant reservoir of faecal bacteria and potentially pose a higher risk of disease than the overlying water. Sediment characteristics and environmental variables can be used to explain large proportions of the spatial and temporal variation of FIO abundance in sediments. It is therefore recommended that monitoring of FIO abundance in sediments is undertaken, and the data used to investigate relationship between contaminated sediments and adverse water quality to inform bathing water regulatory decisions. The results here indicate that future models based on these variables could successfully predict *E. coli* abundance across multiple estuarine systems, in addition to freshwater and coastal sediments. Further multi-disciplinary work is necessary in order to apply this knowledge to bathing water advisory level predictions through the modelling of FIO loading combined with erosion potential of sediments.

References

1. Shuval, H. (2003). Estimating the global burden of thalassogenic diseases: human infectious diseases caused by wastewater pollution of the marine environment. *Journal of Water and Health,* **1**, 53-64.
2. Pond, K. (2005). Water recreation and disease. Plausibility of associated infections: acute effects, sequelae and mortality. (Geneva: IWA Publishing in association with WHO).
3. Georgiou, S., and Langford, I.H. (2002). Coastal bathing water quality and human health risks: a review of legislation, policy, and epidemiology, with an assessment of current uk water quality, proposed standards, and disease burden in England and Wales. *CSERGE, Working Paper ECM 02-06, England*.
4. Fleisher, J.M., Kay, D., Wyer, M., and Godree, A.F. (1998). Estimates of the severity of illnesses associated with bathing in marine waters contaminated with domestic sewage. *International Journal of Epidemiology,* **27**, 722-726.
5. Fleisher, J.M., Fleming, L.E., Solo-Gabriele, H.M., Kish, J.K., Sinigalliano, C.D., Plano, L., Elmir, S.M., Wang, J.D., Withum, K., Shibata, T., Gidley, M.L., Abdelzaher, A., He, G., Ortega, C., Zhu, X., Wright, M., Hollenbeck, J., and Backer, L.C. (2010). The BEACHES Study: health effects and exposures from non-point source microbial contaminants in subtropical recreational marine waters. *International Journal of Epidemiology,* **39**, 1291-1298.
6. Heaney, C.D., Sams, E., Dufour, A.P., Brenner, K.P., Haugland, R.A., Chern, E., Wing, S., Marshall, S., Love, D.C., Serre, M., Noble, R., and Wade, T.J. (2012). Fecal indicators in sand, sand contact, and risk of enteric illness among beachgoers. *Epidemiology,* **23**, 95-106.
7. Directive (2006). 2006/7/EC of the European parliament and of the council of 15 February 2006 concerning the management of bathing water quality and repealing Directive 76/160/EEC. *Official Journal of the European Union,* **L 64/37**.
8. McPhail, C.D., and Stidson, R.T. (2009). Bathing water signage and predictive water quality models in Scotland. *Aquatic Ecosystem Health & Management,* **12**, 183-186.
9. Scott, T.M., Rose, J.B., Jenkins, T.M., Farrah, S.R., and Lukasik, J. (2002). Microbial source tracking: Current methodology and future directions. *Applied and Environmental Microbiology,* **68**, 5796- 5803.
10. Wright, M.E., Solo-Gabriele, H.M., Elmir, S., and Fleming, L.E. (2009). Microbial load from animal feces at a recreational beach. *Marine Pollution Bulletin,* **58**, 1649-1656.
11. Craig, D.L., Fallowfield, H.J., and Cromar, N.J. (2001). The effects of temperature and sediment characteristics on survival of *Escherichia coli* in recreational coastal water and sediment. *Environmental Health,* **1**, 43- 51.
12. You, Y., Rankin, S.C., Aceto, H.W., Benson, C.E., Toth, J.D., and Dou, Z. (2006). Survival of *Salmonella enterica* serovar Newport in manure and manure-amended soils. *Applied and Environmental Microbiology,* **72**, 5777-5783.
13. Brennan, F.P., O'Flaherty, V., Kramers, G., Grant, J., and Richards, K.G. (2010). Long-term persistence and leaching of *Escherichia coli* in temperate maritime soils. *Applied and Environmental Microbiology,* **76**, 1449-1455.

14. Andre, D.A., Weiser, H.H., and Malaney, G.W. (1967). Survival of bacterial enteric pathogens in farm pond water. *Journal of American Water Works Association,* **59**, 503-508.
15. Moore, B.C., Martinez, E., Gay, J.M., and Rice, D.H. (2003). Survival of *Salmonella enterica* in freshwater and sediments and transmission by the aquatic midge *Chironomus tentans* (Chironomidae: Diptera). *Applied and Environmental Microbiology,* **69**, 4556-4560.
16. Avery, L.M., Williams, A.P., Killham, K., and Jones, D.L. (2008). Survival of *Escherichia coli* O157:H7 in waters from lakes, rivers, puddles and animal-drinking troughs. *The Science of the Total Environment,* **389**, 378-385.
17. Rhodes, M.W., and Kator, H. (1988). Survival of *Escherichia coli* and *Salmonella* spp. in estuarine environments. *Applied and Environmental Microbiology,* **54**, 2902- 2907.
18. Won, W.D., and Ross, H. (1973). Persistence of virus and bacteria in seawater. *Journal of the Environmental Engineering Division,* **99**, 205- 211.
19. Shiaris, M.P., Rex, A.C., Pettibone, G.W., Keay, K., McManus, P., Rex, M.A., Ebersole, J., and Gallagher, E. (1987). Distribution of indicator bacteria and *Vibrio parahaemolyticus* in sewage-polluted intertidal sediments. *Applied and Environmental Microbiology,* **53**, 1756- 1761.
20. Hendricks, C.W. (1971). Increased recovery rate of Salmonellae from stream bottom sediments versus surface waters. *Applied Microbiology,* **21**, 379- 380.
21. Goyal, S.M., Gerba, C.P., and Melnick, J.L. (1977). Occurrence and distribution of bacterial indicators and pathogens in canal communities along the Texas Coast. *Applied and Environmental Microbiology,* **34**, 139-149.
22. Haller, L., Pote, J., Loizeau, J.-L., and Wildi, W. (2009). Distribution and survival of faecal indicator bacteria in the sediments of the Bay of Vidy, Lake Geneva, Switzerland. *Ecological Indicators,* **9**, 540- 547.
23. Droppo, I.G., Liss, S.N., Williams, D., Nelson, T., Jaskot, C., and Trapp, B. (2009). Dynamic existence of waterborne pathogens within river sediment compartments. Implications for water quality regulatory affairs. *Environmental Science and Technology,* **43**, 1737-1743.
24. Roper, M.M., and Marshall, K.C. (1974). Modification of the interaction between *Escherichia coli* and bacteriophage in saline sediment. *Microbial Ecology,* **1**.
25. Marshall, K.C. (1969). Orientation of clay particles sorbed on bacteria possessing different ionogenic surfaces. *Biochimica et Biophysica Acta.,* **193**.
26. King, C.M. (1975). Introduction to marine geology and geomorphology., (London: E. Arnold).
27. McLusky, D.S. (1989). The estuarine ecosystem, second edition., (Blackie. USA: Chapman & Hall, New York).
28. Davies, C.M., Long, J.A.H., Donald, M., and Ashbolt, N.J. (1995). Survival of fecal microorganisms in marine and freshwater sediments. *Applied and Environmental Microbiology,* **61**, 1888- 1896.
29. Muirhead, R.W., Collins, R.P., and Bremer, P.J. (2006). Interaction of *Escherichia coli* and soil particles in runoff. *Applied and Environmental Microbiology,* **72**, 3406- 3411.
30. Dawson, M.P., Humphrey, B., and Marshall, K.C. (1981). Adhesion: A tactic in the survival strategy of a marine *Vibrio* during starvation. *Current Microbiology,* **6**, 195-201.
31. Kjelleberg, S. (1993). Starvation in bacteria, (New York: Plenum Press).
32. Oliver, J.D. (1993). Formation of viable but nonculturable cells. In Starvation in Bacteria, S. Kjelleberg, ed. (New York: Plenum Press), pp. 239- 272.

33. Pringle, J.H., and Fletcher, M. (1986). Influence of substratum hydration and adsorbed macromolecules on bacterial attachment to surfaces. *Applied and Environmental Microbiology,* **51**, 1321- 1325.
34. Ao, J., Nishida, K., and Sakamoto, Y. (2009). Modelling sediment- associated *Escherichia coli* in a natural river: Comparison of the reversible and irreversible adsorption. *Annual Journal of Hydraulic Engineering,,* **53**, 187- 192.
35. Malmqvist, T. (1983). Bacterial hydrophobicity measured as partition of palmitic acid between the two immiscible phases of cell surface and buffer. *Acta Pathologica et Microbiologica Scandinavica. Section B,* **91**, 69- 73.
36. Fletcher, M. (1977). The effects of culture concentration and age, time, and temperature on bacterial attachment to polystyrene. *Canadian Journal of Microbiology,* **23**, 1-6.
37. O'Toole, G., Kaplan, H.B., and Kolter, R. (2000). Biofilm formation as microbial development. *Annual Review of Microbiology,* **54**, 49- 79.
38. Kuchma, S.L., and O'Toole, G. (2000). Surface-induced and biofilm-induced changes in gene expression. *Current Opinion in Biotechnology,* **11**, 429- 433.
39. Jefferson, K.K. (2004). What drives bacteria to produce a biofilm? *FEMS Microbiology Letters,* **236**, 163-173.
40. van Loosdrecht, M.C.M., Norde, W., and Zehnder, A.J.B. (1987). Influence of cell surface characteristics on bacterial adhesion to solid supports. In Proceedings of the European Congress on Biotechnology, Volume 4, O.M. Neijsel, R.R. van der Meer and K.C.A.M. Luyben, eds. (Elsevier Science Publishers, Amsterdam).
41. Wrangstadh, M., Conway, P.L., and Kjelleberg, S. (1986). The production and release of an extracellular polysaccharide during starvation of a marine *Pseudomonas* sp. and the effect thereof on adhesion. *Archives of Microbiology,* **145**, 220-227.
42. van Loosdrecht, M.C.M., Lyklema, J., Norde, W., Schraa, G., and Zehnder, A.J.B. (1987). The role of bacterial cell wall hydrophobicity in adhesion. *Applied and Environmental Microbiology,* **53**, 1893- 1897.
43. Palmer, J., Flint, S., and Brooks, J. (2007). Bacterial cell attachment, the beginning of a biofilm. *Journal of Industrial Microbiology and Biotechnology,* **34**, 577-588.
44. van Loosdrecht, M.C.M., Lyklema, J., Norde, W., Schraa, G., and Zehnder, A.J.B. (1987). Electrophoretic mobility and hydrophobicity as a measure to predict the initial steps of bacterial adhesion. *Applied and Environmental Microbiology,* **53**, 1898- 1901.
45. Rutter, P.R., and Vincent, B. (1984). Physicochemical interactions of the substratum, microorganisms, and the fluid phase. In Microbial Adhesion and Aggregation, K.C. Marshall, ed. (Berlin: Springer-Verlag AG), pp. 21-38.
46. van Loosdrecht, M.C.M., Norde, W., Lyklema, J., and Zehnder, A.B. (1990). Hydrophobic and electrostatic parameters in bacterial adhesion. *Aquatic Sciences,* **52**, 103-114.
47. Scholl, M.A., Mills, A.L., Herman, J.S., and Hornberger, G.M. (1990). The influence of mineralogy and solution chemistry on the attachment of bacteria to representative aquifer materials. *Journal of Contaminant Hydrology,* **6**, 321- 336.
48. Hunter, K.A., and Liss, P.S. (1982). Organic matter and the surface charge of suspended particles in estuarine waters *Limnology and Oceanography,* **27**, 322- 335.
49. Loder, T.C., and Liss, P.S. (1985). Control by organic coatings of the surface charge of estuarine suspended particles. *Limnology and Oceanography,* **30**, 418- 421.
50. Soni, K.A., Balasubramanian, A.K., Beskok, A., and Pillai, S.D. (2008). Zeta potential of selected bacteria in drinking water when dead, starved, or exposed to minimal and rich culture media. *Current Microbiology,* **56**, 93-97.

51. Jamieson, R., Joy, D.M., Lee, H., Kostaschuk, R., and Gordon, R. (2005). Transport and deposition of sediment-associated *Escherichia coli* in natural streams. *Water Research,* **39**, 2665-2675.
52. Donlan, R.M. (2001). Biofilm formation: A clinically relevant microbiological process. *Clinical Infectious Diseases,* **33**, 1387-1392.
53. Terada, A., Okuyama, K., Nishikawa, M., Tsuneda, S., and Hosomi, M. (2012). The effect of surface charge property on *Escherichia coli* initial adhesion and subsequent biofilm formation. *Biotechnology and Bioengineering,* **109**, 1745-1754.
54. Marshall, K.C. (1985). Mechanisms of bacterial adhesion at solid- water interfaces. In Bacterial Adhesion, D.C. Savage, Fletcher, M., ed. (New York, NY: Plenum Press), pp. 133- 161.
55. Palmateer, G., McLean, D.E., Kutas, W.L., and Meissner, S.M. (1993). Suspended particulate bacterial interaction in agricultural drains. In Particulate Matter and Aquatic Contaminants, S.S. Rao, ed. (Lewis Publishers), pp. pp. 151-156.
56. Pratt, L.A., and Kolter, R. (1998). Genetic analysis of *Escherichia coli* biofilm formation: roles of flagella, motility, chemotaxis and type I pili. *Molecular Microbiology,* **30**, 285-293.
57. Prigent-Combaret, C., Prensier, G., Le Thi, T.T., Vidal, O., Lejeune, P., and Dorel, C. (2000). Developmental pathway for biofilm formation in curli-producing Escherichia coli strains: role of flagella, curli and colanic acid. *Environmental Microbiology,* **2**, 450-464.
58. DeFlaun, M.F., Marshall, B.M., Kulle, E.P., and Levy, S.B. (1994). Tn5 insertion mutants of *Pseudomonas fluorescens* defective in adhesion to soil and seeds. *Applied and Environmental Microbiology,* **60**, 2637- 2642.
59. O'Toole, G.A., and Kolter, R. (1998). Flagellar and twitching motility are necessary for *Pseudomonas aeruginosa* biofilm development. *Molecular Microbiology,* **30**, 295-304.
60. Barnhart, M.M., and Chapman, M.R. (2006). Curli biogenesis and function. *Annual Review of Microbiology,* **60**, 131-147.
61. Olsen, A., Arnqvist, A., Hammar, M., and Normark, S. (1993). Environmental regulation of curli production in *Escherichia coli*. *Infectious Agents and Disease,* **2**, 272-274.
62. Stock, J.B., and Surette, M.G. (1996). Chemotaxis. In *Escherichia coli* and *Salmonella typhimurium*: Cellular and Molecular Biology, Volume 2, F.C. Neidhardt, R. Curtiss III, J.L. Ingraham, E.C.C. Lin, K.B. Low, B. Magasanik, M. Riley, M. Schaechter and H.E. Umbarager, eds. (Washington, DC:: American Society for Microbiology Press), pp. 1103- 1129.
63. Takahito, S., and Ilno, T. (1980). Isolation and characterization of multiflagellate mutants of *Pseudomonas aeruginosa*. *Journal of Bacteriology,* **143**, 1471- 1479.
64. Jin, F., Conrad, J.C., Gibiansky, M.L., and Wong, G.C.L. (2011). Bacteria use type-IV pili to slingshot on surfaces. *PNAS,* **108**, 12617- 12622.
65. Xicohtencatl-Cortes, J., Monteiro-Neto, V., Saldana, Z., Ledesma, M.A., Puente, J.L., and Giron, J.A. (2009). The type 4 pili of enterohemorrhagic *Escherichia coli* O157:H7 are multipurpose structures with pathogenic attributes. *Journal of Bacteriology,* **191**, 411-421.
66. Korber, D.R., Lawrence, J.R., Sutton, B., and Caldwell, D.E. (1989). Effect of laminar flow velocity on the kinetics of surface recolonization by Mot(+)and Mot(-) *Pseudomonas fluorescens*. *Microbial Ecology,* **18**, 1-19.
67. Rosenberg, M., Bayer, E.A., Declaera, J., and Rosenberg, E. (1982). Role of thin fimbriae in adherence and growth of *Acinetobacter calcoaceticus* RAG-1 on hexadecane. *Applied and Environmental Microbiology,* **44**, 929- 937.

68. Finlay, B.B., and Falkow, S. (1997). Common themes in microbial pathogenicity revisited. *Microbiology and Molecular Biology Reviews,* **61**, 136- 169.
69. Ottemann, K.M., and Miller, J.F. (1997). Roles for motility in bacterial–host interactions. *Molecular Microbiology,* **24**, 1109-1117.
70. Proft, T., and Baker, E.N. (2009). Pili in Gram-negative and Gram-positive bacteria - structure, assembly and their role in disease. *Cellular and Molecular Life Sciences,* **66**, 613-635.
71. Lasaro, M.A., Salinger, N., Zhang, J., Wang, Y., Zhong, Z., Goulian, M., and Zhu, J. (2009). F1C fimbriae play an important role in biofilm formation and intestinal colonization by the *Escherichia coli* commensal strain Nissle 1917. *Applied and Environmental Microbiology,* **75**, 246-251.
72. Austin, J.W., Sanders, G., Kay, W.W., and Collinson, S.K. (1998). Thin aggregative fimbriae enhance *Salmonella enteritidis* biofilm formation. *FEMS Microbiology Letters,* **162**, 295-301.
73. Martino, P.D., Cafferini, N., Joly, B., and Darfeuille- Michaud, A. (2003). *Klebsiella pneumoniae* type 3 pili facilitate adherence and biofilm formation on abiotic surfaces. *Research in Microbiology,* **154**, 9- 16.
74. Watnick, P.I., Fullner, K.J., and Kolter, R. (1999). A role for the mannose-sensitive hemagglutinin in biofilm formation by *Vibrio cholerae* El Tor. *Journal of Bacteriology,* **181**, 3606- 3609.
75. Timmerman, C.P., Fleer, A., Besnier, J.M., De Graaf, L., Cremers, F., and Verhoef, J. (1991). Characterization of a proteinaceous adhesin of *Staphylococcus epidermidis* which mediates attachment to polystyrene. *Infection and Immunity,* **59**, 4187- 4192.
76. Heilmann, C., Hussain, M., Peters, G., and Götz, F. (1997). Evidence for autolysin-mediated primary attachment of Staphylococcus epidermidis to a polystyrene surface. *Molecular Microbiology,* **24**, 1013-1024.
77. Gerba, C.P., and Mcleod, J.S. (1976). Effect of sediments on the survival of *Escherichia coli* in marine waters. *Applied and Environmental Microbiology,* **32**, 114- 120.
78. Perkins, T.L., Clements, K., Baas, J.H., Jago, C.F., Jones, D.L., Malham, S.K., and McDonald, J.E. (2014). Sediment composition influences spatial variation in the abundance of human pathogen indicator bacteria within an estuarine environment. *PLoS ONE,* **9**, e112951.
79. Erkenbrecher, C.W., Jr. (1981). Sediment bacterial indicators in an urban shellfishing subestuary of the lower Chesapeake Bay. *Applied and Environmental Microbiology,* **42**, 484-492.
80. Fries, J.S., Characklis, G.W., and Noble, R.T. (2008). Sediment-water exchange of *Vibrio* sp. and fecal indicator bacteria: implications for persistence and transport in the Neuse River Estuary, North Carolina, USA. *Water Research,* **42**, 941-950.
81. Halliday, E., and Gast, R.J. (2011). Bacteria in beach sands: an emerging challenge in protecting coastal water quality and bather health. *Environmental Science and Technology,* **45**, 370-379.
82. Dorner, S.M., Anderson, W.B., Slawson, R.M., Kouwen, N., and Huck, P.M. (2006). Hydrologic modeling of pathogen fate and transport. *Environmental Science and Technology,* **40**, 4746-4753.
83. Anderson, K.L., Whitlock, J.E., and Harwood, V.J. (2005). Persistence and differential survival of fecal indicator bacteria in subtropical waters and sediments. *Applied and Environmental Microbiology,* **71**, 3041-3048.
84. Van Donsel, D.J., and Geldreich, E.E. (1971). Relationships of Salmonellae to fecal coliforms in bottom sediments. *Water Research,* **5**, 1079- 1087.

85. Sherer, B.M., Miner, J.R., Moore, J.A., and Buckhouse, J.C. (1992). Indicator bacterial survival in stream sediments. *Journal of Environment Quality,* **21**, 591-595.
86. Ashbolt, N.J., Grohmann, G.S., and Kueh, C. (1993). Significance of specific bacterial pathogens in the assessment of polluted receiving waters of Sydney. *Water Science and Technology,* **27**, 449- 452.
87. Grohmann, G.S., Ashbolt, N.J., Genova, M., Logan, G., Cox, P., and Kueh, C. (1993). Detection of viruses in coastal and river water systems in Sydney, Australia. *Water Science and Technology,* **27**.
88. Burton, G.A., Gunnison, D., and Lanza, G.R. (1987). Survival of pathogenic bacteria in various freshwater sediments. *Applied and Environmental Microbiology,* **53**, 633- 638.
89. Tate, R.L. (1978). Cultural and environmental factors affecting the longevity of *Escherichia coli* in histosols. *Applied and Environmental Microbiology,* **35**, 925- 929.
90. Gerba, C.P., Wallis, C., and Melnick, J.L. (1975). The fate of wastewater bacteria and viruses in soil. . *Journal of the Irrigation and Drainage Division,* **101**, 157- 174.
91. Kinzelman, J., McLellan, S.L., Daniels, A.D., Cashin, S., Singh, A., Gradus, S., and Bagley, R. (2004). Non-point source pollution: Determination of replication versus persistence of *Escherichia coli* in surface water and sediments with correlation of levels to readily measurable environmental parameters. *Journal of Water and Health,* **2**, 103-114.
92. Pawar, D.M., Rossman, M.L., and Chen, J. (2005). Role of curli fimbriae in mediating the cells of enterohaemorrhagic *Escherichia coli* to attach to abiotic surfaces. *Journal of Applied Microbiology,* **99**, 418- 425.
93. Rozen, Y., and Belkin, S. (2001). Survival of enteric bacteria in seawater. *FEMS Microbiology Ecology,* **25**, 513- 529.
94. Howell, J.M., Coyne, M.S., and Cornelius, P.L. (1996). Effect of sediment particle size and temperature on fecal bacteria mortality rates and the fecal coliform/fecal Streptococci ratio. *Journal of Environment Quality,* **25**, 1216-1220.
95. Hendricks, C.W. (1971). Enteric bacterial metabolism of stream sediment eluates. *Canadian Journal of Microbiology,* **17**, 551-556.
96. Sutherland, I.W. (1983). Microbial exopolysaccharides - their role in microbial adhesion in aqueous systems. *Critical Reviews in Microbiology,* **10**, 173- 201.
97. Paerl, H.W., and Merkel, S.M. (1982). Differential phosphorus assimilation in attached vs. unattached microorganisms. *Archives of Microbiology,* **93**, 125- 134.
98. Hodson, R.E., Maccubin, A.E., and Pomeroy, L.R. (1981). Dissolved adenosine triphosphate utilization by free-living and attached bacterioplankton. *Marine Biology,* **64**, 43- 51.
99. Williams, A.P., Avery, L.M., Killham, K., and Jones, D.L. (2007). Persistence, dissipation, and activity of *Escherichia coli* O157:H7 within sand and seawater environments. *FEMS Microbiology Ecology,* **60**, 24-32.
100. Oliver, D.M., Clegg, C.D., Heathwaite, A.L., and Haygarth, P.M. (2007). Preferential attachment of *Escherichia coli* to different particle size fractions of an agricultural grassland soil. *Water, Air, and Soil Pollution,* **185**, 369-375.
101. Ling, T.Y., Achberger, E.C., Drapcho, C.M., and Bengston, R.L. (2002). Quantifying adsorption of an indicator bacteria in a soil–water system. *Transactions of the ASAE,* **45**, 669- 674.
102. Gerba, C.P., and Schaiberger, G.E. (1973). Biscayne Bay: bacteriological data interpretation. *Florida Scientist,* **36**, 104- 109.
103. Grimes, D.J. (1980). Bacteriological water quality effects of hydraulically dredging contaminated Upper Mississippi River bottom sediment. *Applied and Environmental Microbiology,* **39**, 782- 789.

104. Blott, S.J., and Pye, K. (2012). Particle size scales and classification of sediment types based on particle size distributions: Review and recommended procedures. *Sedimentology,* **59**, 2071-2096.
105. LaLiberte, P., and Grimes, D.J. (1982). Survival of *Escherichia coli* in Lake Bottom Sediment. *Applied and Environmental Microbiology,* **43**, 623- 628.
106. Cole, J.J., Findlay, S., and Pace, M.L. (1988). Bacterial production in fresh and saltwater ecosystems: a cross- system overview. *Marine Ecology Progress Series,* **43**, 1- 10.
107. Marshall, K.C. (1975). Clay mineralogy in relation to survival of soil bacteria. *Annual Review of Phytopathology,* **13**, 357- 373.
108. Stotzky, G., and Rem, L.T. (1967). Influenceof clay minerals on microorganisms. I. Montmorillonite and kaolinite on bacteria. *Canadian Journal of Microbiology,* **12**, 547-563.
109. England, L.S., Lee, H., and Trevors, J.T. (1993). Bacterial survival in soil: effect of clays and protozoa. *Soil Biology and Biochemistry,* **25**, 525-531.
110. Qualls, R.G., Flynn, M.P., and Johnson, J.D. (1983). The role of suspended particles in ultraviolet disinfection. *Journal of the Water Pollution Control Federation,* **55**, 1280-1285.
111. Oliver, B.G., and Cosgrove, E.G. (1975). The disinfection of sewage treatment plant effluents using ultraviolet light. *Canadian Journal of Chemical Engineering,* **53**, 170-174.
112. Winward, G.P., Avery, L.M., Stephenson, T., and Jefferson, B. (2008). Ultraviolet (UV) disinfection of grey water: particle size effects. *Environmental Technology,* **29**, 235-244.
113. Fujioka, R.S., and Yoneyama, B.S. (2002). Sunlight inactivation of human enteric viruses and fecal bacteria. *Water Science and Technology,* **46**, 291- 295.
114. Carlucci, A.F., and Pramer, D. (1960). An evaluation of factors affecting the survival of *Escherichia coli* in sea water: II. Salinity, pH, and nutrients. *Applied Microbiology,* **8**, 247-250.
115. Mezriouri, N., Baleux, B., and Troussellier, M. (1995). A microcosm study of the survival of *Escherichia coli* and *Salmonella typhimurium* in brackish water. *Water Research,* **29**, 459-465.
116. Munro, P.M., Gauthier, M.J., Breittmayer, V.A., and Bongiovanni, J. (1989). Influence of osmoregulation processes on starvation survival of *Escherichia coli* in seawater. *Applied and Environmental Microbiology,* **55**, 2017-02024.
117. Harvey, H.W. (1955). The chemistry and fertility of sea waters. *Cambridge University Press, London, England*.
118. Faust, M.A., Aotaky, A.E., and Hargadon, M.T. (1975). Effect of physical parameters on the in situ survival of *Escherichia coli* MC-6 in an estuarine environment. *Applied Microbiology,* **30**, 800- 806.
119. Anderson, I.C., Rhodes, M.W., and Kator, H.I. (1983). Seasonal variation in survival of *Escherichia coli* exposed in situ in membrane diffusion chambers containing filtered and nonfiltered estuarine water. *Applied and Environmental Microbiology,* **45**, 1877-1883.
120. Flint, K.P. (1987). The long-term survival of *Escherichia coli* in river water. *Journal of Applied Microbiology,* **63**, 261- 270.
121. Gonthier, A., Guérin-Faublée, V., Tilly, B., and Delignette-Muller, M.L. (2001). Optimal growth temperature of O157 and non-O157 *Escherichia coli* strains. *Letters in Applied Microbiology,* **33**, 352-356.

122. Crabill, C., Donald, R., Snelling, J., Foust, R., and Southam, G. (1999). The impact of sediment fecal coliform reservoirs on seasonal water quality in Oak Creek, ARIZONA. *Water Research,* **33**, 2163-2171.
123. Obiri-Danso, K., and Jones, K. (1999). Distribution and seasonality of microbial indicators and thermophilic campylobacters in two freshwater bathing sites on the River Lune in northwest England. *Journal of Applied Microbiology,* **87**, 822-832.
124. Obiri-Danso, K., and Jones, K. (2000). Intertidal sediments as resevoirs for hippurate negative campylobacters, salmonellae and faecal indicators in three EU recognised bathing waters in north west England. *Water Research,* **34**, 519-527.
125. Oliver, D.M., Clegg, C.D., Haygarth, P.M., and Heathwaite, A.L. (2005). Assessing the potential for pathogen transfer from grassland soils to surface waters. In Advances in Agronomy, Volume 85. (Academic Press), pp. 125-180.
126. Muirhead, R.W., Davies-Colley, R.J., Donnison, A.M., and Nagels, J.W. (2004). Faecal bacteria yields in artificial flood events: quantifying in-stream stores. *Water Research,* **38**, 1215-1224.
127. Guber, A.K., Shelton, D., Pachepsky, Y., Sadeghi, A.M., and Sikora, L.J. (2006). Rainfall-induced release of fecal coliforms and other manure constituents: comparison and modeling. *Applied and Environmental Microbiology,* **72**, 7531- 7539.
128. Gannon, J.J., Busse, M.K., and Schillinger, J.E. (1983). Fecal coliform disappearance in a river impoundment. *Water Research,* **17**, 1595-1601.
129. Schillinger, J.E., and Gannon, J.J. (1985). Bacterial adsorption and suspended particles in urban stormwater. *Journal of Water Pollution Control Federation.,* **57**, 384- 389.
130. Griffith, J.F., Schiff, K.C., Lyon, G.S., and Fuhrman, J.A. (2009). Microbiological water quality at non-human influenced reference beaches in Southern California during wet weather. *Marine Pollution Bulletin,* **60**, 500-508.
131. Balls, P.W., MacDonald, A., Pugh, K.B., and Edwards, A.C. (1997). Rainfall events and their influence on nutrient distributions in the Ythan Estuary (Scotland). *Estuarine, Coastal and Shelf Science,* **44**, 73- 81.
132. Marino, A., Lombardo, L., Fiorentino, C., Orlandella, B., Monticelli, L., Nostro, A., and Alonzo, V. (2005). Uptake of *Escherichia coli*, *Vibrio cholerae* non-O1 and *Enterococcus durans* by, and depuration of mussels (*Mytilus galloprovincialis*). *International Journal of Food Microbiology,* **99**, 281-286.
133. Rowse, A.J., and Fleet, G.H. (1982). Viability and release of *Salmonella charity* and *Escherichia coli* from oyster feces. *Applied and Environmental Microbiology,* **44**, 544-548.
134. Edwards, R.T., and Meyer, J.L. (1987). Bacteria as a food source for black flv larvae in a blackwater river. *Journal of the North American Benthological Society,* **6**, 241- 250.
135. Leff, L.G., McArthur, J.V., and Shimkets, L.J. (1992). Information spiraling: movement of bacteria and their genes in streams. *Microbial Ecology,* **24**, 11- 24.
136. Leff, L.G., and Janakiraman, A. (1995). Introduced bacteria in streams: The effect of macroinvertebrates on survival In Biotechnology Risk Assessment. . (College Park, Maryland: University of Maryland Biotechnology Institute), pp. 156-167.
137. Findlay, S., Meyer, J.L., and Smith, P.J. (1986). Incorporation of microbial biomass by Peltoperla sp. (Plecoptera) and Tipula sp. (Diptera). *Journal of the North American Benthological Society,* **5**, 306- 310.
138. Austin, D.H., and Baker, J.H. (1988). Fate of bacteria ingested by larvae of the freshwater mayfly, Ephemera danica. *Microbial Ecology,* **15**, 323- 332.
139. Leff, L.G., and McArthur, J.V. (1989). Microbial colonization of limnephilid caddisfly cases. *Archives of Microbiology,* **116**, 81- 84.

140. Whitman, R.L., Shively, D.A., Pawlik, H., Nevers, M.B., and Byappanahalli, M.N. (2003). Occurrence of *Escherichia coli* and *Enterococci* in *Cladophora* (Chlorophyta) in Nearshore Water and Beach Sand of Lake Michigan. *Applied and Environmental Microbiology,* **69**, 4714-4719.
141. Byappanahalli, M.N., Shively, D.A., Nevers, M.B., Sadowsky, M.J., and Whitman, R.L. (2003). Growth and survival of *Escherichia coli* and enterococci populations in the macro-alga *Cladophora* (Chlorophyta). *FEMS Microbiology Letters,* **46**, 203-211.
142. Imamura, G.J., Thompson, R.S., Boehm, A.B., and Jay, J.A. (2011). Wrack promotes the persistence of fecal indicator bacteria in marine sands and seawater. *FEMS Microbiology Letters,* **77**, 40-49.
143. Mitchell, R. (1968). Factors affecting the decline of non-marine microorgansims in seawater. *Water Research,* **2**.
144. Puri, A., and Dudley, E.G. (2010). Influence of indigenous eukaryotic microbial communities on the reduction of *Escherichia coli* O157:H7 in compost slurry. *FEMS Microbiology Letters,* **313**, 148-154.
145. McCambridge, J., and McMeekin, T.A. (1980). Relative effects of bacterial and protozoan predators on survival of *Escherichia coli* in estuarine water samples. *Applied and Environmental Microbiology,* **40**, 907-911.
146. Geesey, G.G. (1982). Microbial exopolymers: ecological and economic considerations. *ASM News,* **48**, 9-14.
147. Decho, A.W., and Moriarty, J.W. (1990). Bacterial exopolymer utilization by a harpacticoid copepod: A methodology and results. *Limnology and Oceanography,* **35**, 1039- 1049.
148. Decho, A.W. (2000). Microbial biofilms in intertidal systems: an overview. *Continental Shelf Research,* **20**, 1257- 1273.
149. Stal, L.J., and Defarge, C. (2005). Structure and dynamics of exopolymers in an intertidal diatom biofilm. *Geomicrobiology Journal,* **22**, 341- 352.
150. Paerl, H.W. (1973). Detritus in Lake Tahoe: structural modification by attached microflora. *Science,* **180**, 496-498.
151. Dade, W.B., Davis, J.D., Nichols, P.D., Nowell, A.R.M., Thistle, D., Trexler, M.B., and White, D.C. (1990). Effects of bacterial exopolymer adhesion on the entrainment of sand. *Geomicrobiology Journal,* **8**, 1- 16.
152. Dade, W.B., Self, R.L., Pellerin, N.B., Moffet, A., Jumars, P.A., and Nowell, A.R.M. (1996). The effects of bacteria on the flow behaviour of clay- seawater suspensions. *Journal of Sedimentary Research,* **66**, 39- 42.
153. Dudman, W.F. (1977). The role of surface polysaccharides in natural environments. In Surface Carbohydrates of the Prokaryotic Cell, I.W. Sutherland, ed. (London: Academic Press), pp. 357–454.
154. Otero, A., and Vincenzini, M. (2003). Extracellular polysaccharide synthesis by Nostoc strains as affected by N source and light intensity. *Journal of Biotechnology,* **102**, 143-152.
155. Donot, F., Fontana, A., Baccou, J.C., and Schorr-Galindo, S. (2012). Microbial exopolysaccharides: Main examples of synthesis, excretion, genetics and extraction. *Carbohydrate Polymers,* **87**, 951-962.
156. Underwood, G.J.C., Paterson, D.M., and Parkes, R.J. (1995). The measurement of microbial carbohydrate exopolymers from intertidal sediments. *Limnology and Oceanography,* **40**, 1243- 1253.
157. de Brouwer, J.F.C., Neu, T.R., and Stal, L.J. (2006). On the function of secretion of extracellular polymeric substances by benthic diatoms and their role in intertidal mudflats: A review of recent insights and views. In Functioning of Microphytobenthos

in Estuaries, J.C. Kromkamp, J.F.C. de Brouwer, G.F. Blanchard, R.M. Forster and V. Creach, eds. (Royal Academy of Arts and Sciences, Amsterdam), pp. 45-61.
158. Gerbersdorf, S.U., Westrich, B., and Paterson, D.M. (2009). Microbial extracellular polymeric substances (EPS) in fresh water sediments. *Microbial Ecology,* **58**, 334-349.
159. Flemming, H.C., and Wingender, J. (2001). Relevance of microbial extracellular polymeric substances (EPSs)--Part I: Structural and ecological aspects. *Water Science and Technology,* **43**, 1-8.
160. Hoagland, K.D., Rosowski, J.R., Gretz, M.R., and Roemer, S.C. (1993). Diatom extracellular polymeric substances: Function, fine structure, chemistry and physiology. *Journal of Phycology,* **29**, 537-566.
161. Underwood, G.J.C., Boulcott, M., Raines, C.A., and Waldron, K. (2004). Environmental effects on exopolymer production by marine benthic diatoms: Dynamics, changes in composition, and pathways of production. *Journal of Phycology,* **40**, 293-304.
162. Zhou, J., Mopper, K., and Passow, U. (1998). The role of surface-active carbohydrates in the formation of transparent exopolymer particles by bubble adsorption of seawater. *Limnology and Oceanography,* **43**, 1860-1871.
163. Haynes, K., Hofmann, T.A., Smith, C.J., Ball, A.S., Underwood, G.J., and Osborn, A.M. (2007). Diatom-derived carbohydrates as factors affecting bacterial community composition in estuarine sediments. *Applied and Environmental Microbiology,* **73**, 6112-6124.
164. Smith, D.C., Simon, M., Alldredge, A.L., and Azam, F. (1992). Intense hydrolytic enzyme activity on marine aggregates and implications for rapid particle dissolution. *Nature,* **359**, 139-142.
165. Tolhurst, T.J., Jesus, B., Brotas, V., and Paterson, D.M. (2003). Diatom migration and sediment armouring – an example from the Tagus Estuary, Portugal. *Hydrobiologia,* **503**, 183- 193.
166. J., T.T., Gust, G., and Paterson, D.M. (2002). The influence of an extracellular polymeric substance (EPS) on cohesive sediment stability. In Proceedings in Marine Science, Volume Volume 5, C.W. Johan and K. Cees, eds. (Elsevier), pp. 409-425.
167. Costerton, J.W., Lewandowski, Z., Caldwell, D.E., Korber, D.R., and Lappin- Scott, H.M. (1995). Microbial biofilms. *Annual Review of Microbiology,* **49**, 711- 745.
168. Underwood, G.J., and Paterson, D.M. (2003). The importance of extracellular carbohydrate production by marine epipelic diatoms. *Advances in Botanical Research,* **40**, 183- 240.
169. Makk, J., Acs, E., Marialigeti, K., and Kovacs, G. (2003). Investigations on the Danube gravel- biofilm diatom- associated bacterial communities. *Biologia (Bratisl.),* **58**, 729-742.
170. Balzer, M., Witt, N., Flemming, H.C., and Wingender, J. (2010). Faecal indicator bacteria in river biofilms. *Water Science and Technology,* **61**, 1105-1111.
171. Underwood, G.J., and Kromkamp, J. (1999). Primary production by phytoplankton and microphytobenthos in estuaries. *Advances in Ecological Research,* **29**, 93- 153.
172. Cahoon, L.B. (1999). The role of benthic microalgae in neritic ecosystems. *Oceanography and Marine Biology- an Annual Review,* **37**, 47-86.
173. Admiraal, W. (1984). The ecology of estuarine sediment- inhabiting diatoms. *Biopress,* **3**, 269- 322.
174. Grossart, H.P., Levold, F., Allgaier, M., Simon, M., and Brinkhoff, T. (2005). Marine diatom species harbour distinct bacterial communities. *Environmental Microbiology,* **7**, 860-873.
175. Schafer, H., Abbas, B., Witte, H., and Muyzer, G. (2002). Genetic diversity of 'satellite' bacteria present in cultures of marine diatoms. *FEMS Microbiology Letters,* **42**, 25- 35.

176. Chiovitti, A., Higgins, M.J., Harper, R.E., Wetherbee, R., and Bacic, A. (2003). The complex polysaccharides of the raphid diatom Pinnularia viridis (Bacillariophyceae). *Journal of Phycology,* **39**, 543- 554.
177. Bell, W.H. (1984). Bacterial Adaptation to Low-Nutrient Conditions as Studied with Algal Extracellular Products. *Microbial ecology,* **10**, 217-230.
178. Bruckner, C.G., Rehm, C., Grossart, H.P., and Kroth, P.G. (2011). Growth and release of extracellular organic compounds by benthic diatoms depend on interactions with bacteria. *Environmental Microbiology,* **13**, 1052-1063.
179. Bhaskar, P.V., Grossart, H.P., Bhosle, N.B., and Simon, M. (2005). Production of macroaggregates from dissolved exopolymeric substances (EPS) of bacterial and diatom origin. *FEMS Microbiology Letters,* **53**, 255-264.
180. Grossart, H.P., Czub, G., and Simon, M. (2006). Algae-bacteria interactions and their effects on aggregation and organic matter flux in the sea. *Environmental Microbiology,* **8**, 1074-1084.
181. Gerbersdorf, S.U., Bittner, R., Lubarsky, H., Manz, W., and Paterson, D.M. (2009). Microbial assemblages as ecosystem engineers of sediment stability. *Journal of Soils and Sediments,* **9**, 640-652.
182. Whitehouse, R. (2000). Dynamics of estuarine muds: A manual for practical applications, (Thomas Telford).
183. Postma, H. (1967). Sediment transport and sedimentation in the estuarine environment. In Estuaries, AAAS, Volume 83, G.H. Lauff, ed.
184. Mehta, A.J., and Partheniades, E. (1983). RESUSPENSION OF DEPOSITED COHESIVE SEDIMENT BEDS. Volume 2. pp. 1569-1588.
185. Jamieson, R.C., Joy, D.M., Kostaschuk, R., and Gordon, R.J. (2005). Resuspension of sediment-associated *Escherichia coli* in a natural stream. *Journal of Environment Quality,* **34**, 581- 589.
186. Pandey, P.K., Soupir, M.L., and Rehmann, C.R. (2012). A model for predicting resuspension of *Escherichia coli* from streambed sediments. *Water Research,* **46**, 115-126.
187. Cho, K.H., Pachepsky, Y.A., Kim, J.H., Guber, A.K., Shelton, D.R., and Rowland, R. (2010). Release of *Escherichia coli* from the bottom sediment in a first-order creek: Experiment and reach-specific modeling. *Journal of Hydrology,* **391**, 322-332.
188. Grimes, D.J. (1975). Release of sediment- bound fecal coliforms by dredging. *Applied Microbiology,* **29**, 109- 111.
189. Haag, I., Kern, U., and Westrich, B. (2001). Erosion investigation and sediment qualitymeasurements for a comprehensive risk assessment of contaminated aquatic sediments. *The Science of the Total Environment,* **266**, 249- 257.
190. McNeil, J., and Lick, W. (2004). Erosion rates and bulk properties of sediments from the Kalamazoo River. *Journal of Great Lakes Research,* **30**, 407-418.
191. Le Hir, P., Monbet, Y., and Orvain, F. (2007). Sediment erodability in sediment transport modelling: Can we account for biota effects? *Continental Shelf Research,* **27**, 1116-1142.
192. Paterson, D.M. (1989). Short-term changes in the erodibility of intertidal cohesive sediments related to the migratory behavior of epipelic diatoms. *Limnology and Oceanography,* **34**, 223-234.
193. de Brouwer, J.F., Wolfstein, K., Ruddy, G.K., Jones, T.E., and Stal, L.J. (2005). Biogenic stabilization of intertidal sediments: the importance of extracellular polymeric substances produced by benthic diatoms. *Microbial Ecology,* **49**, 501-512.

194. Austen, I., Andersen, T.J., and Edelvang, K. (1999). The influence of benthic diatoms andinvertebrates on the erodibility of an intertidal a mudflat, the Danish Wadden Sea. *Estuarine, Coastal and Shelf Science,* **49**, 99-111.
195. de Deckere, E.M.G.T., Tolhurst, T.J., and de Brouwer, J.F.C. (2001). Destabilization of cohesive intertidal sediments by infauna. *Estuarine, Coastal and Shelf Science,* **53**, 665-669.
196. Gerbersdorf, S.U., Jancke, T., and Westrich, B. (2007). Sediment properties for assessing the erosion risk of contaminated riverine sites. An approach to evaluate sediment properties and their covariance patterns over depth in relation to erosion resistance. First investigations in natural sediments. *Journal of Soils and Sediments,* **7**, 25-35.
197. Black, K.S., Tolhurst, T.J., Paterson, D.M., and Hagerthey, S.E. (2002). Working with natural cohesive sediments. *Journal of Hydraulic Engineering,* **128**, 2- 8.
198. Andersen, T.J., Jensen, K.T., Lund-Hansen, L., Mouritsen, K.N., and Pejrup, M. (2002). Enhanced erodibility of fine-grained marine sediments by Hydrobia ulvae. *Journal of Sea Research,* **48**, 51- 58.
199. Krone, R.B. (1978). Aggregation of suspended particles in estuaries. In Estuarine Transport Processes, P. Kjerfve and B. W., eds. (Baruch Library in Marine Science, No. 7. Columbia, South Carolina.: University of South Carolina Press), pp. 177-190.
200. van Olphen, H. (1963). An introduction to clay colloid chemistry. *Interscience Publishers, New York*.
201. Spears, B.M., Saunders, J.E., Davidson, I., and Paterson, D.M. (2008). Microalgal sediment biostabilisation along a salinity gradient in the Eden Estuary (Scotland): unravelling a paradox. *Marine and Freshwater Research,* **59**, 313- 321.
202. Flemming, H.C., Wingender, J., Moritz, R., and Mayer, C. (1999). The forces that keep biofilms together. In Biofilms in Aquatic Systems, W. Keevil, A.F. Godfree, D.M. Holt and C.S. Dow, eds. (Cambridge, UK: Royal Society of Chemistry), pp. 1–12.
203. Tolhurst, T.J., Watts, C.W., Vardy, S., Saunders, J.E., Consalvey, M.C., and Paterson, D.M. (2008). The effects of simulated rain on the erosion threshold and biogeochemical properties of intertidal sediments. *Continental Shelf Research,* **28**, 1217-1230.
204. Leach, J.H. (1971). Hydrology of the Ythan Estuary with reference to distribution of major nutrients and detritus. *Journal of the Marine Biological Association of the United Kingdom,* **51**, 137-157.
205. Stove, G.C. (1978). The hydrography, circulation and sediment movements of the Ythan Estuary. In Faculty of Science. (PhD Thesis, Aberdeen University).
206. Balls, P.W. (1994). Nutrient inputs to estuaries from nine Scottish east coast rivers; influence of estuarine processes on inputs to the North Sea. *Estuarine, Coastal and Shelf Science,* **39**, 329-352.
207. Zetsche, E., Paterson, D.M., Lumsdon, D.G., and Witte, U. (2011). Temporal variation in the sediment permeability of an intertidal sandflat. *Marine Ecology Progress Series,* **441**, 49-63.
208. SEPA (2011). Nitrates and pesticides. Impacts and pressures in the Ythan catchment. *Scottish Environment Protection Agency* **2**.
209. SNH (2005). Forvie NNR: The reserve story. (Online) http://www.snh.org.uk/pdfs/publications/nnr/ForvieNNRTheReserveStory. *Scotland's Nature Reserves, Scottish Natural Heritage.* .
210. JNCC (2001). SPA description: Ythan estuary, Sands of Forvie and Meikle loch. In (Online) http://jncc.defra.gov.uk.

211. Gillibrand, P.A., and Balls, P.W. (1998). Modelling salt intrusion and nitrate concentrations in the Ythan Estuary. *Estuarine, Coastal and Shelf Science,* **47**, 695- 706.
212. Raffaelli, D. (1992). Conservation of Scottish estuaries. *Proceedings - Royal Society of Edinburgh, Section B,* **100**, 55-76.
213. Raffaelli, D., Balls, P., Way, S., Patterson, I.J., Hohmann, S., and Corp, N. (1999). Major long-term changes in the ecology of the Ythan estuary, Aberdeenshire, Scotland; how important are physical factors? *Aquatic Conservation: Marine and Freshwater Ecosystems,* **9**, 219-236.
214. Gorman, M., and Raffaelli, D. (1993). The Ythan estuary. *Biologist,* **40**, 10-13.
215. Raffaelli, D. (2000). Interactions between macro-algal mats and invertebrates in the Ythan estuary, Aberdeenshire, Scotland. *Helgoland Marine Research,* **54**, 71-79.
216. Lyons, D.A., Arvanitidis, C., Blight, A.J., Chatzinikolaou, E., Guy-Haim, T., Kotta, J., Orav-Kotta, H., Queirós, A.M., Rilov, G., and Somerfield, P.J. (2014). Macroalgal blooms alter community structure and primary productivity in marine ecosystems. *Global change biology,* **20**, 2712-2724.
217. Raffaelli, D., Limia, J., Hull, S., and Pont, S. (1991). Interactions between the amphipod Corophium volutator and macroalgal mats on estuarine mudflats. *Journal - Marine Biological Association of the United Kingdom,* **71**, 899-908.
218. Kidwai, S., and Raffaelli, D. (2000). Food selection and growth patterns of *Crangon crangon* L. in the presence of macro-algal mats: Field experiment on the Ythan estuary (Aberdeenshire, Scotland). *Pakistan Journal of Zoology,* **32**, 201-206.
219. SEPA (2015). Scottish Bathing Water: 2014-2015. *(Online)* *http://www.sepa.org.uk/media/143136/sepa_bathing_waters_2014-15_web.pdf*.
220. SEPA (2016). Scottish Bathing Water: 2016. *(Online)* *http://www.sepa.org.uk/media/143136/sepa_bathing_waters_2016_web.pdf*.
221. Raffaelli, D. (2015). The robustness of aquatic biodiversity functioning under environmental change: The Ythan Estuary, Scotland. In Aquatic Functional Biodiversity: An Ecological and Evolutionary Perspective. pp. 273-281.
222. Speirs, D.C., and Gurney, W.S.C. (2001). Population persistence in rivers and estuaries. *Ecology,* **82**, 1219-1237.
223. Wiegand, J., Raffaelli, D., Smart, J.C.R., and White, P.C.L. (2010). Assessment of temporal trends in ecosystem health using an holistic indicator. *Journal of Environmental Management,* **91**, 1446-1455.
224. Jarvis, J., and Riley, C. (1987). Sediment transport in the mouth of the Eden estuary. *Estuarine, Coastal and Shelf Science,* **24**, 463- 481.
225. Eastwood, K. (1977). Some aspects of the sedimentology of the superficial deposits of the Eden estuary, Fife. (Geography & Geosciences, PhD Thesis, St. Andrews University.).
226. ECN (2015). The Eden (Fife) ECN site. *(Online)* *http://www.ecn.ac.uk/sites/site/rivers/eden-fife*.
227. UKMO (Accessed 2015). Leuchars climate data. In (Online) http://www.metoffice.gov.uk/public/weather/climate/gfjbwz5gy, U.M. Office, ed.
228. Council, F. (2008). Eden Estuary LNR management plan: 2008- 2013.
229. Owens, N.J.P., and Stewart, W.D.P. (1983). *Enteromorpha* and the cycling of nitrogen in a small estuary. *Estuarine Coastal and Shelf Science,* **17**, 287-296.
230. Taylor, I.S., and Paterson, D.M. (1998). Microspatial variation in carbohydrate concentrations with depth in the upper millimetres of intertidal cohesive sediments. *Estuarine, Coastal and Shelf Science,* **46**, 359-370.
231. Maynard, C., McManus, J., Crawford, R.M.M., and Paterson, D. (2011). A comparison of short-term sediment deposition between natural and transplanted saltmarsh after

saltmarsh restoration in the Eden Estuary (Scotland). *Plant Ecology & Diversity,* **4**, 103-113.
232. Allen, J.W.R. (1985). Principles of physical sedimentology, (London, UK: George, Allen and Unwin.).
233. Tolhurst, T.J., Defew, E.C., and Dye, A. (2010). Lack of correlation between surface macrofauna, meiofauna, erosion threshold and biogeochemical properties of sediments within an intertidal mudflat and mangrove forest. *Hydrobiologia,* **652**, 1-13.
234. Lubarsky, H.V. (2011). The impact of microbial extracellular polymeric substances on sediment stability. In School of Biology, Volume PhD Thesis. (University of St. Andrews).
235. Gerbersdorf, S.U., Manz, W., and Paterson, D.M. (2008). The engineering potential of natural benthic bacterial assemblages in terms of the erosion resistance of sediments. *FEMS Microbiology Ecology,* **66**, 282-294.
236. DuBois, M., Gilles, K.A., Hamilton, J.K., Rebers, P.A., and Smith, F. (1956). Colorimetric method for determination of sugars and related substances. *Analytical Chemistry,* **28**, 350-356.
237. Nielsen, S.S. (2003). Phenol-sulfuric acid method for total carbohydrates. In Food Analysis Laboratory Manual, S.S. Nielsen, ed. (Springer US), pp. 39-44.
238. Gornall, A.G., Bardawill, C.S., and David, M.M. (1949). Determination of serum proteins by means of the biuret method. *Journal of Biological Chemistry,* **177**, 751-766.
239. Olson, B.J., and Markwell, J. (2007). Assays for determination of protein concentration. *Current Protocols in Protein Science*.
240. Masuko, T., Minami, A., Iwasaki, N., Majima, T., Nishimura, S., and Lee, Y.C. (2005). Carbohydrate analysis by a phenol-sulfuric acid method in microplate format. *Analytical Biochemistry,* **339**, 69-72.
241. Raunkjaer, K., Hvitved- Jacobsen, T., and Nielsen, P. (1994). Measurement of pools of protein, carbohydrate and lipid in domestic wastewater. *Water Research,* **28**, 251-262.
242. Tolhurst, T.J., Black, K.S., Shayler, S.A., Mather, S., Black, I., Baker, K., and Paterson, D.M. (1999). Measuring the in situ erosion shear stress of intertidal sediments with the cohesive strength meter (CSM). *Estuarine, Coastal and Shelf Science,* **49**, 281- 294.
243. Vardy, S., Saunders, J.E., Tolhurst, T.J., Davies, P.A., and Paterson, D.M. (2007). Calibration of the high-pressure cohesive strength meter (CSM). *Continental Shelf Research,* **27**, 1190-1199.
244. Singh, H.V., and Thompson, A.M. (2016). Effect of antecedent soil moisture content on soil critical shear stress in agricultural watersheds. *Geoderma,* **262**, 165-173.
245. Ankley, G.T., and Schubauer-Berigan, M.K. (1994). Comparison of techniques for the isolation of sediment pore water for toxicity testing. *Archives of Environmental Contamination and Toxicology,* **27**, 507-512.
246. USEPA (2001). Methods for collection, storage and manipulation of sediments for chemical and toxicological analyses: technical manual.
247. Pachepsky, Y.A., and Shelton, D.R. (2011). *Escherichia coli* and fecal coliforms in freshwater and estuarine sediments. *Critical Reviews in Environmental Science and Technology,* **41**, 1067-1110.
248. Dale, N.G. (1974). Bacteria in intertidal sediments: factors related to their distribution. *Limnology and Oceanography,* **19**, 509- 518
249. Flemming, B.W., and Delafontaine, M.T. (2000). Mass physical properties of muddy intertidal sediments: some applications, misapplications and non-applications. *Continental Shelf Research,* **20**, 1179-1197.
250. Paterson, D.M., Tolhurst, T.J., Kelly, J.A., Honeywill, C., de Deckere, E.M.G.T., Huet, V., Shayler, S.A., Black, K.S., de Brouwer, J., and Davidson, I. (2000). Variations in sediment

properties, Skeffling mudflat, Humber Estuary, UK. *Continental Shelf Research,* **20**, 1373-1396.

251. Mayer, L.M., Rahaim, P.T., Guerin, W., Macko, S.A., Watling, L., and Anderson, F.E. (1985). Biological and granulometric controls on sedimentary organic matter of an intertidal mudflat. *Estuarine, Coastal and Shelf Science,* **20**, 491-503.
252. Venkatramanan, S., Ramkumar, T., and Anithamary, I. (2011). Distribution of grain size, clay mineralogy and organic matter of surface sediments from Tirumalairajanar Estuary, Tamilnadu, east coast of India. *Arabian Journal of Geosciences,* **6**, 1371-1380.
253. Hartke, T., Ressmann, F., Duran, R., Welsh, K., and Sternes, K. (2005). Presence of pathogenic bacteria in the surface water of the Rio Grande Basin. *http://www.meadowscenter.txstate.edu/rg/resources/Sternes__RGB_Pathogens.pdf accessed February 2016*.
254. Atwill, R., Lewis, D., Pereira, M.d.G.C., Huerta, M., Bond, R., Ogata, S.B., and Bass, P. (2007). Characterizing freshwater inflows and sediment reservoirs of fecal coliforms and *E. coli* at five estuaries in Northern California *University of California School of Veterinary Medicine and Cooperative Extension in Sonoma and Marin Counties, Davis, CA. http://cesonoma.ucanr.edu/files/27410.pdf Accessed February 2016*.
255. Garzio, A. (2009). Survival of *E. coli* delivered with manure to stream sediment. *Environmental Science and Policy Honors Thesis. University of Maryland, College Park.*
256. Niewolak, S. (1998). Total viable count and concentration of enteric bacteria in bottom sediments from the Czarna Hańcza River , Northeast Poland. *Polish Journal of Environmental Studies,* **7**, 295-306.
257. Cinotto, P.J. (2005). Occurrence of fecal-indicator bacteria and protocols for identification of fecal-contamination sources in selected reaches of the West Branch Brandywine Creek, Chester County, Pennsylvania. *U.S. Geological Survey Scientific Investigations Report 2005-5039, 91 p.*
258. Davey, M.E., and O' Toole, G.A. (2000). Microbial biofilms- from ecology to molecular genetics. *Microbiology Molecular Biology Reviews,* **64**.
259. Gassman, P.W., Reyes, M.R., Green, C.H., and Arnold, J.G. (2007). The soil and water assessment tool: historical development, applications, and future research directions. *Transactions of the ASABE,* **50**, 1211-1250.
260. Baffaut, C., and Benson, V.W. (2003). A bacteria TMDL for Shoal Creek using SWAT modeling and DNA source tracking. In Total Maximum Daily Load TMDL Environmental Regulations II. ASAE Proceedings, Albuquerque, NM.
261. Kim, J.-W., Pachepsky, Y.A., Shelton, D.R., and Coppock, C. (2010). Effect of streambed bacteria release on *E. coli* concentrations: Monitoring and modeling with the modified SWAT. *Ecological Modelling,* **221**, 1592-1604.
262. Cho, K.H., Pachepsky, Y.A., Kim, J.H., Kim, J.W., and Park, M.H. (2012). The modified SWAT model for predicting fecal coliforms in the Wachusett Reservoir Watershed, USA. *Water Research,* **46**, 4750-4760.
263. Cho, K.H., Pachepsky, Y.A., Kim, M., Pyo, J., Park, M.-H., Kim, Y.M., Kim, J.-W., and Kim, J.H. (2016). Modeling seasonal variability of fecal coliform in natural surface waters using the modified SWAT. *Journal of Hydrology,* **535**, 377-385.
264. Davies, C.M., and Bavor, H.J. (2000). The fate of stormwater-associated bacteria in constructed wetland and water pollution control pond systems. *Journal of Applied Microbiology,* **89**, 349-360.
265. Decamp, O., and Warren, A. (2000). Investigation of *Escherichia coli* removal in various designs of subsurface flow wetlands used for wastewater treatment. *Ecological Engineering,* **14**, 293-299.

266. Ferguson, C.M., Coote, B.G., Ashbolt, N.J., and Stevenson, I.M. (1996). Relationships between indicators, pathogens and water quality in an estuarine system. *Water Research,* **30**, 2045- 2054.
267. Chan, K.-Y., Wong, S.H., and Mak, C.Y. (1979). Effects of bottom sediments on the survival of Enterobacter aerogenes in seawater. *Marine Pollution Bulletin,* **10**, 205-210.
268. Sinclair, J.L., and Alexander, M. (1984). Role of resistance to starvation in bacterial survival in sewage and lake water. *Applied and Environmental Microbiology,* **48**, 410-415.
269. Gerdol, V., and Hughes, R.G. (1994). Feeding behaviour and diet of *Corophium volutator* in an estuary in southeastern England *Marine Ecology Progress Series,* **114**, 103-108.
270. McLusky, D.S. (1968). Some effects of salinity on the distribution and abundance of *Corophium Volutator* in the Ythan Estuary. *Journal - Marine Biological Association of the United Kingdom,* **48**, 443-454.
271. Neill, M. (2004). Microbiological indices for total coliform and *E. coli* bacteria in estuarine waters. *Marine Pollution Bulletin,* **49**, 752-760.
272. Darcan, C., Ozkanca, R., Idil, O., and Flint, K.P. (2009). Viable but non-culturable state (VBNC) of *Escherichia coli* related to EnvZ under the effect of pH, starvation and osmotic stress in sea water. *Polish Journal of Microbiology,* **58**, 307-317.
273. Barcina, I., Gonzalez, J.M., Iriberri, J., and Egea, L. (1990). Survival stragety of *E. coli* and *Enterococcus faecalis* in illuminated fresh and marine systems. *Journal of Applied Microbiology,* **68**.
274. Bogosian, G., Sammons, L.E., Morris, P.J., O'Neil, J.P., Heitkamp, M.A., and Weber, D.B. (1996). Death of the *Escherichia coli* K-12 strain W3110 in soil and water. *Applied and Environmental Microbiology,* **62**, 4114-4120.
275. Ramamurthy, T., Ghosh, A., Pazhani, G.P., and Shinoda, S. (2014). Current perspectives on viable but non-culturable (VBNC) pathogenic bacteria. *Frontiers in Public Health,* **2**, 103.
276. Moore, D.G. (1964). Shear strength and related properties of sediments from experimental mohole (Guadalupe site). *Journal of Geophysical Research,* **69**, 4271-4291.
277. Hamilton, E.L. (1964). Consolidation characteristics and related properties of sediments from experimental mohole (Guadalupe site). *Journal of Geophysical Research,* **69**, 4257-4269.
278. Tolhurst, T.J., Friend, P.L., Watts, C., Wakefield, R., Black, K.S., and Paterson, D.M. (2006). The effects of rain on the erosion threshold of intertidal cohesive sediments. *Aquatic Ecology,* **40**, 533-541.
279. Horman, A., Rimhanen-Finne, R., Maunula, L., von Bonsdorff, C.H., Torvela, N., Heikinheimo, A., and Hanninen, M.L. (2004). *Campylobacter* spp., *Giardia* spp., *Cryptosporidium* spp., noroviruses, and indicator organisms in surface water in southwestern Finland, 2000-2001. *Applied and Environmental Microbiology,* **70**, 87-95.
280. Duris, J.W., Reif, A.G., Krouse, D.A., and Isaacs, N.M. (2013). Factors related to occurrence and distribution of selected bacterial and protozoan pathogens in Pennsylvania streams. *Water Research,* **47**, 300-314.
281. Xu, H.S., Roberts, N., and Singleton, F.L. (1982). Survival and viability of nonculturable *Escherichia coli* and *Vibrio cholerae* in the estuarine and marine environment. *Microbial Ecology,* **8**, 313-323.
282. Anderson, F.E. (1983). The Northern muddy intertidal: seasonal factors controlling erosion and deposition — A review. *Canadian Journal of Fisheries and Aquatic Sciences,* **40**, 143-159.

283. Grabowski, R.C., Droppo, I.G., and Wharton, G. (2011). Erodibility of cohesive sediment: The importance of sediment properties. *Earth-Science Reviews,* **105**, 101-120.
284. SEPA (Accessed 2015). River Ythan 2011-2013 database. *SEPA (© Scottish Environment Protection Agency and database right (2015) All rights reserved)*.
285. SEPA (Accessed 2015). River Eden 2011-2013 database. *SEPA (© Scottish Environment Protection Agency and database right (2015) All rights reserved)*.
286. Howland, R.J.M., Tappin, A.D., Uncles, R.J., Plummer, D.H., and Bloomer, N.J. (2000). Distributions and seasonal variability of pH and alkalinity in the Tweed Estuary, UK. *The Science of The Total Environment,* **251–252**, 125-138.
287. Montague, C.L. (1986). Influence of biota on erodibility of sediments. In Estuarine Cohesive Sediment Dynamics: Proceedings of a Workshop on Cohesive Sediment Dynamics with Special Reference to Physical Processes in Estuaries, Tampa, Florida, November 12–14, 1984, A.J. Mehta, ed. (New York, NY: Springer New York), pp. 251-269.
288. Shikuma, N.J., and Hadfield, M.G. (2010). Marine biofilms on submerged surfaces are a reservoir for *Escherichia coli* and *Vibrio cholerae*. *Biofouling,* **26**, 39-46.
289. Piggot, A.M., Klaus, J.S., Johnson, S., Phillips, M.C., and Solo-Gabriele, H.M. (2012). Relationship between enterococcal levels and sediment biofilms at recreational beaches in South Florida. *Applied and Environmental Microbiology,* **78**, 5973-5982.
290. Feng, F., Goto, D., and Yan, T. (2010). Effects of autochthonous microbial community on the die-off of fecal indicators in tropical beach sand. *FEMS Microbiology Ecology,* **74**, 214-225.
291. Beversdorf, L.J., Bornstein-Forst, S.M., and McLellan, S.L. (2007). The potential for beach sand to serve as a reservoir for *Escherichia coli* and the physical influences on cell die-off. *Journal of Applied Microbiology,* **102**, 1372-1381.
292. Cui, H., Yang, K., Pagaling, E., and Yan, T. (2013). Spatial and temporal variation in enterococcal abundance and its relationship to the microbial community in Hawaii beach sand and water. *Applied and Environmental Microbiology,* **79**, 3601-3609.
293. Mehta, A.J., and Partheniades, E. (1982). Resuspension of deposited cohesive sediment beds. In Coastal Engineering Proceedings, Volume 2. pp. 1569-1588.
294. Defew, E.C., Tolhurst, T.J., and Paterson, D.M. (2002). Site-specific features influence sediment stability of intertidal flats. *Hydrology and Earth System Sciences,* **6**, 971- 982.
295. Gerbersdorf, S.U., Jancke, T., and Westrich, B. (2005). Physico-chemical and biological sediment properties determining erosion resistance of contaminated riverine sediments – Temporal and vertical pattern at the Lauffen reservoir/River Neckar, Germany. *Limnologica - Ecology and Management of Inland Waters,* **35**, 132-144.
296. Underwood, G.J., and Paterson, D.M. (1993). Seasonal changes in diatom biomass, sediment stability and biogenic stabilization in the Severn Estuary. *Journal - Marine Biological Association of the United Kingdom,* **73**, 871-887.
297. Grabowski, R.C. (2014). Measuring the shear strength of cohesive sediment in the field. *Geomorphological Techniques,* **Part 1, Sec. 3.1**.
298. Jepsen, R., Roberts, J., and Lick, W. (1997). Effects of bulk density on sediment erosion rates. *Water, Air, and Soil Pollution,* **99**, 21-31.
299. Amos, C.L., Van Wagoner, N.A., and Daborn, G.R. (1988). The influence of subaerial exposure on the bulk properties of fine-grained intertidal sediment from Minas Basin, Bay of Fundy. *Estuarine, Coastal and Shelf Science,* **27**, 1-13.
300. Dade, W.B., Nowell, A.R.M., and Jumars, P.A. (1992). Predicting erosion resistance of muds. *Marine Geology,* **105**, 285-297.

301. Panagiotopoulos, I., Voulgaris, G., and Collins, M.B. (1997). The influence of clay on the threshold of movement of fine sandy beds. *Coastal Engineering,* **32**, 19-43.
302. Avnimelech, Y., Ritvo, G., Meijer, L.E., and Kochba, M. (2001). Water content, organic carbon and dry bulk density in flooded sediments. *Aquaculture Engineering,* **25**, 25-33.
303. Gerbersdorf, S.U., Jancke, T., Westrich, B., and Paterson, D.M. (2008). Microbial stabilization of riverine sediments by extracellular polymeric substances. *Geobiology,* **6**, 57-69.
304. Aberle, J., Nikora, V., and Walters, R. (2004). Effects of bed material properties on cohesive sediment erosion. *Marine Geology,* **207**, 83-93.
305. Parchure, T.M., and Mehta, A.J. (1985). Erosion of soft cohesive sediment deposits. *Journal of Hydraulic Engineering - ASCE,* **111**, 1308-1326.
306. Spears, B.M., Saunders, J.E., Davidson, I., and Paterson, D.M. (2008). Microalgal sediment biostabilisation along a salinity gradient in the Eden Estuary, Scotland: unravelling a paradox. *Marine and Freshwater Research,* **59**, 313-321.
307. Perkins, R.G., Underwood, G.J., Brotas, V., Snow, G.C., Jesus, B., and Ribiero, L. (2001). Responses of microphytobenthos to light: primary production and carbohydrate allocation over an emersion period. *Marine Ecology Progress Series,* **223**, 101-112.
308. Bhaskar, P.V., and Bhosle, N.B. (2005). Microbial extracellular polymeric substances in marine biogeochemical processes. *Current Science,* **88**, 45-53.
309. Lee, D., Bedford, K., and Yen, C. (1994). Storm and entrainment effects on tributary sediment loads. *Journal of Hydraulic Engineering,* **120**, 81-103.
310. Yang, L., Lin, B., and Falconer, R.A. (2008). Modelling enteric bacteria level in coastal and estuarine waters. *Proceedings of the Institution of Civil Engineers Engineering and Computational Mechanics,* **161**, 179-186.
311. Piorkowski, G., Jamieson, R., Bezanson, G., Truelstrup Hansen, L., and Yost, C. (2014). Reach specificity in sediment *E. coli* population turnover and interaction with waterborne populations. *The Science of the Total Environment,* **496**, 402-413.
312. SEPA (2008). Bathing Waters (Scotland) Regulations 2008. *Scottish Environment Protection Agency*.
313. Venier, C., Figueiredo da Silva, J., McLelland, S.J., Duck, R.W., and Lanzoni, S. (2012). Experimental investigation of the impact of macroalgal mats on flow dynamics and sediment stability in shallow tidal areas. *Estuarine, Coastal and Shelf Science,* **112**, 52-60.
314. Liou, Y. (1970). Hydraulic erodibility of two pure clay systems. Volume Ph.D. Dissertation. (Colorado State University, Fort Collings), p. 148.
315. Doyle, J.D., Tunnicliff, B., Kramer, R., Kuehl, R., and Brickler, S.K. (1992). Instability of fecal coliform populations in waters and bottom sediments at recreational beaches in Arizona. *Water Research,* **26**, 979-988.
316. An, Y.J., Kampbell, D.H., and Breidenbach, G.P. (2002). *Escherichia coli* and total coliforms in water and sediments at lake marinas. *Environmental Pollution,* **120**, 771-778.
317. Quilliam, R.S., Clements, K., Duce, C., Cottrill, S.B., Malham, S.K., and Jones, D.L. (2011). Spatial variation of waterborne *Escherichia coli* - implications for routine water quality monitoring. *Journal of Water and Health,* **9**, 734-737.
318. Ghoul, M., Bernard, T., and Cormier, M. (1990). Evidence that *Escherichia coli* accumulates glycine betaine from marine sediments. *Applied and Environmental Microbiology,* **56**, 551-554.
319. Falkowski, P.G., Barber, R.T., and Smetacek, V. (1998). Biogeochemical controls and feedbacks on ocean primary production. *Science,* **281**, 200-206.

320. Falciatore, A., and Bowler, C. (2002). Revealing the molecular secrets of marine diatoms. *Annual Review of Plant Biology,* **53**, 109-130.
321. Armitage, A.R., and Fong, P. (2004). Upward cascading effects of nutrients: shifts in a benthic microalgal community and a negative herbivore response. *Oecologia,* **139**, 560-567.
322. Posey, M., Powell, C., Cahoon, L., and Lindquist, D. (1995). Top down vs. bottom up control of benthic community composition on an intertidal tideflat. *Journal of Experimental Marine Biology and Ecology,* **185**, 19-31.
323. Sardá, R., Valiela, I., and Foreman, K. (1996). Decadal shifts in a salt marsh macroinfaunal community in response to sustained long-term experimental nutrient enrichment. *Journal of Experimental Marine Biology and Ecology,* **205**, 63-81.
324. Freitag, T.E., Chang, L., and Prosser, J.I. (2006). Changes in the community structure and activity of betaproteobacterial ammonia-oxidizing sediment bacteria along a freshwater-marine gradient. *Environmental Microbiology,* **8**, 684-696.
325. Telesh, I.V., Schubert, H., and Skarlato, S.O. (2011). Revisiting Remane's concept: evidence for high plankton diversity and a protistan species maximum in the horohalinicum of the Baltic Sea. *Marine Ecology Progress Series,* **421**, 1-11.
326. Bouvier, T.C., and del Giorgio, P.A. (2002). Compositional changes in free-living bacterial communities along a salinity gradient in two temperate estuaries. *Limnology and Oceanography,* **47**, 453-470.
327. Troussellier, M., Schafer, H., Batailler, N., Bernard, L., Courties, C., Lebaron, P., Muyzer, G., Servais, P., and Vives-Rego, J. (2002). Bacterial activity and genetic richness along an estuarine gradient (Rhone River plume, France). *Aquatic Microbial Ecology,* **28**, 13-24.
328. Crump, B.C., Hopkinson, C.S., Sogin, M.L., and Hobbie, J.E. (2004). Microbial biogeography along an estuarine salinity gradient: Combined influences of bacterial growth and residence time. *Applied and Environmental Microbiology,* **70**, 1494-1505.
329. Crump, B.C., Armbrust, E.V., and Baross, J.A. (1999). Phylogenetic analysis of particle-attached and free-living bacterial communities in the Columbia River, its estuary, and the adjacent coastal ocean. *Applied and Environmental Microbiology,* **65**, 3192-3204.
330. Selje, N., and Simon, M. (2003). Composition and dynamics of particle-associated and free-living bacterial communities in the Weser estuary, Germany. *Aquatic Microbial Ecology,* **30**, 221-237.
331. Herlemann, D.P.R., Labrenz, M., Jurgens, K., Bertilsson, S., Waniek, J.J., and Andersson, A.F. (2011). Transitions in bacterial communities along the 2000 km salinity gradient of the Baltic Sea. *The ISME Journal,* **5**, 1571-1579.
332. Underwood, G., Phillips, J., and Saunders, K. (1998). Distribution of estuarine benthic diatom species along salinity and nutrient gradients. *European Journal of Phycology,* **33**, 173-183.
333. Nedwell, D.B., and Trimmer, M. (1996). Nitrogen fluxes through the upper estuary of the Great Ouse, England : the role of the bottom sediments. *Marine Ecology Progress Series,* **142**, 273- 286.
334. Ogilvie, B., Nedwell, D.B., Harrison, R.M., Robinson, A., and Sage, A. (1997). High nitrate, muddy estuaries as nitrogen sinks: The nitrogen budget of the River Colne estuary (United Kingdom). *Marine Ecology Progress Series,* **150**, 217-228.
335. Hollibaugh, J.T., Wong, P.S., and Murrell, M.C. (2000). Similarity of particle-associated and free-living bacterial communities in northern San Francisco Bay, California. *Aquatic Microbial Ecology,* **21**, 103-114.

336. Campbell, B.J., and Kirchman, D.L. (2013). Bacterial diversity, community structure and potential growth rates along an estuarine salinity gradient. *The ISME Journal,* **7**, 210-220.
337. Pinhassi, J., and Hagström, A. (2000). Seasonal succession in marine bacterioplankton. *Aquatic Microbial Ecology,* **21**, 245-256.
338. Schäfer, H., Bernard, L., Courties, C., Lebaron, P., Servais, P., Pukall, R., Stackebrandt, E., Troussellier, M., Teresa, G., Vives-Rego, J., and Muyzer, G. (2001). Microbial community dynamics in Mediterranean nutrient-enriched seawater mesocosms: changes in the genetic diversity of bacterial populations. *FEMS Microbiology Ecology,* **34**, 243-253.
339. Lebaron, P., Servais, P., Troussellier, M., Courties, C., Muyzer, G., Bernard, L., Schäfer, H., Pukall, R., Stackebrandt, E., Guindulain, T., and Vives-Rego, J. (2001). Microbial community dynamics in Mediterranean nutrient-enriched seawater mesocosms: changes in abundances, activity and composition. *FEMS Microbiology Ecology,* **34**, 255-266.
340. Ikenaga, M., Guevara, R., Dean, A.L., Pisani, C., and Boyer, J.N. (2010). Changes in community structure of sediment bacteria along the Florida coastal everglades marsh-mangrove-seagrass salinity gradient. *Microbial Ecology,* **59**, 284-295.
341. Fu-Lin, S. (2012). Spatial and vertical distribution of bacteria in the Pearl River estuary sediment. *African Journal of Biotechnology,* **11**.
342. Zheng, B., Wang, L., and Liu, L. (2014). Bacterial community structure and its regulating factors in the intertidal sediment along the Liaodong Bay of Bohai Sea, China. *Microbiological Research,* **169**, 585-592.
343. Wang, L., Liu, L., Zheng, B., Zhu, Y., and Wang, X. (2013). Analysis of the bacterial community in the two typical intertidal sediments of Bohai Bay, China by pyrosequencing. *Marine Pollution Bulletin,* **72**, 181-187.
344. Freitag, T.E., Klenke, T., Krumbein, W.E., Gerdes, G., and Prosser, J.I. (2003). Effect of anoxia and high sulphide concentrations on heterotrophic microbial communities in reduced surface sediments (Black Spots) in sandy intertidal flats of the German Wadden Sea. *FEMS Microbiology Ecology,* **44**, 291-301.
345. Cox, E.J. (1977). The distribution of tube- dwelling diatom species in the Severn estuary. *Journal - Marine Biological Association of the United Kingdom,* **57**, 19-27.
346. Admiraal, W., and Peletier, H. (1980). Distribution of diatom species on an estuarine mudflat and experimental analysis of the selective effect of stress. *Journal of Experimental Marine Biology and Ecology,* **46**, 157-175.
347. Admiraal, W., Peletier, H., and Brouwer, T. (1984). The seasonal succession patterns of diatom species on an intertidal mudflat: An experimental analysis. *Oikos,* **42**, 30-40.
348. Watermann, F., Hillebrand, H., Gerdes, G., Krumbein, W.E., and Sommer, U. (1999). Competition between benthic cyanobacteria and diatoms as influenced by different grain sizes and temperatures *Marine Ecology Progress Series,* **187**, 77-87.
349. Remane, A. (1934). Die brackwasserfauna. *Zoologischer Anzeiger,* **7**, 34-74.
350. Kinne, O. (1971). Salinity: animals- invertebrates. In Marine Ecology, Vol. 1, Environmental Factors, Part 2., O. Kinne, ed. (John Wiley and Sons, New York), pp. 821-996.
351. Khlebovich, V.V. (1969). Aspects of animal evolution related to critical salinity and internal state. *Marine Biology,* **2**, 338-345.
352. Deaton, L.E., and Greenberg, M.J. (1986). There is no horohalinicum. *Estuaries,* **9**, 20-30.

353. Telesh, I., Schubert, H., and Skarlato, S. (2013). Life in the salinity gradient: Discovering mechanisms behind a new biodiversity pattern. *Estuarine, Coastal and Shelf Science,* **135**, 317-327.
354. Feng, B.-W., Li, X.-R., Wang, J.-H., Hu, Z.-Y., Meng, H., Xiang, L.-Y., and Quan, Z.-X. (2009). Bacterial diversity of water and sediment in the Changjiang estuary and coastal area of the East China Sea. *FEMS Microbiology Ecology,* **70**, 236-248.
355. Underwood, G.J., and Provot, L. (2000). Determining the environmental preferences of four estuarine epipelic diatom taxa: growth across a range of salinity, nitrate and ammonium conditions. *European Journal of Phycology,* **35**, 173-182.
356. Barcina, I., Lebaron, P., and Vives-Rego, J. (1997). Survival of allochthonous bacteria in aquatic systems: a biological approach. *FEMS Microbiology Ecology,* **23**, 1-9.
357. Saleem, M., Fetzer, I., Harms, H., and Chatzinotas, A. (2013). Diversity of protists and bacteria determines predation performance and stability. *The ISME Journal,* **7**, 1912-1921.
358. Matz, C., and Kjelleberg, S. (2005). Off the hook- how bacteria survive protozoan grazing. *Trends in Microbiology,* **13**, 302-307.
359. Enzinger, R.M., and Cooper, R.C. (1976). Role of bacteria and protozoa in the removal of *Escherichia coli* from estuarine waters. *Applied and Environmental Microbiology,* **31**, 758-763.
360. Hibbing, M.E., Fuqua, C., Parsek, M.R., and Peterson, S.B. (2010). Bacterial competition: surviving and thriving in the microbial jungle. *Nature Reviews Microbiology,* **8**.
361. Fisher, J.C., Newton, R.J., Dila, D.K., and McLellan, S.L. (2015). Urban microbial ecology of a freshwater estuary of Lake Michigan. *Elementa (Wash D C),* **3**.
362. Vinten, A.J., Artz, R.R., Thomas, N., Potts, J.M., Avery, L., Langan, S.J., Watson, H., Cook, Y., Taylor, C., Abel, C., Reid, E., and Singh, B.K. (2011). Comparison of microbial community assays for the assessment of stream biofilm ecology. *Journal of Microbiological Methods,* **85**, 190-198.
363. Marchesi, J.R., Sato, T., Weightman, A.J., Martin, T.A., Fry, J.C., Hiom, S.J., and Wade, W.G. (1998). Design and evaluation of useful bacterium-specific PCR primers that amplify genes coding for bacterial 16S rRNA. *Applied and Environmental Microbiology,* **64**, 795-799.
364. Hauben, L., Vauterin, L., Swings, J., and Moore, E.R. (1997). Comparison of 16S ribosomal DNA sequences of all Xanthomonas species. *International Journal of Systematic Bacteriology,* **47**, 328-335.
365. Singh, B.K., Nazaries, L., Munro, S., Anderson, I.C., and Campbell, C.D. (2006). Use of multiplex terminal restriction fragment length polymorphism for rapid and simultaneous analysis of different components of the soil microbial community. *Applied and Environmental Microbiology,* **72**, 7278-7285.
366. Nübel, U., Garcia-Pichel, F., and Muyzer, G. (1997). PCR primers to amplify 16S rRNA genes from cyanobacteria. *Applied and Environmental Microbiology,* **63**, 3327-3332.
367. Bérard, A., Dorigo, U., Humbert, J.F., and Martin-Laurent, F. (2005). Microalgae community structure analysis based on 18 S rDNA amplification from DNA extracted directly from soil as a potential soil bioindicator. *Agronomie,* **25**, 1-7.
368. Culman, S.W., Bukowski, R., Gauch, H.G., Cadillo- Quiroz, H., and Buckley, D.H. (2009). T-REX: software for the processing and analysis of T-RFLP data. *BMC Bioinformatics,* **10**.
369. Shyu, C., Soule, T., Bent, S.J., Foster, J.A., and Forney, L.J. (2007). MiCA: A web-based tool for the analysis of microbial communities based on terminal-restriction fragment

length polymorphisms of 16S and 18S rRNA genes. *Journal of Microbial Ecology,* **53**, 562-570.

370. Clarke, K.R., and Gorley, R.N. (2006). PRIMER v6: User Manual/Tutorial, (Plymouth: PRIMER-E).
371. Dorigo, U., Berard, A., and Humbert, J.F. (2002). Comparison of eukaryotic phytobenthic community composition in a polluted river by partial 18S rRNA gene cloning and sequencing. *Microbial Ecology,* **44**, 372-380.
372. Nguyen, T.N.M., Berzano, M., Gualerzi, C.O., and Spurio, R. (2011). Development of molecular tools for the detection of freshwater diatoms. *Journal of Microbiological Methods,* **84**, 33-40.
373. Kwok, S., Kellogg, D.E., McKinney, N., Spasic, D., Goda, L., Levenson, C., and Sninsky, J.J. (1990). Effects of primer-template mismatches on the polymerase chain reaction: human immunodeficiency virus type 1 model studies. *Nucleic Acids Res,* **18**, 999-1005.
374. Beard, W.A., Shock, D.D., and Wilson, S.H. (2004). Influence of DNA structure on DNA polymerase beta active site function: extension of mutagenic DNA intermediates. *The Journal of Biological Chemistry,* **279**, 31921-31929.
375. Stadhouders, R., Pas, S.D., Anber, J., Voermans, J., Mes, T.H.M., and Schutten, M. (2010). The effect of primer-template mismatches on the detection and quantification of nucleic acids using the 5′ nuclease assay. *The Journal of Molecular Diagnostics : JMD,* **12**, 109-117.
376. Liu, W.T., Marsh, T.L., Cheng, H., and Forney, L.J. (1997). Characterization of microbial diversity by determining terminal restriction fragment length polymorphisms of genes encoding 16S rRNA. *Applied and Environmental Microbiology,* **63**, 4516-4522.
377. Jarman, S.N. (2006). Cleaver: software for identifying taxon specific restriction endonuclease recognition sites. *Bioinformatics,* **22**, 2160-2161.
378. Blackwood, C.B., Hudleston, D., Zak, D.R., and Buyer, J.S. (2007). Interpreting ecological diversity indices applied to terminal restriction fragment length polymorphism data: insights from simulated microbial communities. *Applied and Environmental Microbiology,* **73**, 5276-5283.
379. Blackwood, C.B., and Buyer, J.S. (2007). Evaluating the physical capture method of terminal restriction fragment length polymorphism for comparison of soil microbial communities. *Soil Biology and Biochemistry,* **39**, 590-599.
380. Gans, J., Wolinsky, M., and Dunbar, J. (2005). Computational improvements reveal great bacterial diversity and high metal toxicity in soil. *Science,* **309**, 1387-1390.
381. Bolhuis, H., Schluepmann, H., Kristalijn, J., Sulaiman, Z., and Marshall, D.J. (2014). Molecular analysis of bacterial diversity in mudflats along the salinity gradient of an acidified tropical Bornean estuary (South East Asia). *Aquatic Biosystems,* **10**.
382. Ohtomo, R., Minato, K., and Saito, M. (2004). Survival of *Escherichia coli* in a field amended with cow feces slurry. *Soil Science and Plant Nutrition,* **50**, 575-581.
383. Sjogren, R.E. (1995). Thirteen-year survival study of an environmental *Escherichia coli* in field mini-plots. *Water, Air, and Soil Pollution,* **81**, 315-335.
384. Brennan, F.P., Abram, F., Chinalia, F.A., Richards, K.G., and O'Flaherty, V. (2010). Characterization of environmentally persistent *Escherichia coli* isolates leached from an Irish soil. *Applied and Environmental Microbiology,* **76**, 2175-2180.
385. Ma, J., Ibekwe, M.A., Crowley, D.E., and Yang, C.-H. (2014). Persistence of *Escherichia coli* O157 and non-O157 strains in agricultural soils. *The Science of the Total Environment,* **490**, 822-829.
386. van Elsas, J.D., Chiurazzi, M., Mallon, C.A., Elhottovā, D., Krištůfek, V., and Salles, J.F. (2012). Microbial diversity determines the invasion of soil by a bacterial pathogen. *Proceedings of the National Academy of Sciences,* **109**, 1159-1164.

387. Vivant, A.L., Garmyn, D., Maron, P.A., Nowak, V., and Piveteau, P. (2013). Microbial diversity and structure are drivers of the biological barrier effect against Listeria monocytogenes in soil. *PLoS One,* **8**.
388. Fierer, N. (2007). Tilting at windmills: a response to a recent critique of terminal restriction fragment length polymorphism data. *Applied and Environmental Microbiology,* **73**, 8041-8042.
389. Jeng, H.C., England, A.J., and Bradford, H.B. (2005). Indicator organisms associated with stormwater suspended particles and estuarine sediment. *Journal of Environmental Science and Health. Part A, Toxic/Hazardous Substances & Environmental Engineering,* **40**, 779-791.
390. Bai, S., and Lung, W.S. (2005). Modeling sediment impact on the transport of fecal bacteria. *Water Research,* **39**, 5232-5240.
391. Geesey, G.G., and Costerton, J.W. (1979). Microbiology of a northern river: bacterial distribution and relationship to suspended sediment and organic carbon. *Canadian Journal of Microbiology,* **25**, 1058-1062.
392. Ghiglione, J.F., Mevel, G., Pujo-Pay, M., Mousseau, L., Lebaron, P., and Goutx, M. (2007). Diel and seasonal variations in abundance, activity, and community structure of particle-attached and free-living bacteria in NW Mediterranean Sea. *Microbial Ecology,* **54**, 217-231.
393. Allen, G.P., Salomon, J.C., Bassoullet, P., Du Penhoat, Y., and de Grandpré, C. (1980). Effects of tides on mixing and suspended sediment transport in macrotidal estuaries. *Sedimentary Geology,* **26**, 69-90.
394. Guber, A.K., Pachepsky, Y.A., Shelton, D.R., and Yu, O. (2007). Effect of bovine manure on fecal coliform attachment to soil and soil particles of different sizes. *Applied and Environmental Microbiology,* **73**, 3363-3370.
395. Jeng, H.A.C., Englande, A.J., Bakeer, R.M., and Bradford, H.B. (2005). Impact of urban stormwater runoff on estuarine environmental quality. *Estuarine, Coastal and Shelf Science,* **63**, 513-526.
396. Pachepsky, Y.A., Yu, O., Karns, J.S., Shelton, D.R., Guber, A.K., and van Kessel, J.S. (2008). Strain-dependent variations in attachment of *E. coli* to soil particles of different sizes. *International Agrophysics,* **22**, 61-66.
397. Walker, S.L., Redman, J.A., and Elimelech, M. (2004). Role of cell surface lipopolysaccharides in *Escherichia coli* K12 adhesion and transport. *Langmuir,* **20**, 7736- 7746.
398. Sokolov, I., Smith, D.S., Henderson, G.S., Gorby, Y.A., and Ferris, F.G. (2001). Cell surface electrochemical heterogeneity of the Fe(III)-reducing bacteria *Shewanella putrefaciens*. *Environmental Science and Technology,* **35**, 341-347.
399. van der Wal, A., Minor, M., Norde, W., Zehnder, A.J.B., and Lyklema, J. (1997). Electrokinetic potential of bacterial cells. *Langmuir,* **13**, 165-171.
400. Rijnaarts, H.H.M., Norde, W., Lyklema, J., and Zehnder, A.J.B. (1995). The isoelectric point of bacteria as an indicator for the presence of cell surface polymers that inhibit adhesion. *Colloids and Surfaces B: Biointerfaces,* **4**, 191-197.
401. Neihof, R.A., and Loeb, G.I. (1972). The surface charge of particulate matter in seawater. *Limnology and Oceanography,* **17**, 7-16.
402. Tipping, E., Woof, C., and Cooke, D. (1981). Iron oxide from a seasonally anoxic lake. *Geochimica et Cosmochimica Acta,* **45**, 1411-1419.
403. van Loosdrecht, M.C.M., Lyklema, J., Norde, W., and Zehnder, A.J.B. (1989). Bacterial adhesion: a physicochemical approach. *Microbial Ecology,* **17**, 1- 15.
404. Guber, A.K., Shelton, D.R., and Pachepsky, Y.A. (2005). Effect of manure on *Escherichia coli* attachment to soil. *Journal of Environmental Quality,* **34**, 2086-2090.

405. Sharma, M.M., Chang, Y.I., and Yen, T.F. (1985). Reversible and irreversible surface charge modification of bacteria for facilitating transport through porous media. *Colloids and Surfaces,* **16**, 193-206.
406. Dyer, K.R. (1973). Estuaries: A physical introduction, (New York and London: Wiley-Interscience).
407. Malvern (Accessed 2015). Zeta potential- An introduction in 30 minutes. *Malvern Technical Note*.
408. Malvern (Accessed 2013). Zetasizer Nano User Manual.
409. Hiemenz, P.C. (1977). Electrophoresis and other electrokinetic phenomena. In Principles of Colloid and Surface Chemistry, J.J. Lagowski, ed. (New York: Marcel Dekker), pp. 452-487.
410. Hunter, R.J. (1981). Zeta potential in colloid science, (New York: Academic Press).
411. Kaya, A., and Yukselen, Y. (2005). Zeta potential of clay minerals and quartz contaminated by heavy metals. *Canadian Geotechnical Journal,* **42**, 1280-1289.
412. Zhang, R., Liu, B., Lau, S.C., Ki, J.S., and Qian, P.Y. (2007). Particle-attached and free-living bacterial communities in a contrasting marine environment: Victoria Harbor, Hong Kong. *FEMS Microbiology Ecology,* **61**, 496-508.
413. Walker, S.L., Hill, J.E., Redman, J.A., and Elimelech, M. (2005). Influence of growth phase on adhesion kinetics of *Escherichia coli* D21g. *Applied and Environmental Microbiology,* **71**, 3093-3099.
414. Chen, G., and Walker, S.L. (2012). Fecal indicator bacteria transport and deposition in saturated and unsaturated porous media. *Environmental Science and Technology,* **46**, 8782-8790.
415. Zhao, W., Walker, S.L., Huang, Q., and Cai, P. (2014). Adhesion of bacterial pathogens to soil colloidal particles: influences of cell type, natural organic matter, and solution chemistry. *Water Research,* **53**, 35-46.
416. Feng, G., Cheng, Y., Wang, S.-Y., Hsu, L.C., Feliz, Y., Borca- Tasciuc, D.A., Worobo, R.W., and Moraru, C.I. (2014). Alumina surfaces with nanoscale topography reduce attachment and biofilm formation by *Escherichia coli* and *Listeria* spp. *Biofouling,* **30**, 1253-1268.
417. Vigeant, M.A., Ford, R.M., Wagner, M., and Tamm, L.K. (2002). Reversible and irreversible adhesion of motile *Escherichia coli* cells analyzed by total internal reflection aqueous fluorescence microscopy. *Applied and Environmental Microbiology,* **68**, 2794-2801.
418. Gordon, A.S., and Millero, F.J. (1984). Electrolyte effects on attachment of an estuarine bacterium. *Applied and Environmental Microbiology,* **47**, 495-499.
419. Baertsch, C., Paez-Rubio, T., Viau, E., and Peccia, J. (2007). Source tracking aerosols released from land-applied class B biosolids during high-wind events. *Applied and Environmental Microbiology,* **73**, 4522-4531.
420. Clermont, O., Christenson, J.K., Denamur, E., and Gordon, D.M. (2013). The Clermont *Escherichia coli* phylo-typing method revisited: improvement of specificity and detection of new phylo-groups. *Environmental Microbiology Reports,* **5**, 58-65.
421. Altschul, S.F., Gish, W., Miller, W., Myers, E.W., and Lipman, D.J. (1990). Basic local alignment search tool. *Journal of Molecular Biology,* **215**, 403-410.
422. Kauffmann, F., and Dupont, A. (1950). *Escherichia* strains from infantile epidemic gastro enteritis. *Acta Pathologica Microbiologica Scandinavica* **27**, 552-564.
423. Rowe, B., Gross, R.J., and Woodroof, D.P. (1977). Proposal to recognise seroovar 145/46 (Synonyms: 147, Shigella 13, *Shigella sofia*, and *Shigella manolovii*) as a new *Escherichia coli* 0 group, 0164. *International Journal of Systematic Bacteriology,* **27**, 15-18.

424. Watanabe, Y., Ozasa, K., Mermin, J.H., Griffin, P.M., Masuda, K., Imashuku, S., and Sawada, T. (1999). Factory outbreak of *Escherichia coli* O157:H7 infection in Japan. *Emerging Infectious Diseases,* **5**, 424-428.
425. Wirth, T., Falush, D., Lan, R., Colles, F., Mensa, P., Wieler, L.H., Karch, H., Reeves, P.R., Maiden, M.C.J., Ochman, H., and Achtman, M. (2006). Sex and virulence in *Escherichia coli*: an evolutionary perspective. *Molecular Microbiology,* **60**, 1136-1151.
426. Merritt, J.H., Kadouri, D.E., and O'Toole, G.A. (2011). Growing and analyzing static biofilms. *Current Protocols in Microbiology*, 00:B:01B.01:01B.01.01–01B.01.17.
427. O'Toole, G.A., Pratt, L.A., Watnick, P.I., Newman, D.K., Weaver, V.B., and Kolter, R. (1999). Genetic approaches to study of biofilms. *Methods in Enzymology* **310**, 91-109.
428. Wolfe, A.J., and Berg, H.C. (1989). Migration of bacteria in semisolid agar. *Proceedings of the National Academy of Sciences of the United States of America,* **86**, 6973-6977.
429. Brunauer, S., Emmett, P.H., and Teller, E. (1938). Adsorption of gases in multimolecular layers. *Journal of the American Chemical Society,* **60**, 309-319.
430. Malvern (2014). Technical note: Measuring the zeta potential of high conductivity samples using the Zetasizer Nano. In UK, M.I. Ltd, ed.
431. Goude, P.J., Avery, L.M., Williams, A.P., Abel, C., Wyness, A., Vinten, A.J., and Jones, D.L. (2016). Electrolyte and surface coating regulates the binding of an environmental *E. coli* isolate onto kaolinite and montmorillonite clays. *In Press*.
432. Godin, M., Bryan, A.K., Burg, T.P., Babcock, K., and Manalis, S.R. (2007). Measuring the mass, density, and size of particles and cells using a suspended microchannel resonator. *Applied Physics Letters* **91**, 123121.
433. Freeze, R.A., and Cherry, J.A. (1979). Groundwater, (NJ, USA: Prentice Hall).
434. Webmineral (Accessed 2015). Webmineral.com. Volume 2015.
435. Miles, A.A., Misra, S.S., and Irwin, J.O. (1938). The estimation of the bactericidal power of the blood. *The Journal of Hygiene,* **38**, 732-749.
436. Avery, L. (2016). In Prep.
437. Carlsson, S. (2012). Surface characterization of gram-negative bacteria and their vesicles. (Thesis in Chemistry, Umeå University).
438. Niba, E.T.E., Naka, Y., Nagase, M., Mori, H., and Kitakawa, M. (2007). A genome-wide approach to identify the genes involved in biofilm formation in *E. coli*. *DNA Research,* **14**, 237-246.
439. Pravdic, V. (1970). Surface charge characterization of sea sediments. *Limnology and Oceanography,* **15**, 230-233.
440. Martin, J.M., Jednacak, J., and Pravdic, V. (1971). The physico-chemical aspects of trace element behaviour in estuarine environments. *Thalassica Jugoslavica,* **7**, 619-637.
441. Dyer, K.R. (1986). Coastal and estuarine sediment dynamics, (Chichester, New York, Brisbane, Toronto, Singapore: Wiley Interscience).
442. Spears, B.M., Funnel, J., Saunders, J., and Paterson, D.M. (2007). On the boundaries: sediment stability measurements across aquatic ecosystems. In Sediment Dynamics and Pollutant Mobility in Rivers: An Interdisciplinary Approach, B. Westrich and U. Forstner, eds. (Springer, Heidelberg), pp. 68-78.
443. Mulholland, P.J., and Olsen, C.R. (1992). Marine origin of Savannah River estuary sediments: Evidence from radioactive and stable isotope tracers. *Estuarine, Coastal and Shelf Science,* **34**, 95-107.
444. Bullitt, E., and Makowski, L. (1995). Structural polymorphism of bacterial adhesion pili. *Nature,* **373**, 164-167.
445. Beloin, C., Roux, A., and Ghigo, J.M. (2008). *Escherichia coli* biofilms. *Microbial Immunology,* **322**, 249-289.

446. Donlan, R.M. (2002). Biofilms: microbial life on surfaces. *Emerging Infectious Diseases,* **8**, 881-890.
447. Prignent- Combaret, C., Prensier, G., Le Thi, T.T., Vidal, O., Lejeune, P., and Dorel, C. (2000). Developmental pathway for biofilm formation in curli- producing *Escherichia coli* strains: role of flagella, curli and colanic acid. *Environmental Microbiology,* **2**, 450-464.
448. Reisner, A., Krogfelt, K.A., Klein, B.M., Zechner, E.L., and Molin, S. (2006). In vitro biofilm formation of commensal and pathogenic *Escherichia coli* strains: Impact of environmental and genetic factors. *Journal of Bacteriology,* **188**, 3572-3581.
449. Geesey, G.G. (2001). Bacterial behaviour at surfaces. *Current Opinion in Microbiology,* **4**, 296-300.
450. Delpin, M.W., McLennan, A.M., Kolesik, P., and Goodman, A.E. (2000). Comparison of microcolony formation between *Vibrio* sp. strain S141 and a flagellum-negative mutant developing on agar and glass substrata. *Biofouling,* **15**, 183-193.
451. Harris, S.L., Elliott, D.A., Blake, M.C., Must, L.M., Messenger, M., and Orndorff, P.E. (1990). Isolation and characterization of mutants with lesions affecting pellicle formation and erythrocyte agglutination by type 1 piliated *Escherichia coli*. *Journal of Bacteriology,* **172**, 6411-6418.
452. Cookson, A.L., Cooley, W.A., and Woodward, M.J. (2002). The role of type 1 and curli fimbriae of Shiga toxin-producing *Escherichia coli* in adherence to abiotic surfaces. *International Journal of Medical Microbiology,* **292**, 195-205.
453. Moreira, C.G., Carneiro, S.M., Nataro, J.P., Trabulsi, L.R., and Elias, W.P. (2003). Role of type I fimbriae in the aggregative adhesion pattern of enteroaggregative *Escherichia coli*. *FEMS Microbiology Letters,* **226**, 79-85.
454. Orndorff, P.E., Devapali, A., Palestrant, S., Wyse, A., Everett, M.L., Bollinger, R.R., and Parker, W. (2004). Immunoglobulin-mediated agglutination of and biofilm formation by *Escherichia coli* K-12 require the type 1 pilus fiber. *Infection and Immunity,* **72**, 1929-1938.
455. Beloin, C., Valle, J., Latour-Lambert, P., Faure, P., Kzreminski, M., Balestrino, D., Haagensen, J.A., Molin, S., Prensier, G., Arbeille, B., and Ghigo, J.M. (2004). Global impact of mature biofilm lifestyle on *Escherichia coli* K-12 gene expression. *Molecular Microbiology,* **51**, 659-674.
456. Abu-Ali, G.S., Ouellette, L.M., Henderson, S.T., Whittam, T.S., and Manning, S.D. (2010). Differences in adherence and virulence gene expression between two outbreak strains of enterohaemorrhagic *Escherichia coli* O157 : H7. *Microbiology,* **156**, 408-419.
457. Smith, H. (1977). Microbial surfaces in relation to pathogenicity. *Bacteriological Reviews,* **41**, 475-500.
458. Wood, T., González Barrios, A., Herzberg, M., and Lee, J. (2006). Motility influences biofilm architecture in *Escherichia coli*. *Applied Microbiology and Biotechnology,* **72**, 361-367.
459. Harshey, R.M. (1994). Bees aren't the only ones: swarming in Gram-negative bacteria. *Molecular Microbiology,* **13**, 389-394.
460. Cao, Y., Cherr, G.N., Córdova-Kreylos, A.L., Fan, T.W.M., Green, P.G., Higashi, R.M., LaMontagne, M.G., Scow, K.M., Vines, C.A., Yuan, J., and Holden, P.A. (2006). Relationships between sediment microbial communities and pollutants in two California salt marshes. *Microbial Ecology,* **52**, 619-633.
461. Anderson, I.C., Rhodes, M., and Kator, H. (1979). Sublethal stress in *Escherichia coli*: a function of salinity. *Applied and Environmental Microbiology,* **38**, 1147-1152.

462. Abdulkarim, S.M., Fatimah, A.B., and Anderson, J.G. (2009). Effect of salt concentrations on the growth of heat- stressed and unstressed *Escherichia coli*. *Food, Agriculture and Environment,* **7**, 51-54.
463. Shellenberger, K., and Logan, B.E. (2002). Effect of molecular scale roughness of glass beads on colloidal and bacterial deposition. *Environmental Science and Technology,* **36**, 184-189.
464. Muirhead, R.W., Collins, R.P., and Bremer, P.J. (2006). The association of *E. coli* and soil particles in overland flow. *Water Science and Technology,* **54**, 153-159.
465. Auer, M.T., and Niehaus, S.L. (1993). Modeling fecal coliform bacteria—I. Field and laboratory determination of loss kinetics. *Water Research,* **27**, 693-701.
466. Rong, X., Huang, Q., He, X., Chen, H., Cai, P., and Liang, W. (2008). Interaction of *Pseudomonas putida* with kaolinite and montmorillonite: a combination study by equilibrium adsorption, ITC, SEM and FTIR. *Colloids and Surfaces. B, Biointerfaces,* **64**, 49-55.
467. Kirby, R., Henderson, P.A., and Warwick, R.M. (2004). The Severn, UK: Why is the estuary different? *Journal of Marine Science and Environment,* **C2**, 1-17.
468. Jenkins, G.J., Perry, M.C., and Prior, M.J. (2008). The climate of the United Kingdom and recent trends, (Met Office Hadley Centre, Exeter, UK).
469. Murphy, J.M., Sexton, D.M.H., Jenkins, G.J., Boorman, P.M., Booth, B.B.B., Brown, C.C., Clark, R.T., Collins, M., Harris, G.R., Kendon, E.J., Betts, R.A., Brown, S.J., Howard, T.P., Humphrey, K.A., McCarthy, M.P., McDonald, R.E., Stephens, A., Wallace, C., Warren, R., Wilby, R., and Wood, R.A. (2009). UK Climate Projections Science Report: Climate change projections, (Met Office Hadley Centre, Exeter, UK).
470. Feng, Z., Reniers, A., Haus, B.K., Solo-Gabriele, H.M., Wang, J.D., and Fleming, L.E. (2015). A predictive model for microbial counts on beaches where intertidal sand is the primary source. *Marine Pollution Bulletin,* **94**, 37-47.
471. WHO (2003). Guidelines for safe recreational water environments: coastal and fresh waters. (World Health Organization, Geneva, Switzerland).
472. Graczyk, T.K., Sunderland, D., Awantang, G.N., Mashinski, Y., Lucy, F.E., Graczyk, Z., Chomicz, L., and Breysse, P.N. (2010). Relationships among bather density, levels of human waterborne pathogens, and fecal coliform counts in marine recreational beach water. *Parasitology Research,* **106**, 1103-1108.
473. Martinez-Manzanares, E., Moriñigo, M.A., Castro, D., Balebona, M.C., Sanchez, J.M., and Borrego, J.J. (1992). Influence of the faecal pollution of marine sediments on the microbial content of shellfish. *Marine Pollution Bulletin,* **24**, 342-349.
474. Teplitski, M., Wright, A.C., and Lorca, G. (2009). Biological approaches for controlling shellfish-associated pathogens. *Current Opinion in Biotechnology,* **20**, 185-190.
475. EU (2004). Regulation (EC) No 854/2004 of the European Parliament and of the Council of 29th April 2004 laying down specific rules for the organisation of official controls on products of animal origin intended for human consumption. *Official Journal of the European Union,* **L139**, 55-205.
476. Clements, K., Quilliam, R.S., Jones, D.L., Wilson, J., and Malham, S.K. (2015). Spatial and temporal heterogeneity of bacteria across an intertidal shellfish bed: implications for regulatory monitoring of faecal indicator organisms. *The Science of the Total Environment,* **506-507**, 1-9.
477. FEE (Accessed online: December 2016). Blue flag beach criteria and explanatory notes. *Blue Flag programme, the Foundation for Environmental Education.* .
478. BBC (2013). Blue flag: Fewer beaches in Wales win status. (BBC News. 15 May 2013. http://www.bbc.co.uk/news/uk-wales-22529782).

479. BBC (2012). Filey beach Blue Flag loss blamed on heavy rainfall. (BBC News. 6 August 2012. http://www.bbc.co.uk/news/uk-england-york-north-yorkshire-19148604).
480. BBC (2012). Two Southend-on-Sea beaches lose Blue Flag status. (BBC News. 15 August 2012. http://www.bbc.co.uk/news/uk-england-essex-19273686).
481. BBC (2016). Bridlington's North Beach loses Blue Flag award. (BBC News. 19 May 2016. http://www.bbc.co.uk/news/uk-england-36332051).
482. Ashbolt, N.J., Grabow, W.O.K., and Snozzi, M. (2001). Indicators of microbial water quality. In Water Quality: Guidelines, Standards, and Health : Assessment of Risk and Risk Management for Water-related Infectious Disease, L. Fewtrell and J. Bartram, eds. (IWA publishing, World Health Organization (WHO), London).
483. Ishii, S., and Sadowsky, M.J. (2008). *Escherichia coli* in the environment: implications for water quality and human health. *Microbes and Environments,* **23**, 101-108.
484. USEPA (1986). Ambient water quality criteria for bacteria. U.S.E.P. Agency, ed. (Washington, D.C.).
485. Odonkor, S.T., and Ampofo, J.K. (2013). *Escherichia coli* as an indicator of bacteriological quality of water: an overview. *Microbiology Research,* **4**, e2.
486. Pachepsky, Y.A., Sadeghi, A.M., Bradford, S.A., Shelton, D.R., Guber, A.K., and Dao, T. (2006). Transport and fate of manure-borne pathogens: Modeling perspective. *Agricultural Water Management,* **86**, 81-92.
487. Heaney, C.D., Exum, N.G., Dufour, A.P., Brenner, K.P., Haugland, R.A., Chern, E., Schwab, K.J., Love, D.C., Serre, M.L., Noble, R., and Wade, T.J. (2014). Water quality, weather and environmental factors associated with fecal indicator organism density in beach sand at two recreational marine beaches. *The Science of the Total Environment,* **1**, 440-447.
488. Wheeler Alm, E., Burke, J., and Spain, A. (2003). Fecal indicator bacteria are abundant in wet sand at freshwater beaches. *Water Research,* **37**, 3978-3982.

Appendices

Chapters 3 and 4

Table A1 ANOVA summary table for the one- way effect of site on FIO abundance at four sediment types at the Ythan estuary. Significantly different groups obtained using Fisher's LSD test are displayed in brackets under the *p*- value.

		Mud	Mixed Mud	Mixed Sand	Sand	F- Statistic	*p* - Value
Coliforms (log_{10} CFU 100 g dry wt^{-1})	Group Mean	4.62	4.58	3.27	3.84	109.99	<0.001 (M,MM>S>MS)
	Group Standard Deviation	0.69	0.56	0.65	0.56		
	Replicates (n)	77	74	71	68		
E. coli (log_{10} CFU 100 g dry wt^{-1})	Group Mean	3.19	3.21	2.19	2.64	39.81	<0.001 (MM,M>S>MS)
	Group Standard Deviation	0.97	0.79	0.78	0.74		
	Replicates (n)	77	77	71	77		

Table A2 ANOVA summary table for the one- way effect of site on physical sediment characteristics at four sediment types at the Ythan estuary. Significantly different groups obtained using Fisher's LSD test are displayed in brackets under the *p*- value.

		Mud	Mixed Mud	Mixed Sand	Sand	F- Statistic	*p* - Value
Organic Content (%)	Group Mean	4.54	2.70	1.15	0.58	587.65	<0.001 (M>MM>MS>S)
	Group Standard Deviation	0.94	0.74	0.64	0.15		
	Replicates (n)	77	77	70	77		
Water Content (%)	Group Mean	48.99	37.01	21.30	21.30	1471.93	<0.001 (M>MM>S>MS)
	Group Standard Deviation	3.79	4.72	1.60	1.71		
	Replicates (n)	77	77	71	77		
Bulk Density ($g\ cm^3$)	Group Mean	1.72	1.99	2.07	1.96	38.17	<0.001 (MS>MM,S>M)
	Group Standard Deviation	0.22	0.26	0.21	0.19		
	Replicates (n)	77	78	71	77		
Fine Particles (% 0-63 μm)	Group Mean	68.75	52.34	16.86	1.27	1804.56	<0.001 (M>MM>MS>S)
	Group Standard Deviation	3.53	9.32	10.00	2.48		
	Replicates (n)	78	78	72	78		
Median Particle Diameter (μm)	Group Mean	45.99	65.94	258.00	343.59	3052.10	<0.001 (S>MS>MM>M)
	Group Standard Deviation	3.28	25.07	41.70	11.20		
	Replicates (n)	78	78	72	78		
Vol. Weighted Mean Particle Diameter (μm)	Group Mean	55.89	123.11	262.47	356.70	2097.13	<0.001 (S>MS>MM>M)
	Group Standard Deviation	8.80	38.04	37.87	14.99		
	Replicates (n)	78	78	72	78		

Table A3 ANOVA summary table for the one- way effect of site on biogeochemical sediment characteristics at four sediment types at the Ythan estuary. Significantly different groups obtained using Fisher's LSD test are displayed in brackets under the *p*- value. Single asterix (*) denotes analysis run with 'general ANOVA', allowing prediction of missing values. Dagger (†) denotes a square root transformation of the variable prior to analysis.

		Mud	Mixed Mud	Mixed Sand	Sand	F- Statistic	*p* - Value
Colloidal Carbohydrates† ($\mu g\ g^{-1}$)	Group Mean	262.50	289.46	123.52	139.33	65.49	<0.001 (MM,M>S>MS)
	Group Standard Deviation	111.49	214.46	78.24	82.84		
	Replicates (n)	78	78	72	78		
Colloidal Proteins† ($\mu g\ g^{-1}$)	Group Mean	383.26	330.94	158.80	161.52	105.14	<0.001 (M>MM>S,MS)
	Group Standard Deviation	185.40	151.87	115.04	113.65		
	Replicates (n)	78	78	72	78		
Organic Carbon† (% dry wt)	Group Mean	1.57	1.11	0.35	0.23	164.24	<0.001 (M>MM>MS>S)
	Group Standard Deviation	0.32	0.49	0.19	0.07		
	Replicates (n)	24	24	24	24		
Total Carbon† (% dry wt)	Group Mean	3.22	1.90	0.72	0.23	244.92	<0.001 (M>MM>MS>S)
	Group Standard Deviation	0.40	0.68	0.41	0.07		
	Replicates (n)	24	24	24	24		
Total Nitrogen† (% dry wt)	Group Mean	0.22	0.15	0.05	0.03	100.73	<0.001 (M>MM>MS>S)
	Group Standard Deviation	0.04	0.07	0.06	0.05		
	Replicates (n)	24	24	24	24		
Total Carbon/ Nitrogen Ratio	Group Mean	14.95	13.31	17.05	12.07	4.72	0.004 (MS>MM,S) (S<M,MS)
	Group Standard Deviation	1.74	1.12	8.79	3.93		
	Replicates (n)	24	24	24	24		
pH	Group Mean	7.38	7.42	7.31	7.64	30.70	<0.001 (S>MM,M,MS) (MS<MM)
	Group Standard Deviation	0.16	0.22	0.26	0.30		
	Replicates (n)	78	78	66	66		
Salinity*	Group Mean	21.85	17.72	33.00	19.17	86.35	<0.001 (MS>M>S,MM)
	Group Standard Deviation	7.27	7.78	5.16	11.50		
	Replicates (n)	78	78	78	78		

Table A4 ANOVA summary table for the one- way effect of site on erosion resistance variables at four sediment types at the Ythan estuary. Significantly different groups obtained using Fisher's LSD test are displayed in brackets under the *p*- value. Single asterix (*) denotes analysis run with 'general ANOVA', allowing prediction of missing values.

		Mud	Mixed Mud	Mixed Sand	Sand	F- Statistic	*p* - Value
Sediment Shear Strength (kPa)	Group Mean	3.55	8.38	13.12	5.00	178.48	<0.001 (MS>MM>S>M)
	Group Standard Deviation	1.36	2.27	4.55	2.36		
	Replicates (n)	78	78	72	78		
Sediment Stability* (Nm^{-2})	Group Mean	11.16	18.63	23.35	-	12.85	<0.001 (MS,MM>M)
	Group Standard Deviation	9.63	16.34	20.08	-		
	Replicates (n)	78	78	78	-		

Table A5 ANOVA summary table for the one- way effect of season on FIO abundance at four sediment types at the Ythan estuary. Significantly different groups obtained using Fisher's LSD test are displayed in brackets under the *p*- value.

		Spring	Summer	Autumn	Winter	F- Statistic	*p* - Value
Coliforms (log_{10} CFU 100 g dry wt^{-1})	Group Mean	3.70	4.27	4.73	4.00	36.49	<0.001 (A>Su>W>Sp)
	Group Standard Deviation	0.77	0.84	0.69	0.76		
	Replicates (n)	70	65	42	113		
E. coli (log_{10} CFU 100 g dry wt^{-1})	Group Mean	1.96	2.96	3.51	2.98	60.45	<0.001 (A>Su,W>Sp)
	Group Standard Deviation	0.49	1.15	0.65	0.67		
	Replicates (n)	71	70	48	113		

Table A6 ANOVA summary table for the one- way effect of season on physical sediment characteristics at four sediment types at the Ythan estuary. Significantly different groups obtained using Fisher's LSD test are displayed in brackets under the *p*- value.

		Spring	Summer	Autumn	Winter	F- Statistic	*p* - Value
Organic Content (%)	Group Mean	2.35	1.94	2.73	2.22	15.08	<0.001 (A>Sp>W,Su)
	Group Standard Deviation	1.64	1.29	2.15	1.70		
	Replicates (n)	71	69	48	113		
Water Content (%)	Group Mean	31.58	31.24	35.06	32.42	17.70	<0.001 (A>W,Sp,Su)
	Group Standard Deviation	11.43	11.59	14.96	11.52		
	Replicates (n)	72	69	48	113		
Bulk Density ($g\ cm^3$)	Group Mean	2.03	1.87	1.87	1.94	8.36	<0.001 (Sp>W>A,Su)
	Group Standard Deviation	0.20	0.22	0.26	0.29		
	Replicates (n)	72	70	48	113		
Fine Particles (% 0-63 µm)	Group Mean	36.01	37.76	37.71	31.90	22.74	<0.001 (Su,A,Sp>W)
	Group Standard Deviation	28.49	26.42	29.43	28.22		
	Replicates (n)	72	72	48	114		
Median Particle Diameter (µm)	Group Mean	178.49	166.23	173.71	183.76	13.76	<0.001 (W>Sp,A,Su) (Su<Sp,W)
	Group Standard Deviation	131.98	123.49	132.80	131.62		
	Replicates (n)	72	72	48	114		
Vol. Weighted Mean Particle Diameter (µm)	Group Mean	196.86	187.14	191.54	209.13	16.52	<0.001 (W>Sp,A,Su) (Su<Sp,W)
	Group Standard Deviation	123.50	116.12	124.62	123.32		
	Replicates (n)	72	72	48	114		

Table A7 ANOVA summary table for the one- way effect of season on biogeochemical sediment characteristics at four sediment types at the Ythan estuary. Significantly different groups obtained using Fisher's LSD test are displayed in brackets under the *p*- value. Single asterix (*) denotes analysis run with 'general ANOVA', allowing prediction of missing values. Dagger (†) denotes a square root transformation of the variable prior to analysis.

		Spring	Summer	Autumn	Winter	F- Statistic	*p* - Value
Colloidal Carbohydrates† ($\mu g\ g^{-1}$)	Group Mean	263.68	251.54	231.91	127.94	46.52	<0.001 (Sp,Su>W) (W<Sp,Su,A)
	Group Standard Deviation	112.51	197.21	194.41	69.03		
	Replicates (n)	72	72	48	114		
Colloidal Proteins† ($\mu g\ g^{-1}$)	Group Mean	340.10	319.54	251.96	176.77	48.56	<0.001 (Sp,Su>A>W)
	Group Standard Deviation	237.53	160.55	161.18	87.30		
	Replicates (n)	72	72	48	114		
Organic Carbon† (% dry wt)	Group Mean	0.76	0.92	0.90	0.70	5.79	0.001 (Su>W)
	Group Standard Deviation	0.53	0.66	0.82	0.56		
	Replicates (n)	12	36	12	36		
Total Carbon† (% dry wt)	Group Mean	1.48	1.64	1.60	1.37	4.11	0.009 (Su>W)
	Group Standard Deviation	1.16	1.23	1.57	1.20		
	Replicates (n)	12	36	12	36		
Total Nitrogen† (% dry wt)	Group Mean	0.11	0.13	0.11	0.09	5.20	0.002 (Su>W)
	Group Standard Deviation	0.09	0.10	0.11	0.08		
	Replicates (n)	12	36	12	36		
Total Carbon/ Nitrogen Ratio	Group Mean	15.57	13.34	16.81	14.12	1.83	0.147
	Group Standard Deviation	5.24	3.68	9.48	4.37		
	Replicates (n)	12	36	12	36		
pH	Group Mean	7.22	7.41	7.43	7.58	44.79	<0.001 (W>A,Su>Sp)
	Group Standard Deviation	0.21	0.21	0.36	0.20		
	Replicates (n)	71	67	36	114		
Salinity*	Group Mean	30.12	22.87	22.96	17.37	53.42	<0.001 (Sp>A,Su>W)
	Group Standard Deviation	4.81	12.21	5.84	8.88		
	Replicates (n)	67	63	36	114		

Table A8 ANOVA summary table for the one- way effect of season on environmental variables at four sediment types at the Ythan estuary. Significantly different groups obtained using Fisher's LSD test are displayed in brackets under the *p*- value. Double asterix (**) denotes analysis run on mean values for each site at each sampling event rather than all replicates.

		Spring	Summer	Autumn	Winter	F- Statistic	*p* - Value
Min. Grass Temp.** (°C)	Group Mean	8.38	8.98	5.35	2.62	8.48	<0.001 (Su,Sp>W)
	Group Standard Deviation	3.22	2.86	4.63	4.56		
	Replicates (n)	12	12	8	20		
Min. Air Temp.** (°C)	Group Mean	9.23	10.65	7.35	4.96	9.55	<0.001 (Su>A,W) (W<Sp)
	Group Standard Deviation	2.44	2.06	4.05	3.55		
	Replicates (n)	12	12	8	20		
Max. Air Temp.** (°C)	Group Mean	14.48	16.38	11.64	8.95	27.58	<0.001 (Su,Sp>A>W)
	Group Standard Deviation	1.84	3.16	2.16	2.22		
	Replicates (n)	12	12	8	20		
Precip. 1 Day** (mm)	Group Mean	1.83	2.22	2.75	2.40	0.20	0.897
	Group Standard Deviation	1.79	2.68	3.25	3.05		
	Replicates (n)	12	12	8	20		
Precip. 2 Day** (mm)	Group Mean	2.62	5.55	6.65	5.99	0.91	0.445
	Group Standard Deviation	2.19	6.39	8.45	7.06		
	Replicates (n)	12	12	8	20		
Precip. 5 Day** (mm)	Group Mean	8.03	10.75	19.38	12.91	2.42	0.078
	Group Standard Deviation	4.29	8.65	12.45	10.87		
	Replicates (n)	12	12	8	20		
Sea Temp.** (°C)	Group Mean	11.10	14.54	11.56	8.13	55.04	<0.001 (Su>A,Sp>W)
	Group Standard Deviation	2.00	1.50	0.80	0.90		
	Replicates (n)	12	12	8	20		

Table A9 ANOVA summary table for the one- way effect of season on erosion resistance variables at four sediment types at the Ythan estuary. Significantly different groups obtained using Fisher's LSD test are displayed in brackets under the *p*- value. Single asterix (*) denotes analysis run with 'general ANOVA', allowing prediction of missing values.

		Spring	Summer	Autumn	Winter	F- Statistic	*p* - Value
Sediment Shear Strength (kPa)	Group Mean	8.63	7.14	8.43	6.36	10.19	<0.001 (Sp,A>Su,W)
	Group Standard Deviation	6.01	3.45	4.59	3.98		
	Replicates (n)	72	72	48	114		
Sediment Stability* (Nm^{-2})	Group Mean	21.63	19.82	12.15	15.39	3.24	0.024 (Sp>W,A)
	Group Standard Deviation	14.41	12.12	12.99	19.38		
	Replicates (n)	49	24	34	64		

Table A10 ANOVA summary table for the two- way effect of site x season on all variables at four sediment types at the Ythan estuary. Single asterix (*) denotes analysis run with 'general ANOVA', allowing prediction of missing values.

	Residual d.f.	F- Statistic (Interaction)	*p* - Value
Coliforms* (log_{10} CFU 100 g dry wt^{-1})	274	4.96	<0.001
E. coli* (log_{10} CFU 100 g dry wt^{-1})	286	3.96	<0.001
Organic Content* (%)	285	12.82	<0.001
Water Content* (%)	286	8.56	<0.001
Bulk Density* ($g\ cm^3$)	287	4.37	<0.001
Fine Particles* (% 0-63 µm)	290	7.14	<0.001
Median Particle Diameter* (µm)	290	7.57	<0.001
Vol. Weighted Mean Particle Diameter* (µm)	290	5.89	<0.001
Colloidal Carbohydrates*† ($\mu g\ g^{-1}$)	290	8.90	<0.001
Colloidal Proteins*† ($\mu g\ g^{-1}$)	290	8.34	<.001
Organic Carbon† (% dry wt)	80	2.28	0.025
Total Carbon† (% dry wt)	80	2.39	0.019
Total Nitrogen† (% dry wt)	80	1.72	0.097
Total Carbon/ Nitrogen Ratio	80	1.63	0.121
pH*	272	22.37	<0.001
Salinity*	264	7.30	<0.001
Sediment Shear Strength* (kPa)	290	7.32	<0.001
Sediment Stability* (Nm^{-2})	160	15.79	<0.001

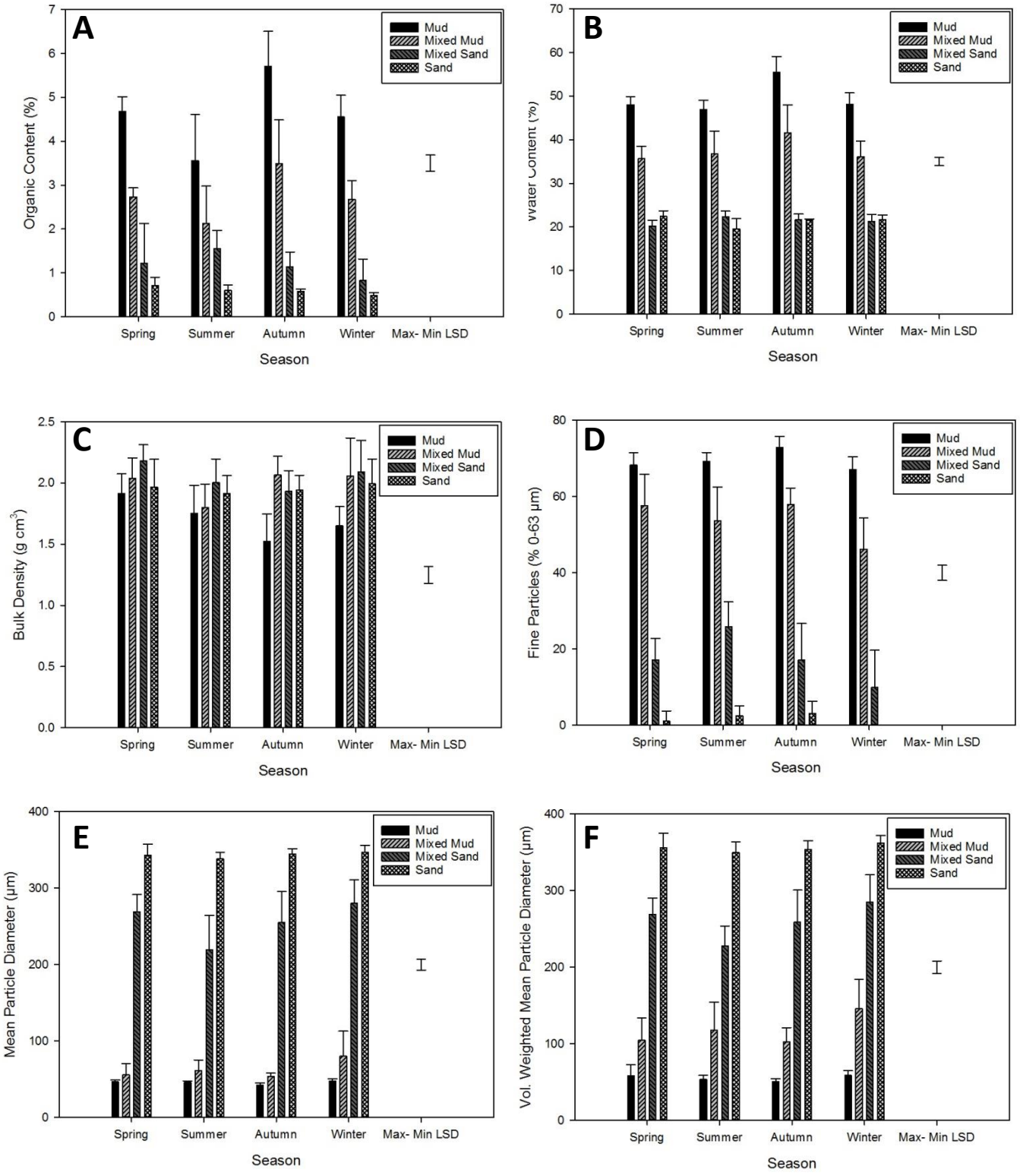

Figure A1 Mean values of organic content (A), water content (B), bulk density (C), fine particle proportion (D), median particle diameter (E) and volume weighted mean particle diameter (F) at four intertidal sediments during each season. Solid fill bars- Mud; light- grey dashed bars- Mixed Mud; dark- grey dashed bars- Mixed Sand; hatched bars- Sand. Error bars indicate standard error from the mean. Floating bar represents maximum – minimum least significant differences (LSD) (due to unequal number of samples within treatments) at p= 0.05 level. Difference between treatment means larger than the LSD bar generally indicates a significant difference.

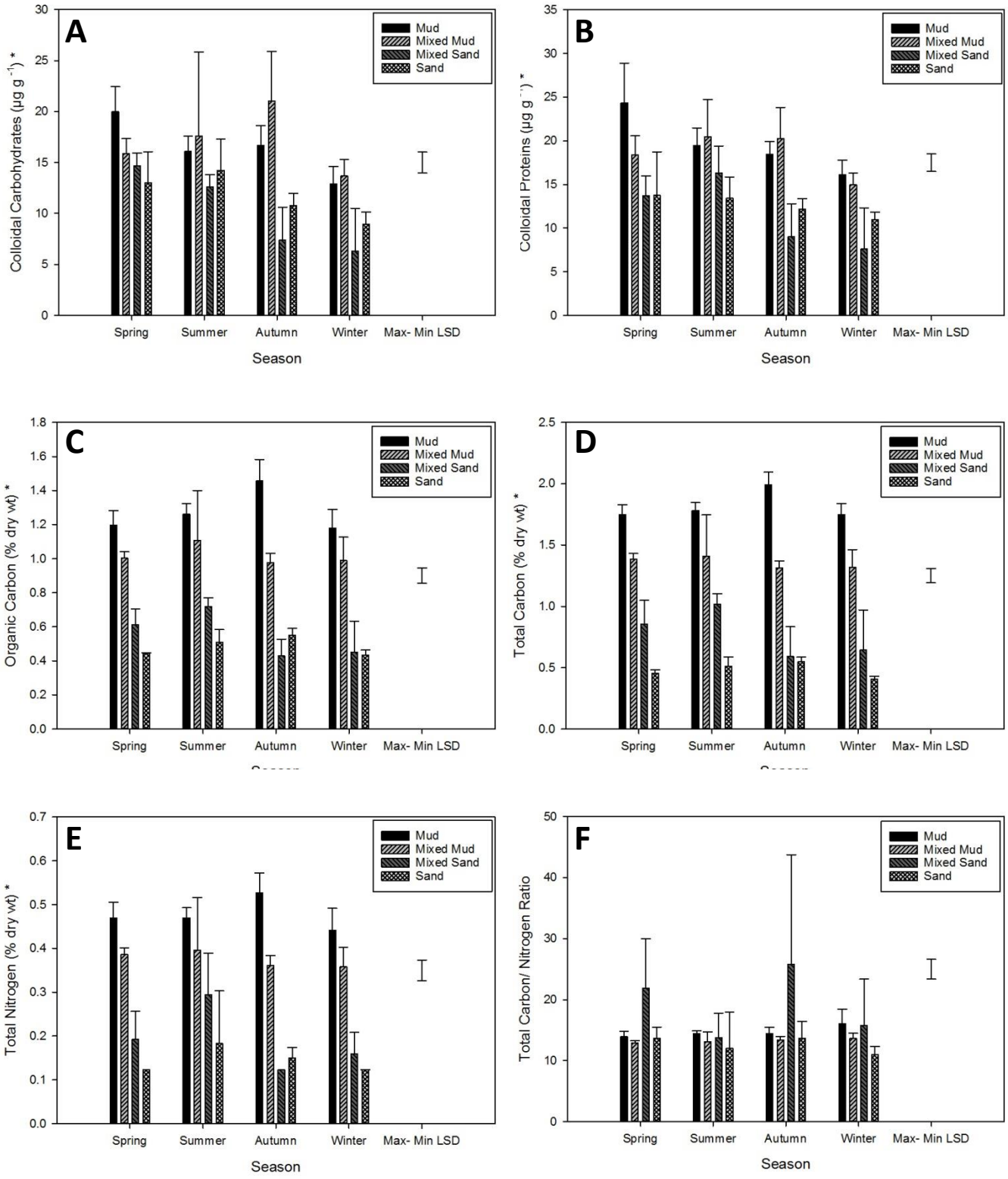

Figure A2 Mean values of colloidal carbohydrates (A), colloidal proteins (B), organic carbon (C), total carbon (D), total nitrogen (E) and the total carbon/total nitrogen ratio (F) at four intertidal sediments during each season. Solid fill bars- Mud; light- grey dashed bars- Mixed Mud; dark- grey dashed bars- Mixed Sand; hatched bars- Sand. Error bars indicate standard error from the mean. Floating bar represents maximum – minimum least significant differences (LSD) (due to unequal number of samples within treatments) at p= 0.05 level. Difference between treatment means larger than the LSD bar generally indicates a significant difference. Asterix (*) denotes a square root transformation of the variable prior to analysis.

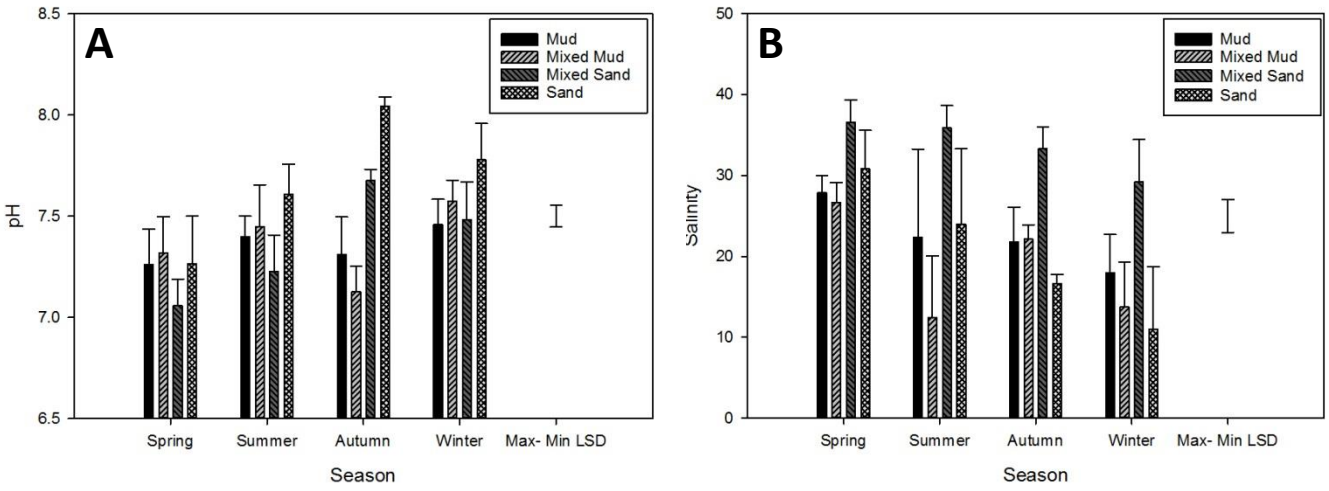

Figure A3 Mean values of pH (A) and salinity (B) at four intertidal sediments during each season. Solid fill bars- Mud; light- grey dashed bars- Mixed Mud; dark- grey dashed bars- Mixed Sand; hatched bars- Sand. Error bars indicate standard error from the mean. Floating bar represents maximum – minimum least significant differences (LSD) (due to unequal number of samples within treatments) at *p*= 0.05 level. Difference between treatment means larger than the LSD bar generally indicates a significant difference.

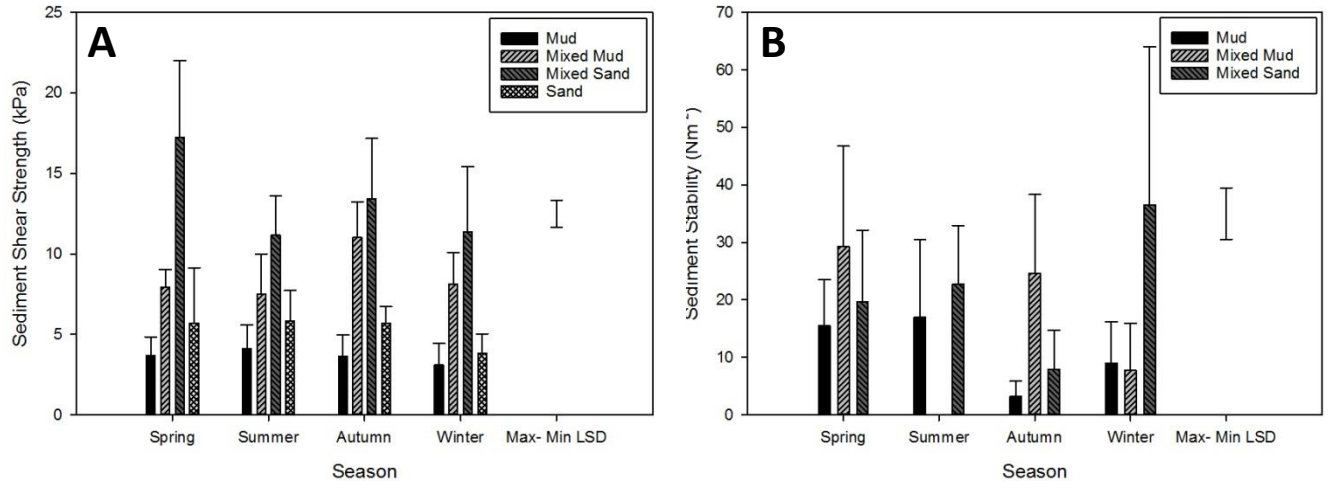

Figure A4 Mean values of sediment shear strength (A) and sediment stability (B) at four intertidal sediments during each season. Solid fill bars- Mud; light- grey dashed bars- Mixed Mud; dark- grey dashed bars- Mixed Sand; hatched bars- Sand. Error bars indicate standard error from the mean. Floating bar represents maximum – minimum least significant differences (LSD) (due to unequal number of samples within treatments) at *p*= 0.05 level. Difference between treatment means larger than the LSD bar generally indicates a significant difference.

Mud

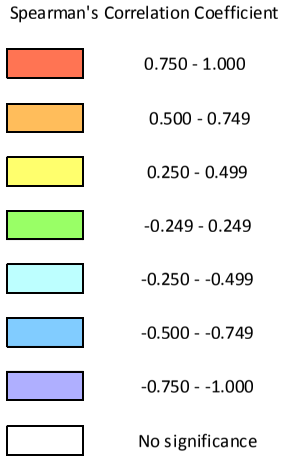

Indicator Organisms	Coliforms	1	1.000 77																
	E. coli	2	.935** 77	1.000 77															
Physical Sediment Characteristics	Organic Content	3	.370** 77	.284* 77	1.000 77														
	Water Content	4	.404** 77	.413** 77	.745** 77	1.000 77													
	Bulk Density	5	-.569** 77	-.664** 77	-.097 77	-.321** 77	1.000 77												
	Fine Particles	6	.393** 77	.241* 77	.403** 77	.279* 77	.073 77	1.000 78											
	Median Particle Diameter	7	-.381** 77	-.217 77	-.433** 77	-.295** 77	-.067 77	-.975** 78	1.000 78										
	Vol. Weighted Mean Particle Diameter	8	-.206 77	-.073 77	-.303** 77	-.210 77	-.240* 77	-.887** 78	.833** 78	1.000 78									
Chemical Sediment Characteristics	Colloidal Carbohydrates	9	-.152 77	-.258* 77	.197 77	.116 77	.449** 77	.339** 78	-.360** 78	-.429** 78	1.000 78								
	Colloidal Proteins	10	-.432** 77	-.544** 77	.072 77	.012 77	.555** 77	.271* 78	-.302** 78	-.383** 78	.836** 78	1.000 78							
	Organic Carbon	11	.302 23	.320 23	.579** 23	.460* 23	-.040 23	.724** 24	-.812** 24	-.578** 24	.399 24	.175 24	1.000 24						
	Total Carbon	12	.304 23	.331 23	.679** 23	.581** 23	-.080 23	.637** 24	-.739** 24	-.531** 24	.263 24	.017 24	.927** 24	1.000 24					
	Total Nitrogen	13	.319 23	.307 23	.690** 23	.478* 23	-.001 23	.659** 24	-.740** 24	-.520** 24	.479* 24	.230 24	.928** 24	.930** 24	1.000 24				
	Carbon/ Nitrogen Ratio	14	-.048 23	-.023 23	-.352 23	-.098 23	-.221 23	-.414* 24	.442* 24	.276 24	-.666** 24	-.557** 24	-.602** 24	-.555** 24	-.781** 24	1.000 24			
	pH	15	.036 77	.189 77	-.411** 77	-.188 77	-.371** 77	-.575** 78	.591** 78	.571** 78	-.370** 78	-.499** 78	-.569** 24	-.501* 24	-.563** 24	.455* 24	1.000 78		
	Salinity	16	-.460** 77	-.605** 77	.125 77	-.018 77	.563** 77	.405** 78	-.437** 78	-.442** 78	.481** 78	.706** 78	.357 24	.306 24	.294 24	-.229 24	-.731** 78	1.000 78	
Erosion Potential	Sediment Shear Strength	17	-.177 77	-.101 77	-.261* 77	-.062 77	.029 77	-.143 78	.119 78	.057 78	.270* 78	.278* 78	.022 24	.023 24	.010 24	-.152 24	.112 78	.147 78	1.000 78
	Sediment Stability	18	-.051 66	-.104 66	-.273* 66	-.344** 66	.270* 66	.016 66	-.067 66	-.004 66	.266* 66	.136 66	-.098 18	-.179 18	-.114 18	-.151 18	.053 66	-.057 66	.228 66
			1	2	3	4	5	6	7	8	9	10	11	12	13	14	15	16	17

Figure A5 Spearman's rank correlation coefficients between all available variables for the Mud site. The upper number in each cell is the correlation coefficient, * denotes two- tailed significance to 0.05 level, ** denotes significance to 0.01 level. Lower number is number of samples in the correlation.

Mixed Mud

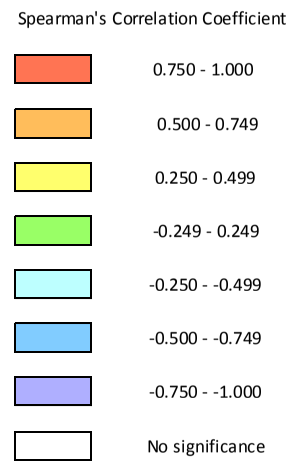

Indicator Organisms	Coliforms	1	1.000 74															
	E. coli	2	.521** 74	1.000 77														
Physical Sediment Characteristics	Organic Content	3	.350** 73	.171 76	1.000 77													
	Water Content	4	.226 73	.334** 76	.628** 77	1.000 77												
	Bulk Density	5	-.003 74	-.232* 77	.156 77	-.123 77	1.000 78											
	Fine Particles	6	.486** 74	-.015 77	.452** 77	.292* 77	-.129 78	1.000 78										
	Median Particle Diameter	7	-.472** 74	.042 77	-.443** 77	-.270* 77	.115 78	-.996** 78	1.000 78									
	Vol. Weighted Mean Particle Diameter	8	-.410** 74	-.009 77	-.456** 77	-.291* 77	.107 78	-.965** 78	.955** 78	1.000 78								
Chemical Sediment Characteristics	Colloidal Carbohydrates	9	.492** 74	.199 77	.690** 77	.332** 77	.128 78	.704** 78	-.689** 78	-.738** 78	1.000 78							
	Colloidal Proteins	10	.572** 74	.299** 77	.339** 77	.294** 77	-.148 78	.722** 78	-.695** 78	-.723** 78	.679** 78	1.000 78						
	Organic Carbon	11	.356 24	.246 24	.493* 23	.348 23	-.215 24	.510* 24	-.511* 24	-.462* 24	.578** 24	.562** 24	1.000 24					
	Total Carbon	12	.149 24	-.009 24	.586** 23	.209 23	-.050 24	.683** 24	-.676** 24	-.654** 24	.720** 24	.446* 24	.876** 24	1.000 24				
	Total Nitrogen	13	.269 24	.040 24	.629** 23	.198 23	-.046 24	.660** 24	-.649** 24	-.634** 24	.759** 24	.528** 24	.910** 24	.973** 24	1.000 24			
	Carbon/ Nitrogen Ratio	14	-.587** 24	-.229 24	-.474* 23	-.197 23	.091 24	-.454* 24	.447* 24	.397 24	-.648** 24	-.691** 24	-.813** 24	-.670** 24	-.801** 24	1.000 24		
	pH	15	-.240* 74	.120 77	-.076 77	-.017 77	.041 78	-.457** 78	.483** 78	.354** 78	-.194 78	-.381** 78	.065 24	.142 24	.122 24	.071 24	1.000 78	
	Salinity	16	-.069 74	-.581** 77	.190 77	-.077 77	.106 78	.481** 78	-.499** 78	-.450** 78	.367** 78	.244* 78	.108 24	.277 24	.260 24	-.117 24	-.599** 78	1.000 78
Erosion Potential	Sediment Shear Strength	17	.119 74	.208 77	.114 77	.057 77	.029 78	-.079 78	.072 78	.045 78	.019 78	-.003 78	-.632** 24	-.599** 24	-.507* 24	.252 24	-.307** 78	.090 78
	Sediment Stability	18	.444** 52	-.068 53	.152 54	.136 54	-.288* 54	.499** 54	-.484** 54	-.525** 54	.515** 54	.548** 54	-.406 12	-.322 12	-.280 12	-.056 12	-.534** 54	.620** 54
			1	2	3	4	5	6	7	8	9	10	11	12	13	14	15	16

Indicator Organisms	Coliforms	1																
	E. coli	2																
Physical Sediment Characteristics	Organic Content	3																
	Water Content	4																
	Bulk Density	5																
	Fine Particles	6																
	Median Particle Diameter	7																
	Vol. Weighted Mean Particle Diameter	8																
Chemical Sediment Characteristics	Colloidal Carbohydrates	9																
	Colloidal Proteins	10																
	Organic Carbon	11																
	Total Carbon	12																
	Total Nitrogen	13																
	Carbon/ Nitrogen Ratio	14																
	pH	15																
	Salinity	16																
Erosion Potential	Sediment Shear Strength	17	.108 24	.277 24	.260 24	-.117 24	-.599** 78	1.000 78										
	Sediment Stability	18	-.632** 24	-.599** 24	-.507* 24	.252 24	-.307** 78	.090 78	1.000 78									
			-.406 12	-.322 12	-.280 12	-.056 12	-.534** 54	.620** 54	.054 54	1.000 54								
			19	20	21	22	23	24	25	26								

Figure A6 Spearman's rank correlation coefficients between all available variables for the Mixed Mud site. The upper number in each cell is the correlation coefficient, * denotes two- tailed significance to 0.05 level, ** denotes significance to 0.01 level. Lower number is number of samples in the correlation.

Mixed Sand

Spearman's Correlation Coefficient

- 0.750 - 1.000
- 0.500 - 0.749
- 0.250 - 0.499
- -0.249 - 0.249
- -0.250 - -0.499
- -0.500 - -0.749
- -0.750 - -1.000
- No significance

Indicator Organisms	Coliforms	1	1.000 71																
	E. coli	2	.762** 71	1.000 71															
Physical Sediment Characteristics	Organic Content	3	.392** 70	.321** 70	1.000 70														
	Water Content	4	.619** 71	.564** 71	.575** 70	1.000 71													
	Bulk Density	5	-.345** 71	-.351** 71	-.219 70	-.234* 71	1.000 71												
	Fine Particles	6	.365** 71	.266* 71	.868** 70	.503** 71	-.067 71	1.000 72											
	Median Particle Diameter	7	-.439** 71	-.361** 71	-.891** 70	-.559** 71	.164 71	-.954** 72	1.000 72										
	Vol. Weighted Mean Particle Diameter	8	-.416** 71	-.334** 71	-.884** 70	-.541** 71	.122 71	-.966** 72	.995** 72	1.000 72									
Chemical Sediment Characteristics	Colloidal Carbohydrates	9	-.297* 71	-.425** 71	.376** 70	-.165 71	.241* 71	.465** 72	-.366** 72	-.390** 72	1.000 72								
	Colloidal Proteins	10	.042 71	-.177 71	.652** 70	.183 71	.096 71	.695** 72	-.642** 72	-.660** 72	.764** 72	1.000 72							
	Organic Carbon	11	.445* 23	.362 23	.821** 23	.495* 23	-.063 23	.935** 24	-.876** 24	-.878** 24	.671** 24	.843** 24	1.000 24						
	Total Carbon	12	.383 23	.383 23	.828** 23	.498* 23	.080 23	.897** 24	-.870** 24	-.870** 24	.603** 24	.815** 24	.940** 24	1.000 24					
	Total Nitrogen	13	.331 23	.159 23	.704** 23	.392 23	.070 23	.842** 24	-.748** 24	-.753** 24	.665** 24	.875** 24	.922** 24	.890** 24	1.000 24				
	Carbon/ Nitrogen Ratio	14	.277 23	.462* 23	.397 23	.231 23	.020 23	.258 24	-.358 24	-.352 24	.217 24	.142 24	.203 24	.305 24	-.051 24	1.000 24			
	pH	15	.384** 65	.493** 65	-.104 64	.294* 65	-.276* 65	-.172 66	.077 66	.102 66	-.776** 66	-.601** 66	-.243 21	-.152 21	-.232 21	-.325 21	1.000 66		
	Salinity	16	-.222 58	-.398** 58	.105 57	-.352** 58	.134 58	.268* 58	-.245 58	-.266* 58	.757** 58	.538** 58	.326 19	.265 19	.472* 19	-.132 19	-.555** 58	1.000 58	
Erosion Potential	Sediment Shear Strength	17	-.270* 71	-.360** 71	-.055 70	-.226 71	.230 71	.121 72	.010 72	-.018 72	.489** 72	.209 72	.088 24	.081 24	.114 24	-.030 24	-.361** 66	.486** 58	1.000 72
	Sediment Stability	18	-.204 50	-.045 50	-.245 49	-.251 50	-.014 50	-.371** 51	.362** 51	.356* 51	-.132 51	-.181 51	-.144 16	-.126 16	.092 16	-.559* 16	.070 47	-.185 39	-.376** 51	1.000 51
			1	2	3	4	5	6	7	8	9	10	11	12	13	14	15	16	17	18

Figure A7 Spearman's rank correlation coefficients between all available variables for the Mixed Sand site. The upper number in each cell is the correlation coefficient, * denotes two- tailed significance to 0.05 level, ** denotes significance to 0.01 level. Lower number is number of samples in the correlation.

Sand

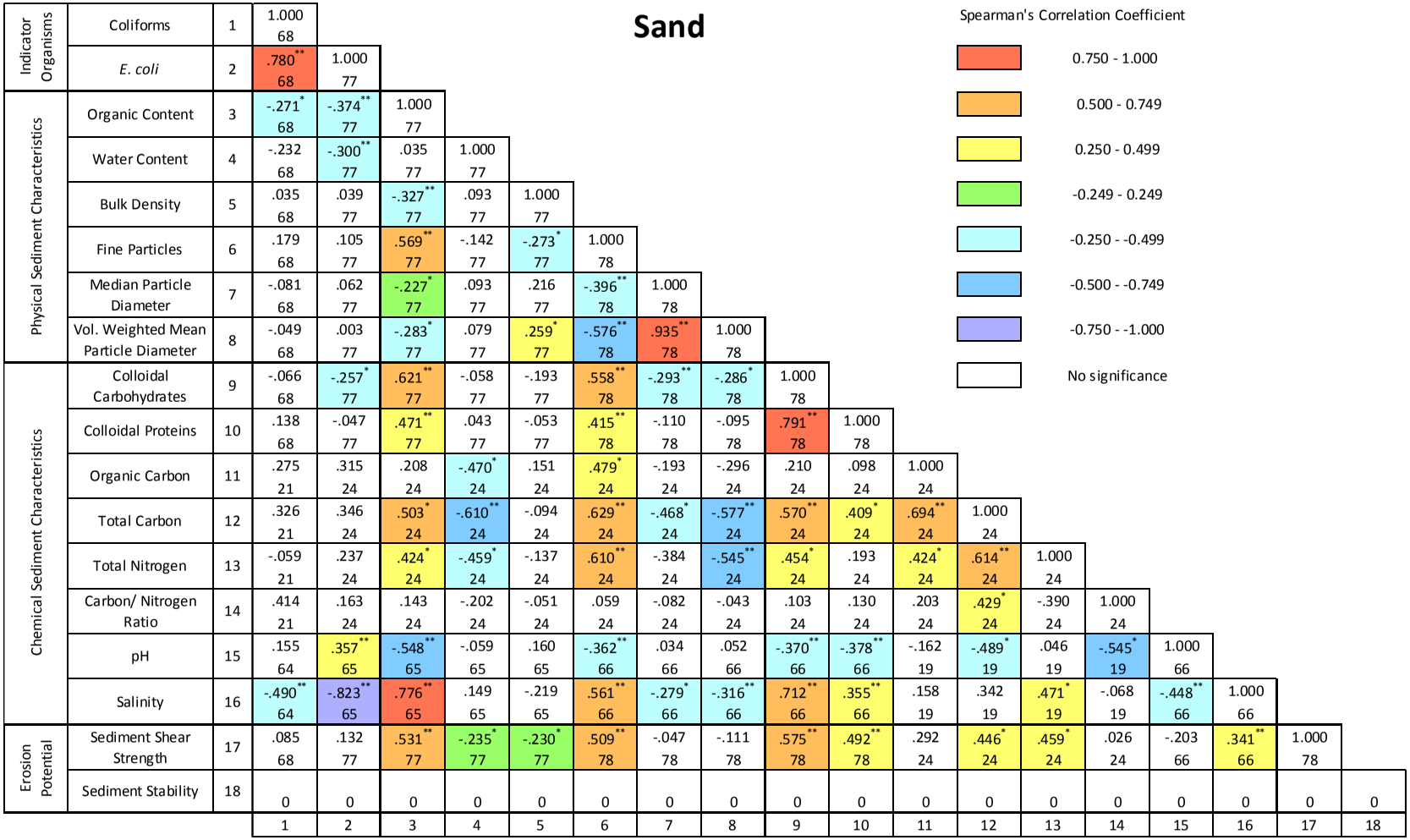

			1	2	3	4	5	6	7	8	9	10	11	12	13	14	15	16	17	18
Indicator Organisms	Coliforms	1	1.000 68																	
	E. coli	2	.780** 68	1.000 77																
Physical Sediment Characteristics	Organic Content	3	-.271* 68	-.374** 77	1.000 77															
	Water Content	4	-.232 68	-.300** 77	.035 77	1.000 77														
	Bulk Density	5	.035 68	.039 77	-.327** 77	.093 77	1.000 77													
	Fine Particles	6	.179 68	.105 77	.569** 77	-.142 77	-.273* 77	1.000 78												
	Median Particle Diameter	7	-.081 68	.062 77	-.227* 77	.093 77	.216 77	-.396** 78	1.000 78											
	Vol. Weighted Mean Particle Diameter	8	-.049 68	.003 77	-.283* 77	.079 77	.259* 77	-.576** 78	.935** 78	1.000 78										
Chemical Sediment Characteristics	Colloidal Carbohydrates	9	-.066 68	-.257* 77	.621** 77	-.058 77	-.193 77	.558** 78	-.293** 78	-.286* 78	1.000 78									
	Colloidal Proteins	10	.138 68	-.047 77	.471** 77	.043 77	-.053 77	.415** 78	-.110 78	-.095 78	.791** 78	1.000 78								
	Organic Carbon	11	.275 21	.315 24	.208 24	-.470* 24	.151 24	.479* 24	-.193 24	-.296 24	.210 24	.098 24	1.000 24							
	Total Carbon	12	.326 21	.346 24	.503* 24	-.610** 24	-.094 24	.629** 24	-.468* 24	-.577** 24	.570** 24	.409* 24	.694** 24	1.000 24						
	Total Nitrogen	13	-.059 21	.237 24	.424* 24	-.459* 24	-.137 24	.610** 24	-.384 24	-.545** 24	.454* 24	.193 24	.424* 24	.614** 24	1.000 24					
	Carbon/ Nitrogen Ratio	14	.414 21	.163 24	.143 24	-.202 24	-.051 24	.059 24	-.082 24	-.043 24	.103 24	.130 24	.203 24	.429* 24	-.390 24	1.000 24				
	pH	15	.155 64	.357** 65	-.548** 65	-.059 65	.160 65	-.362** 66	.034 66	.052 66	-.370** 66	-.378** 66	-.162 19	-.489* 19	.046 19	-.545* 19	1.000 66			
	Salinity	16	-.490** 64	-.823** 65	.776** 65	.149 65	-.219 65	.561** 66	-.279* 66	-.316** 66	.712** 66	.355** 66	.158 19	.342 19	.471* 19	-.068 19	-.448** 66	1.000 66		
Erosion Potential	Sediment Shear Strength	17	.085 68	.132 77	.531** 77	-.235* 77	-.230* 77	.509** 78	-.047 78	-.111 78	.575** 78	.492** 78	.292 24	.446* 24	.459* 24	.026 24	-.203 66	.341** 66	1.000 78	
	Sediment Stability	18	0	0	0	0	0	0	0	0	0	0	0	0	0	0	0	0	0	0

Figure A8 Spearman's rank correlation coefficients between all available variables for the Sand site. The upper number in each cell is the correlation coefficient, * denotes two- tailed significance to 0.05 level, ** denotes significance to 0.01 level. Lower number is number of samples in the correlation.

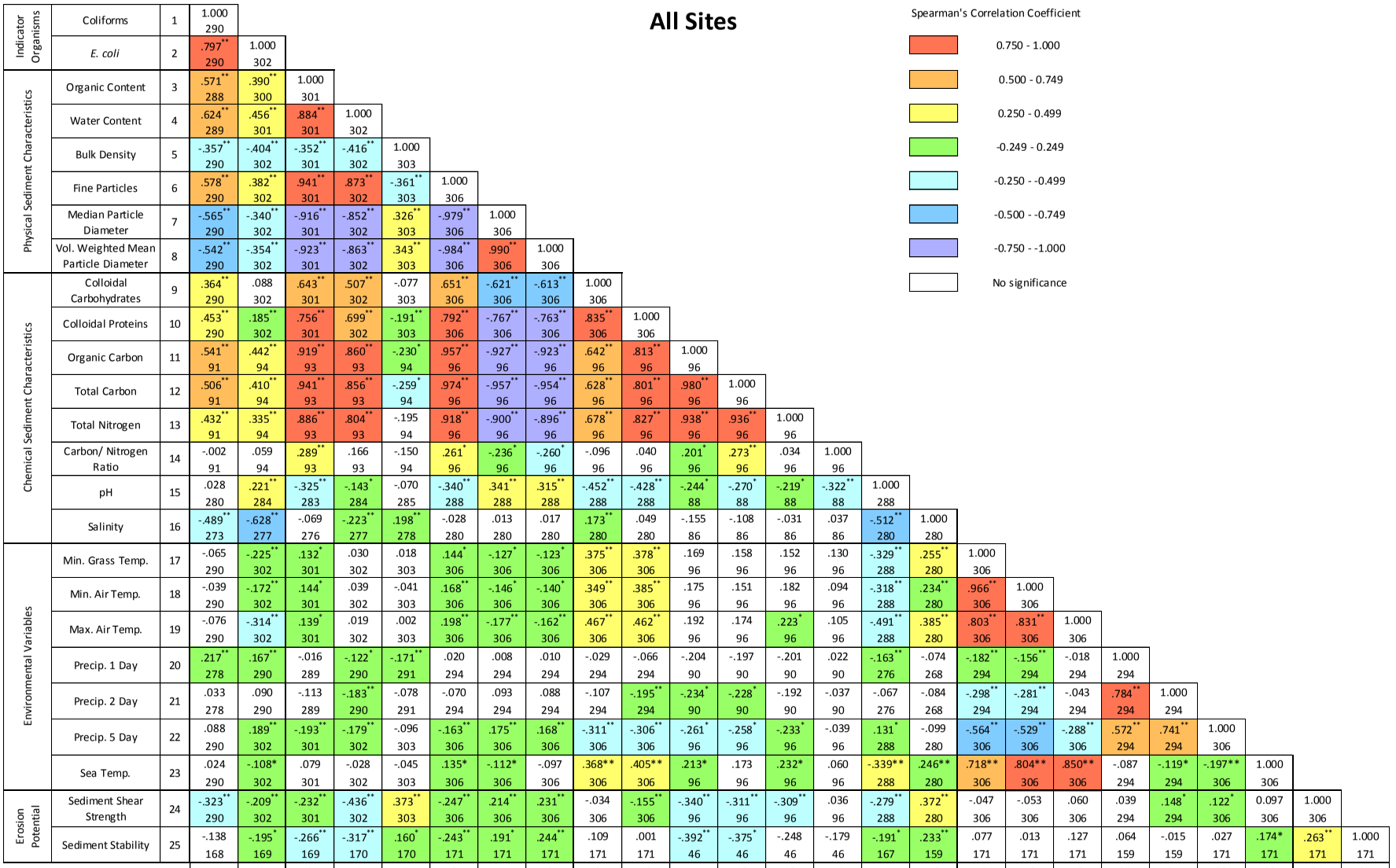

			1	2	3	4	5	6	7	8	9	10	11	12	13	14	15	16	17	18	19	20	21	22	23	24	25
Indicator Organisms	Coliforms	1	1.000 290																								
	E. coli	2	.797** 290	1.000 302																							
Physical Sediment Characteristics	Organic Content	3	.571** 288	.390** 300	1.000 301																						
	Water Content	4	.624** 289	.456** 301	.884** 301	1.000 302																					
	Bulk Density	5	-.357** 290	-.404** 302	-.352** 301	-.416** 302	1.000 303																				
	Fine Particles	6	.578** 290	.382** 302	.941** 301	.873** 302	-.361** 303	1.000 306																			
	Median Particle Diameter	7	-.565** 290	-.340** 302	-.916** 301	-.852** 302	.326** 303	-.979** 306	1.000 306																		
	Vol. Weighted Mean Particle Diameter	8	-.542** 290	-.354** 302	-.923** 301	-.863** 302	.343** 303	-.984** 306	.990** 306	1.000 306																	
Chemical Sediment Characteristics	Colloidal Carbohydrates	9	.364** 290	.088 302	.643** 301	.507** 302	-.077 303	.651** 306	-.621** 306	-.613** 306	1.000 306																
	Colloidal Proteins	10	.453** 290	.185** 302	.756** 301	.699** 302	-.191** 303	.792** 306	-.767** 306	-.763** 306	.835** 306	1.000 306															
	Organic Carbon	11	.541** 91	.442** 94	.919** 93	.860** 93	-.230* 94	.957** 96	-.927** 96	-.923** 96	.642** 96	.813** 96	1.000 96														
	Total Carbon	12	.506** 91	.410** 94	.941** 93	.856** 93	-.259* 94	.974** 96	-.957** 96	-.954** 96	.628** 96	.801** 96	.980** 96	1.000 96													
	Total Nitrogen	13	.432** 91	.335** 94	.886** 93	.804** 93	-.195 94	.918** 96	-.900** 96	-.896** 96	.678** 96	.827** 96	.938** 96	.936** 96	1.000 96												
	Carbon/ Nitrogen Ratio	14	-.002 91	.059 94	.289** 93	.166 93	-.150 94	.261* 96	-.236* 96	-.260* 96	-.096 96	.040 96	.201* 96	.273** 96	.034 96	1.000 96											
	pH	15	.028 280	.221** 284	-.325** 283	-.143* 284	-.070 285	-.340** 288	.341** 288	.315** 288	-.452** 288	-.428** 288	-.244* 88	-.270* 88	-.219* 88	-.322** 88	1.000 288										
	Salinity	16	-.489** 273	-.628** 277	-.069 276	-.223** 277	.198** 278	-.028 280	.013 280	.017 280	.173** 280	.049 280	-.155 86	-.108 86	-.031 86	.037 86	-.512** 280	1.000 280									
Environmental Variables	Min. Grass Temp.	17	-.065 290	-.225** 302	.132* 301	.030 302	.018 303	.144* 306	-.127* 306	-.123* 306	.375** 306	.378** 306	.169 96	.158 96	.152 96	.130 96	-.329** 288	.255** 280	1.000 306								
	Min. Air Temp.	18	-.039 290	-.172** 302	.144* 301	.039 302	-.041 303	.168** 306	-.146* 306	-.140* 306	.349** 306	.385** 306	.175 96	.151 96	.182 96	.094 96	-.318** 288	.234** 280	.966** 306	1.000 306							
	Max. Air Temp.	19	-.076 290	-.314** 302	.139* 301	.019 302	.002 303	.198** 306	-.177** 306	-.162** 306	.467** 306	.462** 306	.192 96	.174 96	.223* 96	.105 96	-.491** 288	.385** 280	.803** 306	.831** 306	1.000 306						
	Precip. 1 Day	20	.217** 278	.167** 290	-.016 289	-.122* 290	-.171** 291	.020 294	.008 294	.010 294	-.029 294	-.066 294	-.204 90	-.197 90	-.201 90	.022 90	-.163** 276	-.074 268	-.182** 294	-.156** 294	-.018 294	1.000 294					
	Precip. 2 Day	21	.033 278	.090 290	-.113 289	-.183** 290	-.078 291	-.070 294	.093 294	.088 294	-.107 294	-.195** 294	-.234* 90	-.228* 90	-.192 90	-.037 90	-.067 276	-.084 268	-.298** 294	-.281** 294	-.043 294	.784** 294	1.000 294				
	Precip. 5 Day	22	.088 290	.189** 302	-.193** 301	-.179** 302	-.096 303	-.163** 306	.175** 306	.168** 306	-.311** 306	-.306** 306	-.261* 96	-.258* 96	-.233* 96	-.039 96	.131* 288	-.099 280	-.564** 306	-.529** 306	-.288** 306	.572** 294	.741** 294	1.000 306			
	Sea Temp.	23	.024 290	-.108* 302	.079 301	-.028 302	-.045 303	.135* 306	-.112* 306	-.097 306	.368** 306	.405** 306	.213* 96	.173 96	.232* 96	.060 96	-.339** 288	.246** 280	.718** 306	.804** 306	.850** 306	-.087 294	-.119* 294	-.197** 306	1.000 306		
Erosion Potential	Sediment Shear Strength	24	-.323** 290	-.209** 302	-.232** 301	-.436** 302	.373** 303	-.247** 306	.214** 306	.231** 306	-.034 306	-.155** 306	-.340** 96	-.311** 96	-.309** 96	.036 96	-.279** 288	.372** 280	-.047 306	-.053 306	.060 306	.039 294	.148* 294	.122* 306	0.097 306	1.000 306	
	Sediment Stability	25	-.138 168	-.195* 169	-.266** 169	-.317** 170	.160* 170	-.243** 171	.191* 171	.244** 171	.109 171	.001 171	-.392** 46	-.375* 46	-.248 46	-.179 46	-.191* 167	.233** 159	.077 171	.013 171	.127 171	.064 159	-.015 159	.027 171	.174* 171	.263** 171	1.000 171

Figure A9 Spearman's rank correlation coefficients between all available variables for all sediment types. The upper number in each cell is the correlation coefficient, * denotes two- tailed significance to 0.05 level, ** denotes significance to 0.01 level. Lower number is number of samples in the correlation.

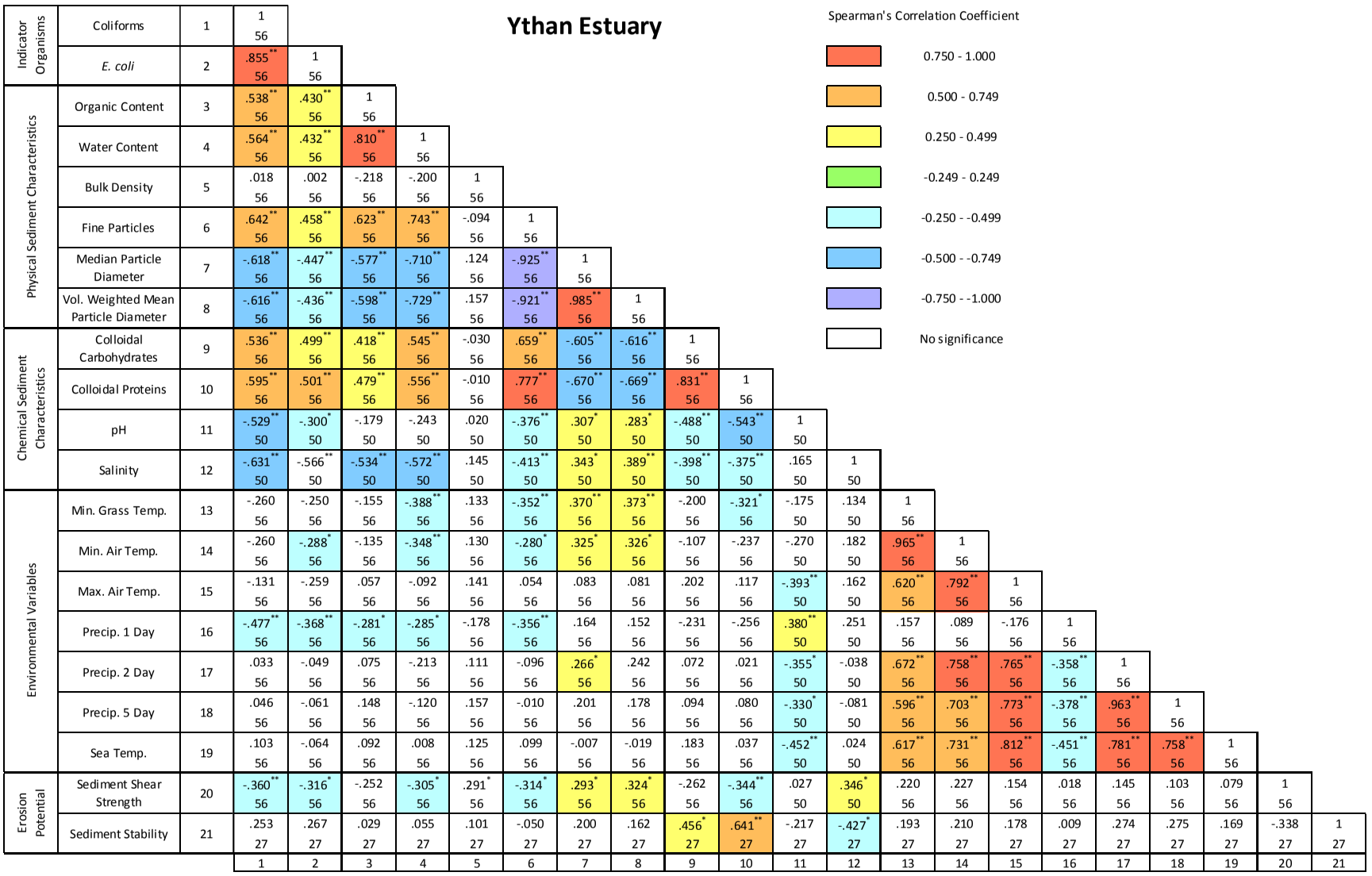

Indicator Organisms	Coliforms	1	1 56																			
	E. coli	2	.855** 56	1 56																		
Physical Sediment Characteristics	Organic Content	3	.538** 56	.430** 56	1 56																	
	Water Content	4	.564** 56	.432** 56	.810** 56	1 56																
	Bulk Density	5	.018 56	.002 56	-.218 56	-.200 56	1 56															
	Fine Particles	6	.642** 56	.458** 56	.623** 56	.743** 56	-.094 56	1 56														
	Median Particle Diameter	7	-.618** 56	-.447** 56	-.577** 56	-.710** 56	.124 56	-.925** 56	1 56													
	Vol. Weighted Mean Particle Diameter	8	-.616** 56	-.436** 56	-.598** 56	-.729** 56	.157 56	-.921** 56	.985** 56	1 56												
Chemical Sediment Characteristics	Colloidal Carbohydrates	9	.536** 56	.499** 56	.418** 56	.545** 56	-.030 56	.659** 56	-.605** 56	-.616** 56	1 56											
	Colloidal Proteins	10	.595** 56	.501** 56	.479** 56	.556** 56	-.010 56	.777** 56	-.670** 56	-.669** 56	.831** 56	1 56										
	pH	11	-.529** 50	-.300* 50	-.179 50	-.243 50	.020 50	-.376** 50	.307* 50	.283* 50	-.488** 50	-.543** 50	1 50									
	Salinity	12	-.631** 50	-.566** 50	-.534** 50	-.572** 50	.145 50	-.413** 50	.343* 50	.389** 50	-.398** 50	-.375** 50	.165 50	1 50								
Environmental Variables	Min. Grass Temp.	13	-.260 56	-.250 56	-.155 56	-.388** 56	.133 56	-.352** 56	.370** 56	.373** 56	-.200 56	-.321* 56	-.175 50	.134 50	1 56							
	Min. Air Temp.	14	-.260 56	-.288* 56	-.135 56	-.348** 56	.130 56	-.280* 56	.325* 56	.326* 56	-.107 56	-.237 56	-.270 50	.182 50	.965** 56	1 56						
	Max. Air Temp.	15	-.131 56	-.259 56	.057 56	-.092 56	.141 56	.054 56	.083 56	.081 56	.202 56	.117 56	-.393** 50	.162 50	.620** 56	.792** 56	1 56					
	Precip. 1 Day	16	-.477** 56	-.368** 56	-.281* 56	-.285* 56	-.178 56	-.356** 56	.164 56	.152 56	-.231 56	-.256 56	.380** 50	.251 50	.157 56	.089 56	-.176 56	1 56				
	Precip. 2 Day	17	.033 56	-.049 56	.075 56	-.213 56	.111 56	-.096 56	.266* 56	.242 56	.072 56	.021 56	-.355* 50	-.038 50	.672** 56	.758** 56	.765** 56	-.358** 56	1 56			
	Precip. 5 Day	18	.046 56	-.061 56	.148 56	-.120 56	.157 56	-.010 56	.201 56	.178 56	.094 56	.080 56	-.330* 50	-.081 50	.596** 56	.703** 56	.773** 56	-.378** 56	.963** 56	1 56		
	Sea Temp.	19	.103 56	-.064 56	.092 56	.008 56	.125 56	.099 56	-.007 56	-.019 56	.183 56	.037 56	-.452** 50	.024 50	.617** 56	.731** 56	.812** 56	-.451** 56	.781** 56	.758** 56	1 56	
Erosion Potential	Sediment Shear Strength	20	-.360** 56	-.316* 56	-.252 56	-.305* 56	.291* 56	-.314* 56	.293* 56	.324* 56	-.262 56	-.344** 56	.027 50	.346* 50	.220 56	.227 56	.154 56	.018 56	.145 56	.103 56	.079 56	1 56	
	Sediment Stability	21	.253 27	.267 27	.029 27	.055 27	.101 27	-.050 27	.200 27	.162 27	.456* 27	.641** 27	-.217 27	-.427* 27	.193 27	.210 27	.178 27	.009 27	.274 27	.275 27	.169 27	-.338 27	1 27
			1	2	3	4	5	6	7	8	9	10	11	12	13	14	15	16	17	18	19	20	21

Figure A10 Spearman's rank correlation coefficients between all available variables for the Ythan estuary transect. The upper number in each cell is the correlation coefficient, * denotes two- tailed significance to 0.05 level, ** denotes significance to 0.01 level. Lower number is number of samples in the correlation.

Eden Estuary

Spearman's Correlation Coefficient

- 0.750 - 1.000
- 0.500 - 0.749
- 0.250 - 0.499
- -0.249 - 0.249
- -0.250 - -0.499
- -0.500 - -0.749
- -0.750 - -1.000
- No significance

Indicator Organisms	Coliforms	1	1.000 56																			
	E. coli	2	.959** 56	1.000 56																		
Physical Sediment Characteristics	Organic Content	3	.618** 56	.590** 56	1.000 56																	
	Water Content	4	.604** 56	.575** 56	.982** 56	1.000 56																
	Bulk Density	5	-.242 56	-.278* 56	-.473** 56	-.484** 56	1.000 56															
	Fine Particles	6	.838** 56	.784** 56	.650** 56	.632** 56	-.293* 56	1.000 56														
	Median Particle Diameter	7	-.779** 56	-.741** 56	-.603** 56	-.588** 56	.288* 56	-.945** 56	1.000 56													
	Vol. Weighted Mean Particle Diameter	8	-.775** 56	-.746** 56	-.590** 56	-.573** 56	.296* 56	-.931** 56	.981** 56	1.000 56												
Chemical Sediment Characteristics	Colloidal Carbohydrates	9	.640** 56	.624** 56	.603** 56	.554** 56	-.092 56	.678** 56	-.617** 56	-.592** 56	1.000 56											
	Colloidal Proteins	10	.471** 56	.450** 56	.605** 56	.552** 56	-.101 56	.584** 56	-.529** 56	-.523** 56	.784** 56	1.000 56										
	pH	11	-.523** 48	-.502** 48	-.242 48	-.172 48	.164 48	-.294* 48	.308* 48	.300* 48	-.200 48	-.125 48	1.000 48									
	Salinity	12	-.644** 48	-.675** 48	-.393** 48	-.454** 48	.356* 48	-.525** 48	.487** 48	.505** 48	-.288* 48	-.122 48	.058 48	1.000 48								
Environmental Variables	Min. Grass Temp.	13	-.469** 56	-.436** 56	-.020 56	-.025 56	.103 56	-.391** 56	.273* 56	.249 56	-.081 56	.079 56	.093 48	.273 48	1.000 56							
	Min. Air Temp.	14	-.380** 56	-.399** 56	-.043 56	-.090 56	.167 56	-.294* 56	.190 56	.171 56	-.028 56	.109 56	-.135 48	.445** 48	.878** 56	1.000 56						
	Max. Air Temp.	15	-.159 56	-.168 56	.099 56	.049 56	.047 56	-.068 56	-.007 56	-.030 56	.216 56	.366** 56	-.094 48	.387** 48	.695** 56	.821** 56	1.000 56					
	Precip. 1 Day	16	-.002 56	.126 56	-.007 56	-.062 56	.193 56	-.106 56	.031 56	.031 56	.046 56	.068 56	-.118 48	.026 48	.250 56	.162 56	-.066 56	1.000 56				
	Precip. 2 Day	17	.344** 56	.374** 56	-.046 56	-.087 56	.128 56	.100 56	-.087 56	-.078 56	.025 56	-.179 56	-.540** 48	.102 48	-.285* 56	-.090 56	-.072 56	.297* 56	1.000 56			
	Precip. 5 Day	18	.234 56	.331* 56	-.022 56	-.062 56	.036 56	-.007 56	-.040 56	-.033 56	-.081 56	-.164 56	-.517** 48	-.042 48	-.081 56	.027 56	-.126 56	.571** 56	.789** 56	1.000 56		
	Sea Temp.	19	-.017 56	-.108 56	-.044 56	-.104 56	.150 56	-.012 56	-.010 56	-.015 56	.085 56	.056 56	-.383** 48	.442** 48	.279* 56	.638** 56	.714** 56	-.239 56	.405** 56	.116 56	1.000 56	
Erosion Potential	Sediment Shear Strength	20	-.136 56	-.096 56	-.062 56	-.053 56	.090 56	-.132 56	.156 56	.178 56	.111 56	.094 56	.214 48	.213 48	-.041 56	-.088 56	-.116 56	.182 56	-.067 56	-.074 56	-.186 56	1.000 56
	Sediment Stability	21	-.297 38	-.151 38	-.158 38	-.225 38	.283 38	-.284 38	.234 38	.274 38	.331* 38	.355* 38	-.082 38	.399* 38	.352* 38	.355* 38	.318 38	.259 38	-.077 38	.066 38	.094 38	-.067 38
			1	2	3	4	5	6	7	8	9	10	11	12	13	14	15	16	17	18	19	20

Figure A11 Spearman's rank correlation coefficients between all available variables for the Eden estuary transect. The upper number in each cell is the correlation coefficient, * denotes two- tailed significance to 0.05 level, ** denotes significance to 0.01 level. Lower number is number of samples in the correlation.

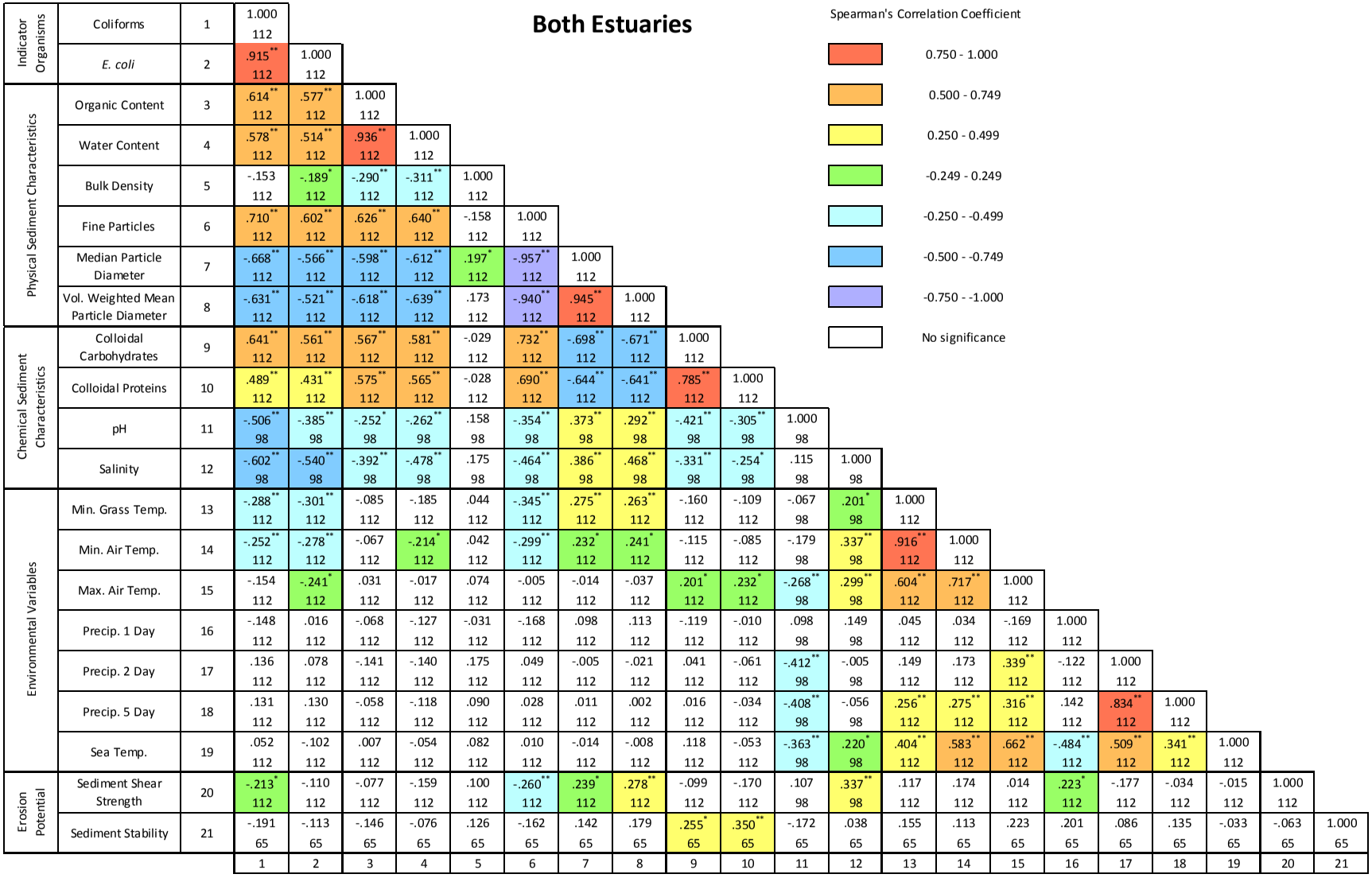

			1	2	3	4	5	6	7	8	9	10	11	12	13	14	15	16	17	18	19	20	21
Indicator Organisms	Coliforms	1	1.000 112																				
	E. coli	2	.915** 112	1.000 112																			
Physical Sediment Characteristics	Organic Content	3	.614** 112	.577** 112	1.000 112																		
	Water Content	4	.578** 112	.514** 112	.936** 112	1.000 112																	
	Bulk Density	5	-.153 112	-.189* 112	-.290** 112	-.311** 112	1.000 112																
	Fine Particles	6	.710** 112	.602** 112	.626** 112	.640** 112	-.158 112	1.000 112															
	Median Particle Diameter	7	-.668** 112	-.566** 112	-.598** 112	-.612** 112	.197* 112	-.957** 112	1.000 112														
	Vol. Weighted Mean Particle Diameter	8	-.631** 112	-.521** 112	-.618** 112	-.639** 112	.173 112	-.940** 112	.945** 112	1.000 112													
Chemical Sediment Characteristics	Colloidal Carbohydrates	9	.641** 112	.561** 112	.567** 112	.581** 112	-.029 112	.732** 112	-.698** 112	-.671** 112	1.000 112												
	Colloidal Proteins	10	.489** 112	.431** 112	.575** 112	.565** 112	-.028 112	.690** 112	-.644** 112	-.641** 112	.785** 112	1.000 112											
	pH	11	-.506** 98	-.385** 98	-.252* 98	-.262** 98	.158 98	-.354** 98	.373** 98	.292** 98	-.421** 98	-.305** 98	1.000 98										
	Salinity	12	-.602** 98	-.540** 98	-.392** 98	-.478** 98	.175 98	-.464** 98	.386** 98	.468** 98	-.331** 98	-.254* 98	.115 98	1.000 98									
Environmental Variables	Min. Grass Temp.	13	-.288** 112	-.301** 112	-.085 112	-.185 112	.044 112	-.345** 112	.275** 112	.263** 112	-.160 112	-.109 112	-.067 98	.201* 98	1.000 112								
	Min. Air Temp.	14	-.252** 112	-.278** 112	-.067 112	-.214* 112	.042 112	-.299** 112	.232* 112	.241* 112	-.115 112	-.085 112	-.179 98	.337** 98	.916** 112	1.000 112							
	Max. Air Temp.	15	-.154 112	-.241* 112	.031 112	-.017 112	.074 112	-.005 112	-.014 112	-.037 112	.201* 112	.232* 112	-.268** 98	.299** 98	.604** 112	.717** 112	1.000 112						
	Precip. 1 Day	16	-.148 112	.016 112	-.068 112	-.127 112	-.031 112	-.168 112	.098 112	.113 112	-.119 112	-.010 112	.098 98	.149 98	.045 112	.034 112	-.169 112	1.000 112					
	Precip. 2 Day	17	.136 112	.078 112	-.141 112	-.140 112	.175 112	.049 112	-.005 112	-.021 112	.041 112	-.061 112	-.412** 98	-.005 98	.149 112	.173 112	.339** 112	-.122 112	1.000 112				
	Precip. 5 Day	18	.131 112	.130 112	-.058 112	-.118 112	.090 112	.028 112	.011 112	.002 112	.016 112	-.034 112	-.408** 98	-.056 98	.256** 112	.275** 112	.316** 112	.142 112	.834** 112	1.000 112			
	Sea Temp.	19	.052 112	-.102 112	.007 112	-.054 112	.082 112	.010 112	-.014 112	-.008 112	.118 112	-.053 112	-.363** 98	.220* 98	.404** 112	.583** 112	.662** 112	-.484** 112	.509** 112	.341** 112	1.000 112		
Erosion Potential	Sediment Shear Strength	20	-.213* 112	-.110 112	-.077 112	-.159 112	.100 112	-.260** 112	.239* 112	.278** 112	-.099 112	-.170 112	.107 98	.337** 98	.117 112	.174 112	.014 112	.223* 112	-.177 112	-.034 112	-.015 112	1.000 112	
	Sediment Stability	21	-.191 65	-.113 65	-.146 65	-.076 65	.126 65	-.162 65	.142 65	.179 65	.255* 65	.350** 65	-.172 65	.038 65	.155 65	.113 65	.223 65	.201 65	.086 65	.135 65	-.033 65	-.063 65	1.000 65

Figure A12 Spearman's rank correlation coefficients between all available variables for the combined estuary transects. The upper number in each cell is the correlation coefficient, * denotes two- tailed significance to 0.05 level, ** denotes significance to 0.01 level. Lower number is number of samples in the correlation.

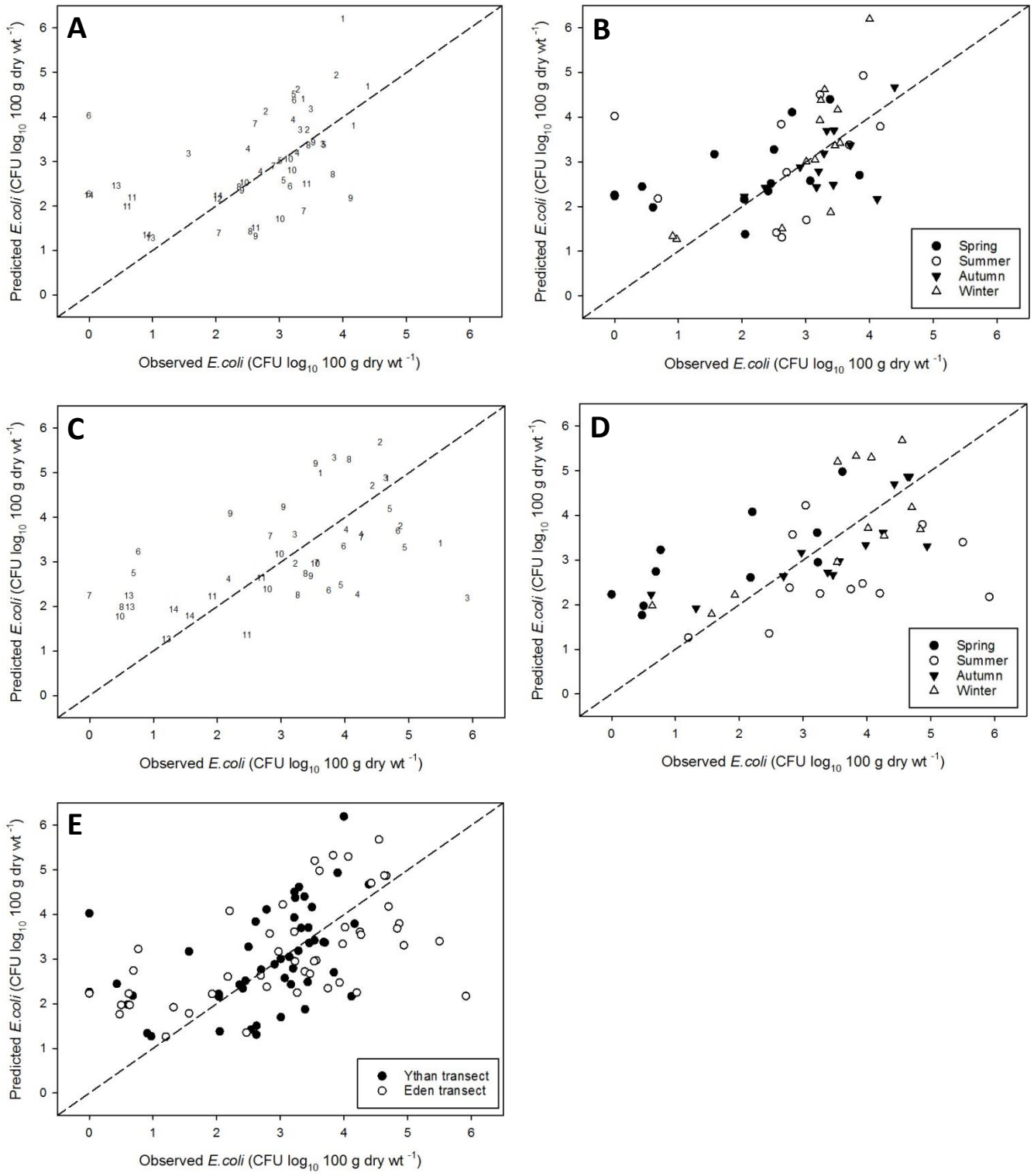

Figure A13. Scatterplots of observed vs. predicted *E. coli* abundance in intertidal sediments using the model constructed on data from the meaned sampling event data of the intensive sampling on the Ythan estuary on the estuary transect datasets. A, B= Ythan estuary; C, D= Eden estuary; E= both estuaries combined. A, C= numbers denote sampling position within the estuary. B, D= solid circles- spring; hollow circles- summer; solid triangles- autumn; hollow triangles- winter. E= solid circles- Ythan estuary; hollow circles- Eden estuary.

Chapter 5

Table A11 Summary of overlaid algal and cyanobacterial TRFs that defined variables in the ordination of microbial communities. Matching phylum, class and order from peak identification using MiCA.

TRF	Phylum	Class/ Sub- class	Order
68B	-	-	-
289B	-	-	-
291B	Chlorophyta	Chlorophyceae	Chlamydomonadales
		Prasinophyceae	Mamiellales
			Pseudoscourfieldiales
	Basidiomycota	Many	Many
295B	Chlorophyta	Chlorophyceae	Chaetophorales
			Chlamydomonadales
			Chlorococcales
			Chlorosarcinales
			Sphaeropleales
			Tetraporales
		Trebouxiophyceae	Chlorellales
			Microthamniales
			incertae sedis
		Ulvophyceae	Trentepohiales
			Ulotrichales
	Basidiomycota	Many	Many
231Y	Cyanobacteria	Nostocophycideae	Nostocales
		Oscillatoriophycideae	Oscillatoriales
			Synechococcales
271Y	Cyanobacteria	Nostocophycideae	Nostocales
		Oscillatoriophycideae	Oscillatoriales
			Chroococcales
349Y	Cyanobacteria	Cyanophyceae	Stigonematales
		Nostocophycideae	Nostocales
		Oscillatoriophycideae	Chroococcales
			Oscillatoriales
		Synechococcophycideae	Synechococcales

Table A12 Summary of overlaid eubacterial TRFs that defined variables in the ordination of microbial communities. Matching phylum, class and order from peak identification using MiCA.

TRF	Phylum	Class/ Sub- class	Order
50G	Proteobacteria	Alphaproteobacteria	Rhodospirillales
52G	Proteobacteria	Alphaproteobacteria	Rhizobiales
		Deltaproteobacteria	Desulfarculales
		Gammaproteobacteria	Alteromonodales Enterobacteriales
60G	-	-	-
166G	Proteobacteria	Gammaproteobacteria	Alteromonodales
171G	Proteobacteria	Betaproteobacteria	Burkholderiales
		Gammaproteobacteria	Alteromonodales Chromotiales Enterobacteriales Pseudomonadales Xanthomonadales
175G	Proteobacteria	Gammaproteobacteria	Alteromonodales Enterobacteriales Vibrionales Xanthomonadales
189G	Proteobacteria	Alphaproteobacteria	Rhizobiales
		Gammaproteobacteria	Alteromonodales Vibrionales
302G	Proteobacteria	Alphaproteobacteria	Rhizobiales
315G	-	-	-
335G	Actinobacteria	Actinobacteria	Actinomycetales
	Proteobacteria	Alphaproteobacteria	Rhizobiales
		Betaproteobacteria	Burkholderiales
		Gammaproteobacteria	Alteromonodales Enterobacteriales Pseudomonadales Vibrionales
338G	Proteobacteria	Alphaproteobacteria	Rhizobiales Rickettsiales
		Deltaproteobacteria	Desulfovibrionales
		Gammaproteobacteria	Alteromonodales Enterobacteriales Pseudomonadales Vibrionales Xanthomonadales
410G	-	-	-
470G	Proteobacteria	Alphaproteobacteria	Rhodobacterales
		Gammaproteobacteria	Alteromonodales

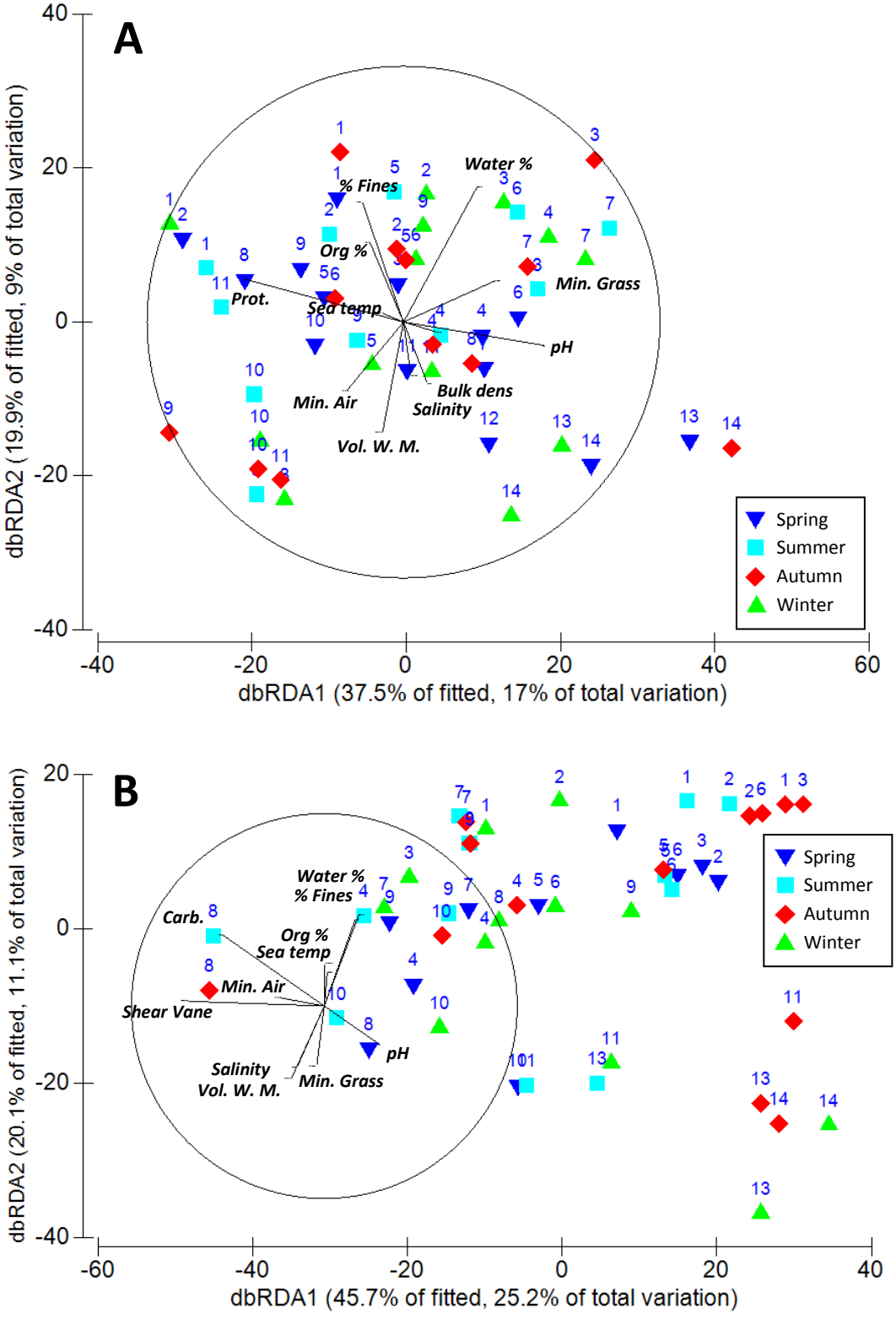

Figure A14 dbRDA ordination of the TRFLP microbial community analysis of the Ythan (A) and Eden (B) estuary transects. Overlaid vectors are of environmental variables that were included in the optimal significant distLM model. Sample labels denote site ID. Blue triangles- spring; turquoise squares- summer; red diamonds- autumn; green triangles- winter.

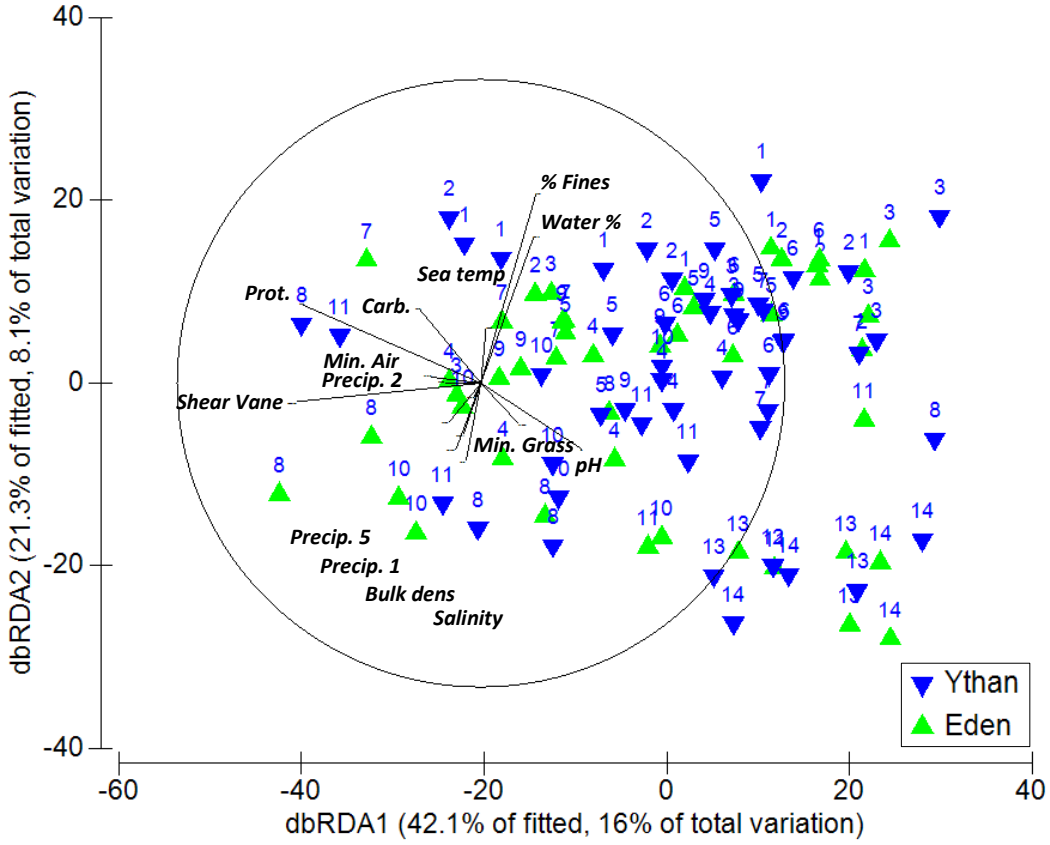

Figure A15 dbRDA ordination of the TRFLP microbial community community analysis of the combined Ythan and Eden estuary transects. Overlaid vectors are of environmental variables that were included in the optimal significant distLM model. Sample labels denote site ID. Blue triangles- Ythan; green triangles- Eden.

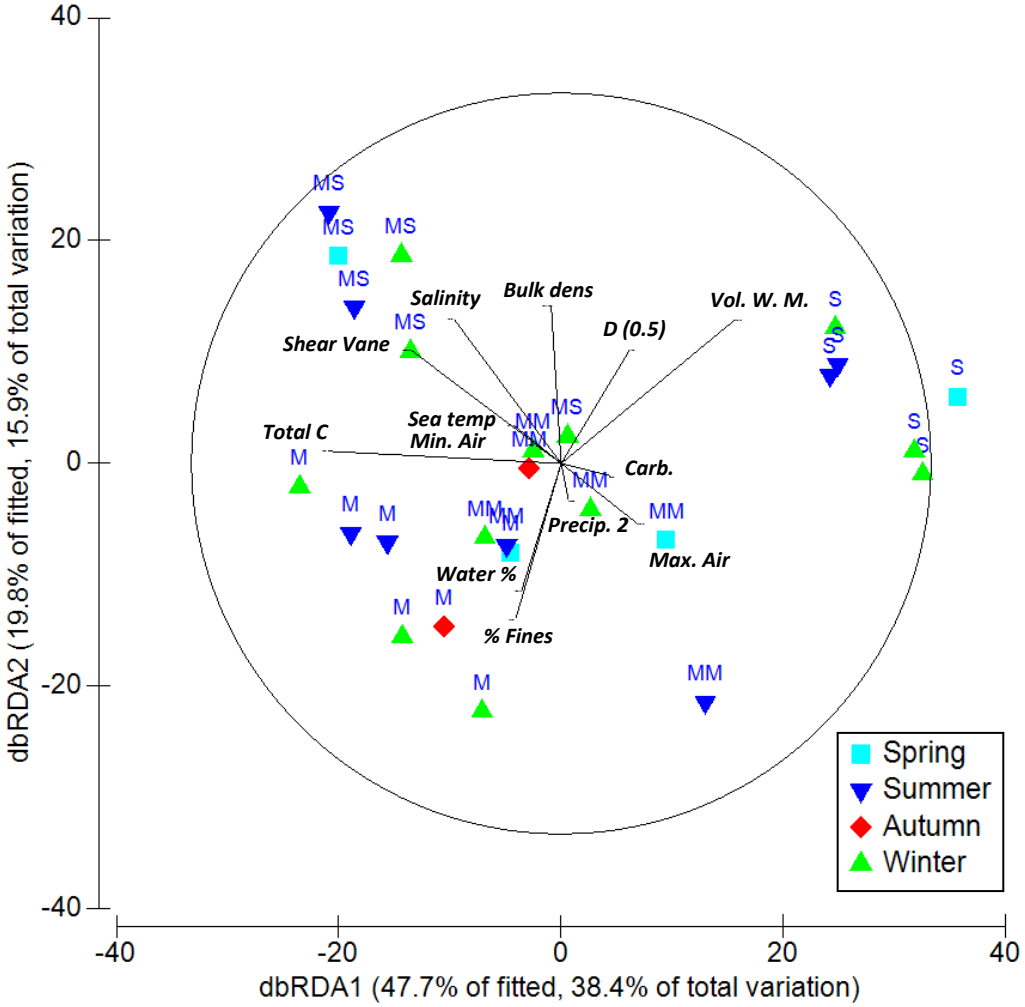

Figure A16 dbRDA ordination of the TRFLP microbial community community analysis of intensively sampled sediments at the Ythan estuary. Overlaid vectors are of environmental variables that were included in the optimal significant distLM model. Sample labels denote site ID. Turquoise squares- spring; blue triangles- summer; red diamonds- autumn; green triangles- winter.